LOCALISATION AND FUNCTION OF MECHANOSENSORY ION CHANNELS IN COLONIC SENSORY NEURONS

Patrick Hughes

Nerve-Gut Laboratory

Department of Physiology

School of Molecular and Biomedical Sciences

University of Adelaide

July 2008

I dedicate this thesis to my wife Sarah and son Blake for their constant support and inspiration throughout

Table of Contents

Abstract

Irritable Bowel Syndrome (IBS) is one of the most common functional disorders of the gastrointestinal tract. Visceral hypersensitivity is the most commonly reported symptom of IBS, yet is the least adequately treated. Mechanosensitive information from the colon is relayed to the CNS by extrinsic colonic primary afferent nerves which have their cell bodies within dorsal root ganglia (DRG). This thesis aims to identify the contribution of several putatively mechanosensitive ion channels (ASIC1, 2 and 3, TRPV4 and TRPA1) toward detection of mechanical stimuli in the colon.

This involvement is assessed by both molecular and functional means. The abundance of each of these channels was assessed by comparing expression within whole DRG against that in specifically colonic DRG neurons using an *in situ* hybridization methodology developed as part of this PhD. The functional role TRPV4 and TRPA1 impart toward colonic mechanosensation was investigated by recording responses to mechanical stimuli from colonic primary afferent fibres and comparing the results from mice genetically modified to lack either TRPV4 or TRPA1 with those of their intact littermates.

The results from these studies indicate expression patterns within whole DRG do not provide accurate representation of the organ of interest, with abundances of each of the channels investigated differing between colonic DRG cells and the whole DRG. In particular ASIC3 and TRPV4 are preferentially expressed in colonic DRG neurons, unlike ASIC2 and TRPA1. Further, TRPV4 is functionally restricted to detection of noxious mechanical stimuli in the colon, while expression of TRPA1 is more widespread and

functionally less restricted. Each of these channels are each potential targets for the treatment of IBS as each affects specific aspects of colonic mechanotransduction.

Declaration of Originality

This work contains no material which has been accepted for the award of any other degree or diploma in any university or other tertiary institution and, to the best of my knowledge and belief, contains no material previously published or written by another person, except where due reference has been made in the text.

I give consent to this copy of my thesis when deposited in the University Library, being made available for loan and photocopying, subject to the provisions of the Copyright Act 1968.

The author acknowledges that copyright of published works contained within this thesis (as listed below) resides with the copyright holders of those works.

Signed :

Patrick Hughes Date

Publications arising from this thesis (bold denotes first authors)

1**: Hughes PA**, **Brierley SM**, Young RL and Blackshaw LA. (2007). Localization and comparative analysis of acid-sensing ion channel (ASIC1, 2, and 3) mRNA expression in mouse colonic sensory neurons within thoracolumbar dorsal root ganglia. J. Comp. Neurol. 500: 863-75

2**: Brierley SM, Page AJ, Hughes PA,** Adam B, Liebregts T, Cooper NJ, Holtmann G, Liedtke W, Blackshaw LA. (2008). Selective Role for TRPV4 ion channels in visceral sensory pathways. Gastroenterol. 134(7):2059-69

3: Brierley SM, Hughes PA, Page AJ, KY Kwan, CM Martin, TA O'Donnell, NJ Cooper, AM Harrington, B Adam; T Liebregts, G Holtmann, DP Corey, G Rychkov, A Blackshaw. (2008) TRPA1 mediates mechanotransduction in sensory neurons and is modulated by algesic stimuli. Neuron (in press).

Acknowledgement of Work Provided by Others

PCR was performed by Stuart Brierley in all cases, however I provided retrogradely labelled tissue for laser capture microdissection. Extracellular recordings from lumbar splanchnic colonic afferents for TRPV4 experiments (Chapter 5) were performed entirely by Stuart Brierley, and were peformed by Stuart Brierley and Chris Martin for TRPA1 experiments (Chapter 6). Vagal gastroesophageal afferents recordings for TRPV4 experiments (Chapter 5) were performed entirely by Amanda Page, and were performed by Amanda Page and Tracey O'Donnell for TRPA1 experiments (Chapter 6). All colonic distension experiments were performed by Tobias Liebregts, Birgit Adam and Gerald Holtmann. TRPV4 immunolabelling (Chapter 5) was performed by Nicole Cooper and Stuart Brierley, and TRPA1 immunolabelling (Chapter 6) was performed by Nicole Cooper, Stuart Brierley and Andrea Harrington.

I am indebted to my principle supervisor, Professor Ashley Blackshaw for providing exciting and rewarding projects. In particular the ability to attend conferences and interact with the global scientific community is greatly appreciated. The support of Amanda Page, my co-supervisor, is also appreciated.

I would also like to thank Stuart Brierley for providing the time and expertise required to learn techniques including colonic electrophysiological recordings.

Finally many thanks also to my wife Sarah and my family, Peter, Marilyn and Bronwyn for their support and encouragement.

CHAPTER 1

INTRODUCTION

Functional Disorders of the Gastrointestinal Tract

Functional disorders of the gastrointestinal tract are extremely common, accounting for greater than 40% of all gastrointestinal practice [1, 2]. This group of illnesses, termed functional as they occur without infectious or metabolic causes and lack structural abnormalities, presently includes more than 20 different disease states [1, 3]. Of these the most common are Irritable Bowel Syndrome (IBS) and functional dyspepsia [3]. These disorders impact significantly on the wellbeing and lifestyle of sufferers and are estimated to cost $41 billion (U.S.) annually in the western world alone [1-4]. The absence of pathological markers and subsequent reliance on patients' perceptions of pain states makes the diagnosis of functional disorders difficult with considerable overlap between the diagnosis of functional dyspepsia and Gastro Oesophageal Reflux Disease (GORD), and less commonly between functional dyspepsia and IBS [3-6]. Altered sensing of mechanical stimuli is implicated in each of these illnesses with sufferers typically reporting lower thresholds for discomfort and / or pain than healthy people [7-16].

Irritable Bowel Syndrome

Irritable Bowel Syndrome (IBS) is defined by Rome criteria as a group of functional bowel disorders in which abdominal discomfort or pain is associated with defecation or a change in bowel habit, and with features of disordered defecation [17-21]. Patients suffering from IBS complain of abdominal pain associated with other symptoms such as changing bowel habits (diarrhoea or constipation, or alternating between diarrhoea and constipation), abdominal bloating, passage of mucus and / or a sense of incomplete rectal evacuation [2, 3, 17-20]. IBS is one of the most common functional disorders of the gastrointestinal tract

with estimates of at least 10% of the population affected in the western world alone [2, 3, 20, 22]. However sufferers do not always seek medical attention, particularly where not readily available [23]. While the prevalence of IBS is similar in developed and undeveloped countries, the gender ratio alternates between female predominant in the developed world and male predominant in the undeveloped world [1]. This difference probably reflects sociological factors, and in turn suggests the true population of IBS is much greater than currently reported. Despite sufferers rarely being referred for specialist treatment the economic impact associated with IBS is substantial and when indirect costs such as work absenteeism are included it is estimated to cost approximately $20 billion per annum in the U.S. alone [2, 23-25].

An understanding of the aetiology of IBS is complex given its functional nature and varied symptomatology and epidemiology. Interdependence of symptoms is yet to be completely understood, and IBS may actually be a group of several disorders with more than one underlying cause. Consistent with the complex symptomatology is the number of theories of the genesis of IBS including abnormal motility, psychological disorders and more recently, previous infection [1, 4, 19, 26]. Visceral hypersensitivity is the most commonly reported symptom and may be the hallmark of IBS sufferers. First described in 1973 and since confirmed in a number of studies, IBS patients consistently demonstrate increased sensitivity to rectal balloon distension when compared to healthy subjects without changes in wall tone or compliance indicating the volume response of the colon wall to pressure is normal (Figure 1) [7-16]. Current evidence from behavioural and functional imaging studies suggest these responses are due to alterations in the periphery rather than higher cortical centres [27, 28]**.** The underlying causes of hypersensitivity of the sensory pathways involved is currently unknown and is an intense area of research, with various hypotheses

suggesting previous exposure to inflammatory mediators, genetic polymorphisms and / or sensitization due to previous injury or stress [1, 10, 14, 29]. .

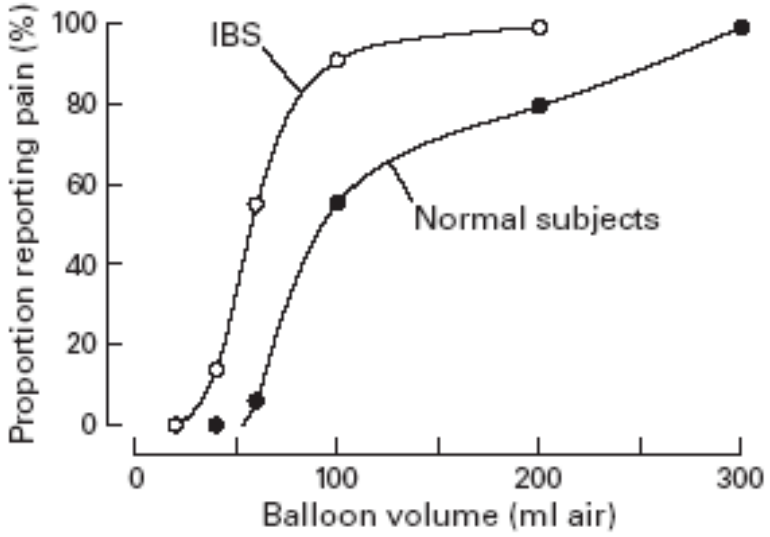

Figure 1: Patients suffering from IBS demonstrate reduced thresholds to rectal balloon pressure compared to healthy subjects. Figure adapted from [7].

Visceral Hypersensitivity Is Not Confined to IBS

Hypersensitivity of gastrointestinal afferents is also implicated in functional disorders of the upper gut including non cardiac chest pain (NCCP), Gastro-Oesophageal Reflux Disease (GORD) and functional dyspepsia. These conditions are prevalent and estimated to account for 5% of all medical consultations. However, as observed with IBS, the majority of sufferers do not seek medical attention and the true incidence may be much higher [3, 30]. Symptoms are varied and include impaired gastric emptying, impaired gastric accommodation and hyperalgesia, with heart-burn predominating in sufferers of gastro-oesophageal reflux disease (GORD) and NCCP [3, 5, 30-32]. While GORD may be causative of NCCP, the pain associated with NCCP and GORD differ and non-GORD related NCCP occurs [31, 32]. Further, GORD is a separate entity to functional dyspepsia and interdependence of the above symptoms in each of these disease states awaits elucidation, similar to the situation observed with IBS. Visceral hypersensitivity of sensory pathways is again implied as intragastric balloons again placed in select regions are perceived at lower distending pressures than in healthy controls [30, 33]. However evidence also suggests psychological disturbances, gastrointestinal motility defects and gastric hypersecretion may also be involved, each of which await integration [30]. While some overlap is observed between sufferers of IBS with GORD or functional dyspepsia this is not common and separate mechanisms are suggested to exist for these illnesses [8].

Treatment of IBS

As the aetiology of IBS is currently unknown treatment is limited to management of symptoms rather than the underlying cause. Hyperalgesia is frequently the most debilitating aspect of IBS, but is the least successfully managed [2, 29, 34, 35]. Motility agents and bulk forming agents have been effective in treatment of constipation (Cisapride, laxatives) or diarrhoea (Loperamide, fibre), but have had little effect on hyperalgesia [1, 29, 36]. Modulation of peripheral 5-HT initially looked promising, with the 5-HT_3 antagonist Alosetron and the 5-HT_4 agonist Tegaserod both providing relief of abdominal cramping and pain associated with either diahorrea predominant (Alosetron) or constipation predominant (Tegaserod) IBS [1, 20, 23, 29, 36, 37]. Unfortunately these drugs have debilitating side effects including cardiac arrhythmia and ischaemic colitis. The seriousness of these side effects led to the initial removal of Cisapride and Alosetron from the marketplace in 2000 and the more recent withdrawal of Tegaserod in 2007. Both Alosetron and Cisapride are currently available on a restricted basis.

The remaining treatments are non-specific, including holistic approaches such as lifestyle management and hypnotherapy, psychotropic medications, probiotics and herbal remedies. Several receptor targets other than 5-HT have been identified, including opiates, tachykinins and proteinases [36, 37]. Currently the most excitement has been generated by Iberogast, a mixture of 9 different herbs demonstrated to modulate intestinal hypersensitivity [39]. Once again these herbs demonstrate efficacious binding to 5-HT_3 and 5-HT_4 receptors, but also to muscarinic and opiate receptors [40]. While each component demonstrated different affinities for each of the above receptors it is unclear whether the benefit achieved is the result of synergistic actions, as observed in a separate study of

caraway and peppermint oils [41]. Also unclear is the actions of these herbs on receptors other than those investigated above.

It is clear management of bowel habit does not treat IBS. More importantly success can be achieved in alleviating pain associated with IBS as demonstrated with 5-HT modulating agents. While hypersensitivity of visceral afferents is clearly demonstrated in patients with IBS and is likely to contribute substantially toward the hyperalgesia suffered, little is known of how this symptom manifests either peripherally or centrally. This is not surprising given the mechanism of transduction of mechanical stimuli remains enigmatic even in healthy systems. Pharmacological targets that reduce sensation specifically in the colon are required in order to clarify the symptomatology of IBS and reduce the potential for side effects. The studies outlined in this thesis aim to identify the involvement several putative mechanosensitive ion channels contribute toward detection of mechanical stimuli in the colon, with the potential of revealing new receptors for treatment of visceral hypersensitivity associated with Irritable Bowel Syndrome.

Pain

The sensation of pain is a common symptom of IBS but is the most poorly treated [34, 35] However pain is inadequately managed in most clinical settings, reflecting a general lack of knowledge of this sense. Despite the initial concept of pain originating millennia ago it is still difficult to define and may either be described in an emotional context, such as suffering, or as an unpleasant sensory experience, such as would be accompanied by hypersensitivity to mechanical stress associated by IBS. The sensing of noxious stimuli resulting in feelings of pain is essential for the survival of organisms in that it acts to warn

away from hostile environments. Receptors tuned to detect noxious stimuli, termed nociceptors, are present on the sensory endings of Aδ and C nerve fibres of the nervous system. Aδ fibres are thinly myelinated and transmit feelings of "sharp" pain, while unmyelinated C fibres are slower and transmit the more "dull" aspects. Despite their description in the early 1900s and subsequent discovery more than 50 years later contention still surrounds the gating of nociceptors [42]. Several theories exist debating whether transduction involves specialised high threshold nociceptors specifically tuned to detect distinct noxious stimuli, or whether the nociceptors are non-specific with a wide dynamic range, encoding innoxious events in response to stimuli of low intensity and noxious events in response to high intensity stimuli [43]. The plasticity of the nervous system, particularly in response to injury, argues for integration of these theories. Mediators released in response to injury specifically act on high threshold nociceptors and / or act to sensitise the nervous system long after their absence, effectively lowering the threshold for noxious signalling [44]. This integration is particularly relevant in chronic pain syndromes such as IBS, whereby noxious events are signalled in the absence of overt pathology.

Detection of Sensory Information in the Colon

Anatomy of the Gastrointestinal Tract

The gastrointestinal tract, with its convoluted lining and massive surface area, is the largest sensory organ in the body. It is essential for survival, acting both as an absorptive layer for nutrients and as a protective layer against toxins. As most of the absorption of nutrients occurs in the lower gastrointestinal tract this area is subjected to a constant barrage of sensory stimuli. Integrated responses are provided by neural, immune and endocrine

systems. These are very extensive and complex, with the gastrointestinal tract containing more neurons than the spinal cord, approximately 75% of the body's immune cells and more than 20 hormones. Most of the processing of sensory information in the gastrointestinal tract does not reach conscious perception and while interactions between these systems are known to occur little is presently known about how they take place. Pathological conditions offer some insight into acute phases, such as bacterial infection resulting in diarrhoea, but chronic disease states such as those present in functional disorders are a much greater enigma. While less is known of the causes of these chronic functional diseases, more is known of the outcomes. Of all the symptoms, pain is the most frequent and often the most debilitating indicating messages must reach the CNS in at the very least the persistent symptoms [34, 35]

The gastrointestinal tract is comprised of mucosal, muscular and serosal layers. The mucosal layer is innermost and consists of three distinct layers; a lining of epithelium in direct contact with gastrointestinal contents that is surrounded by the lamina propria, a layer of loose connecting tissue and the muscular mucosae, a thin layer of smooth muscle. A submucosal layer binds the mucosa to the muscular layers, which are comprised of an inner sheet of circular fibres and an outer sheet of longitudinal smooth muscle. The outermost layer, the serosa, is comprised of a thin serous epithelial membrane coated with connective tissue. Coordination of responses to sensory information in the gastrointestinal tract relies upon innervation of each of these layers by the autonomic, enteric and extrinsic nervous systems. These systems integrate information acquired from a range of stimuli, including chemical, thermal and mechanical, and either initiate (via sensory neurons) or respond (via motor effector neurons) to reflex arcs both within the gut wall and via the CNS to regulate normal gastrointestinal activity.

Sensory Innervation of the Colon

Sensory information is detected in the gastrointestinal tract by afferent nerves within the enteric nervous system, by intestinofugal afferents and by extrinsic afferents. Each of these sensory pathways are primary as they initiate reflex cascades relaying information toward the CNS. Motor innervation of the viscera is provided by the autonomic efferent supply in the form of parasympathetic and sympathetic nerves. Locoal motor control is provided by intrinsic enteric neurons that may function downstream or independantly from extrinsic or autonomic control.

Intrinsic Primary Afferent Neurons

Unlike other viscera the gastrointestinal tract contains its own intrinsic nervous system. Several discoveries at the turn of the 19th century revealed nervous activity in the gastrointestinal tract is retained in the absence of extrinsic connections indicating complete reflex pathways exist in the wall of the gut. Termed the enteric nervous system it is now known to be a vast network comprised of millions of sensory neurons and hence is often termed the ‘second brain’. The enteric nervous system is able to control secretion, motility, blood flow and intestinal transport of nutrients with complete independence from the CNS.

The sensory component of the enteric nervous system is the intrinsic primary afferent neurons (IPANs). IPANs are present in both myenteric and submucosal ganglia**,** where they represent close to one third and one sixth of the total neuronal population respectively [45, 46]. They are characterised by their distinctive Dogiel type II morphology consisting of

several long processes and long after-hyperpolarization potentials [45, 46]. IPANS are sensitive to distension of the intestine, chemical changes within its lumen and distortion of the mucosa and are therefore able to detect alterations in the intestinal state resulting from its contents [45, 46]. Ascending and descending connections with interneurons and both inhibitory and excitatory motorneurons complete the reflex pathways, integrating information received and causing appropriate compensatory changes. As these reflexes are intrinsic properties of the gastrointestinal tract and operate without innervation by the CNS they are thought not to influence conscious perception directly, although they may act indirectly through synapses with intestinofugal or extrinsic afferents [45-47].

Intestinofugal Neurons

Intestinofugal neurons are a rare population that have cell bodies within the gut wall, as in the case with the enteric nervous system, but project to neurons outside the gut wall, as is the case with extrinsic fibres. These neurons have been identified in the myenteric ganglia and influence both motility and the sympathetic innervation of the intestinal wall [46]. As with IPANs there is no evidence that intestinofugal neurons project directly to the CNS, and therefore they are thought not to directly influence conscious perception of painful stimuli.

Extrinsic Primary Afferent Neurons

Extrinsic primary afferents relay sensory information such as pain and nausea from the gastrointestinal tract to the CNS. These nerves in effect act as afferent components of the autonomic nervous system, often travelling with sympathetic and parasympathetic nerves

and passing through prevertebral ganglia where collaterals influence autonomic ganglion cell bodies [38, 48]. They are almost entirely small sparsely myelinated Aδ or very small unmyelinated C fibre nerves with sensitivity to both chemical and mechanical stimuli [48, 49]. These afferents are classed anatomically depending on where the cell soma reside. The cell soma of spinal afferents reside in the dorsal root ganglia (DRG), while that of vagal afferents reside in the nodose and jugular ganglia. Spinal afferents project centrally to the spinal dorsal horn, while vagal afferents project to the nucleus tractus solitarius (NTS) in the brain stem [50, 51]. Both afferent types then connect with second order neurons and project to upper CNS structures such as the hypothalamus, limbic system and thalamus. Spinal afferents are found throughout the gastrointestinal tract whereas vagal afferents are more concentrated in the upper gastrointestinal tract, and are rare in the colon [50, 51].

Spinal and vagal afferent endings are very different both morphologically and physiologically, with differences likely related to anatomical placement within the gastrointestinal tract. For instance both respond to mechanical stimuli within the physiological range yet spinal afferents are also able to respond to noxious mechanical stimuli while the maximal response of vagal afferents is in the physiological range [48, 50-52]. The differences in distribution and physiology suggest vagal afferents are mainly associated with physiological stimuli in the upper GI tract where they influence feelings of satiety, hunger and nausea, while spinal afferents are associated with both physiological and noxious stimuli in the stomach and large intestine and influence feelings of fullness, bloating, discomfort and pain [48, 51, 52]. Spinal afferents are most likely responsible for signalling mechanical stimuli in the colon, such as the degree of distension and therefore filling, and are of most interest for IBS.

Classification of extrinsic primary afferent neurons within anatomical groups is confounded by their polymodal nature, their plasticity and the absence of knowledge of their anatomical specializations. The clearest basis presently available for sub-classification of afferent endings is based on morphological (vagal) and histological (spinal) differences and functionality of these afferents.

Gastrointestinal Mechanosensory Vagal Afferents

While previously stated that vagal endings are rare in the colon it is important to note they do have mechanosensory properties and are well characterised in the upper gut. Three morphologically distinct classes of mechanosensitive afferent endings have been identified for vagal endings; intraganglionic laminar endings (IGLE)s, intramuscular arrays (IMA)s and mucosal endings.

IGLEs were first described in the mid 1940's, but a detailed description was not available until the mid 1970's, when they were named [53]. Detailed profiles since performed throughout the gastrointestinal tract demonstrate a ubiquitous distribution and while concentrations decrease aborally it is important to note they are present in the colon [54-56]. IGLEs form distinct basket like structures wrapping around and possibly entering enteric ganglia sandwiched between longitudinal and circular muscle layers of the gastrointestinal tract. The majority of myenteric ganglion in the oesophagus and approximately half the gastric myenteric ganglia are innervated by IGLEs [55, 56]. These endings are likely to represent mechanosensory endings that respond to low intensity stretch or shearing forces [50, 57-59]

Intramuscular arrays (IMAs) were not described until 1992 and not named until the mid 1990's [54, 60]. These endings have terminals in longitudinal and circular muscle where they branch extensively and run parallel with smooth muscle bundles [54, 60]. They are suggested to be in-series tension receptor endings responding to passive stretch or active contraction of the muscle, although this function has more recently been described as a feature of IGLEs and IMAs have not been correlated functionally with mechanosensory sites [52, 54, 58, 61]. In a constrast to the widespread distribution of IGLEs throughout the gastrointestinal tract, IMAs are more selectively distributed with localisation particularly in the walls of the stomach and sphincters [56, 62].

Vagal mucosal afferents predominate in the upper gastrointestinal tract, particulary in the oesophagus [62-64]. Their morpholgy is diverse with several different subtypes evident. Thick calibre afferents display complex branching, as previously described for IGLEs, and run close to or penetrate the epithelial layer [62, 63]. Thin calibre fibres form dense networks of afferents in the submucosa and are comprised of either simple unbranched varicose fibres or fibres with short branches extending toward the epithelium [62].

Functional studies of gastroesophageal afferent endings have also revealed three distinct types of receptor; mucosal, tension and tension / mucosal afferents. Mucosal afferents respond to light stroking of the mucosa, are generally silent at rest and do not respond to circular stretch [65, 66]. Tension receptors respond to circular stretch with a slowly adapting relationship, often have a resting discharge and do not respond to light stroking of the mucosa [65, 66]. Tension / mucosal afferents respond to both light mucosal stroking and circular stretch and have so far only been identified in the oesophagus but not the stomach of the ferret [65]. It is currently difficult to correlate functionality with

morphology and particularly confounding are the morphology of tension / mucosal endings and the functional role of IMAs.

Gastrointestinal Mechanosensory Spinal Afferents

Spinal afferents are found throughout the gastrointestinal tract and are responsible for the majority of sensory processing in the colon [50-52]. The vertebral DRG level in which cell bodies of spinal afferents are located is dependent on the individual viscera examined and decreases aborally, with cell bodies corresponding to innervation of the stomach located in vertebral DRG levels above that of the colon. Spinal afferents are polymodal and therefore classified anatomically on the basis of the histological tissue level in which their receptive field is observed, that is muscular, mucosal or serosal. Functional studies using electrophysiological techniques have provided evidence of distinct mechanosensory properties within these classes. Muscular afferents are distension sensitive, while serosal afferents are activated by distension only at high thresholds and mucosal afferents are silent at rest and do not respond to distension [50, 51, 67]. As serosal afferents are only activated at high thresholds they are thought to signal sharp pain such as that encountered at the onset of spasm or excessive distension [50, 51, 67]. Muscular afferents respond much more readily to distension, but still may contribute to discomfort and pain as they encode distending stimuli into the noxious range [50, 51, 67]. While mucosal afferents are distension insensitive they are mechano (i.e. fine tactile stimulation), chemo and thermo sensitive [50, 51, 67]. It is important to note that thresholds for mechanosensation are not fixed but are influenced by a wide range of modulators. These modulators are released in response to injury, ischemia and inflammation and often sensitise endings by decreasing the threshold needed for activation [52, 68]. Also important is the presence of silent

nociceptors, which are quiescent to mechanosensation at rest, but are sensitised in conditions of inflammation or injury [38, 47, 51, 52, 67, 68].

Lumbar Splanchnic vs Pelvic Colonic Innervation

Innervation of the colon by spinal afferents has been demonstrated to be bimodal in several animal models (Figure 2) [69-73]. One population has cell soma residing in thoracolumbar DRG vertebral levels and follows lumbar splanchnic innervation, while the other has cell soma in the lumbosacral DRG vertebral levels and follows pelvic innervation. While the mechano and chemosensory properties of both splanchnic and pelvic innervation of the colon has been described in several models direct comparisons are confounded by the use of various experimental techniques in different species [74-78]. In an effort to directly compare these pathways Brierley *et. al.* have recently used a flat colonic sheet preparation in the mouse to characterise mechanosensory and chemosensory properties [79-81]. Anatomical differences in the location of receptive fields were discovered with lumbar splanchnic afferents innervating the colon in wide-spread area distinctly above the rectal area, while pelvic afferents innervating a distinctly distal colonic and rectal region [79-81]. The three classes of afferent previously described (muscular, mucosal and serosal) were conserved between pathways, yet had significantly different distribution and activation thresholds. For example, mucosal and muscular afferents were rare in the lumbar splanchnic afferent innervation, but very common in the pelvic afferent innervation. Further, the threshold of mechanical activation for the serosal class was lower in pelvic afferents than in lumbar splanchnic afferents and the response generated was much greater, indicating lumbar splanchnic serosal afferents adapt more rapidly than their pelvic counterparts [80]. In addition each pathway also contained a unique class of ending, with

mesenteric afferents found in the lumbar splanchnic pathway and muscular / mucosal afferents found in the pelvic pathway [80]. Mesenteric afferents were located on or near blood vessels supplying the serosa and have been proposed to detect twisting and torsion of the colon and changes in blood pressure. Muscular / mucosal afferents display response profiles similar to both mucosal (i.e. low threshold) and muscular (i.e. distension sensitive) afferents. The physiological role of this type of afferent ending is unknown at present, however it has been postulated that they may be responsible for the detection of rapidly moving boluses. [51, 65].

The chemosensory properties of these two pathways have also been contrasted using similar methodology. Lumbar splanchnic afferent innervation is suggested to be tuned toward detection of noxious stimuli as serosal afferents contain more nociceptive receptors (P_2X_3 and TRPV1) than pelvic serosal afferents and respond more often to bradykinin, an inflammatory mediator [79, 81]. Further, mechanically insensitive afferents were recruited by bradykinin and agonists of P_2X_3 receptor in lumbar splanchnic afferents, but not in pelvic afferents [79, 81]. However, this may be presumptive in that not all afferent classes nor nociceptive properties have been investigated. The studies outlined above only compared serosal afferent classes yet the other pelvic afferent classes respond to mechanical stimuli into the noxious range and also respond to nociceptive agents [38, 47, 78-81]. None the less lumbar splanchnic afferents are mainly quiescent until acted upon by noxious stimuli while pelvic afferents are much more easily activated suggesting pelvic afferents signal distension that is maintained by movement of the bolus over the mucosal epithelium, while the lumbar splanchnic pathway signals transient events such as onset of rapid distension and presence of nociceptive mediators.

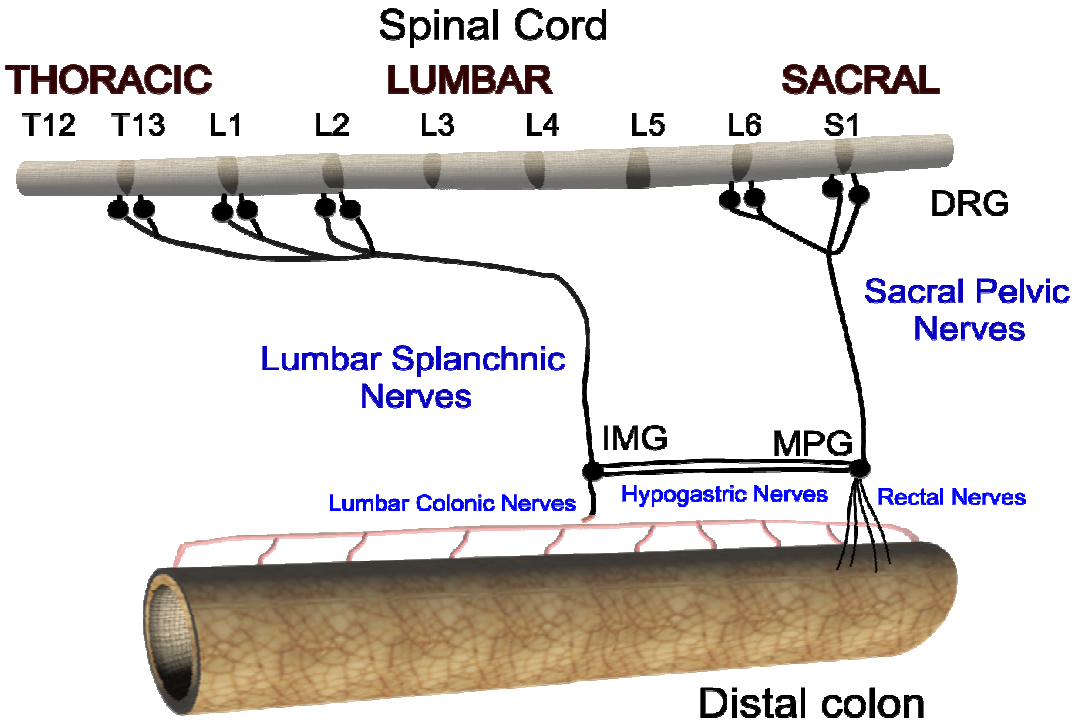

Figure 2: Colonic afferent innervation is bimodal. The colon is innervated by afferents with cell soma in either the thoracolumbar or lumbosacral DRG vertebral levels.

Extrinsic Colonic Innervation by Other Afferent Classes

rIGLEs

While it is generally accepted spinal nerve terminals are unspecialised free endings, more complex IGLE like endings have been described [47, 50, 57, 58, 82]. These afferents innervate the colon and rectum via rectal but not splanchnic nerves and have been termed rectal IGLEs (rIGLEs) as they share morphological characteristics with the IGLEs observed in the upper gastrointestinal tract, albeit they are much simpler in structure [47, 50, 80]. Electrophysiological properties are also similar between both populations as recordings from rIGLEs revealed low threshold slowly adapting mechanoreceptors and may correspond to the muscular afferent observed in the pelvic pathway [79, 81].

Rectospinal and Colospinal Afferents

The majority of colonic sensory processing is conducted via the splanchnic and pelvic nerves described above. However two other populations of extrinsic afferent exist that project directly toward the CNS, bypassing the dorsal root ganglia. The first discovered of these, rectospinal afferents, was described 20 years ago while the other, colospinal afferents, is much more recent [83-85]. While both of these pathways are presumed to be sensory as they demonstrate immunoreactivity similar to that observed in DRG neurons functional studies are currently lacking.

Of clinical interest is the degree of involvement of each of these pathways in functional disorders of the colon. Balloon distension of the colon demonstrates involvement of mechanosensory afferent pathways in IBS and the lumbar splanchnic pathway may be more finely tuned to detect mechanical and chemical stress in normal healthy subjects [7, 79-81]. The role of central sensitisation also cannot be ignored as NMDA receptors activated by injury or inflammation are able to modulate primary afferent responses [86]. The relationship between afferent ending and IBS is currently far from delineated and while activation thresholds are generally reduced in patients suffering from IBS the effect on activation thresholds of specific afferent types is far from defined. Unclear is whether IBS causes changes in abundance of particular afferents, reduction in activation thresholds, changes in adaptation profiles or all of the above. This is not surprising given the nature of mechanosensation is far from understood in the healthy colon, or for that matter in other sensory organs such as skin and the ear.

Mechanotransduction

Mechanotransduction is the process whereby mechanical stimulation of a neuron is converted into a neural action potential. This process plays a fundamental role in determining how organisms respond to their environment. It underlies a wide range of sensory information, including touch, hearing, proprioception and several aspects of somatic pain. In addition a constant stream of mechanosensory information reaches the brain from the viscera. This provides the perceptions of sensation of pain, and also autonomic reflex control of digestive, cardiovascular, respiratory and endocrine functions [87].

To be considered mechanosensitive a channel must contain several key elements. Firstly it must be able to respond very rapidly [88, 89]. Secondly it must be extremely sensitive, with the kinetics of activation dependent on the amplitude of the stimuli, yet also remain adaptive, in that it must be able to adapt to sometimes intense environmental mechanical stimuli and still maintain sensitivity to extremely small changes [88, 89]. This is particularly relevant in low threshold mechanoreceptors, such as those in the auditory system where high sensitivities must be achieved. Thirdly a mechanically dependent physiological outcome must occur following activation [90]. Two different gating models have been proposed that fit these criteria: the lipid bilayer model and the tethered model (Figure 3) [89-91]. The lipid bilayer model originates from prokaryotes and proposes tension on the bilayer alone directly gates mechanically sensitive ion channels found there (Figure 3A) [89-91]. The tethered model is slightly more complex, in that the mechanically sensitive channel is anchored between intra and extracellular structures such as cytoskeletal and / or extracellular matrix proteins (Figure 3B) [89-91]. These tethers may be gated directly by mechanical stimuli, or they may be gated indirectly in that force may be conveyed to an accessory protein that in turn induces a conformation change and activation of the channel (Figure 3C) [89]. In an extension of the tethered model the whole transduction apparatus may be indirectly gated and acted upon by signalling intermediaries (Figure 3D) [89, 90]. A criticism of this final model is that activation of these channels may be too slow due to the reliance on second messenger pathways. However, the latencies of activation of some purportedly mechanosensitive neurons, such as bristle cells in *Drosophila*, are greater than that required for activation of channels in this manner [90]. It remains to be determined whether these neurons directly transduce mechanical stimuli, or instead are merely sensitive to mechanical stimuli. It is important to keep the physiological relevance in mind when assessing these criteria, and as such question whether a channel should be discounted as a potential target if it is indirectly mechanosensitive,

particularly if expressed in appropriate places and quantities. These channels may in fact prove to be better targets through manipulation of second messenger systems that are open to exploitation.

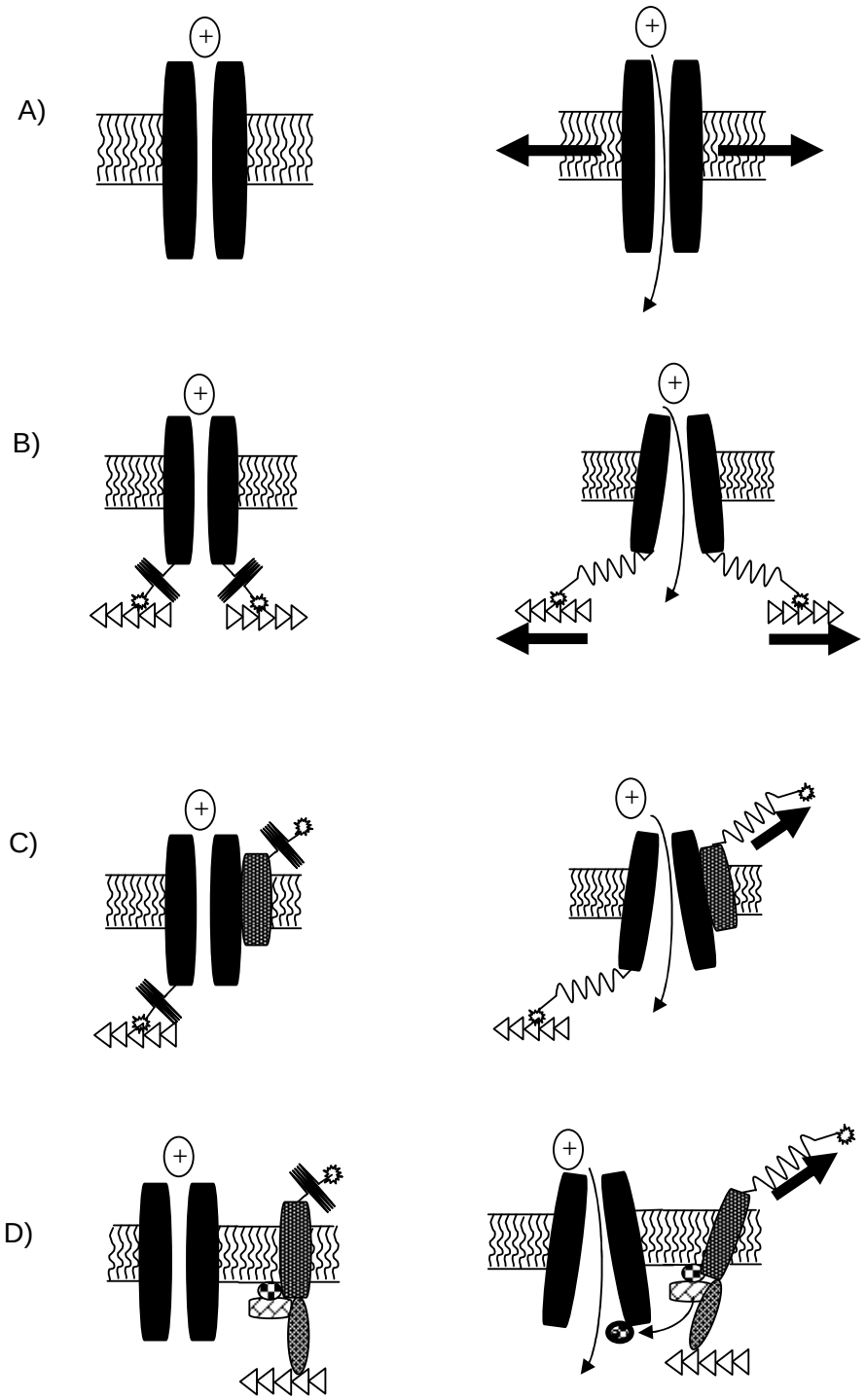

Figure 3: Gating mechanisms of mechanotransduction channels. Channels may either be activated by stretch (A), gated directly (B), or indirectly via attached accessory proteins (C) or activated by intermediatories (D). Figure adapted from [89].

Much more is known about bacterial mechanosensory ion channels than those in eukaryotes. Three of the known mechanosensitive ion channels in *E. coli*, MscL (MechanoSensitive channel of Large conductance), MscS (Smaller conductance) and $MscK^{+}$ (Potassium regulated) have each been cloned, sequenced and are well characterised [91, 92]. The crystal structures have also been determined for MscS and MscL, allowing investigation into gating mechanisms [91, 92]. The lipid bilayer model is the generally accepted model for prokaryotic mechanotransduction, particularly for functions such as osmosensation, [87, 91, 92]. Evidence supporting the lipid bilayer theory of gating includes the ability of these channels to retain their mechanosensitivity when reconstituted in vitro [87]. This is not without controversy however as these experiments involved patch clamping of the membrane, which in itself causes deformation of the lipid bilayer and may induce mechanosensory currents [92]. Despite the relative abundance of knowledge of these channels homologues are yet to be discovered in eukaryotes [91].

The tethered model is proposed as the general model for the eukaryotic mechanotransduction apparatus, although recent evidence suggests some eukaryotic mechanosensory channels are more aligned with the lipid bilayer model [91]. In this model deflection of the extracellular structure relative to the intracellular structure causes the transduction channel to change its probability of being open and therefore the firing of action potentials at the sensory ending [87]. This is again somewhat controversial as it is also proposed that the cytoskeletal and extracellular matrix proteins may not directly gate the channel, but instead stretch the bilayer in the immediate vicinity of the mechanosensitive channel [87, 90, 91]. In this case is unclear whether the true mechanosensor is in fact in the lipid bilayer, or whether these channels are indirectly mechanosensitive.

Eukaryotic Models of Mechanosensation

Insight into the eukaryotic mechanosensitive apparatus has been achieved using both invertebrate and vertebrate models. These models mainly include testing the responses to specific touch stimuli in mutant nematode worms (*Caenorhabditis elegans*) and flies (*Drosophila*), but have also included vertebrates models such as zebrafish (*Danio rerio*) and mouse (*Mus musculus*). These models prove especially useful as mechanosensory information detected by eukaryotes, such as touch hearing and proprioception, are much more complex than that detected by prokaryotes which mainly consists of osmotic regulation [87].

The *C. elegans* model is a relatively simple forward genetic screen where mechanical stress is used to prod the worms and deficiencies are recorded [93, 94]. Mechanical stress ranges from "gentle touch" (prodding the nematode with an eyelash), the nose touch response (further divided into head on collision response and head withdrawal response), the harsh touch response (evident in the absence of gentle touch), the proprioception response (coordination) and tap withdrawal response (retreat in response to tap on culture plate) [94, 95]. Each of these stresses employ a different set of cells and pathways and ablations of these cells or mutations specific to each pathway have been described [94, 95]. As yet over 450 mutations in 18 different genes (mainly labelled *mec* for mechanosensitive) have been identified for the gentle touch stimulus alone [93, 95].

Drosophila is another invertebrate with a rich genetic history. It offers the added ability to perform electrophysiological recordings that are somewhat difficult in *C. elegans*. Mechanosensory cells in *Drosophila* are classified into two types depending on whether they have one to three ciliated dendrites and are supported by accessory cells (type I), or

multiple non ciliated dendrites with no accessory cells (type II) [94, 95]. Type I cells can be further divided into external sensory and chordontal organs. Examples of extrasensory cells include bristle cells, which can be recorded from electrophysiologically, while chordontal examples include Johnstons organ, the fly's hearing receptor [94, 95]. Forward screens of the larva of *Drosophila* using similar techniques as the *C. elegans* coupled with electrophysiological methodology of adult bristle have also uncovered several mechanosensitive genes, including the *unc* and *uncl* (uncoordinated and uncoordinated like), and the *nomp* (no mechanoreceptor potential) and *remp* (reduced mechanoreceptor potential) gene families, of which several have sequence homologies with higher and lower class organisms, such as those of the Degenerin / Epithelial Sodium Channel (DEG/ENaC) and Transient Receptor Potential (TRP) families [94, 95].

The zebrafish model (*Danio rerio*) extends the information garnered from invertebrate models and incorporates it into a relatively simple vertebrate [94, 95]. This model also has two major mechanosensing cells, the Rohon-beard cells and the hair cells. Rohon-Beard cells are embryonic cells that respond to gentle touch along the trunk, and eventually degenerate and are replaced by dorsal root ganglion sensory cells [95]. Forward genetic screens have again been used to identify two phenotypes – circular and touch [95]. Mutants with the circular phenotype swim in circles, and are presumed to have defects in hair cells as upright swimming requires an intact vestibular system [95]. Mutants with the touch phenotype are insensitive to tail touch by a probe, but otherwise swim normally, and are thought to have defective Rohon-Beard cells [95]. Genetic analysis has currently identified over 20 genes in the circular mutants, and three genes in the touch mutants [94, 95].

Putative Mammalian Mechanotransducers

While a plethora of putatively mechanosensory genes have been uncovered from invertebrate models much less is known about mammalian mechanotransduction. This large gap in information stems from a lack of specific antagonists, the costs of generating knock out mice, both monetary and time, and the technical difficulty of most mammalian preparations. Physiological information does not often correlate between mammals and lower organisms, either due to differences in expression patterns, differences in functionality or a lack of mammalian homologues. Despite the potential for setbacks, intense interest in this area has generated several candidates, including ATP gated channels (P_2X), tetrodotoxin resistant Na+ channels ($NaV_{1.8}$, $NaV_{1.9}$), the stretch activated potassium channel *trek*, members of the Deg / ENaC family and members of the TRP family [42, 90, 96, 97]. Members of each of these channels are expressed in small diameter DRG cells and are implicated in mediation of pain sensing. Mice mutated to lack any of these channels demonstrate deficits in specific aspects of mechanotransduction. Mice lacking the P_2X_3 receptor demonstrate reduced bladder emptying, implying stretch activated mechanoreceptors in the bladder are disrupted [97]. Reductions in mechanical activation thresholds have also been observed in $NaV_{1.8}$ (-/-) mice, although it is currently contentious as to whether this results in altered nociception [98-100]. TREK (-/-) mice also demonstrate increased sensitivity to innocuous touch, but not to noxious pressure implying specific deficits in low threshold mechanical stimuli that again may not be nociceptive [90, 96]. The most promising candidates for mediation of colonic mechanotransduction currently are members of the Deg/ENaC family and members of the TRP family.

Degenerin / Epthelial Sodium Channel (DEG / ENaC) Family

Genetic, molecular and electrophysiological studies have recently implicated receptors of the Deg/ENaC family in mechanotransduction. Genetic screening of mutated *C. elegans* with impaired responses to touch initially produced several candidate molecules forming the degenerin family (DEG, UNC and MEC) [95, 101-109]. At present this family comprises over 30 members from various organisms (Figure 4) [110].

Acid Sensing Ion Channels (ASICs)

ASIC channels are H^+ gated channels with varied pH sensitivities and kinetics. To date four separate ASIC genes have been cloned with several splice variants ASIC1 (spliced into ASIC1a and ASIC1b), ASIC2 (spliced into ASIC2a and ASIC2b), ASIC3 and ASIC4 [110, 111]. While this family of ion channels is functionally polymodal and shares little amino acid identity individual subunits share common structural properties consisting of two transmembrane domains (M1 and M2), intracellular carboxyl and amino termini and a large cysteine rich extracellular domain thought to serve as a receptor for external stimuli (Figure 5) [111]. Certain physiological properties are also shared including permeability to Na^+, inhibition by amiloride and lack of voltage gating [112]. ASIC1, 2 and 3 have each been identified in mechanosensory structures and sensory ganglia [113-123], and each has demonstrated mechanosensitivity, although this varies according to tissue and afferent type [78, 114, 124, 125]. ASIC1 has previously been suggested to be the most abundant member of the ASIC family, with the splice variant ASIC1a more prevalent than ASIC1b in DRG, although both are present in small to medium diameter DRG cells [116, 123, 126]. ASIC2a and ASIC2b are also both expressed in DRG and are postulated to be more abundant in medium to large

DRG cells, while ASIC3 has been identified in small, medium and large DRG neurons [114, 116, 118, 121, 123].

While each of the above studies suggest the cell type individual ASIC members are expressed in differs it is important to note ASIC channels are heteromeric in their native state [116, 127-129]. The exact stoichiometry of ASIC channels is currently unknown, and is likely to differ between functional roles and tissue types. There are demonstrated functional differences in tissue types depending on subunit deleted. Specifically deletion of ASIC1a results in substantial increases in sensitivity of visceral but not cutaneous afferents, while deletion of ASIC2 caused afferent type dependant increases or decreases in mechanosensitivity in both visceral and cutaneous afferents, and finally ASIC3 potently decreases mechanosensitivity in visceral afferents while only moderately affecting cutaneous afferents [78, 124, 125]. These experiments demonstrate ASIC3 is the most important member for colonic mechanotransduction, while ASIC1 is more important in the gastrointestinal tract than in skin and ASIC2 more important in skin than the gastrointestinal tract [124, 125].

Stomatin

Recent research in *C. elegans* has identified MEC-2 from the DEG family as a putative intracellular anchor protein for the ASIC complexes linking the ion channel complex to the intracellular membrane [130, 131]. There is high homology between MEC-2 and the vertebrate protein stomatin and stomatin-like protein. These homologues have been identified in DRG neurons where they colocalise with ASIC family members [130-132]. Further, ASIC members are also co-immunoprecipitated with these homologues and they modulate the activity of ASIC members [131, 132]. Finally, mice genetically

altered to lack either stomatin or homologues demonstrate marked deficiencies in mechanotransduction [132, 133].

ENaCs

The ENaC family is comprised of three subunits, α, β and γ, which heteromultimerize to form functional channels. ENaCs are essential for the regulation of Na+ transport, and thus are found in numerous epithelia in organs such as the kidney and colon. However a mechanosensory function has also been postulated as they are identified in sensory ganglia and in specialized mechanosensory structures in the skin and the baroreceptor [134, 135].

Figure 4: Phylogeny tree of Deg/ENaC family. Shown are mammalian, nematode, insect and mollusc subfamilies divided according to amino acid homology. Figure adapted from [110].

Figure 5: Structure of ASIC member. N and C termini are cytoplasmic, with large extracellular domain between the two transmembrane domains. Figure adapted from [111].

Transient Receptor Potential (TRP) Family

Since the discovery of the first TRP channel in the late 1970's and its subsequent cloning in the early 1990's interest in this class of ion channels has intensified [136, 137]. Currently there are 28 mammalian members classified into seven subclasses based on amino acid homology (Figure 6). TRP proteins generally have 6 transmembrane domains with a pore forming loop between domains 5 and 6 (Figure 7 and 8). The N- and C- termini are cytoplasmic and contain a number of additional domains depending on the subfamily, including the "TRP box" of the "TRP domain", a uniquely conserved region at the C-termini within TRPC and TRPM but not TRPV subfamilies, and multiple ankyrin repeats at the N-termini of TRPV, TRPA and TRPC, but not TRPM subfamilies. At present little insight toward function can be gleaned from these two domain types as the role of the TRP box is yet to be determined, and ankyrin repeats are one of the most common protein-protein interactions in nature, found in proteins of diverse function and they do not recognize specific sequences or structural motifs. Functional channels are weakly Ca^{2+} permeable and are formed by tetrameric assembly in either homo or heteromeric fashion [138, 139].

Vanilloid TRPV Family

The vanilloid TRPV subfamily (TRPV) was established with the discovery of TRPV1, as it is activated by the vanilloid capsaicin, the active ingredient in chilli [140]. Subsequent investigations indicated mice genetically engineered to lack this channel have deficiencies in responses to painful stimuli, thereby implicating the TRPV family in nociception [141]. Currently there are six members of the TRPV family, TRPV1 to TRPV6, with TRPV5 and 6 more distantly related to TRPV1 to 4. Functional channels are either homomeric (TRPV1-4) or heteromeric (TRPV5 and 6) tetramers [138, 139].

TRPV4

TRPV4 was cloned shortly following the discovery of TRPV1 [142]. Interest in TRPV4 arose due to its homology with *osm-9*, a mechanically sensitive gene from the invertebrate *c. elegans* family [143]. TRPV4 is expressed in most tissues including kidney, heart, brain, lung, the gastrointestinal tract and sensory tissues such as DRG, nodose ganglia and trigeminal ganglia and also in sites of mechanotransduction including the skin and inner ear [142, 144, 145]. TRPV4 has also been identified in nodose neurons retrogradely labelled from the stomach, providing evidence it is present in sensory neurons innervating the gut [145].

TRPV4 is implicated in detection of mechanical stress generated by cell swelling and shear stress / fluid flow [146-151] . TRPV4 is polymodally gated, like the majority of TRP channels, with agonists including acidic pH, citrate, phorbol esters, anadamide and several of its metabolites and some herbal extracts [140, 146-152]. TRPV4 is also gated by temperature, but it is active at physiological temperatures, unlike TRPV1 and TRPV2 [147]. Despite this polymodality there is persuasive evidence of inherent mechanosensitivity. Mice genetically engineered to lack TRPV4 display abnormal osmotic regulation and abnormal responses to noxious cutaneous pressure and acoustic stress, each implying mechanosensory deficits [149, 153-156]. While the deficit to noxious cutaneous pressure is compelling the response by individual cutaneous afferents is yet to be determined. The results of the above studies suggest TRPV4 is mechano–nociceptive however a more thorough investigation of all afferent classes (with their varying thresholds to mechanical stress) is required before this conclusion is reached.

TRPA1

TRPA1 is the sole mammalian member of the TRPA family. Interest in TRPA1 stemmed from its an ankyrin rich N-terminus, more than other mammalian TRP members and previously only observed in TRPN1, an invertebrate mechano-nociceptive channel [157]. As with TRPV4, expression of TRPA1 is widespread, including in the CNS, spleen, reproductive organs, buccal mucosa and colon [158-161]. TRPA1 has also been identified in sensory neurons, although the abundance is currently controversial and ranges from 5 to 50% of DRG cells [162-167]. Despite this disagreement, it is clear TRPA1 is primarily expressed in small to medium putatively nociceptive neurons (Neurofilament-200 negative; CGRP and substance P positive) [163-165, 167]. TRPA1 is gated by noxious stimuli at sufficient concentrations including allyl isothiocyanate, cinnamaldehyde, gingerol, allicin, eugenol and also by noxious cold temperature [165-172]. TRPA1 may also be coupled with either bradykinin, an inflammatory mediator, or TRPV1. Investigations using mice genetically engineered to lack TRPA1 demonstrate sensitivity to bradykinin is lost without TRPA1 [166, 173]. TRPA1 also commonly colocalizes with TRPV1 in DRG neurons raising the possibility these channels may also be coupled [159, 165, 167]. Several lines of evidence suggest TRPA1 is mechanosensory, including the loss of specific mechanosensory responses in invertebrates such as *C. elegans* and zebrafish when *trpa1* expression is disrupted [174, 175]. Due to a lack of selective antagonists, investigations in higher organisms are limited to mice genetically engineered to lack *trpa1*, where deficits in response to noxious mechanical stimuli in cutaneous afferents are observed while responses to non-noxious mechanical stimuli are unaltered [166, 173]. However, as observed previously with TRPV4, the role of individual afferent subtypes has not been investigated and a more comprehensive investigation is warranted.

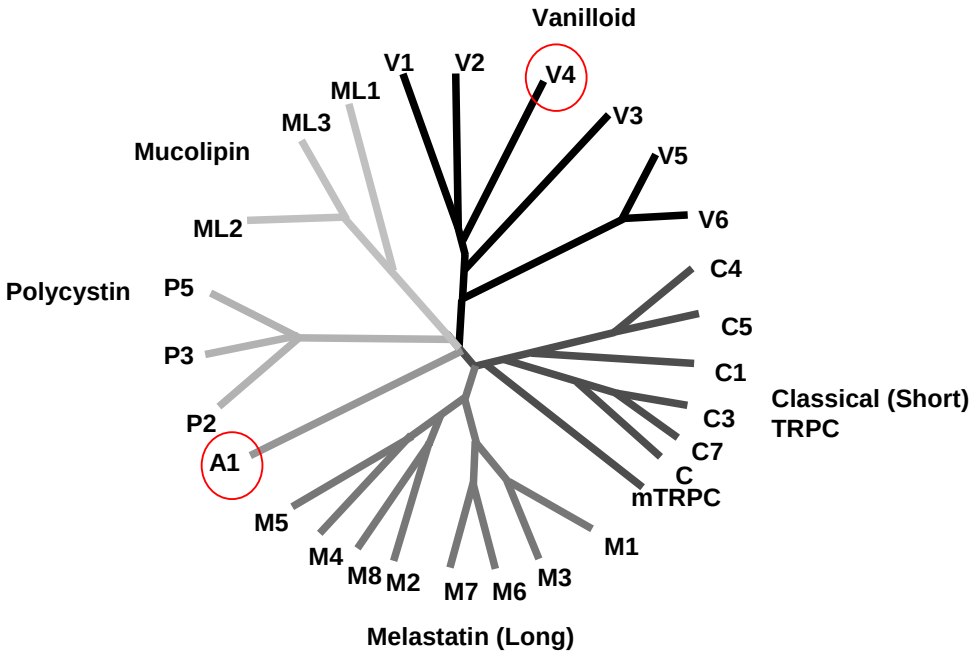

Figure 6: Phylogeny tree of TRP family. Shown are seven subfamilies divided according to amino acid homology. Circled are the TRP channels focused on as part of this PhD. Figure adapted from [157].

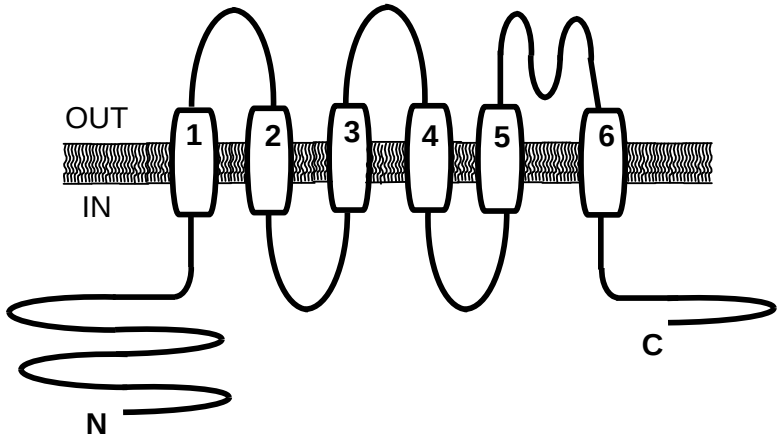

Figure 7: Structure of TRPV4 protein. N and C termini are cytoplasmic, with pore loop between transmembrane domains 5 and 6. Figure adapted from [142].

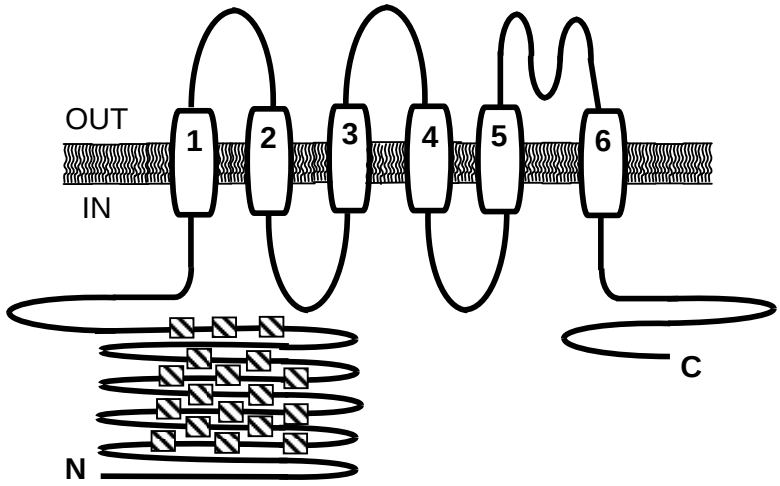

Figure 8: Structure of TRPA1 channel. N and C termini are cytoplasmic, with pore loop between transmembrane domains 5 and 6. Ankyrin repeats are highlighted by N-terminal striped squares. Figure adapted from [176].

CHAPTER 2

SPECIFIC AIMS

Aims

1) To develop and optimize an oligonucleotide based fluorescent in situ hybridization technique for detection of low abundance genes in dorsal root ganglia.

2) To compare the expression of the putative mechanosensitive ion channels ASIC1, 2 and 3, TRPV4 and TRPA1 in whole DRG with that specifically in colonic cells within dorsal root ganglia and gastric cells within nodose ganglia.

Hypothesis: Sensory ganglia are heterogeneous and expression patterns differ depending on viscera innervated and therefore quantification of expression in sensory ganglia as a whole is misleading.

3) To determine the contribution the putatively mechanosensitive ion channels TRPV4 and TRPA1 impart toward colonic mechanosensation mediated by extrinsic spinal afferents.

Hypothesis: TRPV4 and TRPA1 are both mechanosensitive but mediate different aspects of colonic mechanosensation.

CHAPTER 3

OLIGONUCLEOTIDE BASED FLUORESCENCE *IN SITU* HYBRIDIZATION FOR DETECTION OF GENES OF LOW ABUNDANCE

Abstract

In situ hybridization provides the detection of mRNA within morphologically preserved tissue sections. Oligonucleotide probes present an attractive alternative to riboprobe *in situ* hybridizations but have previously lacked sensitivity unless isotopic labels are used. The following describes the optimisation of a protocol for *in situ* hybridization using non-isotopically labelled oligonucleotide probes for the detection of genes of low abundance. Signal amplification is required for detection of these genes, and was provided through the use of tyramide based catalysed reporter deposition (CARD). It is expected this protocol will be able to be used to detect any given gene so long as the characteristics of the oligonucleotide probes outlined in this chapter are adhered to.

Introduction

In the post genome era it is becoming increasingly important to determine not only in which tissues specific genes are found, but also in which cell type within these tissues. This requires studies where tissue morphology is conserved, precluding the use of molecular techniques such as PCR and microarray. *In situ* hybridization (ISH) is an attractive alternative to these techniques as it identifies the cellular localisation of specific nucleic acid sequences in morphologically preserved tissue sections. ISH involves the targeting of a specific genetic sequence of interest by a nucleic acid probe. The probe is labelled by various means providing at minimum semi-quantitative detection. This provides not only information about the expression of the target sequence, as in PCR, but also the cells it is found in, and can also be used to provide information about relationships within or between cells. ISH was originally developed independently by two separate groups in 1969 and has transformed from an unwieldy technique confined to expression of limited targets of high expression to an extremely sensitive procedure a conventional laboratory can use to detect single copy sequences [177, 178]. ISH is especially powerful when combined with complementary techniques whereby specific mRNA species can be detected in distinct subsets of cells such as those traced from individual tissues (nerve tract tracing), with other mRNA species (in combination with laser microdissection and PCR / microarray), or with proteins (immunohistochemistry). As ISH directly targets nucleic acid sequences it may also prove to be more specific than immunohistochemistry, particularly when investigating newly discovered sequences where commercial antibodies are either non-existent or unreliable. The aim of these experiments is to generate a highly sensitive ISH protocol that is readily accessible for use in a conventional laboratory setting.

The fundamental decisions that must be made before attempting ISH experiments are the choice of probe and the detection technique to be used. These choices are made bearing in mind the sensitivity required, whether the protocol will be combined with others (such as nerve tract tracing) and the equipment required for probe production and detection.

Probe Design

The choice of probe is at the foundation of ISH and greatly influences the protocol used. It is essential to design a probe that is specific for the gene of interest. There are two quite different types of probe commonly used, riboprobes and oligonucleotide probes. Riboprobe production involves isolation of the gene of interest, cloning it into a vector to produce large quantities and finally purification of the single stranded cRNA probe for use on the tissue of interest. This time-consuming technique requires detailed molecular knowledge and therefore these probes are most commonly produced in-house. Oligonucleotide probes are much shorter single stranded cDNA probes based on published sequences. They are economically produced by commercial suppliers using DNA synthesizers. As oligonucleotide probes are cDNA they are inherently more stable than riboprobes as they are not susceptible to degradation by RNAse enzymes. The shorter length of oligonucleotide probes allows them to target members within genetic families that have high homology between their members. This is generally more difficult with the longer riboprobes, which typically overlap across conserved regions. While it is generally presumed riboprobes are the more sensitive of the two probe types, recent improvements in detection techniques, as outlined below, have resolved this problem [179, 180]. Oligonucleotide probe-based *in situ* hybridization therefore offers an attractive alternative to the more commonly used riboprobe-based *in situ* hybridization.

Oligonucleotide probes are constructed to be antisense to a specific segment of the targeted gene. Databases, such as those provided by the National Centre for Biotechnology Information (NCBI), are used to compare the sequence of the target gene against all other known sequences in order to find these specific segments. Certain characteristics must then be conformed to when designing the probe, such as length, percentage of guanine (G) and cytosine (C) nucleotides, and the number of certain nucleotides in a row. The complementary sense probe is often used as a negative control and must also be compared against the database to ensure it does not match known sequences. The characteristics of the probe determine its melting temperature, and therefore the temperature at which the hybridization and following stringency washes will be carried out. The melting temperature (T_m) is the temperature at which 50% of an oligonucleotide probe and its perfect complement are in duplex. As observed in the following formula, T_m is governed by the length of the probe (n) and the percentage of G and C nucleotides as the concentration of sodium ions and the percentage of formamide are constant. It is important to note that T_m is reduced by approximately 1.4°C for every 1% of probe mismatch. In general hybridizations are carried out at 5-15°C lower than the melting temperature of the probe.

$$Tm = 81.5+ 16.6 (\log Na+) + 0.41(\%GC) -0.61(\%formamide)– (500/n)$$

nb:1XSSC=195mM Na^+

Probe Labelling and Detection

In order to visualize the probe it must be labelled. There are several choices for labelling the probe, requiring decisions based on the sensitivity and morphology required and the instrumentation available for detection. In the earlier days of ISH,

probes were labelled randomly with radioisotopes that were detected autoradiographically. While these labels generally work very well and are still in use today, limitations within the technique motivated development of non-isotopic labels. These labels result in the deposition of either fluorescent or colorimetric reaction products. Non-isotopic labels are not only more stable (an inherent problem with isotopically labelled probes), but also take much less time to develop, are safer to use and produce better morphology than isotopic labels which tend to produce a non-specific scatter across the tissue. While it is agreed that isotopically labelled probes offer greater sensitivity than their non-isotopic counterparts, the improved detection techniques outlined below and hinted at in the oligonucleotide vs riboprobe discussion are again valid here [180].

Non-isotopic probes incorporate either a direct label into the probe or bind a hapten molecule that is able to be further amplified to increase sensitivity. The label or hapten are added using either enzymatic addition or chemical modification, both of which have been significantly improved upon since they were first published in the early 1980's. Direct detection methods would not provide the sensitivity required for detection of low abundance genes and were not attempted. Haptens are incomplete antigens that react with specific antibodies (or secondary reporter molecules) to amplify signals. Common haptens include digoxigenin (DIG), a steroid that occurs naturally in only a select plant type, and biotin, a water soluble B vitamin. All probes used in this protocol are labelled with DIG, as it does not naturally occur in mammals and non-specific staining will therefore be limited. In this case all probes were purchased pre-labelled by GeneDetect, however there are kits available that allow probe labelling to be performed easily in the laboratory, such as the oligonucleotide tailing kit from Roche.

Three different detection techniques were used in working up the ISH protocol. These ranged from low sensitivity (anti-DIG rhodamine conjugated Fab fragments (Roche)), medium sensitivity (anti-DIG alkaline phosphatase (AP) conjugated Fab fragments (Roche)) and high sensitivity (anti-DIG horse radish-peroxidase (HRP) conjugated Fab fragments combined with tyramide based catalysed reporter deposition (CARD) amplification (Perkin Elmer)). Sensitivity is achieved by increasing the number of rounds of amplification of the signal (Figure 1).

The least sensitive of the indirect approaches, anti-DIG rhodamine, undergoes no amplification and is able to be observed using a fluorescent microscope with filters attached to allow excitation at 555nm and emission at 580nm (Figure 1). The anti-DIG AP antibody permits a single round of amplification, and when nitro blue tetrazolium chloride / 5-Bromo-4-chloro-3-indolylphosphate (NBT/BCIP) solution is added a dark blue / brown precipitate is visible under light microscopy (Figure 1). The tyramide based CARD detection system was first developed for signal amplification in immunoblotting and ELISA assays, and has since successfully been adapted for detection of cellular mRNA [179-185]. This approach increases the amplification of the signal via several amplification rounds (Figure 1). Firstly anti-DIG HRP binds to the DIG labelled probe. The HRP then catalyses the deposition of tyramide radicals to tyrosine moieties of proteins in the vicinity of the site of synthesis. These tyramide radicals are conjugated with biotin, which is then used to bind streptavidin conjugated fluorescent reporters. The fluorophore used in this case is Alexa Fluor 546 which has emission (556nm) and excitation (573nm) maxima similar to the anti-DIG rhodamine used previously.

Preservation of mRNA and Tissue Morphology

mRNA is extremely labile, mainly due to the presence of endogenous RNAse enzymes. These enzymes are very stable and able to withstand temperatures above 100°C. In order to remove RNAses all chemicals must be molecular grade (free from DNAse and RNAse), and solutions and equipment used treated with diethylpyrocarbonate (DEPC) and autoclaved.

Fixation of tissue is important not only to preserve mRNA integrity, but also to preserve tissue morphology. It is important that the morphology is preserved in this protocol as it is envisioned it will be combined with other labelling techniques such as nerve tract tracing. A range of fixatives are available and each must be used with care as overfixation may lead to issues of tissue and mRNA degredation and / or autofluorescence. Four conditions were compared in this protocol – no fixation, ethanol post-fixation, 4% paraformaldehyde perfusion fixation, and 4% paraformaldehyde perfusion fixation followed by post-fixation in the same solution

After choices of fixation, probe type and detection technique have been made there are several steps within the protocol itself that must be optimised in order to produce a protocol of highest sensitivity. As hybridizations must be performed in order to make these decisions, they are outlined below with the relevant experimental conditions.

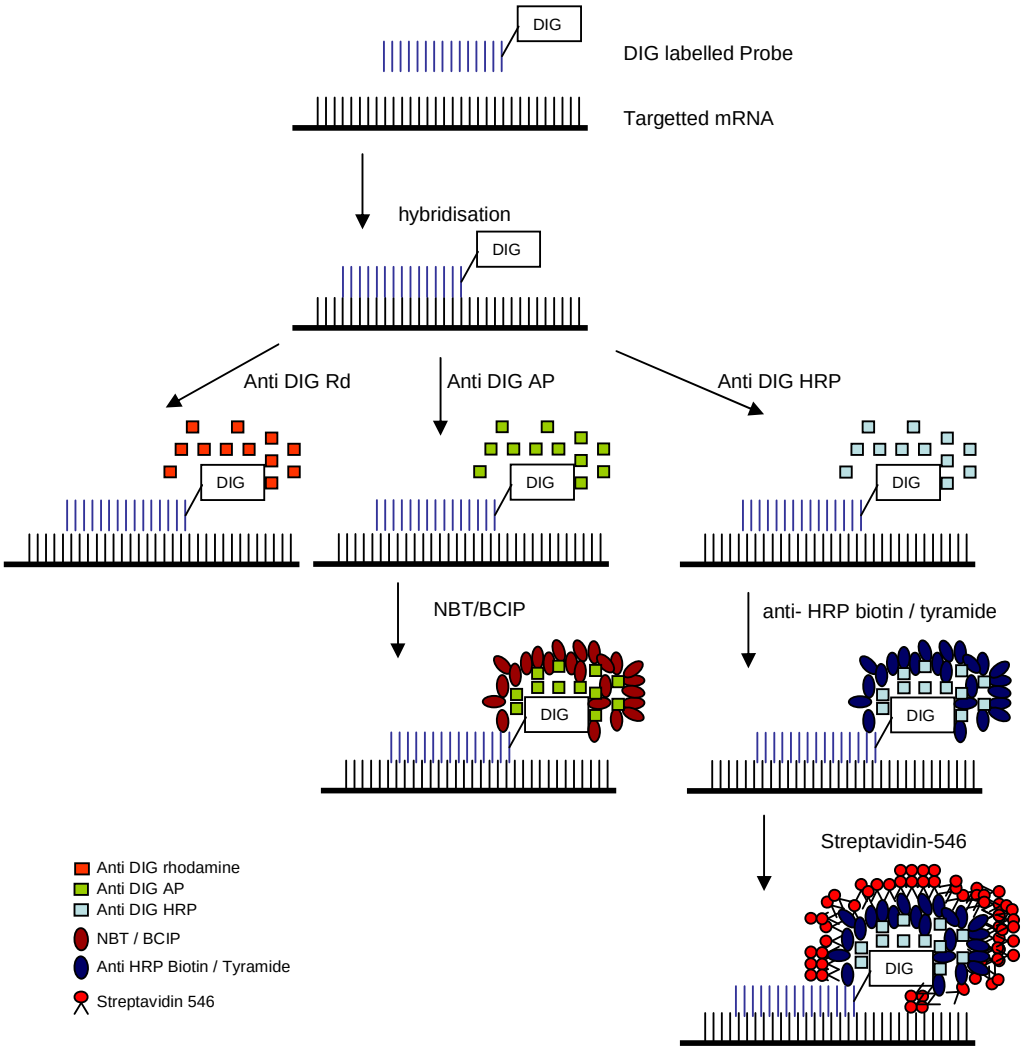

Figure 1: Detection of probe by anti-DIG Rhodamine, anti-DIG AP or CARD methods. Signal strength is increased in each method by increasing the number of rounds of amplification.

Target

It was decided that members of the Acid Sensing Ion Channel (ASIC) were the first ion channels to be targeted, as electrophysiological and molecular studies have demonstrated their presence in dorsal root ganglion (DRG) cells [125]. ASIC3 mRNA was the first choice of the ASIC family to pursue as ASIC1 contains splice variants known to be present in the DRG, and ASIC2 was thought to be too abundant to use as a signal for working up the ISH protocol.

Aim

The aim of the following experiments is to optimise the use of digoxigenin labelled oligonucleotide probes for *in situ* hybridization of low copy number genes in dorsal root ganglion cells and seeks to resolve issues of fixation, probe characteristics and method of detection.

Methodology

All solutions were made using molecular grade reagents where available. All solutions and equipment were treated with 0.1% diethylpyrocarbonate (DEPC) (Sigma, USA) and autoclaved wherever possible. All washes were at room temperature unless stated.

Ethics

All experiments were performed in accordance with the guidelines of the Animal Ethics Committees of the Institute for Medical and Veterinary Science and the University of Adelaide, Adelaide, Australia.

In situ Hybridization

Tissue Processing

Mice that were not perfused were killed via CO_2 inhalation and cervical dislocation. Mice that were perfused were first deeply anaesthetised with Nembutal (100mg/kg Virbac Animal Health, Australia). Transcardial perfusion was then performed with warm sterile heparinized saline followed by ice cold 4% paraformaldehyde (pH 7.4). In both cases DRG from thoracolumbar vertebral levels (T10-L1) were removed bilaterally using the costae fluctuantes as an anatomical guide. These DRG were then pooled and transferred to 20% sucrose solution until sunk at room temperature. The sucrose was then removed, and the ganglia snap frozen in Tissue-Tek O.C.T. embedding medium (Sakura Finetek, Japan) by brief immersion in liquid nitrogen cooled isopentane (-30°C) and either processed immediately or stored for a maximum of two days at -80°C.

Prehybridization

Serial frozen sections (12μm) were cut through the whole tissue block at -20°C and thaw mounted onto Superfrost + slides (Menzel-Glaser, Germany). The tissue sections were then subjected to either ethanol or 4% PFA post fixation where applicable and air-dried for one hour at room temperature in a sterile environment. The sections were then rehydrated and endogenous biotin blocked using 0.3% H_2O_2 / 0.1M phosphate buffer for 10 minutes if the CARD amplification technique was to be used. They were then acetylated (freshly prepared 0.1M triethanolamine (Sigma, USA) pH 8 (HCl) / 0.25% acetic anhydride (Sigma, USA)) for a further 10 minutes before being equilibrated in 5X SSC (saline sodium citrate buffer).

Sections were prehybridised with 100μl hybridization buffer, coverslipped with parafilm and placed in an airtight moist hybridization container for two hours at 37°C. The hybridization buffer solution consisted of 50% formamide (Sigma, USA)), 250μg/ml bakers yeast tRNA type X (Sigma, USA), 250μg/ml salmon sperm DNA (Sigma, USA), 1% Denhardts solution (1% each bovine serum albumin, polyvinylpyrolidone and ficoll) (Sigma), 10mg/ml poly(a) (Roche, USA), 5X SSC, and 20% dextran sulphate (Sigma).

Probes and Hybridization

All probes were obtained from GeneDetect (New Zealand) already labelled with DIG (3′ Greenstar). The specificity of each probe was compared against all other known sequences using the BLAST program (NCBI) prior to use. Table 1 outlines the characteristics of each probe. Each probe was serially diluted for optimization of signal. Negative controls included the complementary sense strand at the same dilution as the

antisense probe, removal of probe from the hybridization buffer and the use of unlabelled probe in excess concentration in an attempt to outcompete labelled probe

Probe was dissolved in hybridization buffer and applied to sections (100 µl / slide) that were then coverslipped with parafilm and hybridised overnight in an airtight moist hybridization chamber at 37°C. Following hybridization, the parafilm was floated off in 5XSSC and the sections were washed firstly in 1XSSC, then 0.5XSSC for 30 minutes each at temperatures from 50-60°C. They were then equilibrated to room temperature in 0.5XSSC. Note that the characteristics of the probe used to detect all mRNA is unusual in that it does not contain G or C nucleotides, and consequently has a much lower melting temperature than the other probes. Therefore hybridization and stringency washes were both carried out at room temperature when this probe was used.

Detection of DIG-Labelled Hybrids

Several detection techniques were assessed in order to determine the sensitivity required for the use of oligonucleotide probes. These ranged from low sensitivity (anti-DIG Rhodamine Fab fragments (Roche, USA)), medium sensitivity (anti-DIG alkaline phosphatase (AP) Fab fragments (Roche) followed by Nitro blue tetrazolium chloride / 5-Bromo-4-chloro-3-indolylphosphate (NBT/BCIP) (Sigma, USA), and high sensitivity (tyramide based catalysed reporter deposition (CARD) (Perkin-Elmer, USA)).

Detection Using Anti-DIG Rhodamine

The slides were equilibrated in Tris buffered saline (TBS) and incubated firstly in blocking solution (Perkin-Elmer, USA) for 30 minutes then anti-DIG rhodamine

conjugated Fab fragments at a dilution of 1:200 in blocking solution overnight at 4°C. Slides were then washed in TBS and readied for coverslipping.

Detection Using anti-DIG-AP

The slides were equilibrated in TBS and incubated firstly in blocking solution (Perkin-Elmer, USA) for 30 minutes then anti-DIG AP conjugated Fab fragments at a dilution of 1:200 in blocking buffer overnight at 4°C. Slides were then washed in TBS and the AP precipitant detected using NBT/BCIP solution and readied for coverslipping.

Probe target	gene	sequence (5' to 3')	antisense to	% homology in mouse	% GC	melting temp
ASIC3	*ACCN3*	CCGCTCAGCCACCTGGTAGAGGAAGGCCGCCAGCGACAGGAGTACAGC	406-453	100	66	68
NaV 1.8	*SCN10a*	TTCCCTGGGGAGTGACACGCCATCCTCCTCAGCCCTGGGCACATGCAG	5629-5676	100	64	67
β-actin	*actb*	GCCGATCCACACGGAGTACTTGCGCTCAGGAGGAGCAATGATCTTGAT	1059-1105	97 (47/48)	54	63
mRNA		Poly d(t) 48 mer - binds to poly (a) tail	poly a tail	100	0	40
nonsense		CCTCCCATCCGGTAGAACACTAGAGACATGTGGGTTTTGCGTCTTTAC		0	50	61

Table 1: Characteristics of probes used for *in situ* hybridization work up.

Detection Using CARD

The slides were equilibrated in TBS and incubated firstly in blocking solution (Perkin-Elmer, USA) for 30 min then anti-DIG horse radish peroxidase (HRP) conjugated Fab fragments (Roche, USA) at dilutions of 1:50 to 1:200 in blocking solution for a further 30 minutes. The slides were then incubated for 20 minutes in biotin labelled tyramide (Perkin Elmer, USA) diluted 1:50 in the amplification buffer, before being incubated with Alexa Fluor 546 at 1:50 to 1:800 in blocking solution for 50 minutes. Slides were then washed in TBS and readied for coverslipping.

Sections were either coverslipped with buffered glycerol for colorimetric detection or coverslipped with Prolong antifade (Invitrogen, USA) for fluorescent detection to prevent photo-bleaching. They were then screened under an epifluorescent microscope (Olympus BX51) using either light microscopic conditions or the appropriate filter for rhodamine and SA546.

A number of controls were built into the study design to ensure the results obtained are accurate and reproducible. In the case of fluorescent detection camera exposure times were optimised for positively labelled neurons, and these same times were used across all negative control slides (sense probes and unlabelled probes). Serial sections were used with alternating antisense probe and negative controls. Postitive labelling was identified by the clear presence of cytoplasmic labelling at an intensity above that in the adjacent negative control tissue, both visually and by spot intensity measurements. Image control, including brightness and contrast levels are consistent within experiments.

Results

Fixation

Considerable morphological losses resulted from using either unfixed tissue or a light ethanol fix. A substantial improvement was observed when the 4% PFA solution was perfused, which was further enhanced with 4% PFA post-fixation. No increases in autofluorescence were observed using 4% PFA post-fixation making this the protocol of choice.

Detection of mRNA

The first experiments performed were designed to determine whether mRNA could be detected in dorsal root ganglia (DRG) using oligonucleotide probes. The probe against mRNA was combined with the anti-DIG rhodamine detection technique. The presence of mRNA is clearly demonstrated in Figure 2, where the negative control has probe omitted from the hybridization buffer.

Once it was demonstrated mRNA could be detected, experiments were performed to determine whether mRNA is degraded at -80°C and therefore the length of time sections can be stored. This involved using the mRNA probe combined with Anti-DIG AP and using NBT/BCIP for detection. As the time taken for precipitation of the reaction product is indicative of mRNA quality, it was used to assess the effect of changes in protocol. Tissue sections were cut onto slides and stored at -80°C for up to two weeks. It was found that storage longer than 96 hours had a detrimental effect on mRNA quality. While this does not directly indicate ASIC3 mRNA has degraded, it does imply total mRNA deteriorates over time, even when stored at -80°C, and as ion channels

generally have low copy number it is presumed they would also degrade. Therefore whenever possible hybridizations were performed on the same day as dissection or tissue was stored in snap frozen blocks for a maximum of 48 hours.

Detection of β-actin

The next gene to be identified was β-actin, a structural housekeeping gene present in all cells and therefore commonly used as a positive control in molecular studies. The hybridization was carried out at 37°C, stringency washes at 50°C and detection performed using CARD amplification. It should be possible to detect β-actin using detection techniques of lower sensitivity than the CARD amplification, but as ASIC3 would require high sensitivity it was necessary to keep as much of the protocol constant as possible. β-actin was observed in cells in thoracolumbar DRG and the observed signal is decreased either when the probe is diluted or when unlabelled probe is added in excess indicating the probe is specific for β-actin (Figure 3).

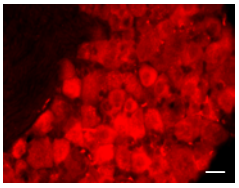

mRNA probe

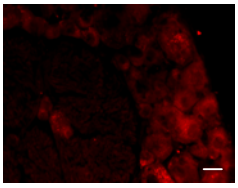

Negative control (no probe)

Figure 2: mRNA detection in dorsal root ganglion cells. The DIG labelled probe is targeted to poly (A) tails, present on all mRNA sequences. Detection is via anti-DIG rhodamine. Probe is omitted from the hybridisation buffer for the negative control. Scale bar denotes 25μm.

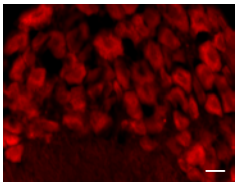

Antisense β-actin (1:200)

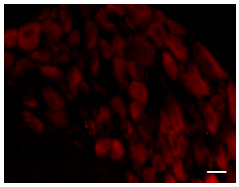

Antisense β-actin (1:800)

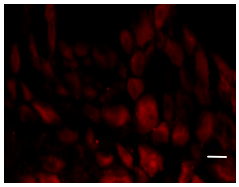

Excess unlabelled β-actin

Figure 3: Successful detection of β-actin with CARD amplification. Dilution of probe lower than 1:200 substantially reduced the amount of signal observed, and the labelled antisense probe was successfully outcompeted by the addition of excess unlabelled β-actin probe to the hybridisation buffer indicating the signal is specific for the β-actin probe. Scale bar denotes 25μm.

Detection of ASIC3

The ASIC3 probe was initially hybridised at 37°C, washed at 50°C and detected using CARD amplification**.** ASIC3 mRNA transcripts were observed under these conditions, however when unlabelled nonsense probe was added in excess with the ASIC3 probe the amount of signal observed decreased (Figure 4). The nonsense probe has no homology with any known sequences and is therefore useful as a negative control as it provides information about the specificity of the probe and stringency of the hybridization. If the stringency is not high enough, such as in this case, the nonsense probe competes successfully for binding sites, and as it is unlabelled the amount of signal observed decreases. This indicates the ASIC3 probe is binding non-specifically to the tissue and stringency must therefore be increased.

In order to increase the stringency it was decided to maintain hybridization at 37°C, but increase the temperature of the following SSC washes by 5°C to 55°C. The signal achieved for ASIC3 mRNA was again observed to be greater than negative controls, in this case the DIG labelled sense probe (Figure 5). As a further control unlabelled ASIC3 probe was added in excess with DIG labelled ASIC3, and the amount of signal decreased, indicating the signal is specific for the ASIC3 probe (Figure 5). Attempts were also made at this temperature with the β-actin probe, but no signal was observed suggesting the stringency was too high. Unfortunately this also means the nonsense probe would be of no use at this temperature as it has similar T_m as the β-actin probe. In order to optimise the stringency washes, the temperature was again increased 5°C to 60°C. This resulted in decreased signal observed when compared to the negative controls, indicating conditions are too stringent for the ASIC3 probe (results not shown). The optimal conditions for the ASIC3 probe are hybridization at 37°C followed by stringency washes in 1X and 0.5X SSC at 55°C.

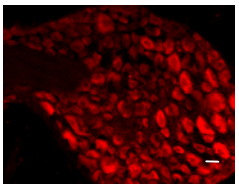

ASIC3

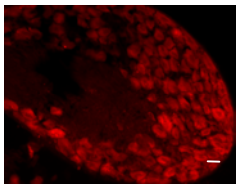

ASIC3 + nonsense

Figure 4: Unlabelled nonsense probe successfully outcompetes ASIC3 when stringency washes are carried out at 50°C. The signal observed from the ASIC3 probe is greatly decreased when unlabelled nonsense probe is added in excess, indicating the ASIC3 probe is binding non-specifically at this temperature. Scale bar denotes 25μm.

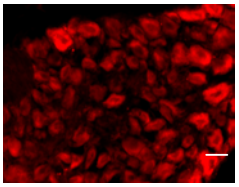

ASIC3

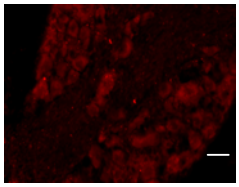

ASIC3 Sense

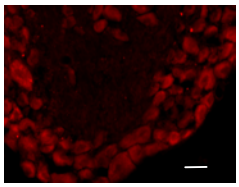

ASIC3 unlabelled

Figure 5: The signal generated by the ASIC3 probe is specific for ASIC3 when stringency temperatures of 55°C are used. The amount of signal generated by the antisense probe is much greater than that observed when the complementary sense probe is used, and also is successfully outcompeted by excess unlabelled ASIC3 probe. Scale bar denotes 25μm.

Optimisation of the CARD Detection Technique

CARD amplification can result in non-specific binding, and serial probe dilutions were therefore performed with both antisense and sense probes in order to maximise the signal to noise ratio. As this is a function of the probe rather than the tissue, it must be performed each time a new probe is purchased. Dilutions of the ASIC3 probe from 1:200 to 1:1600 were performed and optimal conditions were achieved at 1:400 for the ASIC3 probe (Figure 6). Concentrations above this resulted in non-specific scatter across the slide, while those lower resulted in loss of signal.

In an attempt to further increase the signal to noise ratio, and in particular to determine which stage of the assay produced the most noise, each step in the CARD protocol was optimised. Firstly the anti-DIG HRP complex and the fluorophore conjugated complex (SA546) were separately serially diluted. The optimal dilution of anti-DIG HRP was observed to be 1:100, while the SA546 was 1:200 (Figure 7 and results not shown). The biotin/tyramide reaction was also optimised and as this is a time dependent reaction two incubation times were used, 10 (manufacturers recommendations) and 20 minutes. No increases in non specific binding were observed when the slides were incubated for 20 minutes (results not shown). The anti-DIG HRP step produced the greatest amount of noise, which is not surprising as it is most closely related to probe concentration.

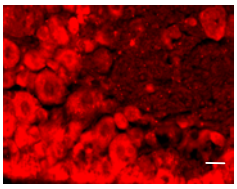

ASIC3 1:200

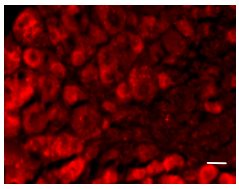

ASIC3 1:400

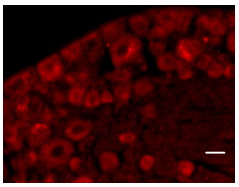

ASIC3 1:1600

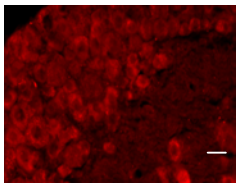

ASIC3 sense (1:400)

Figure 6: Optimisation of ASIC3 probe concentration for use with CARD amplification. A dilution of 1:400 was found to be optimal. Scale bar denotes 25µm.

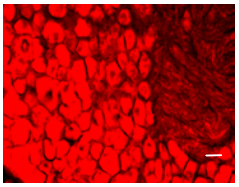

1:50

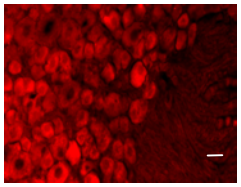

1:100

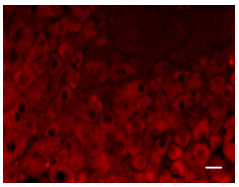

1:200

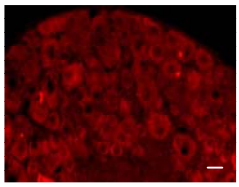

no probe

Figure 7: Optimisation of Anti-DIG HRP dilutions for use with CARD amplification. A dilution of 1:100 was found to be optimal. Scale bar denotes 25µm.

Confirmation of Specificity

In order to confirm the protocol works for targets other than ASIC3, it was essential to validate it with genes of similar physiology. $NaV_{1.8}$ is a sodium channel known to be expressed in a specific population of DRG cells [186]. A probe against $NaV_{1.8}$ was purchased DIG labelled from GeneDetect and was designed to have similar characteristics to the ASIC3 probe (T_m of 67°C and 68°C respectively (see Table 1)). As demonstrated in Figure 8, positive labelling was observed when the antisense $NaV_{1.8}$ was used, and no labelling was observed when this was outcompeted by excess labelled probe or when the sense probe was used.

The availability of null mutant mice lacking the ASIC3 gene in the laboratory provided an opportunity further validation of this protocol. PCR of the ASIC3 gene previously demonstrated the absence of this transcript in these mice [125]. As the T_m of both the ASIC3 probe and the $NaV_{1.8}$ probe are similar it was possible to use them in serial sections with the same protocol. Figure 8 clearly demonstrates the absence of ASIC3 mRNA and the presence of $NaV_{1.8}$ mRNA in these mice.

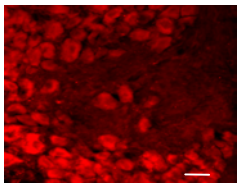

NaV 1.8

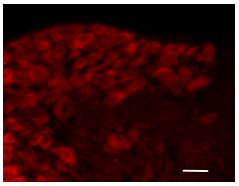

NaV 1.8 sense

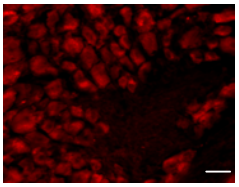

NaV 1.8 unlabelled

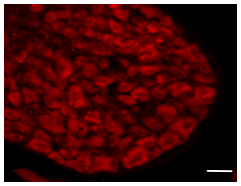

ASIC3

Figure 8: *In situ* hybridization against $NaV_{1.8}$ or ASIC3 in ASIC3 null mutant mice (-/-). A specific signal is observed when the antisense $NaV_{1.8}$ probe is used in DRG sections. No signal is observed for ASIC3 in mice lacking the ASIC3 gene, further validating the in situ protocol. Scale bar denotes 25μm.

Discussion

The aim of these experiments was to design and optimise a sensitive oligonucleotide based *in situ* hybridization (ISH) technique that was able to be detected non-isotopically. Oligonucleotide probes represent an attractive alternative to the more cumbersome riboprobe method of ISH, but until recently lacked the sensitivity required for detection of genes of low abundance without the use of isotopic labels. However the development of detection methodology which utilizes several rounds of amplification, such as CARD, greatly increases the signal generated by non-istopic labels, providing the sensitivity needed for oligonucleotide probes to detect genes of low abundance. While this protocol is designed to be used on mouse DRG it is expected it will be able to be used with little change to detect targeted mRNA in various tissue types across species.

Hybridization conditions are determined by the characteristics of the probe, and therefore as long as oligonucleotide probes are designed with similar melting points this protocol may be used. To encourage the maximum amount of binding possible, it was decided to use a relatively low hybridization temperature (37°C) and remove non-specific binding by using stringent washing conditions immediately after the hybridization. The stringency of these washes is determined by the salt concentration and also the temperatures used. An example of the difference probe melting points can make is the loss of detection of β-actin using stringency washes of 55°C, and the non-specific binding by the ASIC3 probe when stringency washes of 50°C were used. It is intuitive that the stringency would have to be lower for the β-actin probe despite its abundance as not only does it have a lower melting point than the ASIC3 probe but there is also a 3% mismatch in probe homology, further reducing the melting temperature available for binding to this gene.

The use of CARD amplification is an essential component of this protocol, as detection methods of less sensitivity did not provide sufficient labelling. However the use of CARD amplification is not straightforward and introduces several parameters which must be addressed. Most importantly is the issue of probe concentration, which is typically at least 10 fold less than when unamplified protocols are used [180, 187]. As this is a function of probe rather than tissue or cell type, each probe used must be serially diluted to determine the optimum signal to noise ratio before routine use. Optimisation of the CARD detection steps were also performed in this protocol. The issues involved in optimisation of these steps are more likely to be related to tissue or gene targeted than probe concentration. As the CARD technique is used exclusively for detection of lowly abundant mRNA, it is unlikely these steps would require alteration. However if probe dilution does not result in reduction of non-specific staining, dilution of the anti-DIG HRP would be the most likely next step.

Tissue fixation is an important component of the protocol as it acts to conserve mRNA and tissue morphology. However overfixation through use of a strong fixative can lead to cross linking of mRNA strands and prevent the probe binding to its target sequence. While proteinase treatment can resolve these issues somewhat, it can also lead to degradation of mRNA and tissue. An advantage of oligonucleotide probes is their small size, facilitating access to target sequences. Nonetheless proteinase treatment was trialled in this protocol (proteinase K., Sigma, USA) in an effort to determine whether the signal could be bolstered, without success (results not shown). However proteinase treatment is often necessary if paraffin embedded tissue or riboprobes are used and can potentially damage the integrity of the mRNA investigated.

Background autofluorescence is also present in a small number of cells per section, as identified by the use of filters outside of the range of emission and excitation spectra of SA-546. The use of fluorophores with long wavelengths, such as SA546, have been reported to minimize the effects of autofluorescence, yet it is not completely removed [188]. The autofluorescence observed is most likely due to endogenous tissue constituents rather than the probe, as it is observed on the negative control sections where probe is not added. A number of additional techniques were attempted to abolish the autofluorescence, including sodium borohydride, but these were found to also dampen the strength of signal emitted from positively stained cells (results not shown). It is likely that the amount of autofluorescence observed within tissue sections is dependant on tissue type, and the use of these techniques may have to be reassessed if alternate tissue is to be used. While the number of autofluorescent cells is negligible they must be taken into account in order to achieve an accurate determination of the abundance of signal when quantification of positive cells is to be attempted.

This protocol provides a relatively straightforward and rapid means of detecting mRNA of low abundance in morphologically preserved tissue. Oligonucleotide probes have several advantages over the more established riboprobes in that they are much easier to use and able to be economically purchased from any number of commercial enterprises. The use of the CARD system with non-isotopic labels not only increases safety, but also greatly reduces the time needed to complete an experiment without compromising sensitivity. This protocol is now validated for genes of low abundance, and in the following chapters will be used to identify members of the ASIC and TRP family in dorsal root ganglion cells.

CHAPTER 4

LOCALISATION AND COMPARATIVE ANALYSIS OF ACID-SENSING ION CHANNEL (ASIC1, 2, AND 3) MRNA EXPRESSION IN MOUSE COLONIC SENSORY NEURONS WITHIN THORACOLUMBAR DORSAL ROOT GANGLIA.

Abstract

Reducing colonic mechanosensitivity is an important potential strategy for reducing visceral pain. Mice lacking Acid Sensing Ion Channels ASIC1, 2 & 3 show altered colonic mechanosensory function, implicating ASICs in the mechanotransduction process. Deletion of ASICs affects mechanotransduction in visceral and cutaneous afferents differently, suggesting differential expression. We determined relative expression of ASIC1, 2 & 3 in mouse thoracolumbar dorsal root ganglia (DRG) by quantitative RT-PCR analysis (QPCR) and specifically in retrogradely traced colonic neurons isolated via laser capture microdissection. Localisation of ASIC expression in thoracolumbar (T10-L1) and lumbosacral (L6-S1) DRG was determined using fluorescence *in situ* hybridization (FISH) and retrograde tracing. QPCR of whole thoracolumbar DRG revealed abundance of ASIC2 > ASIC1 > ASIC3. Similarly, FISH of all neurons in thoracolumbar DRG demonstrated ASIC2 was expressed in the most (40 ± 1%) neurons, followed by ASIC3 (24 ± 1%) then ASIC1 (18 ± 1%) Analysis of lumbosacral DRG revealed ASIC3 to be in similar abundance (23 ± 1%) to the thoracolumbar DRG. Retrograde tracing from the distal colon labelled 4 ± 1% of neurons in T10-L1 DRG and 2 ± 0.3% of neurons in L6-S1 DRG. In contrast to whole DRG, FISH of colonic neurons showed ASIC3 expression in 73 ± 2%, ASIC2 in 47 ± 0.5% and ASIC1 in 30 ± 2% in thoracolumbar DRG. ASIC3 was also highly expressed in lumbosacral DRG neurons (60 ± 4%). QPCR of laser captured colonic neurons revealed that ASIC3 was the most abundant ASIC transcript, followed by ASIC1 then ASIC2. We conclude that ASIC1, 2 &3 are expressed preferentially in colonic neurons within thoracolumbar DRG, and ASIC3 is also preferentially expressed in lumbosacral colonic DRG neurons. In particular ASIC3, the least abundant in the general population, is the most abundant ASIC transcript in colonic neurons. The prevalence of ASIC3 in neurons innervating the colon supports electrophysiological data showing it makes a

major contribution to colonic mechanotransduction and therefore may be a target for the treatment of visceral pain.

Introduction

Mechanotransduction plays a fundamental role in determining how organisms respond to their environment, both external and internal. Mechanical stimuli in the gastrointestinal tract such as colorectal distension induce peristalsis and defecation, and lead to sensations of urgency, cramping and severe pain in pathophysiological conditions [2, 7, 12]. Irritable bowel syndrome (IBS) is one of the most prevalent gut disorders, affecting approximately 10% of the population**,** and is characterised by hypersensitivity to distension of the colon or rectum [2, 7]. Current evidence suggests hypersensitivity may be due to altered peripheral mechanosensory mechanisms [27, 28].

While the molecular nature of mechanotransduction is yet to be conclusively elucidated, several lead molecules have been identified, including members of the Acid Sensing Ion Channel (ASIC) family. ASICs are members of the degenerin / epithelial sodium channel (DEG/ENaC) family. Four ASIC genes have so far been cloned in mammals; ASIC1, with splice variants ASIC1a and 1b [113, 126], ASIC2 with splice variants ASIC2a and 2b [114, 131, 189, 190], ASIC3 [113, 191, 192] and ASIC4 [193-195]. These channels were initially implicated in mechanotransduction because their phylogenetic relatives in *Caenorhabditis elegans* (*C. elegans),* the degenerins, are essential for perception of touch. Specifically, mutations disrupting the DEG/ENaC proteins *MEC-4* and *MEC-10* impair responses to touch [101-104, 107], whilst *MEC-6* is a part of the degenerin channel complex that may mediate mechanotransduction in touch cells [95]. Moreover, *UNC-8* has been implicated in proprioception [108] whilst *UNC-105* is implicated in the detection of muscle stretch [105, 106]. Importantly this corresponds with the expression of a multitude of *MEC* genes in the touch receptor neuron responsible for gentle touch in *C. elegans* [109].

Expression of ASICs

Indirect evidence has since supported a mechanosensory role of DEG/ENaCs in mammals, including the localisation of three members of the ASIC family (ASIC1, 2 and 3) to peripheral mechanosensory structures and sensory ganglia [113-123].

Price *et al.* described the first ASIC gene when they cloned ASIC2 and found it to be related structurally to the ENaC family [131]. All members of the ASIC family have since been identified in sensory neurons although the specific distribution is not without controversy. ASIC1 is suggested to be the most abundant member of the ASIC family in DRG neurons [116]. Expression has been confirmed in both peripherin and neurofilament positive cells, indicative of small and medium to large neurons respectively [116, 123, 126]. ASIC1 has two splice variants, ASIC1a and ASIC1b. ASIC1a is suggested to be the most abundant variant and predominantly co-localises with peripherin, unlike ASIC1b which predominantly colocalises with neurofilament markers [126]. However these results are somewhat controversial given a separate group demonstrated similar abundances of both splice variants exist in small diameter DRG neurons [123].

When first discovered ASIC2a was thought to be isolated to the CNS while ASIC2b was found in both the CNS and sensory neurons [120]. More recently ASIC2a transcripts have been identified in DRG, although at a lower abundance than ASIC2b [114, 116, 118]. Both transcripts and protein have been observed in large and small DRG neurons however expression is more abundant in medium to large neurons which coexpress NF-200, with relatively little coexpression with peripherin observed [114, 116, 118]. Immunohistochemical experiments demonstrate both splice variants colocalise in the same neuron [116].

Since first reported in 1997 ASIC3 has been described as predominantly expressed in both large and small diameter sensory neurons. However both northern blot and RT-PCR have demonstrated ASIC3 expression in the CNS [126, 196]. ASIC3 expression is again controversial with suggestions of predominance in NF-200 positive and peripherin negative neurons, while others have described coexpression with substance P (a marker of nociceptive C fibres), indicating ASIC3 is likely to be expressed in both medium to large putatively mechanosensitive and small putatively nociceptive neurons [116, 121, 123]. .

Functional ASIC Channels Are Heteromeric

All ASIC members except ASIC2b have the ability to form active homomeric channels when expressed in cell culture and examined using electrophysiological means. However the evidence gained at present suggests that in their native state ASIC channels form heteromultimers. While certain properties of acid evoked currents elicited from native DRG have been observed in homomeric cultures, no individual homomultimer has been described which produces all of these properties [127]. In fact native DRG desensitise faster than any of the homomeric cultures, suggesting individual subunits confer specific properties to the heteromeric complex to produce unique currents. Functional pair-wise heteromeric formation has been observed for all combinations of ASIC1a, 1b, 2a and 3 in cell culture [128], although this is contentious as Alvarez de la Rosa *et.* al. had previously indicated that ASIC1+3 combinations do not occur [116]

Further evidence of heteromultimerization comes from genetically modified mice lacking individual ASIC channels. Cell cultures of DRG explants from these mice

suggest that deletion of any one subunit does not abolish H+ gated currents, but instead alters them when compared to wild types. The resultant H+ gated currents are consistent with those found in cell cultures coexpressing the two remaining subunits[127, 129].

Physiological Evidence

In the absence of specific pharmacological agents for individual ASIC members, more direct evidence of the involvement of these channels in mechanosensation has been provided by mutant mice lacking individual members of the ASIC family [114, 121, 124, 125]. Interestingly the change in response elicited is dependent on tissue and afferent type. Deletion of *ASIC1a* causes a potent increase in the sensitivity of visceral afferents, but no change in cutaneous mechanoreceptors [124, 125]. Deletion of *ASIC2* caused increases or decreases in mechanosensitivity in different populations of visceral and cutaneous afferents. In particular *ASIC2* disruption led to potent increases in the sensitivity of colonic splanchnic serosal afferents [125], yet potent decreases were observed in gastro-oesophageal vagal tension receptors and 2 out of 5 types of cutaneous mechanoreceptor in *ASIC2* -/- mice [114, 125]. Importantly for the gastrointestinal tract, *ASIC3* disruption potently decreased mechanosensitivity in splanchnic and pelvic colonic afferents and in one class of gastro-oesophageal afferent, indicating a widespread positive influence of ASIC3 on visceral mechanosensation [78, 125]. In contrast, the effect of *ASIC3* disruption in skin was restricted to a moderately increased sensitivity of rapidly adapting mechanoreceptors and a decreased sensitivity of AM mechanonociceptors [121]. This suggests ASIC3 may be a more important potential target for modulating mechanosensory function in the gut, particularly in colonic high-threshold afferents.

The results described above suggest there may be tissue specific expression of ASIC channels; however characterisation of ASIC channels in cell bodies of sensory neurons in dorsal root ganglia (DRG) is currently restricted to the mid-lumbar segments of the spinal cord, specifically L3-L5 [118, 119, 122, 123, 126]. These spinal regions are in fact devoid of colonic afferent neuronal cell bodies in rodents, which instead project to thoracolumbar (T10-L1) and lumbosacral (L6-S1) DRG [69, 71, 72, 75, 79]. Our recent data indicate that thoracolumbar splanchnic afferents are specifically tuned to convey nociceptive mechano- and chemosensory information [79-81, 124, 125].

Aim

The aim of this study was to determine whether distinctive expression of ASIC1, 2 or 3 transcripts occurred in thoracolumbar and lumbosacral colonic afferent neurons.

Methodology

Ethics

All experiments were performed in accordance with the guidelines of the Animal Ethics Committees of the Institute for Medical and Veterinary Science and the University of Adelaide, Adelaide, Australia.

Retrograde Labelling

Male or female adult (7-10 week) mice were anaesthetised with halothane (Astra Zeneca, Wilmington DE; 5% induction using induction box, 1.5-2% maintenance), and, following midline laparotomy, three injections (10uL total, 26s gauge Hamilton syringe) of the fluorescent retrograde neuronal tracer cholera toxin subunit B conjugated to fluorescein isothiocyanate (CTB-FITC ;Sigma,St. Louis, MO; 0.5% in 0.1M phosphate buffer (PB), pH 7.4) were made submucosally within the wall of the descending colon approximately 2 cm from the anus. The viscera were carefully rinsed with sterile saline after each injection to ensure dye was not incorporated into structures other than the colon wall, and the overlying muscle and skin were then sutured closed. Following surgery, but prior to regaining consciousness, mice were given an analgesic (5mg/kg butorphenol s.c.; Intervet, Australia), and an antibacterial (10mg/kg oxytetracycline; Pfizer, Groton, CT). Recovery for all animals was under constant observation in a warm environment. Postoperative health, including body weight, was recorded for the following three days, during which time additional soft food was provided to supplement their normal diet. A tracing time of three days was used, as this had been previously determined to provide optimal results. Colons removed after the tracing procedure showed no obvious signs of inflammation or damage.

In Situ Hybridization

Tissue Processing

Mice were deeply anaesthetised with Nembutal (100mg/kg Virbac Animal Health, Australia) and transcardial perfusion was performed first with warm sterile heparinized saline followed by ice cold 4% paraformaldehyde (PFA) / 0.1M PB, pH 7.4. Following fixation, thoracolumbar DRG from bilateral spinal levels T10-L1 (corresponding to the splanchnic innervation of the colon) and lumbosacral DRG from bilateral levels L6-S1 (corresponding to the pelvic innervation of the colon) were removed, using the costae fluctuantes as an anatomical guide, under sterile conditions in ice cold saline, and pooled in to 20% sucrose / 0.1M PB until sunk. The pooled ganglia were then snap-frozen in Tissue-Tek O.C.T. embedding medium (Sakura Finetek, Japan) by brief immersion in liquid nitrogen cooled isopentane and either processed immediately or stored for a maximum of two days at -80°C.

In Situ Hybridization

The in situ hybridization protocol used was essentially that optimised in chapter 3.

All solutions were made using molecular grade reagents where available. All solutions and equipment were treated with 0.1% diethylpyrocarbonate (DEPC; Sigma) and autoclaved wherever possible. All washes were at room temperature unless stated.

Probes

48mer digoxigenin (DIG) labelled oligonucleotide probes (refer to table 1 for sequence) were used to target ASIC1, 2 or 3, with complementary sense probes used as negative controls. The ASIC1 and 2 probes were designed to target conserved areas across the splice variants. Each probe was 100% homologous with the mouse genome. The ASIC3 probe was provided DIG labelled (3' Greenstar) by GeneDetect (New Zealand). HPLC grade probes for ASIC 1 and 2 were provided unlabelled (Geneworks, Australia) and 3' tailed with DIG using the oligonucleotide tailing kit (Roche, Nutley, NJ), according to manufacturer's instructions.

Probe	gene	sequence (5' to 3')	antisense to
ASIC3	*ACCN3*	CCGCTCAGCCACCTGGTAGAGGAAGGCCGCCAGCGACAGGAGTACAGC	406-453
ASIC2	*ACCN1*	GGGCTATGCCACCTGAGCTTGCTGTCCCCTGTCCTGGGTCTTGGGCCT	2170-2217
ASIC1	*ACCN2*	TTGGCAGCGTACGTCATCCCGGCAGGATGTCCTCGGAGGCTCTCGCAG	1675-1722

TABLE 1: In situ Hybridization digoxigenin (DIG)-labelled Oligonucleotide Probes used to target ASIC1, 2 or 3.

Probe Labelling

Probe was diluted to a concentration of 100pmol / 9μL, as determined by spectrophotometric calculation. Probe labelling was performed according to manufacturer's instructions. Briefly, 4 μL of reaction buffer (1 M potassium cacodylate, 0.125 M Tris-HCl, 1.25 mg / mL bovine serum albumin, pH 6.6), 4 μL $CoCl_2$ (Cobaltous chloride), 1 μL DIG-dUTP/dATP (1mM), 1 μL dATP (10mM) and 1 μL terminal transferase (400 U / uL terminal transferase in 60 mM K-phosphate (pH 7.2), 150 mM KCL, 1 mM 2-Mercapto-ethanol, 0.5% Triton X-100, 50% glycerol) were added to 100 pmol / 9 μL probe on ice. The solution was mixed by brief vortex and centrifugation, and incubated at 37° C for 15 minutes, then placed on ice. The reaction was stopped by the addition of 2 μL 0.2 M EDTA (pH 8.0).

Determination of Efficiency of Labelling

Serial dilutions were made of labelled probe (30 to 1 fmol / μL) and 1 μL blots were aliquoted onto positively charged nylon membranes (Roche). These dilutions were then cross linked (UV Stratalinker 1800, Stratagene, Cedar Creek, Texas) and prepared for detection using alkaline phosphatase (AP). Briefly, the blot was rinsed in wash buffer (0.1 M Maleic acid, 0.15 M NaCl, pH 7.5 0.3% Tween 20 (Roche)), and a blocking solution was then applied (Roche propriety solution, 10% in Maleic acid buffer (0.1 M Maleic acid, 0.15 M NaCl, pH 7.5) for 30 minutes at room temperature. Anti-DIG conjugated AP Fab fragments (Roche) was then applied at a dilution of 1:5000 for 30 min. The blot was then rinsed again in wash buffer and transferred to the detection buffer (0.1 M Tris-HCl, pH 9.5, 0.1 M NaCl (Roche)) for 5 minutes. Nitro blue tetrazolium chloride / 5-Bromo-4-chloro-3-indolylphosphate (NBT/BCIP) (Sigma, USA) was then added overnight in a darkened environment for detection. Only those

probes that incorporated sufficient label as demonstrated by the blot with comparison to a positive control (pre DIG-tailed oligonucleotide provided in kit) were used in the following experiments. An example of a representative dot blot is described below (Figure 1).

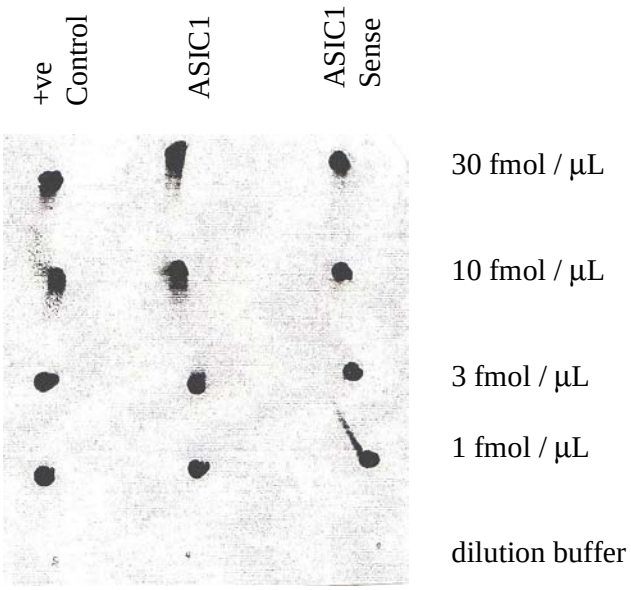

Figure 1: Dot blot of ASIC1 and ASIC1 sense oligonucleotide probe demonstrating the efficiency of the DIG labelling reaction. The positive control in this case is a DIG tailed 48 mer oligonucleotide provided in the tailing kit. The negative control is dilution buffer (sterile water). Positive labelling is observed for both the ASIC1 and ASIC1 sense probe at equal dilutions, indicating the kit labelled both probes equally as efficiently.

Prehybridization

Serial frozen sections (12μm) were cut through the whole tissue block at -20°C and thaw mounted onto Superfrost + slides (Menzel-Glaser, Germany). Sections were then post fixed in 4% PFA for 10 minutes at 4°C and air-dried for one hour at room temperature in a sterile environment. Sections were then rehydrated, endogenous biotin blocked using 0.3% H_2O_2 / 0.1M PB for 10 minutes, and acetylated (freshly prepared 0.1M triethanolamine (Sigma, USA) pH 8 (HCl) / 0.25% acetic anhydride (Sigma, USA)) for a further 10 minutes before being equilibrated in 5X saline sodium citrate (SSC) buffer. The slides were prehybridised with hybridization buffer, coverslipped with parafilm and placed in an airtight moist hybridization container for two hours at 37°C. The hybridization buffer solution consisted of 50% formamide (Sigma), 250μg/ml bakers yeast tRNA type X (Sigma), 250ug/ml salmon sperm DNA (Sigma), 1% Denhardts solution (1% each bovine serum albumin, polyvinylpyrrolidone and ficoll) (Sigma), 10mg/ml poly(a) (Roche), 5XSSC, and 20% dextran sulphate (Sigma). Sections were then washed in 5X SSC for 10 minutes at room temperature. Individual probes were dissolved in hybridization buffer, applied to sections, and hybridised overnight at 37°C. Following hybridization, sections were washed first in 1XSSC then 0.5XSSC for 30 minutes each at 55°C. Sections were then equilibrated to room temperature in 0.5XSSC.

Detection of DIG-labelled hybrids

Detection of the DIG label was performed using CARD amplification (Perkin-Elmer, Oak Brook, IL) combined with streptavidin conjugated Alexa Fluor 546 (SAF 546) (Invitrogen, La Jolla, CA). The slides were equilibrated in Tris buffered saline and incubated firstly in blocking solution (Perkin-Elmer) for 30 min then anti-DIG horse

radish peroxidase conjugated Fab fragments (Roche) at a dilution of 1:100 in blocking solution for a further 30 min. The slides were then incubated for 20 minutes in biotin labelled tyramide (Perkin Elmer) diluted 1:50 in the provided amplification buffer, before being incubated with SAF 546 at 1:200 in blocking solution for 50 minutes. Slides were then coverslipped with Prolong antifade (Invitrogen) to prevent photo-bleaching and screened under an epifluorescent microscope (Olympus BX51) using the appropriate filters for FITC and SA546.

Quantification and Statistical Analysis

Digital images were captured (Cool Snap Fx, Photometrics, Tucson, AZ) and processed using V++ software v 4.0 (Digital Optics, New Zealand). Only cells with intact nuclei were included in this study. UTHSCSA Image tool v3.0 (University of Texas Health Science Center, San Antonio, TX) was used to quantify labelled cells and measure their diameters. The number of labelled neurons was expressed as a percentage of neurons in the whole DRG section; the latter could be counted by increasing image brightness and contrast. This measure was determined from 4-8 DRG sections per mouse and averaged across 5-6 mice per target.

A number of controls were built into the study design to ensure that the results were accurate and reproducible. The number of neurons labelled by each antisense probe was compared with several negative control experiments including the use of complementary sense probe, omission of probe from the hybridization buffer, and competition with excess unlabelled probe. A low level of autofluorescence was observed in these control experiments, however this was negligible when compared to the antisense probe. Moreover, the amount of labelling generated by the sense probe was not significantly different to that observed when the probe was completely omitted

from the buffer (results not shown), confirming an inherent autofluorescence of DRG. To determine positive ASIC labelled DRG neurons, serial sections were alternately hybridised with either positive antisense probe or negative complementary sense probe. Slides were scored by a single observer who was blinded to their prior processing. A neuron was counted as ASIC positive if the majority of the cytoplasm was fluorescent at a level that was clearly above the maximum that could be attributed to autofluorescence. This was assessed both visually and by spot intensity measurements. Exposure times and brightness / contrast levels were consistent between ASIC probe and its negative control. There was a distance of at least 100 µm between each positively labelled section, ensuring the same neurons were not repeatedly counted. Proportions of positive neurons for each target in whole DRG were the same regardless of whether or not ganglia were retrogradely labelled, indicating that no induction of expression had taken place because of interventions during retrograde tracing. Cross sectional diameter was averaged over a representative 96 neurons per label (n = 6). One-way ANOVAs or unpaired t-tests were used to determine differences in ASIC expression between populations ($P < 0.05$).

As an additional control to RT-PCR experiments ASIC1, 2 and 3 primers were used on thoracolumbar DRG from the respective *ASIC1*, *2* or *3* knockout mice, where available. These mice were of C57/BL6 background and generated by homologous recombination in embryonic stem cells as previously described [114, 121, 197]. Heterozygote pairs of mice were mated to generate animals for this investigation. No labelling or PCR products were observed when the primers were used on thoracolumbar DRG from the respective *ASIC* knockout mice (data not shown). Further, in situ hybridization was also performed for ASIC3 using ASIC3 knockout mice, for which no labelling was observed, as detailed in chapter 2.

Quantitative RT-PCR

Tissue Processing and RNA Extraction of Whole Ganglia

Thoracolumbar (T10-L1) DRG were removed bilaterally from five male or female mice (20-30g) and the level of each noted and recorded, using the costae fluctuantes as an anatomical guide. DRG from each level were pooled and stored in RNAlater® (Qiagen, Australia) at -20°C for subsequent RNA extraction. RNA was isolated from these DRG using homogenisation and TRIzol reagent (Invitrogen, Australia), followed by isopropanol precipitation. RNA quantification was determined by measuring the absorbance at 260 nm (A260) using a spectrophotometer (Biorad, Australia) RNA quality was estimated by the A260 and A280 nm ratio.

Laser capture microdissection and RNA extraction

Thoracolumbar DRG (T10–L1), corresponding to the splanchnic innervation of the mouse colon, were harvested 2-3 days after retrograde labelling with CTB-FITC as described above. DRG were transferred to a 20% RNAse free sucrose solution until sunk at room temperature. The sucrose was then removed, and the pooled ganglia snap frozen in Tissue-Tek O.C.T. embedding medium (Sakura Finetek, Japan) by brief immersion in liquid nitrogen cooled isopentane (-30°C) and processed immediately for laser capture microdissection. Cryosections (10 μm) were mounted onto Superfrost + slides (Menzel-Glaser, Germany) washed with RNase free water, fixed with 75%, 100% ethanol and air dried before commencing laser-capture microdissection which was performed on a P.A.L.M.® Microlaser Technologies microbeam microdissection system. The retrogradely labelled colonic neurons were microdissected and catapulted directly into a lysis and stabilization buffer (Buffer RLT, RNeasy Micro RNA

extraction Kit, (Qiagen, Australia) containing 0.14M β-Mercaptoethanol (Sigma-Aldrich, Australia). The RNA from these cells was then isolated using an RNeasy Micro RNA extraction Kit as per the manufacturers instructions (Qiagen, Australia). This process utilized RNeasy MinElute Spin Columns, allowing adsorption of RNA to the silica membrane, an on-column DNase digestion treatment, removal of contaminants with simple wash steps and elution of the RNA with RNase-free water. RNA quantification was determined by measuring the absorbance at 260 nm (A260) using a spectrophotometer (Biorad, Australia) RNA quality was estimated by the A260 and A280 nm ratio.

Determination of Relative ASIC Transcript Expression

Quantitative reverse transcription polymerase chain reactions (RT-PCR) reactions were performed using a Chromo4 (MJ Research) real-time instrument (designed to detect SYBR® green fluorescence and therefore amplified cDNA products) attached to a PTC-200 Peltier thermal cycler (MJ Research) and analysed using Opticon Monitor software (MJ Research). Reverse transcription (RT) and polymerase chain reactions (PCR) were performed using a Qiagen QuantiTect® SYBR® Green RT-PCR one-step RT-PCR kit (Qiagen, Australia) according to the manufacturers specifications, with primers used as indicated in Table 2, under the following conditions: Reverse Transcription: 50°C for 30mins; Initial PCR activation: 95°C for 15 mins; PCR cycles; 94°C for 15 sec, 47°C for 30 sec and 72°C for 30 sec repeated for 44 cycles. Confirmation of the amplified products were resolved by 3% agarose gel electrophoresis and visualized via ethidium bromide staining. Each assay was run in at least triplicate in separate experiments. Control PCRs were performed by substituting RNA template with distilled RNAse-free water. All primers were designed with Primer 3.0 software (Applied Biosystems) and tested for specificity using NCBI's BLAST software. All product lengths were

restricted between 100-150bp, to allow the highest efficiency of reaction when using SYBR® Green.

Target	**Gene**	**FORWARD PRIMER (5' – 3')**	**REVERSE PRIMER (5' – 3')**	**PRODUCT LENGTH (bp)**
ASIC1	*ACCN2*	CAGATGGCTGATGAAAAGCA	AAGTGGCACGAGAGAAGCAT	140
ASIC2	*ACCN1*	TGACATTGGTGGTCAAATGG	ATCATGGCTCCCTTCCTCTT	139
ASIC3	*ACCN3*	AGGGAGAAGTCCCAAAGCAT	GACACTCCATTCCCAGGAGA	107
β-actin	*ACTB*	GACCTCTATGCCAACACAGT	GATCTTCATGGTGCTAGGAG	108

Table 2: Nucleotide primer sequence Used for Relative Quantification of ASIC transcripts Using Quantitative RT-PCR

Data Analysis of Quantitative RT-PCR

The comparative CT method was used to quantify the abundance of target transcripts in whole thoracolumbar DRG and LCM colonic neurons from thoracolumbar DRG, as previously described (PE Applied Biosystems User Bulletin 2 and [198]). The read-out for quantitative RT-PCR using the Opticon monitor software was given as the number of PCR cycles or the "cycle threshold" (CT) needed to achieve a certain level of fluorescence. To obtain relative expression values for ASIC transcripts the CT for each ASIC transcript was compared to the internal reference β–actin using the equation ΔCT (Cycle threshold (CT) of ASICx transcript - Cycle threshold (CT) of β-actin). Briefly, the greater the ΔCT value the less of the target transcript present. To determine the relative expression of these transcripts in whole thoracolumbar DRG and LCM colonic neurons from thoracolumbar DRG, the ΔΔCT was calculated using the following formula ΔΔCT=ΔCT [ASICx whole DRG] - ΔCT [ASICx LCM neurons] and the relative fold differences calculated using the formula $2^{-\Delta\Delta CT}$. As such fold changes were calculated relative to the level of β-actin RNA in the same sample. CT values for β–actin were highly reproducible between samples and between methods of RNA preparation. Quantitative data are expressed as mean ± SD, and significant differences in transcript expression determined by a Mann-Whitney test at a significance level of $P < 0.05$

Verification of Relative Expression Data From Quantitative RT-PCR

To be able to accurately quantify and compare transcript expression we incorporated extensive controls and calibrators. A melting curve program verified the specificity and identity of the RT-PCR products and no primer dimers were observed. To confirm

amplification efficiencies and therefore the validity of the comparative CT method, titration curves were obtained by taking template RNA of known concentration from thoracolumbar DRG and using them to create a five log dilution series of RNA. The linearity of the plots indicated equal amplification of the assay over a range of input RNA concentrations for β-actin, ASIC1, ASIC2 and ASIC3. These curves demonstrated that the efficiencies of targets (i.e. ASICs) and reference (β-actin) were equal. Further validation was indicated by calculating ΔCT (Cycle threshold (CT) of ASICx transcript - Cycle threshold (CT) of β-actin) from the titration curves for thoracolumbar DRG. A slope of less than 0.1 indicated that the efficiencies of target (i.e. ASICs) and the reference (ie. β-actin) were equal and therefore relative comparative analysis using the comparative CT method was appropriate.

Results

Expression and Quantification of ASIC1, 2 and 3 in Whole Thoracolumbar DRG Using Quantitative RT-PCR and *in situ* Hybridization

First we investigated ASICs in the thoracolumbar (T10-L1) DRG to establish expression levels and patterns in all sensory neurons. Using gel electrophoresis we confirmed the size of the amplified products generated by the QuantiTect® SYBR® Green RT-PCR Kit with primers specific for ASIC1, 2, 3 and β–actin, showing intense single bands, corresponding to the predicted sizes of ASIC1, 2 and 3 transcripts *(*Figure 2). This confirmed our previous findings [124, 125] that ASIC1, 2 and 3 transcripts are expressed in thoracolumbar DRG. Quantitative RT-PCR analysis of whole thoracolumbar DRG revealed that using β–actin as a reference CT value, ASIC2 was the most abundant ASIC transcript, significantly more than ASIC1 ($P < 0.0001$) and ASIC3 ($P < 0.0001$). Specifically there was a 12.19 ± 0.98 fold greater abundance of ASIC2 than ASIC1, a 21.57 ± 2.07 fold greater abundance of ASIC2 than ASIC3. There was a 1.78 ± 0.24 fold greater abundance of ASIC1 than ASIC3 (Figure 3). Transcripts for ASIC1, 2 and 3 were not observed in thoracolumbar DRG from the respective *ASIC1, 2 or 3* knockout mice (data not shown).

Using fluorescence *in situ* hybridization (FISH) we investigated the proportion of neurons within thoracolumbar DRG expressing ASIC1, 2 and 3 mRNA. Specifically, 40 ± 1% of thoracolumbar DRG neurons expressed transcripts for ASIC2, whilst ASIC3 was observed in 24 ± 1% of neurons and ASIC1 in 18 ± 1% of neurons (N=6 for each probe (Figure 4). Therefore significantly more neurons within thoracolumbar DRG expressed ASIC2 than ASIC1 ($P < 0.001$) or ASIC3 ($P < 0.001$), whilst significantly more neurons expressed

ASIC3 than ASIC1 ($P < 0.01$). The average cell diameter of ASIC1 expressing neurons was 18.4 ± 0.4 µm, ASIC2 18.5 ± 0.4 µm and ASIC3 16.7 ± 0.4 µm (n=96 cells per target). The restricted variability of cellular diameter indicated labelling of a single population of neurons, with diameter from 10 µm to 25µm, consistent with small-medium diameter neuron bodies (Figure 5). No labelling was evident in non-neuronal cells.

Further the lumbosacral DRG (L6-S1) was also examined for ASIC3 expression in neurons representing the pelvic innervation of the colon. 23 ± 1% (N=6) of lumbosacral DRG neurons were found to express ASIC3, similar to that observed in thoracolumbar DRG (Figure 6). The average diameter of these neurons was found to be 19.63 ± 0.5 µm. Once again the diameter was restricted to within 10 µm to 25µm, indicating small to medium sized neurons (Figure 7).

Overall, the results of both quantitative RT-PCR analysis and FISH experiments indicate mRNA transcripts of ASIC2 are clearly the most abundant in terms of relative transcript quantification and the number of neurons expressing the transcripts in the general thoracolumbar population, followed by ASIC1 and ASIC3. ASIC3 was also found to have similarly low levels of expression in lumbosacral DRG.

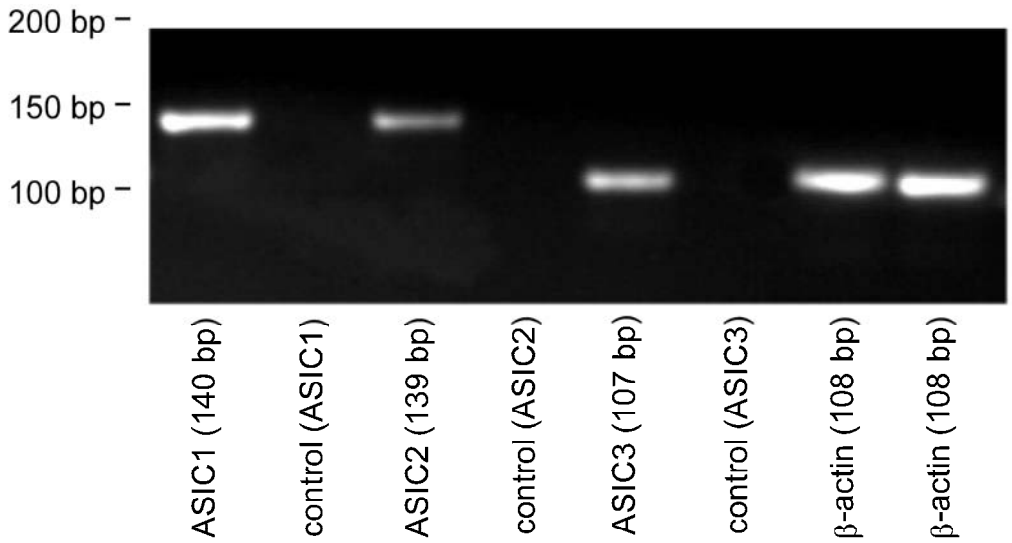

Figure 2: Detection of ASIC transcripts in whole mouse thoracolumbar (T10-L1) DRG. ASIC 1, 2, and 3 transcripts were all detected in whole mouse thoracolumbar (T10-L1) DRG. Where the RNA template was substituted with distilled water no evidence of an amplified product was observed. PCR analysis for the detection of ASIC1, 2 and 3 and β-actin was carried out by using specific primers (Table 1b) as described in the materials and methods. PCR products from quantitative RT-PCR experiments were separated on a 3% agarose gel to confirm the presence of transcripts in whole mouse thoracolumbar (T10-L1) DRG and validate the products obtained during quantitative analysis.

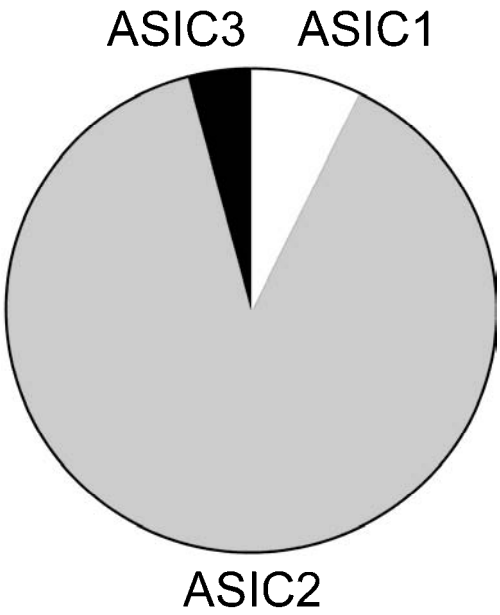

Figure 3: Relative Expression of ASIC transcripts in whole mouse thoracolumbar (T10-L1) DRG. Quantitative RT-PCR analysis of whole thoracolumbar DRG revealed that relative to β–actin ASIC2 had the highest ASIC transcript expression, followed by ASIC1 and ASIC3 respectively. Specifically there was a 12.19 ± 0.98 fold greater abundance of ASIC2 than ASIC1, and a 21.57 ± 2.07 fold greater abundance of ASIC2 than ASIC3. There was a 1.78 ± 0.24 fold greater abundance of ASIC1 than ASIC3. These relative expression data indicate that ASIC2 is by far the most predominant ASIC transcript in whole thoracolumbar DRG, followed by ASIC1 and ASIC3. Experiments were performed in at least triplicate in separate PCR studies. Fold differences are calculated relative to β–actin mRNA levels.

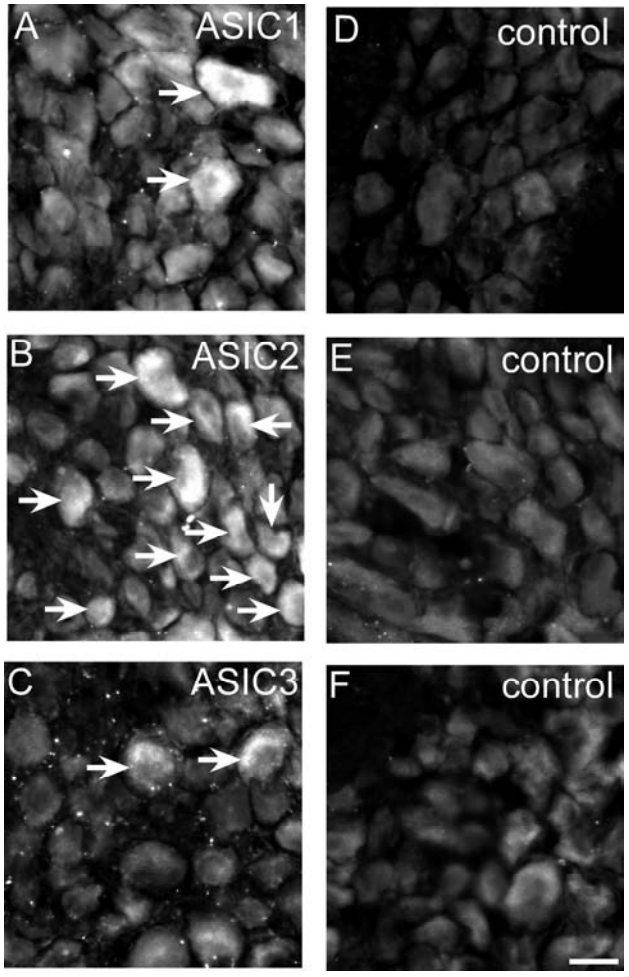

Figure 4: In situ hybridisation targeting ASIC1 (A), ASIC2 (B) or ASIC3 (C) with streptavidin-546 detection in thoracolumbar (T10-L1) DRG. Sections of thoracolumbar DRG showing (A) ASIC1, (B) ASIC2, and (C) ASIC3 mRNA expression in neurons. Arrows denote examples of positively labelled neurons. D-F: The specificity of the mRNA signals were confirmed using negative control studies using the complementary sense probe and serial sections, imaged at identical microscope and software settings. All ASIC-positive neurons are indicated. Scale bar = 25 μm.

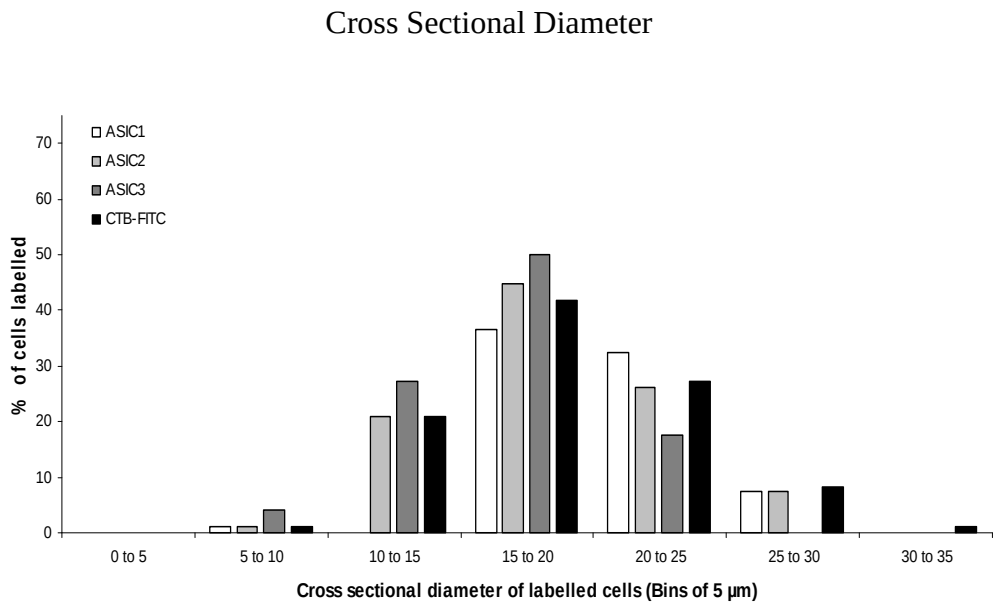

Figure 5: The distribution of the diameters of thoracolumbar DRG neurons labelled by either ASIC1, 2 and 3 or CTB-FITC overlap. This graph shows that the neurons expressing ASIC1, 2 and 3 have a cross-sectional diameter of 10 – 30 µm irrespective of label, consistent with small-to-medium diameter neurons. Similarly, retrogradely labelled colonic neurons have a similar cross-sectional diameter, consistent with classification as small-to-medium diameter neurons.

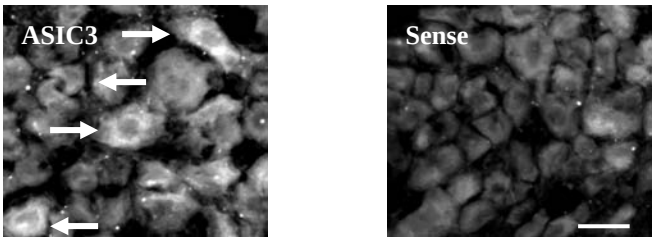

Figure 6: In situ hybridisation targeting ASIC3 with streptavidin-546 detection in lumbosacral (L6-S1) DRG. Arrows denote examples of positively labelled neurons. The specificity of the mRNA signals were confirmed using negative control studies using the complementary sense probe and serial sections, imaged at identical microscope and software settings. All ASIC3-positive neurons are indicated. Scale bar = 25 μm.

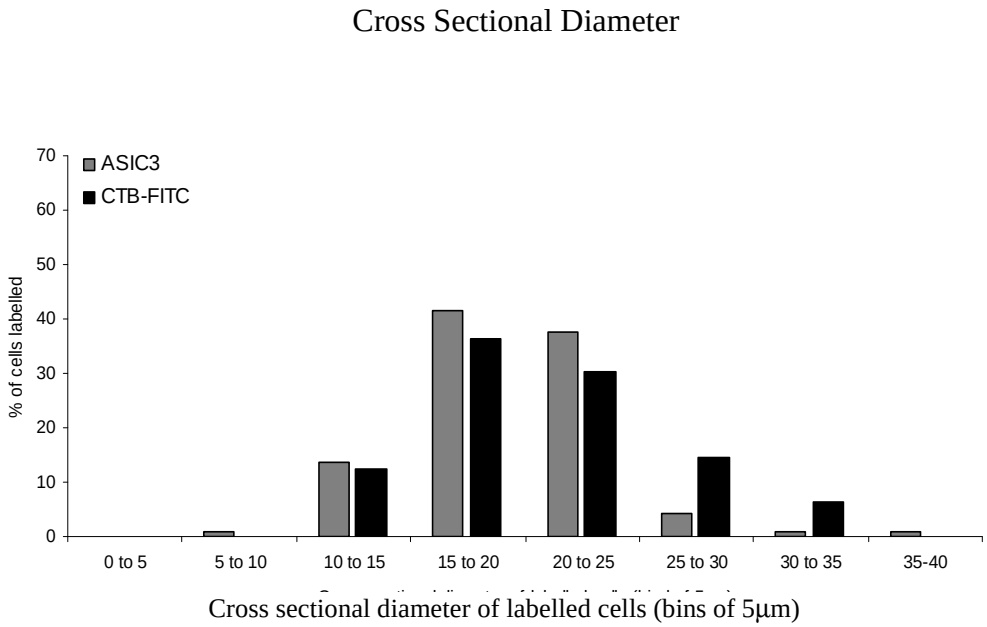

Figure 7: The distribution of the diameters of neurons labelled by either ASIC3 or CTB-FITC overlap in lumbosacral DRG. This graph shows that the neurons expressing ASIC3 have a cross-sectional diameter of 10 – 30 μm irrespective of label, consistent with small-to-medium diameter neurons. Similarly, retrogradely labelled colonic neurons have a similar cross-sectional diameter, consistent with classification as small-to-medium diameter neurons.

Expression and Quantification of ASIC1, 2 and 3 in Retrogradely Labelled Colonic Neurons within Thoracolumbar DRG using Quantitative RT-PCR and *in situ* Hybridization

Subserosal CTB-FITC injections in the distal colon resulted in labelling of 4 ± 1% (N=8) of neurons in thoracolumbar (T10-L1) DRG and 2 ± 0.3% (N=6) of neurons in lumbosacral (L6-S1) DRG, confirming that colonic afferents represent a small subpopulation of thoracolumbar DRG neurons [69, 71, 79]. In thoracolumbar DRG, the average diameter of retrogradely labelled neurons was 19 ± 0.4 µm, with the majority of labelled neurons ranging from 10 to 25 µm (Figure 5). In lumbosacral DRG, the average diameter of retrogradely labelled neurons was 20.9 ± 0.56 µm (Figure 7). This is consistent with small-medium diameter neuron bodies observed previously.

To determine the relative expression of ASIC1, 2 and 3 transcripts in colonic neurons we used laser capture microdissection in conjunction with quantitative RT-PCR to specifically isolate neurons within the thoracolumbar DRG that had been retrogradely labelled. Gel electrophoresis and UV analysis of quantitative RT-PCR products from laser capture microdissected retrogradely labelled colonic neurons revealed intense single bands, corresponding to the predicted sizes of ASIC1, 2 and 3 (Figure 8). This confirmed that the correct ASIC1, 2 and 3 transcripts were amplified from laser captured neurons. Quantitative RT-PCR analysis revealed in colonic neurons that, relative to β-actin, ASIC3 had the most abundant ASIC transcript expression, significantly more than ASIC1 ($P < 0.05$) and ASIC2 ($P < 0.01$) respectively. Specifically there was a 2.27 ± 0.56 fold greater abundance of ASIC3 than ASIC1 and a 5.13 ± 0.84 fold greater abundance of ASIC3 than ASIC2. There was a 2.26 ± 0.12 fold greater abundance of ASIC1 than ASIC2 (Figure 9).

In order to investigate proportions of colonic afferents expressing ASIC1, 2 and 3, we carried out FISH experiments in conjunction with retrograde tracing. ASIC3 was observed in 73 ± 2% (N=6) of retrogradely labelled neurons, while ASIC2 and ASIC1 were observed in 47 ± 1% (N=5) and 30 ± 2% (N=5) of colonic neurons respectively (Figure 10). Therefore significantly more colonic neurons within the thoracolumbar DRG expressed ASIC3 than ASIC1 ($P < 0.001$) or ASIC2 ($P < 0.001$), whilst significantly more neurons expressed ASIC2 than ASIC1 ($P <0.01$). Further, ASIC3 was found to be expressed in 60 ± 4% (N=6) of colonic lumbosacral DRG neurons (Figure 11), indicating this pathway also expresses ASIC3 in high abundance.

Overall, the results of both the quantitative RT-PCR analysis and FISH experiments indicate that in colonic neurons mRNA transcripts of ASIC3 are clearly the most abundant both in terms of relative quantification and the number of neurons expressing the transcript, followed by ASIC1 and ASIC2 at lower amounts.

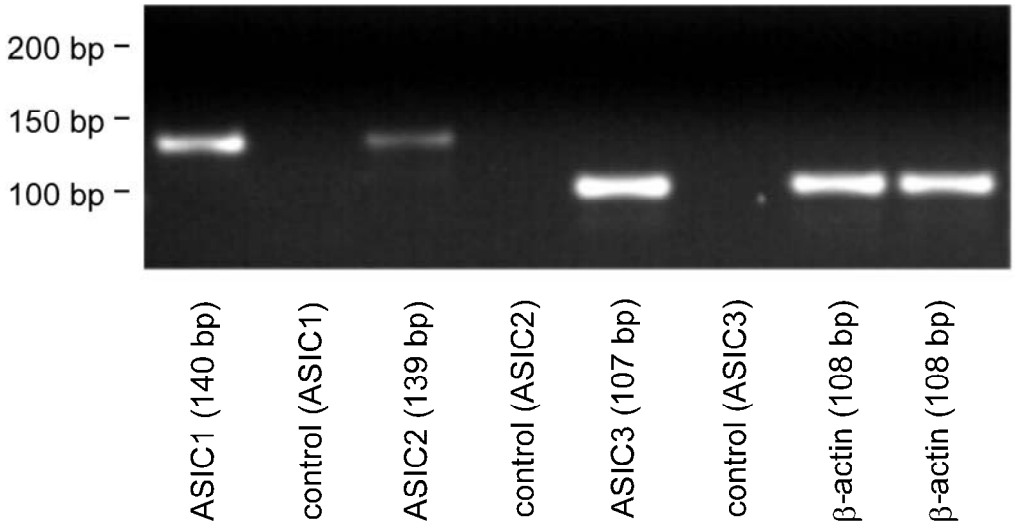

Figure 8: Detection of ASIC1, 2 and 3 transcripts in colonic neurons isolated from thoracolumbar (T10-L1) DRG using laser capture microdissection. ASIC 1, 2, and 3 transcripts were all detected specifically within colonic neurons which were identified by CTB-FITC retrograde tracing and isolated by laser capture microdissection from thoracolumbar (T10-L1) DRG.

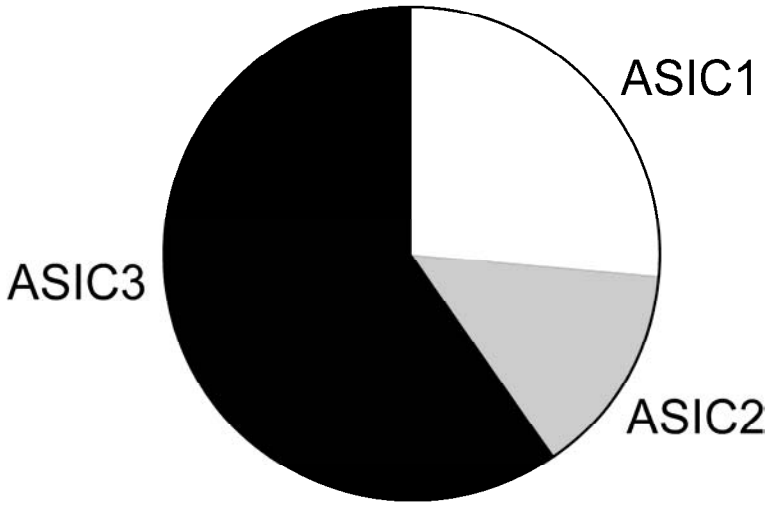

Figure 9: Relative expression of ASIC1, 2 and 3 transcripts in colonic neurons isolated from thoracolumbar (T10-L1) DRG using laser capture microdissection. Quantitative RT-PCR data revealed that in these laser capture microdissected colonic neurons that relative to β-actin ASIC3 had the highest ASIC transcript expression, followed by ASIC1 and ASIC2 respectively. Specifically there was a 5.13 ± 0.84 fold greater abundance of ASIC3 than ASIC2, a 2.27 ± 0.56 fold greater abundance of ASIC3 than ASIC1. There was a 2.26 ± 0.12 fold greater abundance of ASIC1 than ASIC2. Experiments were performed in at least triplicate. Fold differences are calculated relative to β–actin mRNA levels.

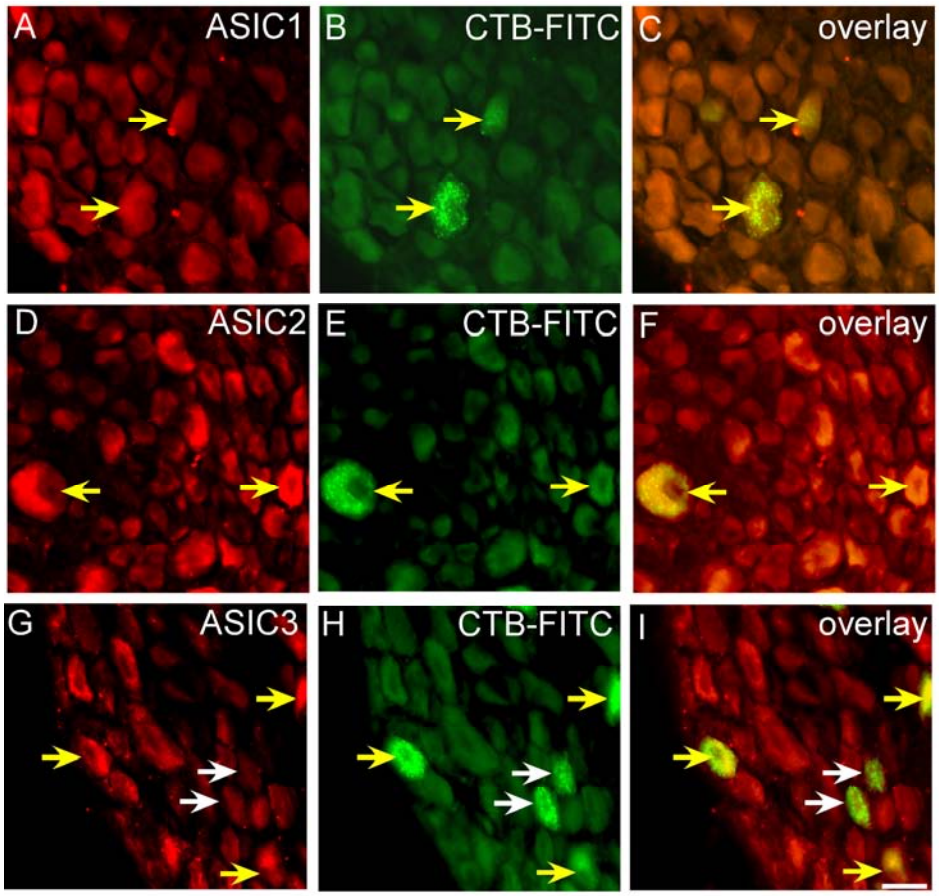

Figure 10: In situ hybridisation targeting of ASIC1, 2 and 3 in retrogradely labelled colonic neurons within thoracolumbar DRG. In situ hybridisation using probes against ASIC1 (A), ASIC2 (D), and ASIC3 (G) labelled with strepavidin-546 (red) in sections, with retrogradely labelled colonic thoracolumbar DRG neurons (B, E, H) also labelled with CTB-FITC (green), and overlaid images of both (C, F, I). Yellow arrows indicate neurons retrogradely traced from the colon with CTB-FITC that were also ASIC-positive. White arrows indicate colonic neurons, labelled with CTB-FITC, that were ASIC-negative. Scale bar = 25 μm.

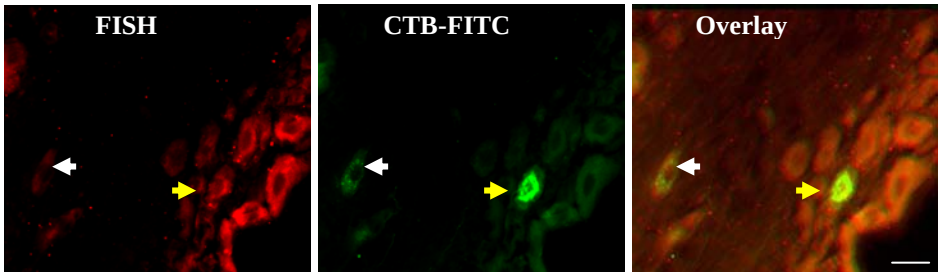

Figure 11: In situ hybridisation targeting of ASIC 3 in retrogradely labelled colonic neurons within lumbosacral DRG. In situ hybridisation using probes against ASIC3 labelled with strepavidin-546 (red), with retrogradely labelled colonic lumbosacral DRG neurons also labelled with CTB-FITC (green), and overlaid image of both (merge). Yellow arrows indicate neurons retrogradely traced from the colon with CTB-FITC that were also ASIC3-positive. White arrows indicate colonic neurons that were ASIC-negative Scale bar = 25 μm.

Comparison of ASIC1, 2 and 3 in Colonic Neurons With Whole Thoracolumbar DRG

73 ± 2% of retrogradely labelled colonic neurons expressed ASIC3 compared with only 24 ± 1% of neurons in the general population. These data indicate that ASIC3 positive neurons are significantly more prevalent by 204% ($P < 0.0001$) in the colonic population compared with the general thoracolumbar population (Figure 12). ASIC1 and 2 positive neurons were also significantly more abundant in the colonic innervation, however not to the same extent. ASIC1 was expressed in 30 ± 2% of colonic neurons compared with only 18 ± 1% of neurons in the general population resulting in an 83% greater expression of ASIC1 in colonic neurons ($P < 0.0001$) (Figure 12). ASIC2 was expressed in 47 ± 0.5% of colonic neurons, compared with 40 ± 1% of neurons in the general population (25% greater expression; $P < 0.001$, Figure 12). In addition, ASIC3 was also found to be much more abundant in colonic neurons in lumbosacral DRG, with expression increasing from 23 ± 1% in the general population to 60 ± 4% in colonic lumbosacral DRG neurons, representing an increase of 160% ($P<0.0001$) (Figure 13).

Analysis of the quantitative RT-PCR data also indicated that although transcripts for each of the ASIC members were present in colonic neurons within thoracolumbar DRG, the magnitude of expression varied compared to the general thoracolumbar DRG population. Although ASIC3 was the least expressed of the ASIC transcripts in the whole DRG, in colonic neurons ASIC3 had the highest relative expression, with a 5.22 ± 0.13 fold greater ($P < 0.05$) relative abundance of ASIC3 in colonic neurons compared to the general DRG population (Figure 14). ASIC1 had a 1.30 ± 0.09 fold greater relative abundance in colonic neurons vs. the general population (Figure 14). ASIC2, on the other hand, was 17.76 ± 1.97

fold less abundant ($P < 0.001$) in colonic neurons than in thoracolumbar DRG population (Figure 14).

Overall, the results of both the quantitative RT-PCR analysis and in situ hybridization experiments indicate a significantly enhanced expression of ASIC3 within colonic neurons (Table 3).

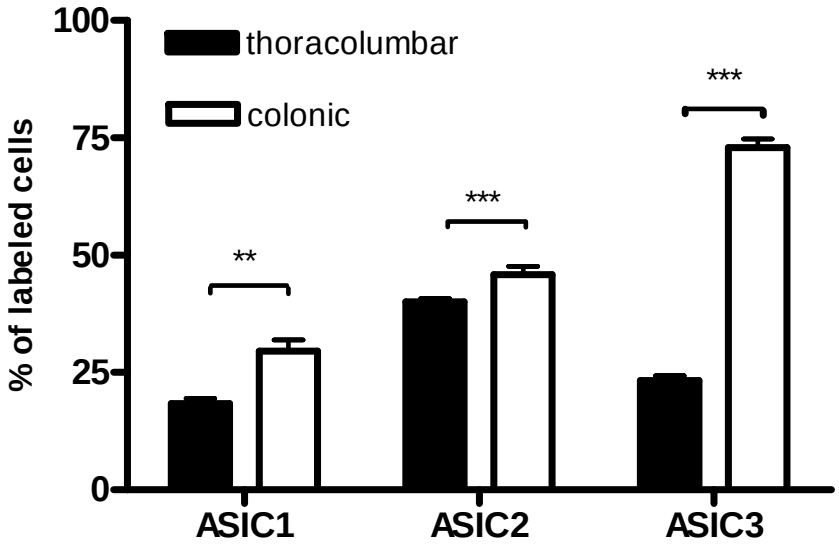

Figure 12: In situ hybridisation comparison of the proportions of neurons expressing ASIC1, 2 and 3 in the general thoracolumbar DRG vs colonic neurons. Transcript expression of ASIC1, 2 or 3 is each significantly more abundant in CTB-FITC labelled colonic thoracolumbar DRG neurons when compared to expression in the general thoracolumbar DRG population when quantified by in situ hybridisation. This indicates expression of ASIC members is more abundant on a tissue level in colonic neurons. Data are means ± SEM. (* $P < 0.01$, ** $P < 0.001$, *** $P<0.0001$)

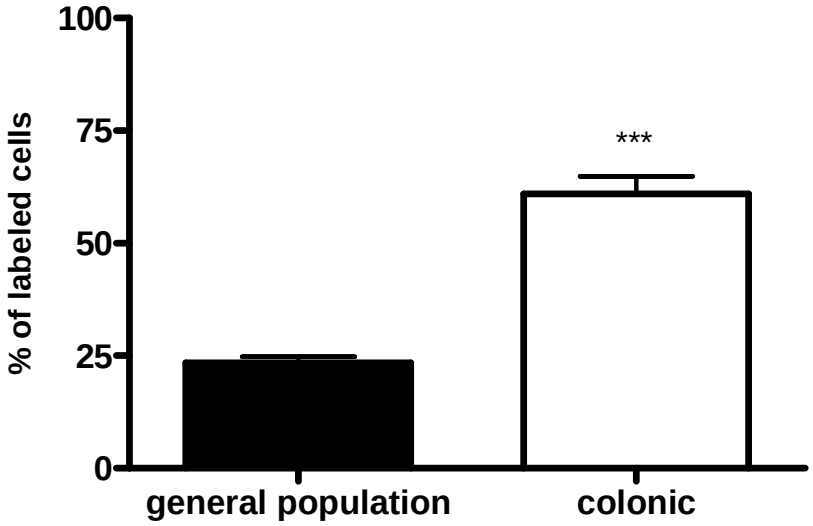

Figure 13: In situ hybridisation comparison of the proportions of neurons expressing ASIC3 in the general lumbosacral DRG vs colonic neurons. Transcript expression of ASIC3 is each significantly more abundant in CTB-FITC labelled colonic lumbosacral DRG neurons when compared to expression in the general lumbosacral DRG population when quantified by in situ hybridisation. This indicates expression of ASIC members is more abundant on a tissue level in colonic neurons. Data are means ± SEM. (*** $P<0.0001$)

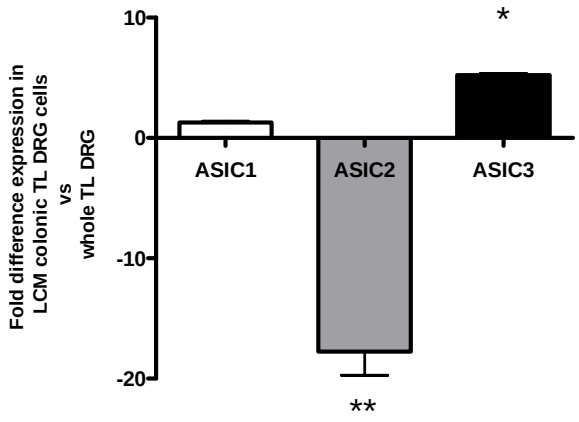

Figure 14: Comparative expression of ASIC1, 2 and 3 in whole thoracolumbar DRG vs. colonic neurons isolated with laser capture microdissection using quantitative RT-PCR. ASIC3 had the highest relative expression in colonic neurons, but was the least expressed of the ASIC transcripts in the whole DRG, which translated to a 5.22 ± 0.13 fold greater relative abundance of ASIC3 in colonic neurons vs. the general population (*P < 0.05). ASIC1 had the second greatest relative abundance in the general population. ASIC1 also had the second greatest relative abundance in colonic neurons. Overall this translated to a 1.30 ± 0.09 fold greater relative abundance of ASIC1 in colonic neurons vs. the general population. Although ASIC2 had by far the highest ASIC transcript expression in whole thoracolumbar DRG, ASIC2 was the least expressed ASIC transcript in the colonic neurons. Overall this translated to ASIC2 being 17.76 ± 1.97 fold less abundant in colonic neurons compared with the general population, indicating a dramatic decrease in the contribution of ASIC2 to colonic neurons compared with the general population (**P < 0.01).

Table 3: Relative abundance or expression of ASIC transcripts in thoracolumbar DRG neurons versus colonic neurons

	Quantitative RT-PCR			Fluorescent *in situ* hybridization		
	ASIC1	**ASIC2**	**ASIC3**	**ASIC1**	**ASIC2**	**ASIC3**
Thoracolumbar	**	***	*	**	**	*
Colonic	**	*	***	**	**	***

*** (greater than 50% of neurons or at least 5 fold greater abundance than least abundant ASIC)

** (25-50% of neurons or 2.5-5 fold greater abundance than least abundant ASIC)

* (less than 25% of neurons or over 2.5 fold less abundant than other ASICs)

Discussion

Using FISH and quantitative RT-PCR we have identified ASIC1, 2 and 3 mRNA transcripts within the general population of mouse T10-L1 thoracolumbar DRG neurons, but most importantly and for the first time we have identified ASIC1, 2 and 3 specifically within colonic neurons. Findings from both techniques were in agreement that ASIC2 was the most abundant ASIC transcript expressed in the general thoracolumbar DRG population of neurons, followed by ASIC1 and ASIC3. To identify colonic afferent neurons we injected tracer into the distal colon, and in conjunction with either FISH or laser capture microdissection plus quantitative RT-PCR, examined ASIC expression in identified colonic DRG neurons. In contrast to whole DRG, ASIC3 was the most abundant ASIC transcript in colonic neurons, followed by ASIC1 and ASIC2. This shows that different populations of spinal afferent neurons express different proportions of ASICs. Of particular interest is the stark contrast between ASIC2 predominance in the general thoracolumbar population and ASIC3 predominance in colonic neurons. Notably ASIC3 has the lowest abundance in the general population, but is the most highly expressed ASIC transcript in colonic neurons. ASICs exist as heteromultimers in sensory neurons [127], however our data suggests that the composition of heteromultimers must differ markedly between different types of sensory neurons.

ASIC3

In studies on knockout mice we have previously shown that of all ASICs, ASIC3 has the largest contribution of all ASICs towards visceral mechanosensation [125]. It could be argued that mRNA expression may not directly translate into functional ASIC protein

expression contributing to afferent mechanosensory complexes. However, the predominance of ASIC3 mRNA in neurons innervating the colon in the current study supports these recent functional data indicating that in this case transcript expression correlates well with functional significance. ASIC3 expression was detected by FISH in 73% of colonic thoracolumbar DRG neurons, which is 26-43% more than those expressing ASIC 1 or 2 respectively. Quantitative RT-PCR analysis of laser captured colonic DRG neurons showed that ASIC3 transcript expression was at 2 - 5 fold higher levels than other ASICs, corroborating our localisation data. In our previous electrophysiological studies on knockouts we showed that disrupting expression of *ASIC3* had the greatest impact on mechanosensitivity of colonic serosal and mesenteric afferents, which account for 86% of all thoracolumbar splanchnic colonic sensory neurons, indicating a widespread positive influence of ASIC3 on colonic mechanosensation [125]. Therefore the molecular, localisation and functional outcomes of disrupting *ASIC3* agree that it is potentially a major target for modulating mechanosensory function in the gut, particularly in colonic high-threshold splanchnic afferents.

Very recent studies indicate that this may also be the case for lumbosacral pelvic colonic afferents, which are more involved with transmission of non-noxious sensory information. Immunohistochemistry has previously showed ASIC3 protein in comparable proportions of rat thoracolumbar (43%) and lumbosacral (42%) labelled colonic sensory neurons [71], which is less than the expression noted in the current study, but does not correlate as well with functional data. *In situ* hybridization studies conducted in parallel with those on thoracolumbar DRG in this study indicate significant ASIC3 transcript expression in the majority of colonic neurons within mouse lumbosacral DRG (60%). Furthermore, disrupting expression of *ASIC3* decreases the mechanosensitivity of mouse pelvic colonic

afferent fibres [78], indicating a similar role of ASIC3 in this pathway to that in splanchnic afferents.

The significance of the abundant ASIC3 expression in colonic neurons becomes more apparent when it is compared with that in the DRG as a whole, the vast majority of which comprises neurons innervating skin and skeletal muscle. In whole DRG ASIC3 was the least prevalent transcript, therefore its prevalence is increased from the 22-fold least expressed transcript in DRG to the 5-fold most expressed in colonic neurons. The lower proportion of neurons expressing ASIC3 and the low levels of transcript are reflected in a relatively small change in cutaneous mechanosensitivity when ASIC3 is deleted [121], which occurs in only one of 5 classes of afferents. Previous reports of ASIC3 expression in whole DRG, using a variety of methods and from different spinal levels, are in general agreement with our study. In addition to immunohistochemical evidence cited above, Northern Blot and RT-PCR analysis have also detected mRNA transcripts for ASIC3 in rat lumbar DRG [126, 199]. Previous studies using *in situ* hybridization in rat showed ASIC3 transcripts are expressed in 30–35% of neurons, mainly in small-to-medium diameter neurons [122, 123, 126, 199], which compares with the 24% we observed in the present study. Importantly, this transcript expression translates to protein expression, because in the same levels of rat DRG, Western blot analysis reveals expression of ASIC3 [116]. ASIC3 transcript and protein have also been previously shown in lumbar DRG of mouse, using RT-PCR [121, 125] or Northern blot analysis [117]. ASIC3 protein has also been located at the sites of cutaneous sensation and is present in mechanosensory lanceolate nerve endings surrounding the hair shaft and other cutaneous sensory structures [121]. Overall the location of ASIC3 corresponds directly with the deficits observed in cutaneous mechanosensation and behavioural responses in mice with disruptions to the *ASIC3* [117,

121] gene, which taken together indicate it plays a specific but minor role in cutaneous mechanotransduction.

ASIC1 and ASIC2

We found ASIC1 expression in the smallest number of colonic neurons (30%) but it was quantitatively the second most abundant ASIC transcript. This suggests that ASIC1 is highly expressed in a sub-population of colonic neurons, although there are technical considerations besides (see later). Deletion of *ASIC1a* in our previous studies caused a widespread increase in the sensitivity of 2 classes of splanchnic colonic afferents, which suggests that ASIC1a may serve to dampen the mechanotransduction process in these afferents [124, 125].

ASIC2 was expressed in 47% of colonic neurons, yet was the least expressed ASIC transcript, 5-fold less than ASIC3 and 2-fold less than ASIC1, suggesting its expression is common but thinly spread. Our previous functional data indicated ASIC2 contributed the least to colonic mechanosensation as deletion of *ASIC2* led to changes in only one class of colonic splanchnic afferent [125], in which an increase in sensitivity was seen. As the only changes observed in the *ASIC1a* and *ASIC2* knockout mice were an increase in mechanosensitivity of splanchnic colonic afferents, it appears that ASIC1a and ASIC2 make little if any direct contribution to their mechanotransduction [124, 125].

Previous publications have reported the distribution of ASIC mRNA transcripts by PCR-analysis, Northern blot analysis or *in situ hybridization* and the distribution of ASIC proteins by Western blot analysis and immunohistochemistry. Such studies have been

performed in rat and mouse lumbar DRG mainly in the context of other systems, particularly cutaneous sensation. Northern Blot and RT-PCR analysis have detected mRNA transcripts for ASIC1 [113], ASIC1a and ASIC1b [126], ASIC2a [118], ASIC2b [120] in rat lumbar DRG. More specifically, *in situ hybridization* reveals transcript expression of ASIC1a in 20-25% of neurons with predominantly small neuron diameters [113, 122, 123, 126]. The other splice variant of ASIC1, ASIC1b has transcript expression in between 10-25% of neurons with small, medium and large diameters [122, 123, 126]. ASIC2a transcripts are primarily expressed in large-diameter DRG neurons in an unspecified number of neurons in rat [118], whilst ASIC2b transcripts are also expressed but in an unspecified number of neurons with unspecified diameters [112, 120]. Our current observations indicate ASIC1 and ASIC2 only in small-medium diameter neurons in mouse. Transcript expression correlates with protein expression, as Western blot analysis reveals expression of both proteins [116]. Immunohistochemical studies indicate that within rat DRG neurons ASIC proteins are present mainly on the plasma membrane of the soma and cellular processes [116]. Two spliced forms, ASIC2a and ASIC2b, colocalize in the same population of DRG neurons [116, 199] with ASIC2a protein expressed by 21% of L4 and L5 DRG neurons [118]. Ligation studies have indicated that ASIC2a can be transported from DRG cell bodies to sensory nerve terminals in the periphery, where they are located specifically at specialized cutaneous mechanosensory terminals, including lanceolate, Meissner, Merkel, penicillate, reticular, and hair follicle palisades as well as some intraepidermal and free myelinated nerve endings [118].

In addition to the above data from rat, ASIC1 and 2 transcripts and proteins have also been found previously in mouse lumbar DRG. Specifically, they have been located in DRG using RT-PCR [114, 117, 121, 124, 125] or Northern blot analysis [117] where they

heteromultimerize with ASIC3 [127, 129]. ASIC2 protein has also been located at mouse cutaneous nerve endings [114, 121]. Correspondingly there are deficits in cutaneous mechanosensation in mice lacking *ASIC2* [114]. Disruption of ASIC1a has no effect on cutaneous mechanical or thermal sensation, in contrast to its role in gut [124]. The role of ASIC1 expression in non-colonic DRG is therefore unclear, although we observed only 18% of neurons in whole DRG expressing ASIC1, suggesting it may play a role in afferents innervating neither colon nor skin, such as those innervating skeletal muscle or other viscera.

Functional Implications of Differential ASIC Expression

Little is presently known of the exact stoichiometry of ASIC channel formation other than it is heteromultimeric in nature consisting of various combinations of ASICs [112, 116, 120, 127, 129]. The proportions observed in the present study for each individual ASIC member differed between whole DRG and colonic neurons, suggesting the heteromultimeric complexes formed by these members differ in composition depending on the regions they innervate. We cannot deduce from current data how many of each ASIC subunit comprises the heteromultimeric complex, but it follows that ASIC3 is more highly represented in those within colonic sensory neurons. The rich diversity in mechanosensitivity of afferents in the skin and the gastrointestinal tract may be a result of the expression of diverse heteromultimeric species. Indeed, the range of alterations of mechanosensitivity in different afferent populations (colonic, gastro-oesophageal and cutaneous) in *ASIC1a*, *2* and *3* mutant mice would support this concept [114, 121, 124, 125]. What is also apparent from these studies on *ASIC* mutant mice is that disruption of any one of the *ASIC* genes fails to abolish any one sensory modality completely; and

instead, the loss of the deleted subunits results in modified sensory transduction suggesting that ASIC subunits may have both overlapping functions and some functional redundancy. Such changes in ASIC knockouts are likely a direct result from the specific loss of the individual *ASIC* gene as deletion of *ASIC2 or 3* does not result in compensatory changes in the expression of other ASICs in DRG [114, 121], spinal cord, brainstem, and brain [117] or ASIC4, TRPV1, or TRPV2 expression [117]. Similarly, deletion of *ASIC1, 2 or 3* does not result in compensatory changes in the expression of other ASIC transcripts in thoracolumbar DRG as determined by quantitative RT-PCR (SM Brierley unpublished observation). Differences in function between different afferent types and tissues is perhaps not surprising given the likely number of functionally active heteromultimeric complexes formed by ASIC members [128] and the variety of different acid-evoked current profiles recorded from DRG [127, 128]. The present study provides further evidence that the extent of expression of individual ASIC members appears to be tissue specific. The development of agonists or antagonists specific for ASIC members and the use of double or triple ASIC knockout mice lacking combinations of these channels will provide much needed information as to the formation of the heteromultimeric complexes and their functionality.

Technical Considerations

Both FISH and laser capture microdissection combined with quantitative RT-PCR were used to quantify mRNA expression of ASIC members in this study. While each of these techniques detects the expression of mRNA, slight differences are apparent. *In situ* hybridization provides analysis of expression at the tissue level as it specifically labels cells expressing targeted mRNA whilst keeping morphology intact. The density of staining within a given cell indicates presence or absence of targeted mRNA; allowing the

percentage of cells expressing the target to be calculated. However, analytical constraints, such as limits of detection of fluorescent label, may underestimate the number of cells expressing the targeted mRNA and confounding factors, such as the presence of autofluorescence, make analysis of abundances on the cellular level difficult to perform. On the other hand, quantitative RT-PCR does quantify the abundance of a targeted mRNA within a given population of cells, although tissue morphology is lost. However, the advent of laser capture microdissection provides the ability to capture specific populations of cells, such as those traced in the present study, allowing quantification of targeted mRNA expression. These factors may contribute to the slight differences observed in ASIC expression and abundance when comparing FISH and quantitative PCR analysis. However, these two techniques combined provide a powerful analysis of the proportions of cells expressing ASIC transcripts and their relative expression in specific population of cells and both agree that ASIC3, which has the lowest abundance in the general thoracolumbar population, is the most highly expressed ASIC transcript in colonic neurons.

Final Conclusions

We conclude that although ASIC1, 2 and 3 are expressed in the general population of thoracolumbar DRG, these transcripts are highly localised specifically within colonic neurons. In particular ASIC3, which has the lowest abundance in the general population, is the most highly expressed ASIC transcript in colonic neurons. The prevalence of ASIC transcripts in neurons innervating the colon supports electrophysiological data showing they make a major contribution to colonic mechanotransduction and therefore may be targets for the treatment of visceral pain.

CHAPTER 5

SELECTIVE ROLE FOR TRPV4 ION CHANNELS IN VISCERAL SENSORY PATHWAYS.

Abstract

Current evidence suggests hypersensitive responses to mechanical stimuli underpin painful sensations experienced by patients suffering from Irritable Bowel Syndrome. TRPV4 is a putatively mechanosensitive ion channel but is yet to be investigated in the gastrointestinal tract. We have quantified the expression of TRPV4 in colonic Dorsal Root Ganglion (DRG) neurons and gastric nodose neurons, and compared these populations with expression in the global DRG or nodose populations respectively. Further, we have assessed the responses to mechanical stimuli applied to the gastrointestinal tract in mice lacking *trpv4* and compared this to their intact littermates. TRPV4 was found to be specifically expressed in colonic DRG neurons in that both the number of cells expressing TRPV4 ($P<0.0001$) and the transcript abundance were significantly ($P<0.001$) greater in colonic DRG neurons than the global DRG population and also the gastric nodose population ($P<0.05$). Functional studies indicate TRPV4 is expressed in nociceptive afferents as responses to mechanical stimuli were significantly ($P<0.001$) decreased in TRPV4 (-/-) mice in those afferent types with high mechanical thresholds but not in those afferents with lower thresholds. Further, immunohistochemical studies indicate TRPV4 is predominantly expressed in the serosal wall and in fibres on the mesenteric blood vessels where it colocalises with CGRP. Finally *trpv4* (-/-) mice demonstrate significantly decreased EMG responses to colorectal distension and TRPV4 is upregulated in patients suffering from active colitis, a syndrome characterized by recurrent abdominal pain. The above results demonstrate TRPV4 is an attractive target for the pharmacological mediation of painful colonic syndromes such as Irritable Bowel Syndrome.

Introduction

Patients suffering Irritable Bowel Syndrome (IBS) demonstrate hypersensitivity to mechanical stimuli in the colon. This is likely to be mediated peripherally by extrinsic afferents projecting from the colon to the spinal cord. The nature of mammalian mechanotransduction is currently an area of intense research. TRPV4 is a putatively mechanosensitive ion channel of the transient receptor potential (TRP) family, but is yet to be characterised in the gastrointestinal tract.

TRPV4

The vanilloid TRPV subfamily (TRPV) was established with the discovery of the nociceptive channel TRPV1 with TRPV4 cloned shortly after [140-142]. Interest in TRPV4 arose due to its homology with *osm-9*, a mechanically sensitive gene from the invertebrate *C. elegans* family [143, 155]. Worms lacking this gene display insensitivity to touch at the worm's anterior or "nose" end, osmotic regulation and some odorants [143]. Interestingly, when mammalian *trpv4* was replaced into *C. elegans* lacking *osm-9*, it was found to rescue the nose touch and osmoregulatory defects [155]. The olfactory defects were not recovered implying divergence in the role of *osm-9* and *trpv4* in olfaction.

Expression

Expression of TRPV4 is widespread, with transcript detected in most tissues, including kidney, heart, brain and lung [142]. Of particular interest is its identification in sensory tissue, including DRG, nodose and trigeminal ganglia, and in mechanosensitive structures

such as the cochlear hair cells, cutaneous nerve endings and merkel cells [142, 144]. In the gastrointestinal tract transcripts of TRPV4 are present throughout the muscular and mucosal layers of the stomach and colon. Further, it is also present in retrogradely labelled gastric nodose neurons, providing evidence it is present in sensory neurons innervating the gut [145]. More recently TRPV4 protein has been identified in rat DRG from spinal levels L3-L6 and mouse DRG from levels L5-L6, spinal regions which do not innervate the colon [144, 200]. TRPV4 protein expression was observed in approximately 10% of mouse DRG [144]. While expression levels were not quantified in the rat, co-labelling was observed with the nociceptive markers Calcitonin Gene Related Peptide (CGRP), Substance P (SP) and PAR_2 (Protease Activated Receptor) [200]. As has been demonstrated with the ASIC family in the previous chapter expression in whole DRG is not necessarily reflective of that in the colonic population and low abundances such as that observed for TRPV4 in the mouse DRG may not correlate with the colonic DRG population [201]. It is entirely plausible that TRPV4 may be widely expressed in all tissues, but the abundance may differ markedly between organs. The first aim of this project is therefore to determine the expression of TRPV4 in mouse colonic DRG neurons relative to that in the DRG as a whole.

TRPV4 Gating

The first description of TRPV4 was its identification as an osmoreceptor activated by cell swelling under hypotonic conditions [142]. Homeostasis of the osmotic balance within the cell is dependent on the ability of the cell to shrink or swell in response to environmental conditions. This is regarded as a form of mechanical stimulation as the extent to which the cell is able to swell or shrink is governed by membrane tension. Since these initial studies

outlining the osmotic activation of TRPV4 it has also been demonstrated to be activated *in vitro* by temperature, shear stress / fluid flow (another form of mechanical stimulus), phorbol esters, anandamide and arachidonic acid, acidic pH, citrate and Bisandrographolide from the Chinese herb *Andrographis paniculata* [146-151]. Temperature is a common activator of TRP channels, but unlike TRPV1, 2 and 3, TRPV4 is activated at temperatures below 30°C [147]. It is also active under physiological temperatures, unlike TRPV1 and 2 which are only thermosensitive to noxious heat [140, 152]. This is important as TRPV4 responds to fluid flow and stress from mechanical shearing at physiological temperatures but not at room temperature, and physiological temperatures potentiate responses to hypotonic stimuli, indicating temperature sensitizes TRPV4 activation [146]. Interestingly TRPV4 mediates mechanical hyperalgesia induced by inflammatory mediators [202].

The polymodality of TRPV4 activation is not only represented by its plethora of ligands but also by the various gating mechanisms discovered so far. The only endogenous ligand discovered as yet is 5'6'-EET, a cytochrome P-450 metabolite of anandamide [151]. Synthetic phorbol esters activate TRPV4 directly (or protein kinase C independently) as is the case for 4αPDD, and indirectly (or protein kinase C dependently) as is the case for PMA [146, 150]. Interestingly these agonists have been used to demonstrate osmotic stimulation of TRPV4 is dependent on phosopholipase A_2 metabolism of anandamide to 5'6'EET, while activation of TRPV4 by temperature and 4αPDD is via an alternate pathway that is either PKC dependent or independent [146, 203]. Further, the induction of mechanical hyperalgesia induced by activation of TRPV4 via inflammatory mediators is mediated by both PKC and PKA second messenger systems [202]. This promiscuity of gating coupled with widespread expression suggests TRPV4 may be an integrator of environmental stimuli, rather than a generator of signals from one type of stimuli.

TRPV4 and Mechanosensation

Despite the complexity concerning TRPV4 gating, there is still compelling evidence that TRPV4 is mechanosensitive, including its localisation in cutaneous and auditory mechanosensitive complexes, the abnormal responses of the *osm-9* mutant to touch and the osmotic / shearing forces gating TRPV4 [142, 144, 146, 154, 155]. Much of this evidence comes from TRPV4 knock out mice as antagonists specific for TRPV4 are yet to be developed. These TRPV4 null mutants demonstrate the expected abnormal osmotic and thermal regulation but also display abnormal responses to pressure, noxious acid and acoustic stress [149, 153-156] . It is interesting to note the altered acoustic response is suggested to be related to a neuroprotective effect rather than mechanosensory role for TRPV4, and possibly represents another function of this diverse receptor.

From a mechanosensitive point of view, the response to tail pressure is of most interest [149]. Both the activation threshold and frequency of discharge of putatively noxious pressure sensing nerves were significantly reduced in response to noxious pressure in mice lacking TRPV4 compared to intact mice. This indicates a greater pressure stimulus is required to activate the channel in mice lacking TRPV4 compared to intact mice. However the pressure response relationship (inactivation by pressure reduction) and mean conductance was unchanged in TRPV4 knock out mice, as was the response to non-noxious touch. This indicates in the skin TRPV4 may function specifically in the detection of noxious mechanical stimuli. However afferent innervation of the skin contains several classes, each of which is tuned to detect different stimuli, and a more thorough investigation of all afferent classes is required before reaching this conclusion [204]. With

these findings in mind we aim to investigate the influence TRPV4 has on mechanosensation in all afferent classes innervating the colon, encompassing low, medium and high threshold afferent classes.

Previous experimental approaches in our laboratory have provided insight into the influence individual ASIC members have on mechanosensation [124, 125]. A similar approach is again to be used, comparing mechanosensation in mice lacking the TRPV4 gene with their intact litter mates. Briefly, extracellular electrophysiological recordings will be made from the pelvic nerve while attached to the colon, as detailed in Figure 1. There are four distinct classes of pelvic afferent ending in the colon, each of which has different thresholds for mechanical stimulation [79-81]. These include the high threshold serosal afferent class which respond only to blunt probing of the serosa, the medium threshold afferent class which respond to circular stretch, the low threshold mucosal afferent class which respond to fine mucosal stroking but not stretch, and the muscular mucosal class which respond both to circular stretch and fine mucosal stroking and are also low threshold [79-81]. In normal events, low threshold afferents would respond to chemical insults and movement of villi on the mucosal surface and medium threshold afferents would respond to distension and contraction of the colon as induced by peristalsis. Neither of these events would be considered to be noxious and are unlikely to reach conscious perception. However the high threshold serosal afferent class would only respond to stress on the outermost layer of the colon, events which would almost certainly be considered to be noxious and would generate pain signals in the CNS. Simultaneous experiments in the laboratory will investigate the mechanosensory role of TRPV4 in the lumbar splanchnic colonic preparation (predominately high threshold) and in the vagal oesophageal preparation (predominately low to mid threshold).

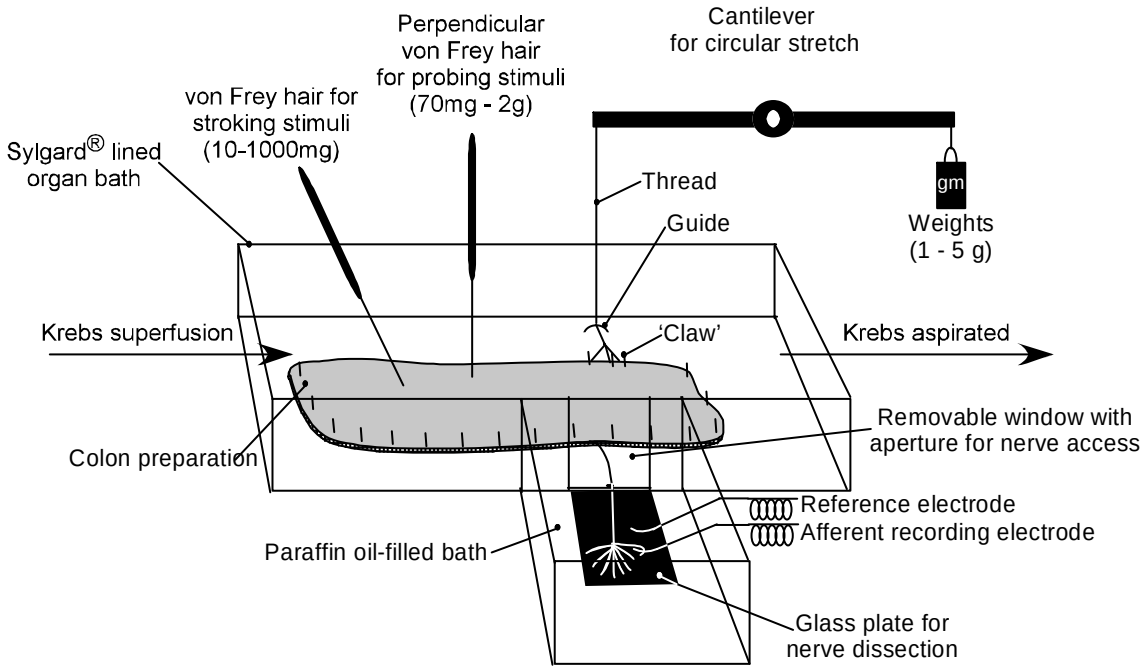

Figure 1: Colonic organ bath. The colon is cut longitudinally and pinned flat in a Krebs filled organ bath. Attached nerves (lumbar splanchnic or pelvic) sit in a paraffin chamber for extracellular electrophysiological recordings.

Aims

The aims are two fold. Firstly we aimed to determine the expression of TRPV4 in colonic versus the general DRG population, and secondly to determine the influence TRPV4 has on colonic mechanosensation.

Methodology

Ethics

All studies were performed in accordance with the guidelines of the Animal Ethics Committees of the Institute for Medical and Veterinary Science, and University of Adelaide.

The methodology used for both retrograde labelling and *in situ* hybridization were essentially as outlined in the previous chapter [201].

Colonic and Gastric Retrograde Labelling

Male or female adult (7-10 week) mice were anaesthetised using inhaled halothane, and, following midline laparotomy either three injections (10uL total) or six injections (20uL total) of cholera toxin subunit B conjugated to fluorescein isothiocyanate (CTB-FITC (Sigma,USA)) were made into the submucosal layer of the descending colon or stomach respectively. The viscera was carefully rinsed with sterile saline after each injection to ensure dye was not incorporated into structures other than the wall of the colon or stomach, and the muscle and skin were then sutured closed. Recovery for all animals was under constant observation in a warm environment. A tracing time of three days was used as this had been previously determined to provide optimal results.

FISH

Probe

A 48mer DIG labelled oligonucleotide probe was designed antisense to 1750-1797 mRNA of the TRPV4 gene (refer to Table 1 for sequence), with the complementary sense probe used as a negative control. They were each provided unlabelled (Geneworks) and 3' tailed with DIG using the oligonucleotide tailing kit (Roche) according to manufacturer's instructions. The efficiency of this reaction was determined prior to use as per the previous chapter and only those probes that had incorporated sufficient label were used.

gene	sequence (5' to 3')	antisense to
TRPV4	TGTGCTGGTGGTTGTCTCTGCGGCGCTCTACCTGGCTGGGATCGAGGC	1750-1797

Table 1: Oligonucleotide code for TRPV4 probe.

Dorsal Root Ganglion and Nodose Ganglion Preparation

Animals were deeply anaesthetized and transcardial perfusion was performed firstly with warm sterile heparinized saline, then ice cold 4% paraformaldehyde (PFA) / 0.1M phosphate buffer followed by ice cold 20% sucrose in 4% paraformaldehyde (PFA) / 0.1M phosphate buffer. Following fixation, DRG from bilateral spinal levels T10-L1 and L6-S1 or nodose ganglion were removed and pooled separately in 20% sucrose / 0.1M phosphate buffer until sunk, then snap frozen in embedding medium.

Hybridization

Serial frozen sections (12μm) were cut, post fixed in 4% PFA at 4°C for 10 minutes and air dried for one hour at room temperature in a sterile environment. Sections were then rehydrated, endogenous biotin blocked and acetylated before being equilibrated in 5X saline sodium citrate (SSC) buffer. The slides were prehybridised with hybridization buffer for two hours at 37°C. Sections were then washed in 5XSSC for 10 minutes at room temperature. Individual probes were dissolved in hybridization buffer, applied to sections and hybridised overnight in an airtight moist hybridization chamber at 37°C. Following hybridization sections were washed firstly in 1XSSC then 0.5XSSC for 30 minutes each at 55°C. They were then equilibrated to room temperature in 0.5XSSC

Detection of DIG-Labelled Hybrids

Detection of the DIG label was performed using CARD amplification (Perkin-Elmer) combined with streptavidin conjugated 546 (Invitrogen, La Jolla, CA). Sections were incubated firstly in blocking solution (Perkin-Elmer) for 30 minutes then anti-DIG horse radish peroxidase conjugated Fab fragments (Roche) at a dilution of 1:100 in blocking solution for a further 30 minutes. The sections were then incubated for 20 minutes in biotin labelled tyramide (Perkin Elmer) diluted 1:50 in the provided amplification buffer, before being incubated with Alexa Fluor 546 conjugated streptavidin at 1:200 in blocking solution for 50 minutes. Slides were then coverslipped with Prolong antifade (Invitrogen) and screened under an epifluorescent microscope (Olympus BX51) using filters appropriate for FITC and SA546 labelling.

Quantification + Statistics

Digital images were captured (Cool Snap Fx, Photometrics, USA) and processed using V++ software v 4.0 (Digital Optics, New Zealand). Only neurons with intact nucleus were included in this study. UTHSCSA Image tool v3.0 (The University of Texas Health Science Centre, San Antonio, TX, USA) was used to quantify labelled neurons and measure their diameters. The abundance of labelled neurons was expressed as percentage of neurons labelled in whole DRG section. This was counted from at least 6 DRG sections per mouse and averaged across six mice. The amount of neurons labelled non-specifically, as detected on the serial sense slide and confirmed using a filter outside the emission spectra of FITC or SA546, was subtracted from the amount of staining recorded on positively labelled tissue. The cross sectional diameter was measured from two different angles (shortest and longest distances) and averaged for measurements of diameter in a representative 96 neurons per targeted tissue (n=6). Exposure times and brightness/contrast levels are constant between TRPV4 probe and its negative control. Unpaired t-tests were used to determine differences between populations ($P<0.05$).

Colonic Electrophysiological Recordings

Generation of TRPV4 Knock Out Mice

Mice with disrupted TRPV4 gene were generated at Duke University, North Carolina, USA as previously described and kindly donated by W. Liedtke [154]. Briefly the gene for TRPV4 was disrupted by *cre-lox* mediated excision of the pore loop domain and adjacent transmembrane domains [154]. Heterozygote pairs (+/-) were mated to generate animals for

the current experiments. Homozygous TRPV4 (+/+) or (-/-) mice were randomly selected after genotyping. Mice lacking TRPV4 and their wild type littermates were indistinguishable by body weight, general behaviour or gross anatomical features of the gut or elsewhere.

Pelvic Nerve Dissection

Male and female mice (TRPV4 (+/+) or (-/-)) 20-30 gm were sacrificed via CO_2 inhalation and cervical dislocation. The colon (5-6cm) and mesentery were removed into ice cold Krebs' with the major pelvic ganglion and pelvic nerve attached. Extraneous tissue was removed from pelvic nerve and the distal colon was then opened longitudinally along the anti-mesenteric border. The tissue was pinned flat, mucosal side up, in a specialized organ bath consisting of two adjacent compartments machined from clear acrylic (Danz Instrument Service, Adelaide, South Australia), the floors of which were lined with Sylgard (Dow Corning Corp., Midland, MI, USA.). The pelvic nerve was gently extended from the tissue onto a mirror in the adjacent recording chamber. A moveable wall containing a small opening to allow passage of nerve was lowered into position and the recording bath filled with paraffin oil. The colonic compartment was superfused with a modified Krebs' solution (in mM: 117.9 NaCl, 4.7 KCl, 25 $NaHCO_3$, 1.3 NaH_2PO_4, 1.2 $MgSO4(H_2O)_7$, 2.5 $CaCl_2$, 11.1 d-glucose), bubbled with carbogen (95% O_2 / 5% CO_2) at a temperature of 34°C. All preparations contained the L-type calcium channel antagonist nifedipine (1 µM) to suppress smooth muscle activity and the prostaglandin synthesis inhibitor indomethacin (3 µM) to suppress potential inhibitory actions of endogenous prostaglandins. Under a dissecting microscope the nerve sheath encasing the pelvic nerve was gently peeled back to expose the nerve trunk, which was then finely teased into 6-10 bundles. Each bundle was placed

individually onto a platinum recording electrode. A platinum reference electrode rested on the mirror in a small pool of Krebs' solution adjacent to the recording electrode.

Characterisation of Pelvic Afferent Properties

Receptive fields were identified by systematically stroking the mucosal surface and mesenteric attachment with a brush of sufficient stiffness to activate all types of mechanosensitive afferent. Once identified, receptive fields were assessed with three distinct mechanical stimuli to enable classification: focal compression of the receptive field via a perpendicular probing stimulus with calibrated von Frey hairs (70, 160, 600, 1000 and 2000mg; each force applied 5 times for a period of 3 seconds with a 10 second interval), mucosal stroking with calibrated von Frey hairs (10, 200, 500 and 1000mg force; each force applied 10 times) and circular stretch (1-5 gm in 1 gm increments; each weight applied for a period of 1 minute with a 1 minute interval between each application). Stretch was applied via a "claw" made from bent dissection pins attached to the tissue adjacent the receptive field and connected via a cantilever system via thread. Weights were applied to the opposite end of the cantilever system to initiate graded colonic stretch. This system ensures circular and not longitudinal stretch is applied to the tissue. Categorisation of afferent properties was accorded based on previously published classification and consisted of serosal (responding to focal compression only), mucosal (responding to fine mucosal stroking (10mg von Frey hair)), muscular (responding to stretch, but not fine mucosal stroking) or muscular mucosal (responding to both stretch and fine mucosal stoking) [80].

Drug Addition to Receptive Fields

Chemosensitive properties of pelvic nerve afferents to the selective TRPV4 agonist 5'6' epoxyeicosatrienoic acid (5'6' EET) (Cayman Chemical, Michigan, USA) or non selective TRPV4 antagonist Ruthenium Red (Sigma) were determined after mechanical thresholds and stimulus response functions had been established. A small metal ring was placed over the receptive field of interest, residual Krebs' aspirated, and drug applied to the mucosal surface for either 2 (5'6' EET) or 10 (Ruthenium Red) minutes. The drug was then aspirated and mechanical sensitivity of receptive field re-determined. Previous descriptions of this route of administration ensure activation of all layers of the colonic wall [79].

Data Recording and Analysis

Electrical signals generated by nerve fibres placed on the platinum recording electrode were fed into a differential amplifier, filtered, sampled at a rate of 20kHz using a 1401 interface (Cambridge Electronic Design, Cambridge, UK) and stored onto PC. The amplified signal was also used for online audio monitoring. Action potentials were analysed off-line using the Spike 2 wavemark function and discriminated as single units on the basis of distinguishable waveform, amplitude and duration. A maximum of two active units on each recorded strand was allowed to avoid potential errors in discrimination. Data are expressed as mean +/- SEM. n = the number of individual afferents. Data were analysed using the Prism 4 software (Graphpad Software, San Diego, CA, USA), and when appropriate, were analysed using either one or two way analysis of variance (ANOVA). Differences were considered significant at a level of $P < 0.05$.

Stimulus-response functions were constructed by assessing the minimum time between action potentials (maximum instantaneous frequency), mean number of action potentials per bin (mean frequency), mean number of action potentials across the total time (mean rate) and actions potentials per second (spikes per second) generated in response to mechanical stimulus. These measures reflect changes in the initial dynamic stage (instantaneous frequency), and the overall response (mean frequency, spike rate and spikes / sec).

Results

Expression Studies

TRPV4 Expression in Whole DRG and Nodose Ganglia

Using fluorescence *in situ* hybridization (FISH) we investigated the proportion of neurons within thoracolumbar (T10-L1) and lumbosacral (L6-S1) DRG, and nodose ganglia expressing TRPV4 mRNA. Specifically, 22 ± 1% of thoracolumbar DRG neurons, 19 ± 1% of lumbosacral DRG neurons and 22 ± 1% of nodose ganglia neurons expressed transcripts for TRPV4 (N=6 for each probe (Figure 2)). The average cell diameter of TRPV4 expressing neurons in thoracolumbar DRG was 18.3 ± 0.4 µm, while in lumbosacral DRG it was 20.9 ± 0.5 µm and in nodose ganglia it was 14.1 ± 0.3 µm (n=96 neurons per targeted tissue). The restricted variability of cellular diameter indicated labelling of a single population of neurons, with diameter from 10 µm to 30 µm, consistent with small-medium diameter cell bodies (Figure 3) [201]. No labelling was evident in non-neuronal cells.

TRPV4 Expression in Colonic DRG

Subserosal CTB-FITC injections in the distal colon resulted in labelling of 3 ± 0.1% (N=6) neurons in thoracolumbar (T10-L1) DRG and 2 ± 0.2% (N=6) of neurons in lumbosacral (L6-S1) DRG, confirming that colonic afferents represent a small subpopulation of thoracolumbar DRG neurons [69, 71, 79, 201]. In thoracolumbar DRG, the average diameter of retrogradely labelled neurons was 19 ± 0.4 µm. In lumbosacral DRG, the average diameter of retrogradely labelled neurons was 21 ± 0.5 µm (Figure 3). The

diameter of the majority of retrogradely labelled neurons again ranged from 10 to 30 µm in both DRG populations, consistent with small-medium cell bodies observed previously (Figure 3) [69, 201].

In order to investigate proportions of colonic afferents expressing TRPV4, we carried out FISH experiments in conjunction with retrograde tracing. TRPV4 was observed in 65 ± 4% and 58 ± 2% (N=6) of retrogradely labelled thoracolumbar or lumbosacral DRG neurons respectively (Figure 4).

TRPV4 Expression in Gastric Nodose Neurons

Subserosal CTB-FITC injections in the stomach resulted in labelling of 5 ± 0.6% (N=6) neurons in nodose ganglion, confirming that gastric afferents represent a small subpopulation of nodose neurons [205, 206]**.** The average diameter of retrogradely labelled neurons was 15 ± 0.3 µm, with the majority of labelled neurons ranging from 10 to 20 µm (Figure 3). This is consistent with small-medium diameter cell bodies observed previously [206]**.**

In order to investigate proportions of gastric afferents expressing TRPV4, we carried out FISH experiments in conjunction with retrograde tracing. TRPV4 was observed in 43 ± 4% (N=6) of retrogradely labelled nodose ganglia (Figure 4).

In both DRG and nodose ganglia the amount of labelling of TRPV4 was the same regardless of whether ganglia were retrogradely labelled or not, indicating no alterations in TRPV4 expression were induced by the surgical procedure.

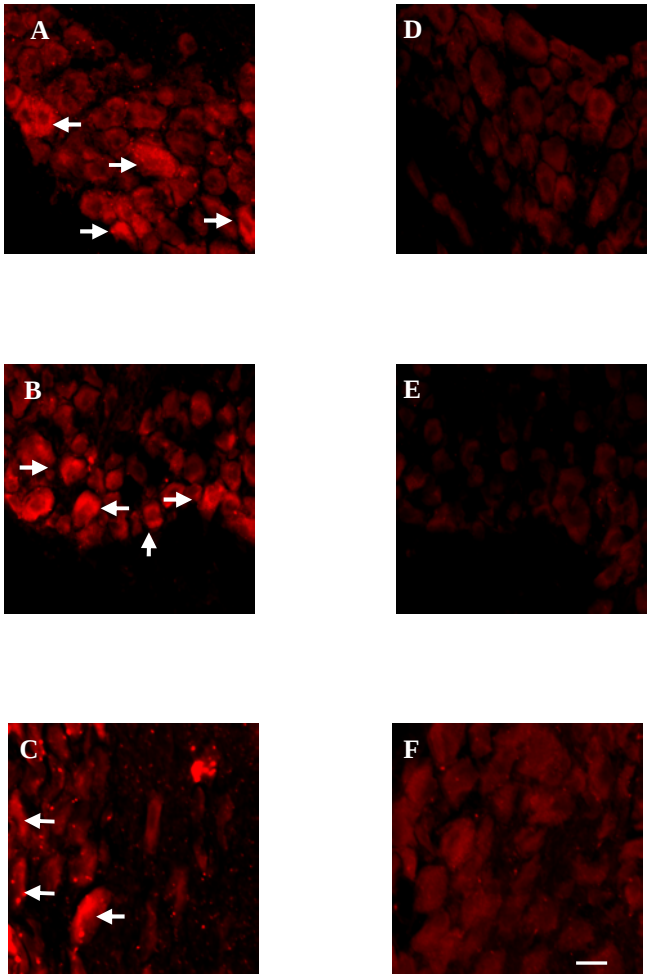

Figure 2: *In situ* hybridisation targeting TRPV4 with streptavidin-546 detection in thoracolumbar (T10-L1) (A), lumbosacral (L6-S1) (B) or nodose (C) ganglia. TRPV4 mRNA expression in **(A)** thoracolumbar, **(B)** lumbosacral, and **(C)** nodose ganglia neurons. Arrows denote examples of positively labelled neurons. **D-F:** The specificity of the mRNA signals were confirmed using negative control studies using the complementary sense probe and serial sections, imaged at identical microscope and software settings. All TRPV4-positive neurons are indicated. Scale bar = 25 μm.

A)

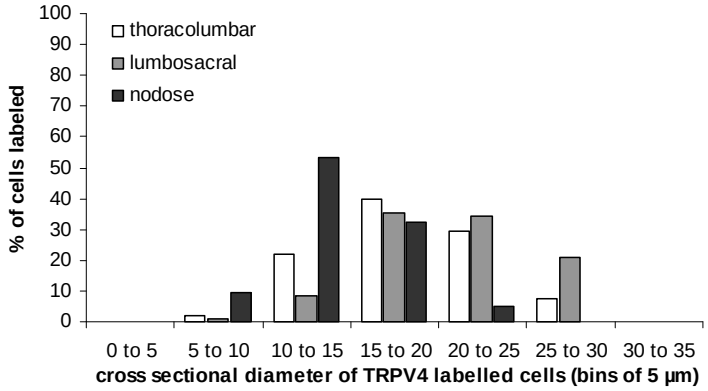

B)

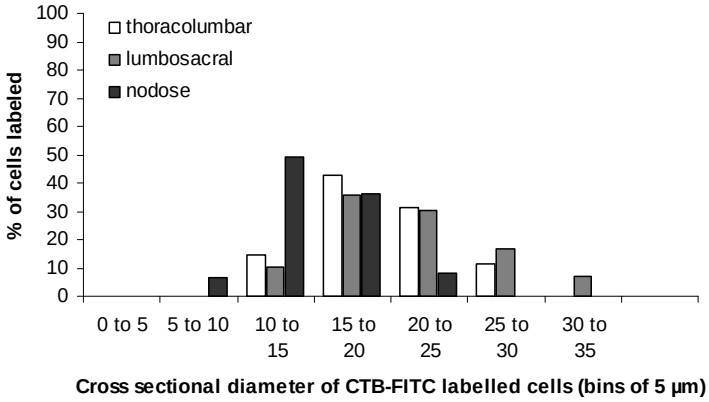

Figure 3: The distribution of the diameters of thoracolumbar or lumbosacral DRG or nodose ganglion neurons labelled by either (A) TRPV4 or (B) CTB-FITC overlap. This graph shows that the neurons expressing TRPV4 have a cross-sectional diameter of 10 – 30 µm, consistent with small-to-medium diameter cells. Similarly, retrogradely labelled colonic neurons have a similar cross-sectional diameter, consistent with classification as small-to-medium diameter cells.

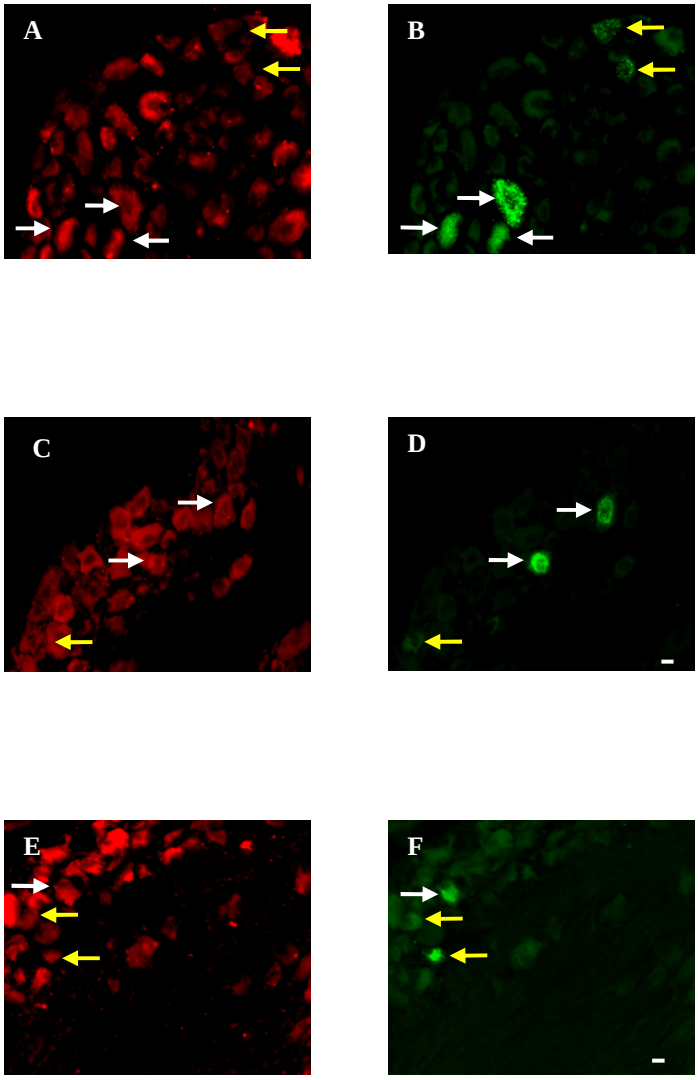

Figure 4: *In situ* hybridisation targeting of TRPV4 in retrogradely labelled colonic or gastric neurons within thoracolumbar and lumbosacral DRG and nodose ganglia. *In situ* hybridisation using probes against TRPV4 labelled with strepavidin-546 (red) in thoracolumbar (A), lumbosacral (C) and nodose (E) sections, with corresponding retrogradely labelled colonic neurons (B, D, F) labelled with CTB-FITC (green). White arrows indicate neurons retrogradely traced from the colon or stomach with CTB-FITC that were also TRPV4-positive. Yellow arrows indicate colonic or gastric neurons, labelled with CTB-FITC, that were TRPV4-negative. Scale bar = 25 μm.

Comparison of Colonic, Gastric and Whole Ganglia Expression

In the thoracolumbar DRG region, 65 ± 4% of retrogradely labelled colonic neurons expressed TRPV4 compared with only 22 ± 1% of neurons in the general population. These data indicate that TRPV4 positive neurons are significantly more prevalent by 195% ($P < 0.0001$) (Figure 5) in the colonic population compared with the general thoracolumbar population. Similar results were observed in the lumbosacral DRG region, where 58 ± 2% of retrogradely labelled colonic neurons expressed TRPV4 compared to only 19 ± 1% in the general population, resulting in an increase of 205% ($P < 0.0001$) (Figure 5).

An increase in TRPV4 abundance was observed in retrogradely labelled gastric neurons (43 ± 4% in gastric cells vs 22 ± 1% in the general population), however this resulted in an increase of only 95% ($P < 0.0001$) (Figure 5).

Overall, the results of the *in situ* hybridization experiments indicate a significantly enhanced expression of TRPV4 within colonic neurons and gastric neurons, but also that more colonic neurons express TRPV4 compared to gastric neurons ($P<0.01$ (thoracolumbar DRG) and $P<0.05$ (lumbosacral DRG))

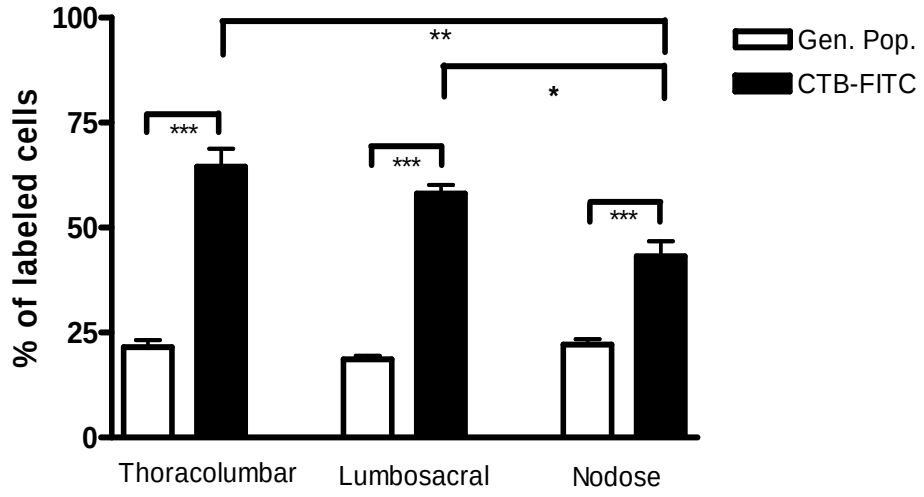

Figure 5: *In situ* hybridisation comparison of the proportions of neurons expressing TRPV4 in the general DRG or nodose population vs colonic (DRG) or gastric (nodose) neurons. Transcript expression of TRPV4 is significantly more abundant in CTB-FITC labelled colonic thoracolumbar and lumbosacral DRG neurons and gastric nodose neurons when compared to expression in the general populations as quantified by *in situ* hybridisation. Expression is also more abundant in colonic neurons than in gastric neurons. This indicates expression of TRPV4 members is more abundant on a tissue level in colonic neurons. Data are means ± SEM. (*** $P<0.0001$, ** $P<0.001$, * $P<0.05$)

Colonic Electrophysiological Recordings

Four classes of colonic mechanosensitive afferent are able to be distinguished from recordings from the pelvic afferent. Characterisation of these classes is dependant on responses to different stimuli, including those that respond only to focal compression with von Frey hair only (serosal class), those that respond to focal compression and mucosal stroking with fine von Frey hair (mucosal), those that respond to focal compression and circular stretch, but not fine mucosal stroking (muscular) and those that respond to focal compression, fine mucosal stroking and circular stretch (muscular / mucosal) (Figures 6 and 7). Of these four classes, serosal afferents account for 20% of the total afferent observed, mucosal for 34%, muscular for 19% and muscular / mucosal for 27% (Figure 8). No differences were observed between afferent proportions in TRPV4 (+/+) and (-/-) mice.

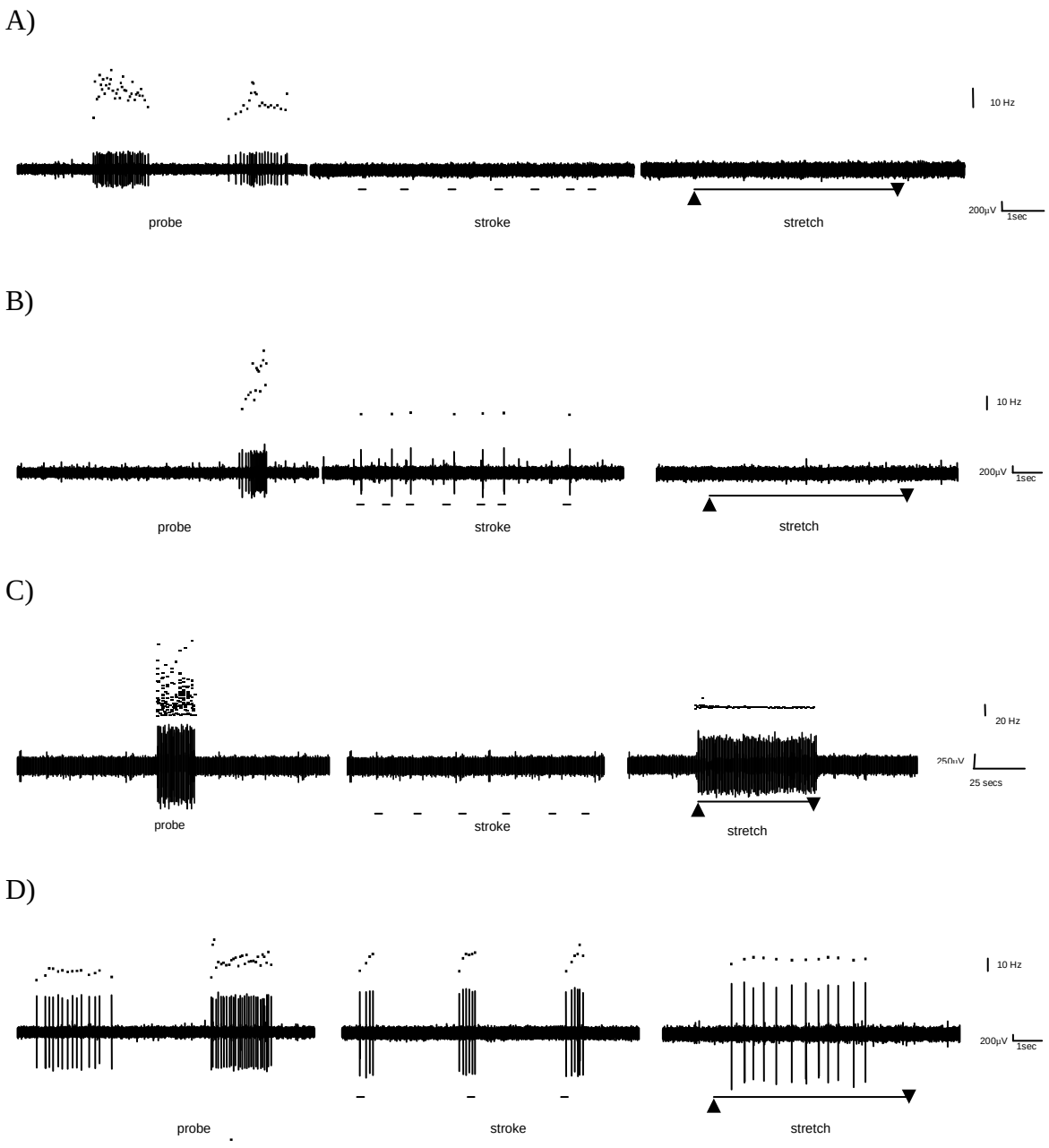

Figure 6: Four classes of pelvic afferent nerve. Four classes of afferent were able to be distinguished in the pelvic afferent, A) serosal, B) mucosal, C) muscular and D) muscular mucosal. Serosal afferents respond only to blunt probing. Mucosal afferents respond to stroking of the mucosa with fine von Frey hair, but not stretch, while muscular afferents respond to circular stretch but not fine stroking and muscular mucosal afferents respond to both fine stroking and circular stretch.

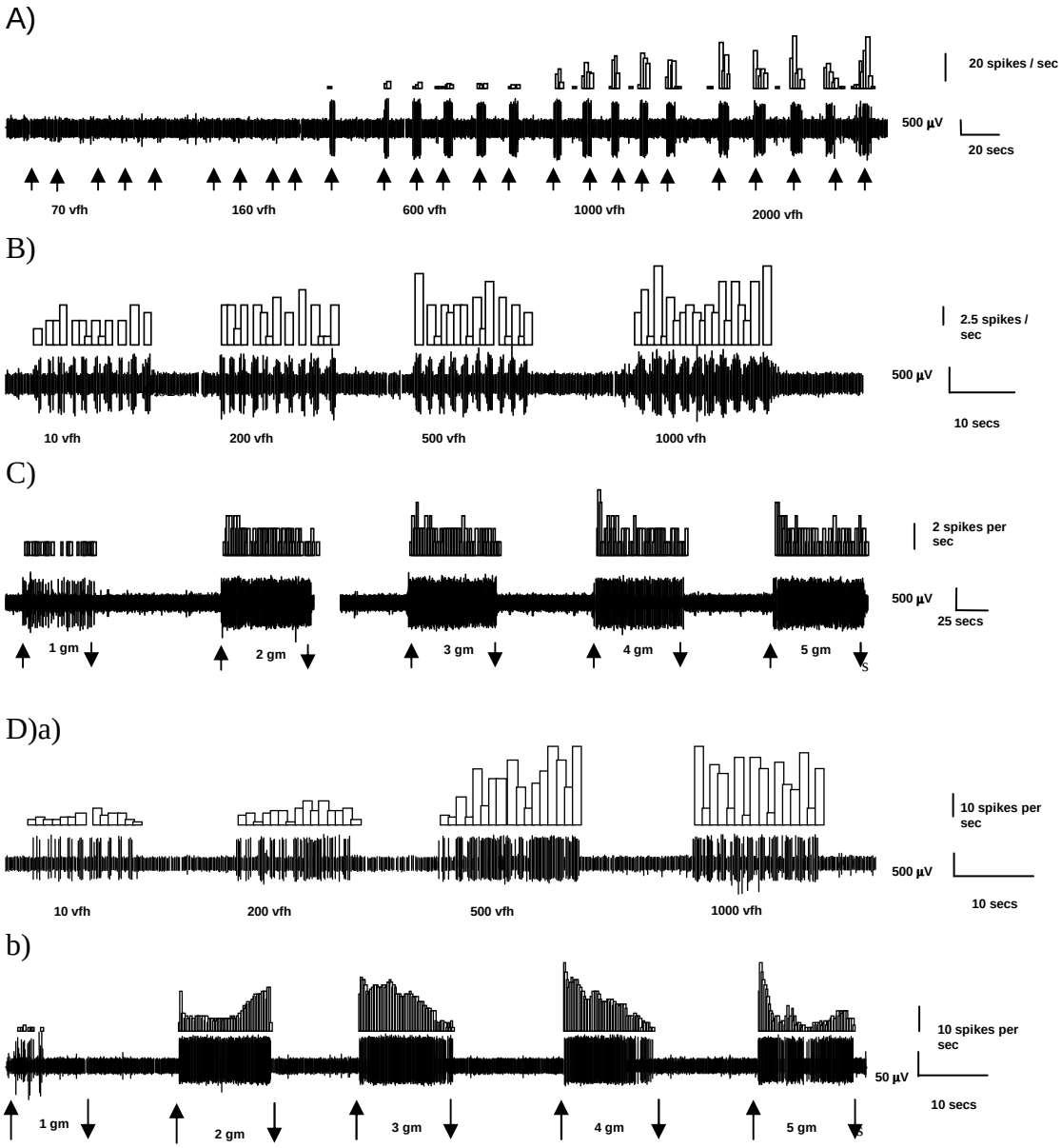

Figure 7: Pelvic afferents respond to mechanical stimuli in a graded manner. Each afferent type responds in a graded manner to specific stimuli. A) Serosal afferent responses to increasing thickness von Frey hairs. B) Mucosal afferent responses to calibrated von Frey hairs. C) Muscular afferent responses to graded circular stretch D) Muscular mucosal responses to calibrated von Frey hairs (a) and graded circular stretch (b).

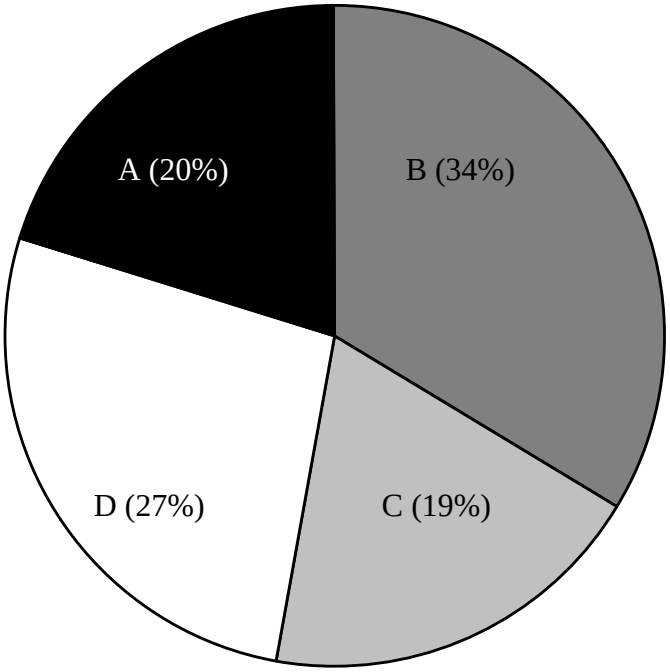

Figure 8: The distribution of afferent classes recorded from the pelvic nerve. The serosal afferent class (A) accounted for 20% of the total afferents observed, mucosal afferents (B) accounted for 34%, muscular afferents (C) accounted for 19%, and muscular mucosal (D) accounted for 27%.

Effect of *trpv4* Deletion on Pelvic Afferents

When responses to mechanical stimuli were compared between TRPV4 (+/+) and their (-/-) litter mates, significant deficits were observed in the serosal afferent subclass (Figure 9). These deficits were significant in all analysis variations tested (i.e. mean instantaneous frequency, mean frequency, rate and spikes per second), indicating the deficits are not restricted to the initial dynamic phase of the stimuli, but affect mechanotransduction throughout the stimulus period (Figure 9). Responses to von Frey hair strengths from 600-2000 mg were significantly decreased in TRPV4 (-/-) mice, with a maximal deficit of 52% recorded at 600 mg von Frey hair when calculated in spikes per second (Figure 9). No alterations in activation threshold were observed in TRPV4 (-/-) mice (data not shown).

No differences to mechanical stimuli were observed between TRPV4 (+/+) and (-/-) mice in mucosal (Figure 10), muscular (Figure 11) or the muscular or mucosal components of muscular mucosal afferents (Figures 12 and 13 respectively). Once again the results were similar between the different analysis variations (mean instantaneous frequency, mean frequency, rate and spikes per second).

Pharmacological Modulation of TRPV4

5’6’ EET Activates Serosal Afferents

5’6’ EET is an endogenous agonist of TRPV4 activity [151]. Significant increases in mechanosensation were observed following addition of this agonist in the serosal afferent population (Figure 14), but not in the mucosal, muscular or muscular mucosal afferent

classes (Figure 15). These results are expressed in spikes per second. Similar results were observed for the other analysis variations.

A dose dependant effect of 5'6' EET was observed when applied for 2 minute incubations in concentrations ranging from 10^{-7} to 10^{-5}M (Figure 14). A maximal increase of 53% was observed in these afferents. To ensure these results were due to activation of TRPV4 and not an as yet uncharacterised target of 5'6' EET these experiments were repeated in TRPV4 (-/-) mice. No significant differences in serosal afferents were observed in TRPV4 (-/-) mice following the addition of 5'6' EET (Figure 14). As the other classes of afferent did not respond to 5'6' EET their responses were not examined in TRPV4 (-/-) mice.

Ruthenium Red Inhibits Serosal Afferents

Selective antagonists for TRPV4 are currently unavailable, and while ruthenium red antagonises TRPV4, it is non-selective and also antagonises other ion channels, such as TRPV1 [207]. Despite this it is currently the only available antagonist of TRPV4. As only the serosal afferent class was affected by TRPV4 deletion, and was also the only afferent class to respond to 5'6' EET, the effect of ruthenium red was tested in this afferent class only. Serosal afferents responded in a dose dependant manner from 10^{-5} to 10^{-4} M, significant at 30^{-5} and 10^{-4} M (Figure 16). A maximal decrease of 57% was observed at 10^{-4} M concentration. Once again the results are expressed as spikes per second, although similar results were observed from the other analysis variations. In order to determine how much of this effect can be attributed to TRPV4 receptor antagonism these experiments were repeated in TRPV4 (-/-) mice. While it is known ruthenium red acts on channels other than

TRPV4, no further decrease in mechanosensation was observed when ruthenium red was added in TRPV4 (-/-) mice (Figure 16).

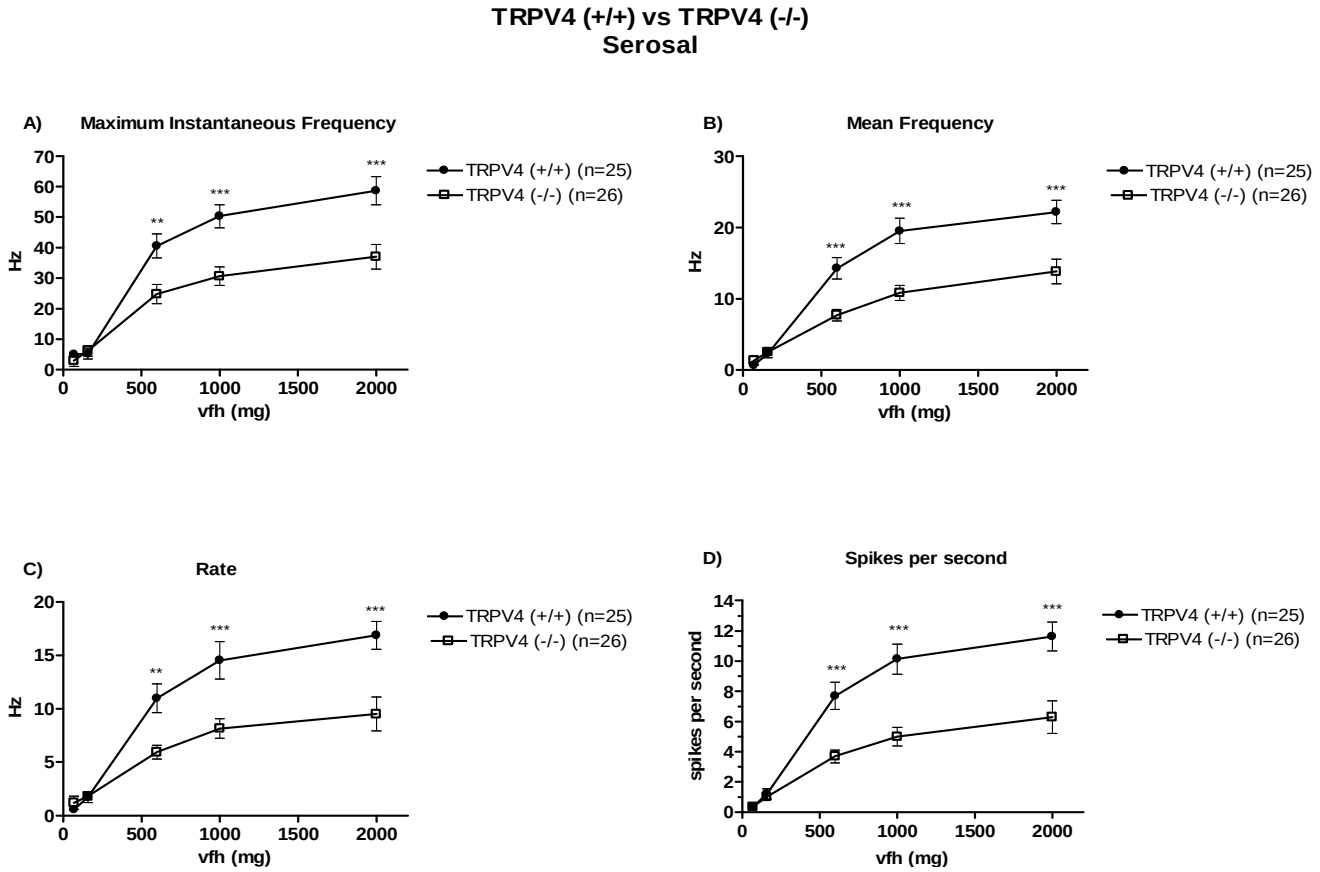

Figure 9: Effect of TRPV4 disruption on pelvic serosal afferent mechanosensitivity. Disruption of TRPV4 resulted in decreased mechanosensitivity when expressed as (A) maximum instantaneous frequency, (B) mean frequency, (C) rate or (D) spikes per second. Data analysed via two way ANOVA with Bonferoni post-hoc test (***P<0.001, **P<0.01)

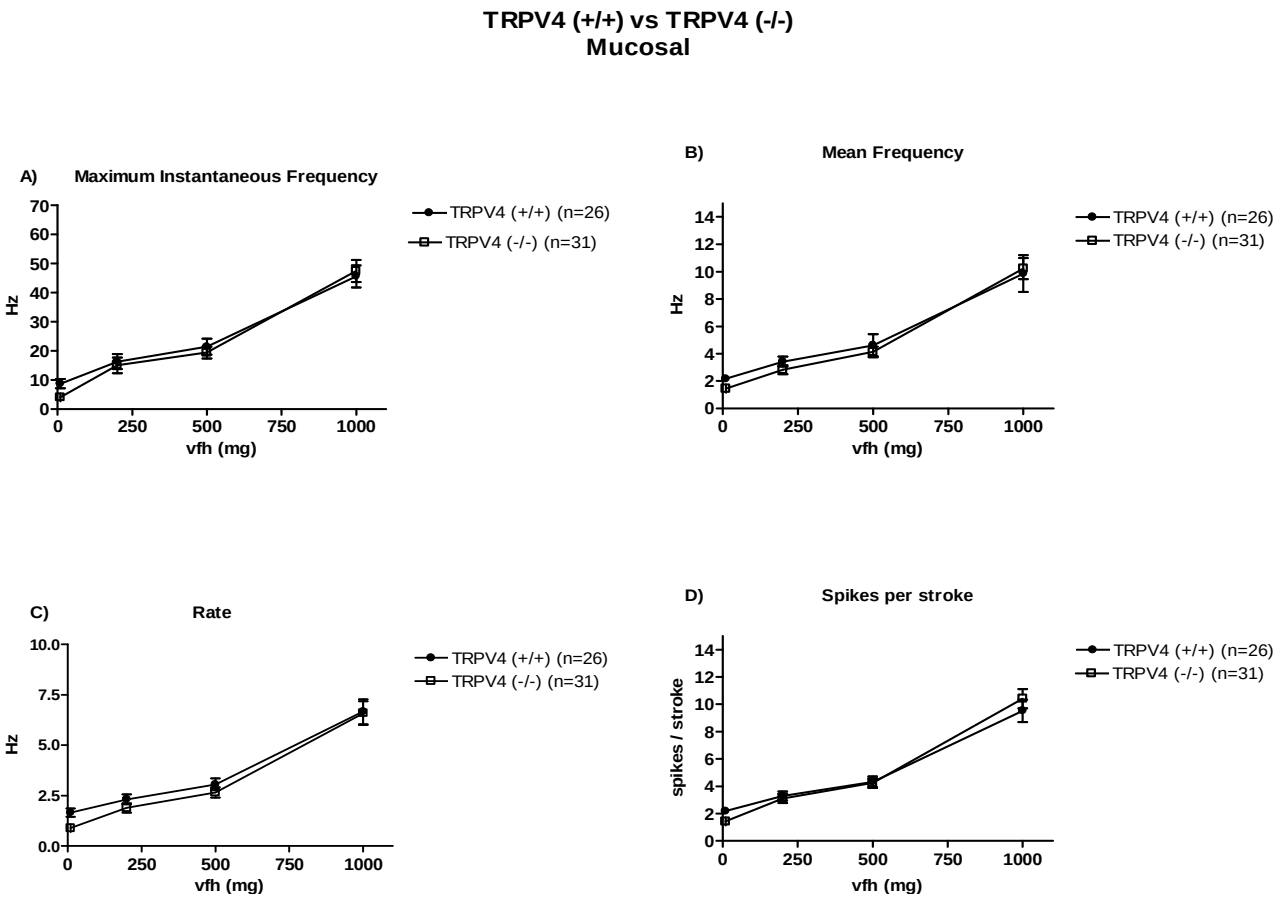

Figure 10: Effect of TRPV4 disruption on pelvic mucosal afferent mechanosensitivity. Disruption of TRPV4 resulted in no change mechanosensitivity when expressed as (A) maximum instantaneous frequency, (B) mean frequency, (C) rate or (D) spikes per second. Data analysed via two way ANOVA with Bonferoni post-hoc test (***P<0.001, **P<0.01)

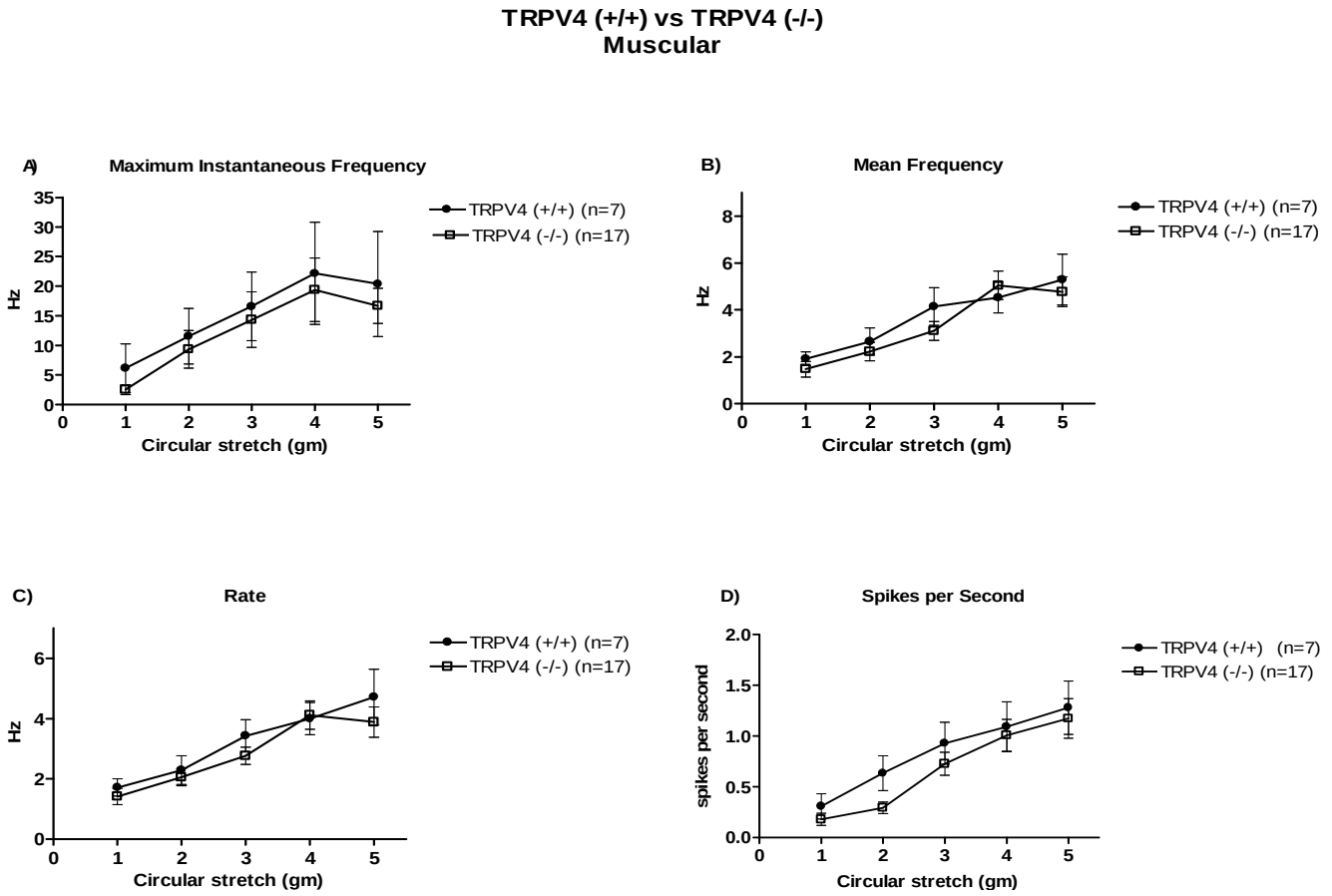

Figure 11: Effect of TRPV4 disruption on pelvic muscular afferent mechanosensitivity. Disruption of TRPV4 resulted in no change mechanosensitivity when expressed as (A) maximum instantaneous frequency, (B) mean frequency, (C) rate or (D) spikes per second. Data analysed via two way ANOVA with Bonferoni post-hoc test (***P<0.001, **P<0.01)

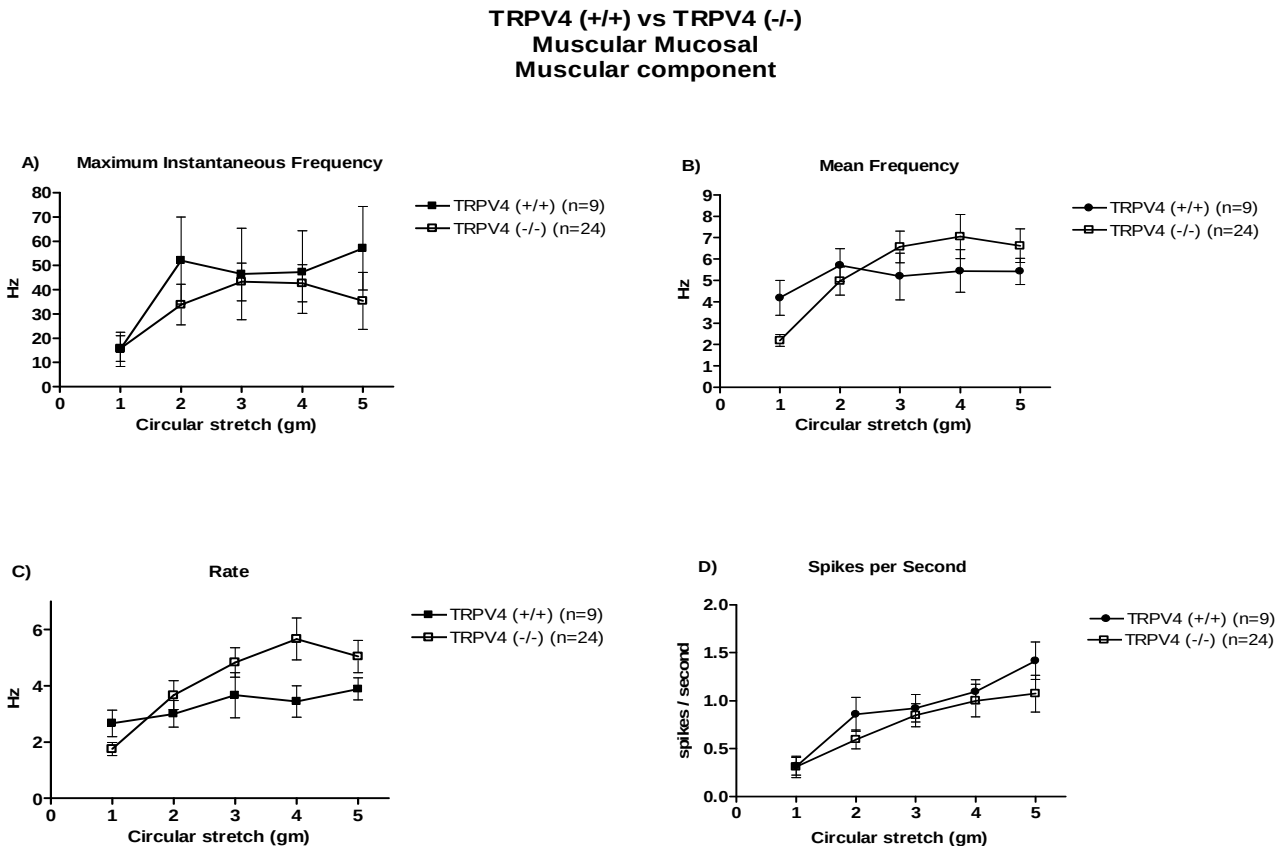

Figure 12: Effect of TRPV4 disruption on the muscular component of the pelvic muscular mucosal afferent mechanosensitivity. Disruption of TRPV4 resulted in no change mechanosensitivity when expressed as (A) maximum instantaneous frequency, (B) mean frequency, (C) rate or (D) spikes per second. Data analysed via two way ANOVA with Bonferoni post-hoc test (***P<0.001, **P<0.01)

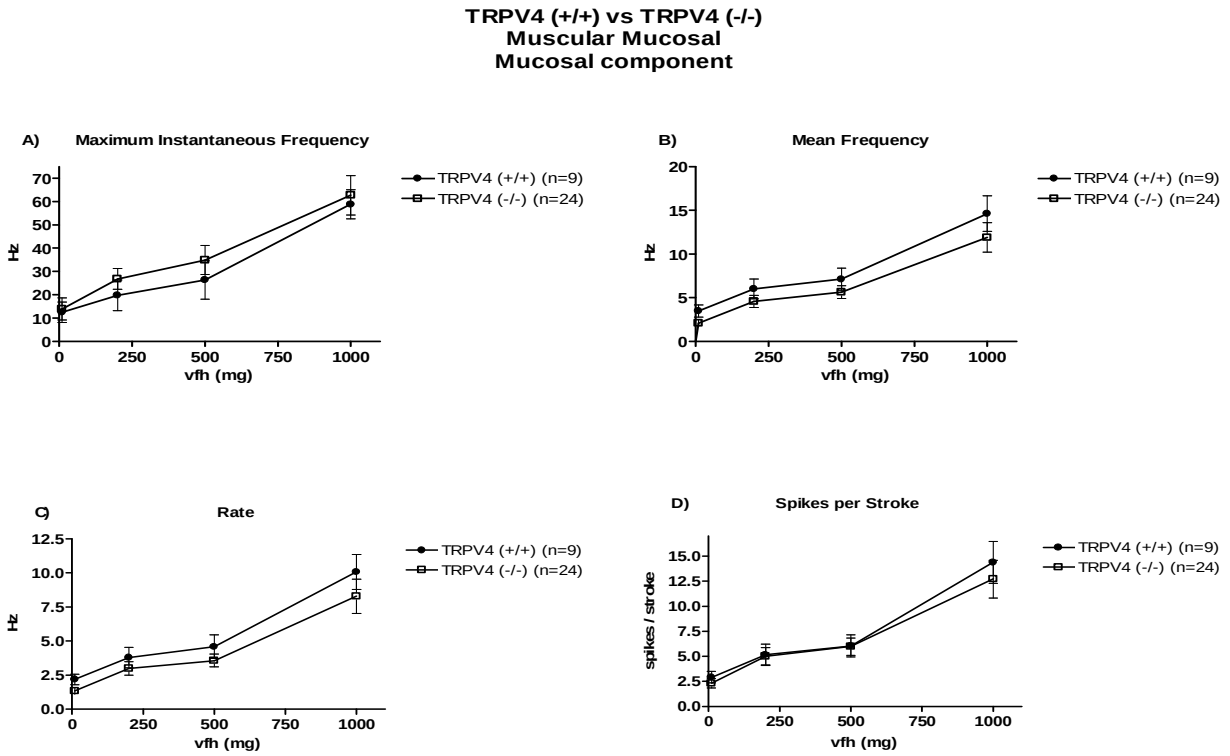

Figure 13: Effect of TRPV4 disruption on the mucosal component of the pelvic muscular mucosal afferent mechanosensitivity. Disruption of TRPV4 resulted in no change mechanosensitivity when expressed as (A) maximum instantaneous frequency, (B) mean frequency, (C) rate or (D) spikes per second. Data analysed via two way ANOVA with Bonferoni post-hoc test (***P<0.001, **P<0.01)

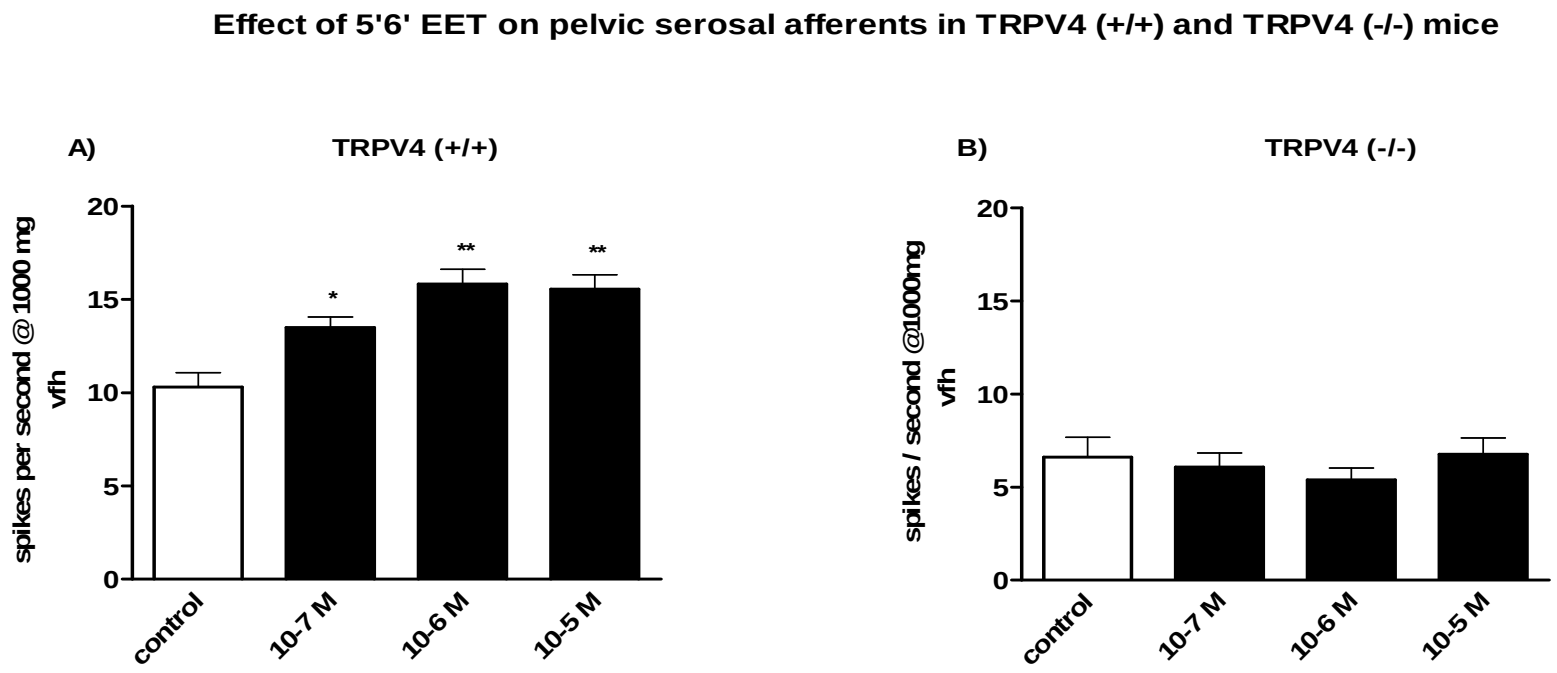

Figure 14: Mechanosensory effect of the TRPV4 agonist 5'6' EET on serosal afferents in A) TRPV4 (+/+) mice and B) TRPV4 (-/-) mice. Effect on mechanosensation expressed as change in spikes per second response at 1000 mg von Frey hair to increasing concentrations of 5'6' EET as compared to control. Addition of 5'6' EET to pelvic serosal afferents resulted in a significant increase in mechanosensation in TRPV4 (+/+) mice (A) which was not observed in TRPV4 (-/-) mice (B). Data analysed via one way ANOVA with Dunnett post-hoc test (**P<0.01, *P<0.05)

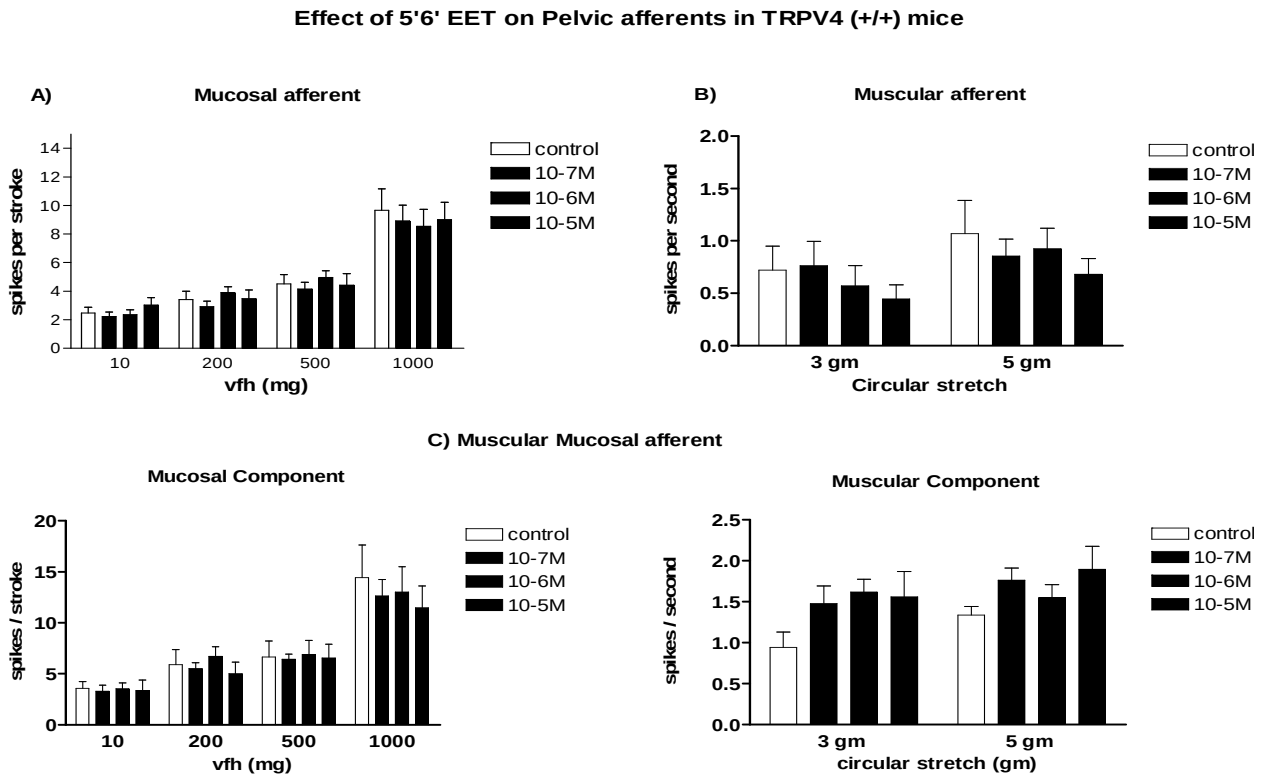

Figure 15: Mechanosensory effect of the TRPV4 agonist 5'6' EET on A) mucosal, B) muscular and C) muscular mucosal afferents in TRPV4 (+/+) mice. Effect on mechanosensation expressed as change in spikes per second response to increasing concentrations of 5'6' EET as compared to control. Addition of 5'6' EET to pelvic serosal afferents did not result in significant changes in mechanosensation in TRPV4 (+/+) in these afferent classes. Data analysed via two way ANOVA with Bonferonni post-hoc test (**P<0.01, *P<0.05)

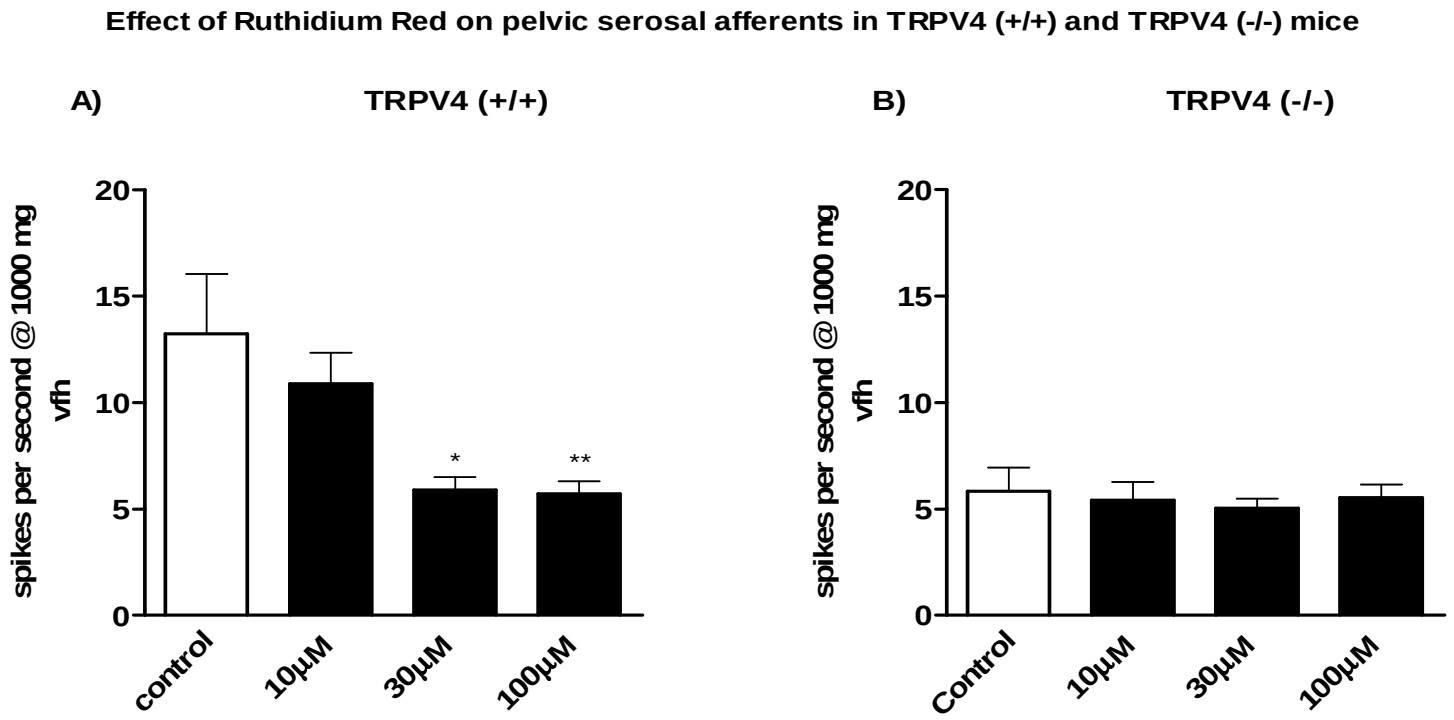

Figure 16: Mechanosensory effect of the TRPV4 anatagonist Ruthenium Red on serosal afferents in A) TRPV4 (+/+) mice and B) TRPV4 (-/-) mice. Effect on mechanosensation expressed as change in spikes per second response at 1000 mg von Frey hair to increasing concentrations of Ruthenium Red as compared to control. Addition of Ruthenium Red to pelvic serosal afferents resulted in a significant decrease in mechanosensation in TRPV4 (+/+) mice (A) which was not observed in TRPV4 (-/-) mice (B). Data analysed via one way ANOVA with Dunnetts' post-hoc test (**P<0.01, *P<0.05)

Discussion

Compelling evidence suggests TRPV4 is involved in mechanosensation, including its localisation in cutaneous and auditory mechanosensitive structures, and specific mechanosensitive deficits following genetic disruption in both invertebrate and mammalian models [142, 144, 149, 155]. Despite this, its role in colonic mechanosensation is yet to be characterized. The aims of this project were firstly to determine the expression of TRPV4 in colonic dorsal root ganglia, and secondly to determine the contribution TRPV4 imparts toward colonic mechanosensation.

TRPV4 Expression

Colonic Expression

Transcripts corresponding to TRPV4 were positively identified by PCR in dorsal root ganglia neurons innervating the colon from both thoracolumbar (T10-L1) and lumbosacral (L6-S1) spinal levels (Figure 17 adapted from Brierley et. al. Gastroenterol. 2008). Two independent lines of inquiry were then used to determine the relative expression of TRPV4 in specifically colonic DRG neurons with that in the general DRG population. Firstly, experiments utilizing FISH technology indicate a significantly greater proportion of colonic DRG neurons express TRPV4 compared to the general thoracolumbar or lumbosacral DRG populations, with increases of approximately 200% observed for each pathway. Secondly, quantitative PCR of laser capture microdissected retrogradely labelled colonic DRG neurons indicated TRPV4 expression was much more abundant in colonic neurons compared to the general population (Figure 18 adapted from Brierley et. al. Gastroenterol. 2008). Further, expression was observed to be much more abundant in colonic neurons innervating the

thoracolumbar DRG regions compared to the lumbosacral regions (Figure 18 adapted from Brierley et. al. Gastroenterol. 2008).

Gastric Expression

TRPV4 expression was also positively identified in gastric nodose ganglia neurons (Figure 17 adapted from Brierley et. al. Gastroenterol. 2008). FISH analysis of retrogradely labelled gastric nodose neurons indicate a significantly greater number of gastric nodose cells express TRPV4 compared to the whole ganglia, however LCM-qPCR analysis indicate a similar abundance of mRNA between the two populations (Figure 18 adapted from Brierley et. al. Gastroenterol. 2008), suggesting more cells express a lower abundance of TRPV4 mRNA in specifically gastric nodose cells compared to the nodose as a whole.

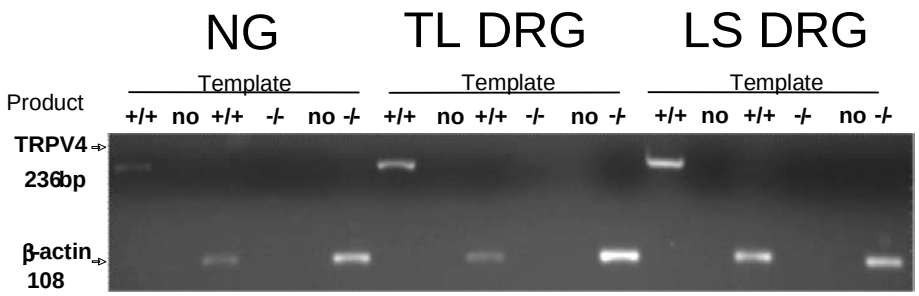

Figure 17: PCR gel of TRPV4 in nodose ganglia (NG), thoracolumbar dorsal root ganglia (TL) and lumbosacral dorsal root ganglia. TRPV4 is present in intact animals (+/+), and not present in TRPV4 knock out animals (-/-) in each of these ganglia. These results are confirmed by the presence of β-actin in (-/-) animals and the absence of product in water controls (no). (adapted from Brierley et. al. Gastroenterol. 2008)

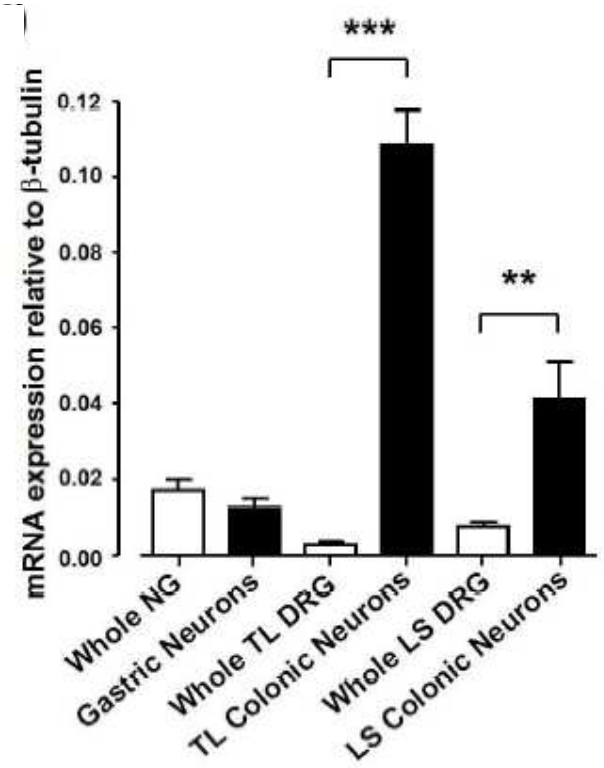

Figure 18: Q-PCR comparison of TRPV4 abundance in whole nodose ganglia, thoracolumbar DRG and lumbosacral DRG vs gastric and colonic populations. The abundance of TRPV4 is greater in whole nodose ganglia (NG) than in whole thoracolumbar (TL) or whole lumbosacral (LS) ganglia. TRPV4 expression is similar in specifically gastric nodose neurons compared to whole nodose ganglia. TRPV4 expression is much greater in colonic thoracolumbar DRG than in whole thoracolumbar DRG, and is also significantly greater in colonic lumbosacral DRG compared to whole thoracolumbar DRG. (adapted from Brierley et. al. Gastroenterol. 2008)

Conclusions From Analysis of Expression

This is the first study to demonstrate TRPV4 expression in colonic DRG and quantify this expression both in proportion of cellular expression and cellular abundance in colonic DRG and gastric nodose neurons. Previous studies have demonstrated expression of TRPV4 is widespread, and it has been identified in dorsal root ganglia and mucosal and muscular layers of the small intestine and stomach and in gastric nodose neurons [142, 144, 145]. As is often the case however, the dorsal root ganglia have previously been taken from spinal levels devoid of colonic innervation (i.e. L4-L5) and quantification of TRPV4 expression has not been undertaken [69]. As demonstrated in the previous chapter with expression of ASIC channels, the abundance in whole ganglia does not necessarily reflect the innervation of the organ of interest [201]. In the case of TRPV4, as observed for ASIC3, the abundance in whole ganglia actually provides an inaccurate representation of the abundance in colonic DRG neurons.

Similar proportions of whole DRG and nodose ganglia neurons expressed TRPV4. These expression levels are in the order previously observed for ASIC1 and ASIC3, and are considered to be low, particularly when compared with other ion channels such as ASIC2 [201]. However the situation in colonic DRG is reversed, with transcript present much more abundantly and in a significantly greater proportion of colonic DRG and gastric nodose neurons than in their respective general populations. Further, a significantly greater proportion of colonic DRG neurons express TRPV4 than the gastric nodose neurons. A similar proportion of colonic neurons express TRPV4 in thoracolumbar and lumbosacral DRG, but the abundance of TRPV4 is much greater in the thoracolumbar colonic population. This indicates that while TRPV4 is present in a similar number of colonic thoracolumbar and lumbosacral DRG neurons, it is present in a much greater concentration (or copy number) in the colonic thoracolumbar DRG

neurons. Together these results indicate TRPV4 may be much more important in the afferent innervation of the colon than the upper gastrointestinal tract. In particular it may be of greater relevance in lumbar splanchnic innervation of the colon than the pelvic innervation.

Influence of TRPV4 on Colonic Mechanosensation

The above studies provide solid rational for experiments to further delineate the role TRPV4 imparts toward colonic mechanotransduction. In an indication of the functional relevance of TRPV4, the increase in expression is similar to that previously demonstrated for ASIC3 [201], which has a demonstrated involvement in colonic mechanotransduction [78, 125]. The afferent innervation of the colon is represented by the lumbar splanchnic and pelvic spinal nervous pathways, while the upper gut is innervated by the vagal nervous pathways. Mechanosensory and chemosensory stimuli from these afferents have previously been investigated in our laboratory and eight different afferent types are able to be distinguished [80, 125]. Six of these are colonic spinal afferents, and the remaining two gastric vagal afferents. These afferent types each have different thresholds for mechanical stimulation depending on the types of stimuli they respond to.

Afferent Innervation of the Colon

Important similarities and differences exist between the lumbar splanchnic and pelvic afferent innervation of the colon [80]. Both of these pathways contain low threshold mucosal afferents, mid threshold muscular afferents and high threshold serosal afferents [80]. Additionally the pelvic pathway also contains low threshold muscular / mucosal afferents which are not present in the lumbar splanchnic pathway, and the lumbar

splanchnic pathway contains high threshold mesenteric afferents which are not present in the pelvic afferent pathway. Afferent proportions also differ between pathways, with the splanchnic pathway predominately comprised of high threshold serosal and mesenteric afferents, while a more even spread of afferent types is represented in the pelvic pathway, with approximately one quarter serosal, one quarter muscular, one quarter mucosal and one quarter muscular mucosal [80]. This means these pathways convey very different information to the spinal cord and CNS. For example, in normal digestion low threshold mucosal afferents would be activated by movement of villi on the mucosal surface, while mid threshold afferents would be activated by distension or contraction as induced by normal peristalsis. Neither of these stimuli are considered to be painful, and it can be argued that neither of these afferents convey information that reaches conscious perception. However in the case of noxious stimuli, such as severe distension or torsion on the mesentery, the higher threshold serosal and mesenteric afferents are activated. Both of these events are considered noxious, and presumably result in painful sensations from the colon. Neither serosal nor mesenteric afferent types would be activated in normal circumstances.

Effect of TRPV4 Deletion on Colonic Innervation

TRPV4 mice engineered to lack the TRPV4 gene (*trpv4* (-/-)) and their wild type litter mates (*trpv4* (+/+)) were used in these studies as antagonists specific for TRPV4 are currently not available. Further, 5’6’ EET, an endogenous agonist selective for TRPV4, and ruthenium red, a non-selective TRPV4 antagonist, were used to determine whether mechanosensitive responses are able to pharmacologically manipulated [150, 151].

TRPV4 (-/-) mice and their (+/+) wild type litter mates were observed to be healthy with no obvious defects. PCR analysis of these mice demonstrates TRPV4 is lacking from

the (-/-) mice (Figure 16). A full complement of afferent classes were observed in both TRPV4 (+/+) and (-/-) mice and no differences were observed between afferent proportions. Electrical activation thresholds and conduction velocities were also observed to be similar between TRPV4 (+/+) and (-/-) mice, indicating disruption of TRPV4 does not alter the biophysical properties of colonic afferents (Figure 19 adapted from Brierley et. al. Gastroenterol. 2008). Hence it is reasonable to infer any alterations in colonic mechanosensitivity are due solely to the removal of TRPV4 and not to extraneous effects associated with genetic disruption.

Pelvic Afferents

Significant reductions in mechanosensation were observed only in the serosal afferent class of the pelvic nerve. No difference was observed in activation threshold, indicating the there is no change in the amount of mechanical stimuli required to activate TRPV4, but there are significant deficits in response generated by mechanical stimuli. No alterations were observed in muscular, mucosal or either of the muscular or mucosal components of the muscular mucosal afferent class. These results were further validated by the use of 5'6' EET, an endogenous TRPV4 agonist, which induced significant increases in mechanosensation in the serosal afferent class and not muscular, mucosal or muscular / mucosal afferent classes. This effect was lost in TRPV4 (-/-) mice implying the selectivity of 5'6 EET for TRPV4. Significant dose dependant decreases in mechanosensation in serosal afferents were observed following the addition of ruthenium red, and again this effect was lost in TRPV4 (-/-) mice. Given the non-selectiveness of this antagonist, including its reputed effects on TRPV1 and structurally related ECaC (Epithelial Ca^{2+}) channels, it was surprising that no further deficits in mechanosensation were observed in the serosal afferent class in TRPV4 (-/-) mice particularly as the concentrations used should be sufficient to antagonise TRPV1 [150,

207, 208]. This is despite the reported involvement of TRPV1 in colonic mechanosensation, particularly in noxious colonic distension [78]. However the authors of this study chose to omit the serosal afferent population, instead focussing on the muscular and mucosal pelvic afferent population. As the effect of deletion of TRPV1 was limited to the muscular afferent class, it is implied mucosal afferents do not express TRPV1. Ruthenium red was not applied to muscular or mucosal afferents in our study, and one explanation of our results is that TRPV1 is not expressed in serosal afferents, and therefore no further deficits are observed in TRPV4 (-/-) mice. However this is unlikely given the colonic distension was in the noxious range activating serosal afferents and the range of painful states this channel has previously been shown to be involved in [78, 209]. More likely, TRPV1 may be expressed in high threshold afferent subclasses, but the impact on mechanotransduction in high threshold colonic afferents may be less than that mediated by TRPV4. In this scenario disruption of TRPV4 lowers mechanosensitivity to levels below the influence of TRPV1, and therefore antagonism of TRPV1 cannot further reduce mechanosensation.

Lumbar Splanchnic Colonic and Vagal Gastric Afferents

Simultaneous experiments investigating lumbar splanchnic innervation of the colon and vagal innervation of the upper gut provided evidence complementing that observed in pelvic afferents. Significant reductions in mechanosensory response and activation threshold were observed in both serosal and mesenteric afferents recorded from the lumbar splanchnic nerve (Figure 20 and 21 adapted from Brierley et. al. Gastroenterol. 2008), while no deficits were observed in either muscular or mucosal afferent classes recorded from the vagal nerve (Figure 22). This indicates both the amount of mechanical stimuli needed to activate the channel is reduced in the splanchnic and the response generated is decreased. Due to the scarcity of muscular and mucosal afferent

classes in the lumbar splanchnic nerve, recordings were not made from these classes. 5’6’ EET and ruthenium red again dose dependently increased or decreased mechanosensation respectively in both serosal and mesenteric lumbar splanchnic afferents in a manner similar to that observed in the pelvic serosal population (results not shown).

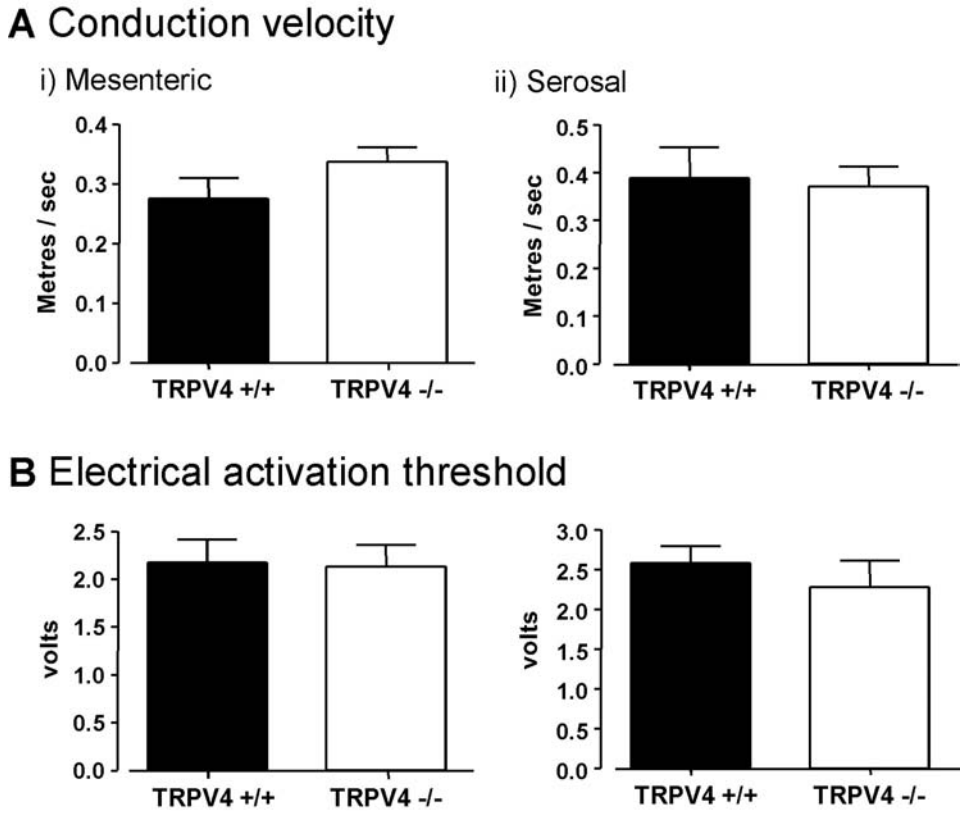

Figure 19: Conduction velocities and electrical activation thresholds are similar in TRPV4 (+/+) and (-/-) mice. This indicates no alterations in biophysical properties of colonic afferents occurs from deletion of TRPV4. (adapted from Brierley et. al. Gastroenterol. 2008).

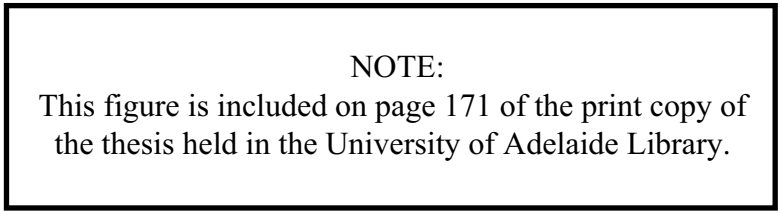

Figure 20: Effect of TRPV4 disruption on lumbar splanchnic A) mesenteric and B) serosal afferent mechanosensitivity. Disruption of TRPV4 resulted in decreases in mechanosensitivity in both mesenteric and serosal afferent types. Data analysed via two way ANOVA with Bonferoni post-hoc test (***P<0.001, **P<0.01) (adapted from Brierley et. al. Gastroenterol. 2008).

Figure 21: Effect of TRPV4 disruption on threshold of activation in lumbar splanchnic A) mesenteric and B) serosal afferent mechanosensitivity. Disruption of TRPV4 resulted in an increase in activation threshold in both mesenteric and serosal afferent types. Data analysed via Fisher's exact test at each point. (**P<0.01, *P<0.05) (adapted from Brierley et. al. Gastroenterol. 2008).

NOTE:
This figure is included on page 173 of the print copy of the thesis held in the University of Adelaide Library.

Figure 22: Effect of TRPV4 disruption on vagal gastric afferent mechanosensitivity. Disruption of TRPV4 resulted in no changes to mechanosensitivity in both mucosal and muscular (tension) afferents (adapted from Brierley et. al. Gastroenterol. 2008).

Further Evidence of the Involvement of TRPV4 in Colonic Mechanosensation

Several experiments conducted concurrently with those above further demonstrate the involvement of TRPV4 in colonic mechanonociception. Firstly, immunohistological staining of mouse colon for TRPV4 demonstrated its predominance in the outermost serosal layer of the colon and scarcity in the muscular and mucosal layers (Figure 21). This corresponds well with our electrophysiological studies indicating its importance in the serosal layer. TRPV4 has previously been described as colocalising with CGRP, a marker of nociceptive neurons in rat DRG neurons [200]. Co-localisation was also demonstrated in our hands, with TRPV4 and CGRP expression overlapping in the serosal layers of the mouse colon, further highlighting its putative role as a colonic nociceptor (Figure 23 adapted from Brierley et. al. Gastroenterol. 2008).

Colorectal balloon experiments replicate symptoms of chronic visceral pain experienced by patients suffering irritable bowel syndrome, namely voluntary contractions of the external abdominal muscles indicative of pain [16, 27, 210, 211]. This represents the behavioural response to visceral nociceptor activation and is relevant to clinical observations. Dramatic reductions of abdominal EMG responses to noxious colorectal distension were observed in mice lacking the TRPV4 gene (Figure 24 adapted from Brierley et. al. Gastroenterol. 2008). No other signs of changes in behaviour or conscious sensory capacity were observed in these mice. This demonstrates the observed changes at the cellular level correspond with alterations in sensory function in intact animals, and correlates well with the putative role of TRPV4 as a nociceptive mechanosensor.

Finally, immunohistological studies in human colon also demonstrated localisation of TRPV4 predominately in fibres innervating the submucosa and serosa, where it was observed usually in close association with blood vessels (Figure 25 adapted from Brierley et. al. Gastroenterol. 2008). As in the mouse circular and longitudinal smooth muscle layers were largely negative. Again this correlates well with the functional studies in mouse, and demonstrates a clear correlation between species. Further, in tissue from patients with active colitis (ulcerative colitis and Crohn's disease), which is characterised by recurrent abdominal pain, increased TRPV4 immunoreactivity was observed in nerve fibres when compared to non-inflamed, uninvolved tissue (Figure 25 adapted from Brierley et. al. Gastroenterol. 2008) [15]. This was particularly evident in the serosa and on those nerves surrounding blood vessels. This again demonstrates an involvement of TRPV4 in painful conditions across mouse and human species.

NOTE:
This figure is included on page 176 of the print copy of the thesis held in the University of Adelaide Library.

Figure 23: Colocalisation of CGRP (red) and TRPV4 in peripheral endings in mouse colon. TRPV4 was predominately identified in the outermost serosal layer of the colon (H), while CGRP labelling was observed throughout the colon (G). Colocalisation was restricted to the outer layers as highlighted by arrows. Mesenteric blood vessels are also flanked by fibres colocalising for TRPV4 (J) and CGRP (I) highlighted by arrows. Whole mounts of mesenteric blood vessels also show colocalisation of TRPV4 (L) and CGRP (K), highlighted by arrows. Scale bars are 250 μm. (adapted from Brierley et. al. Gastroenterol. 2008).

NOTE:
This figure is included on page 177 of the print copy of the thesis held in the University of Adelaide Library.

Figure 24: EMG response to colorectal distension in conscious TRPV4 (+/+) or (-/-) mice. Significantly reduced responses (approx 55%) to colorectal distension were observed in TRPV4 (-/-).(adapted from Brierley et. al. Gastroenterol. 2008).

NOTE:
This figure is included on page 178 of the print copy of the thesis held in the University of Adelaide Library.

Figure 25: Localisation of TRPV4 in human colon from patients suffering from Crohn's disease. TRPV4 labelling was observed in serosal blood vessels (B), in longitudinal muscle within 100µm of serosal border (C), in serosal / mesentery approximately 2 cm from colon, and not observed in muscular or mucosal layers (D). B). bv = blood vessel, ser = serosa, lm = longitudinal muscle, cm = circulat muscle. B-D = 40µm, E = 500µm. (adapted from Brierley et. al. Gastroenterol. 2008).

Is TRPV4 the Colonic Mechanonociceptor?

Previous studies have identified several putatively mechanosensitive ion channels, including members of the ASIC family, NaV1.8, CaV and members of the TRP family. Studies focussing on colonic mechanosensation have so far identified ASIC3 and TRPV1 as mediators of mechanical stimuli [78, 125]. Despite very similar preparations used in these previous studies as to those in the current study, direct comparisons are complicated. For example, serosal afferents were ignored in the study investigating the role of ASIC3 and TRPV1 in colonic mechanosensation mediated by the pelvic afferent population which instead focussed on mucosal and muscular afferents [78]. However ASIC3 was investigated in serosal and mesenteric afferents in the lumbar splanchnic afferent population in an identical manner to that in the current study [125]. Despite being bred on different backgrounds, similar baseline values were observed for ASIC3 (+//+) and TRPV4 (+/+) mice, but the deficits in mechanosensation were much more pronounced in mice lacking TRPV4 than ASIC3. This indicates TRPV4 has a more pronounced role in detection of mechanical stimuli in the lumbar splanchnic innervation of the colon. As ASIC3 and TRPV1 each have previously been described as also mediating muscular afferent mechanosensitivity [78], TRPV4 is also the first colonic mechanosensor described to mediate only high threshold mechanosensation.

Final Conclusions

The results of this study demonstrate the importance of TRPV4 in mediating noxious stimuli in colonic afferents. Expression studies demonstrate TRPV4 is much more abundant in gastrointestinal sensory neurons than in the general sensory cell population, and it is also

much more abundant in colonic DRG than gastric DRG. *In vivo* functional studies indicate mice lacking TRPV4 do not respond to painful stimuli such as that induced by colorectal distension. More thorough examinations of this response using *in vitro* preparations demonstrate modulation of mechanosensation by TRPV4 is restricted to the high threshold (pain sensing) serosal and mesenteric afferent classes. Further, immunohistological staining demonstrates TRPV4 is present in the serosal layer of the colon, but absent in muscular and mucosal layers in both mouse and human tissue. Finally it is also upregulated in painful conditions affecting the colon in humans, such as those experienced in colitis.

TRPV4 is therefore an obvious mediator of noxious mechanical stimuli in the colon, making it an attractive candidate for pharmacotherapeautic treatment of disease states such as Irritable Bowel Syndrome.

CHAPTER 6

TRPA1 MEDIATES DIVERSE QUALITIES OF VISCERAL MECHANOSENSATION

Abstract

The expression of TRPA1 in sensory ganglia is contentious, as are its purported mechanosensory role. We quantified the expression of TRPA1 specifically in colonic Dorsal Root Ganglia (DRG) and gastric nodose ganglia neurons and compared its expression to the global DRG and nodose ganglia populations. Almost half of all DRG or nodose neurons expressed TRPA1 in the global populations. Significantly ($P<0.0001$) more colonic DRG and gastric nodose neurons express TRPA1 than in the global DRG or nodose populations, although the percentage difference observed is numerically small and may not translate to physiological differences. Functional studies indicated TRPA1 is necessary for normal sensing of mechanical stimuli in the gastrointestinal tract. *trpa1* (-/-) mice demonstrated mechanosensensory deficits in afferent subtypes that respond to mucosal stroking in both the colon and upper gut, and those that respond to blunt probing (serosal afferents) in the colon, but not those that respond to circular stretch (muscular afferents) in either the colon or the upper gut. These results indicate TRPA1 has widespread expression, and expression differs between muscular afferent populations in the colon and upper gastrointestinal tract. TRPA1 mediates mechanosensation detected by both high and low threshold afferent classes throughout the gastrointestinal tract, indicating it is not restricted to detection of sensing of painful stimuli.

Introduction

Hypersensitive responses to mechanical stimuli mediate the painful aspects of Irritable Bowel Syndrome. The peripheral sensory endings represent good targets for modulation of this sensation, yet the nature of mechanotransduction at these endings is yet to be deduced. TRPA1 represents a putative mechanosensitive ion channel, but is yet to be characterised in the colon.

TRPA1

TRPA1, the sole member of the TRPA family, was first identified in 1999 [212]. It shares similar topology with other TRP family members, with six transmembrane domains and a pore forming region between the 5^{th} and 6^{th} domains, and functional channels are expected to be homo - tetrameric, although this is yet to be conclusively demonstrated [157, 212]. TRPA1 is distinguished from other TRP members by an ankyrin rich N-terminus estimated to contain approximately 14-18 members [157, 173, 174, 212]. While this number of ankyrin domains is unique in the mammalian TRP family, it is also observed in TRPN1 (NOMPC), a invertebrate mechano-nociceptive TRP channel characterized by 29 ankyrin repeats at the N-terminus [213, 214]. The mammalian homologue of TRPN1 is yet to be identified and TRPA1 is phylogenically distinct. Despite this, the uniqueness of the shared ankyrin repeat motif generated interest in TRPA1 as a mechanosensor. Indeed it has been demonstrated multiple ankyrin repeats of the quantity observed in TRPA1 can act as a gating spring for mechanotransduction in hair cells [215]. Thus interest in TRPA1 as a mechanosensor initiated from its structural properties, unlike the other mechanosensors

described in previous chapters (ASICs and TRPV4) which were based on evidence gleaned from invertebrate models.

TRPA1 is Nociceptive

TRPA1 has been localised to sensory neurons and is gated by noxious stimuli such as noxious cold, pungent compounds (e.g. mustard oil) and inflammatory mediators such as bradykinin, indicating it is likely to confer nociceptive properties.

Expression in Sensory Ganglia

Initial studies identified TRPA1 in mouse DRG neurons but are currently contentious on a number of grounds [165]. In the first instance expression was described as restricted to sensory ganglia (DRG, nodose and trigeminal ganglia) and inner ear, in that it was absent from brain, spinal cord, heart, lung, whiskers and paw skin in mouse [164, 165]. It has since been demonstrated to be present in a much more widespread manner than first reported. Expression has been confirmed in sensory ganglia [159, 162, 167, 168] and transcripts also identified in the CNS, spleen, reproductive organs, buccal mucosa and colon [158-161]. Further, agonists selective for TRPA1 have a demonstrated effect in bladder strips [158]. The abundance of TRPA1 within DRG is also contentious, with estimates ranging from very low (< 5% of neurons), to high (40%-56% of neurons) [162-165]. It is unlikely these issues relate to technical or species issues, as the studies purporting TRPA1 expression to be restricted to DRG differ in abundances observed (5% compared to 40%) and were both in mouse, while those reporting high expression levels were in either mouse (40%) or rat (37% or 56%) [162-164]. The differences in abundances

are more likely to be explained by variations in expression in different levels of DRG. This is difficult to resolve as the levels at which the DRG are taken are for the most part omitted from these reports.

Despite the contentions above, it is clear TRPA1 is primarily expressed in small to medium neurons (Neurofilament 200 negative) that are likely to be nociceptive (CGRP and substance P positive) [163-165, 167]. Interestingly co-localisation of TRPA1 with TRPV1, a nociceptive channel, is observed in the majority of TRPA1 positive DRG neurons raising the possibility that these channels are coupled [159, 165, 167].

Gating by Noxious Stimuli

Expression of TRPA1 in nociceptive neurons is consistent with their activation by known agonists of TRPA1. Initially identified as a thermosensor of noxious cold, it has since been demonstrated to be activated by a number of pungent compounds, all of which are noxious at sufficient concentration, including allyl isothiocyanate (mustard oil), cinnamaldehyde (cinnamon), gingerol (ginger), allicin (garlic) and eugenol (cloves) [165-172]. Interestingly allyl isothiocyanate, cinnamaldehyde and allicin have anti-microbial properties and another anti-microbial with noxious properties, methyl paraben, also activates TRPA1 [216]. While the mechanism of activation is unclear methyl paraben demonstrates selectivity for TRPA1 in that members of the TRPV family are not activated [216]. Antagonists of TRPA1 are limited, with camphor demonstrated to block TRPA1, but also activate TRPV1 and TRPV3 [217].

The electrophilic nature of the pungent chemicals indicates they are likely to act via covalent modification of cysteine residues at the N-terminus rather than directly via the channel pore. Indeed mutations in TRPA1 at cysteine residues resulted in decreased sensitivity to isothiocyanate and cinnamaldehyde, but receptor operated activity is retained as expected as cysteine residues are not present in the pore forming loop [171, 172, 218, 219]. This indicates distinct modes of activation exist for TRPA1, each independent of the other [219].

TRPA1 May be Coupled With Other Nociceptive Mediators

TRPA1 is also activated by the potent inflammatory peptide bradykinin in an indirect manner involving Phospholipase-C (PLC) [168, 170, 172, 220, 221]. Investigations in two separate lines of mice with disrupted TRPA1 demonstrate TRPA1 is indeed necessary for sensitivity to bradykinin since these mice experienced reductions in the nociceptive behaviours and mechanical hyperalgesia [166, 167, 173]. TRPA1 has also been implicated in the actions of TRPV1, a mediator of nociceptive stimuli [141]. TRPA1 is commonly coexpressed with TRPV1 and responses by DRG neurons that respond to both mustard oil and the TRPV1 agonist capsaicin are lost in TRPA1 (-/-) mice, while those DRG neurons that only respond to capsaicin are unaffected [163, 165, 167, 168, 173]. These results indicate TRPA1 may also be coupled with TRPV1. Interestingly intracellular Ca^{2+} is an endogenous ligand of TRPA1, and it has been suggested the activation of TRPA1 mediated by bradykinin or TRPV1 channels may involve the increases in intracellular Ca^{2+} accompanied with activation of these channels [168, 222, 223].

While there is a consensus regarding the involvement of TRPA1 in mediating bradykinin sensitivity, this is not the case with other noxious stimuli. Most obviously, sensing of noxious cold is disrupted in one knock out mouse line, but is intact in another [166, 173]. Several possible reasons exist for this discrepancy. Firstly, there are differences in thresholds to cold between the sexes, with females having a much lower threshold than males [224]. Accordingly Kwan *et. al.* demonstrate a much larger difference was observed in the female knock out line compared to the males, while Bautista *et. al.* used only male mice. Secondly, despite using the same stimuli (acetone and cold plate) each group assessed the changes by different means. Kwan *et. al.* examined the number of times the mouse responded over a period of time, a measure of sensitization, while Bautista *et. al.* examined the time taken for the mice to respond to the stimuli, a measure of the acute component. While it is difficult to directly compare these results, physiological responses to noxious cold do contain both an acute and a more long term response [224]. These results indicate TRPA1 may be involved in sensitization to noxious cold.

A further discrepancy arises with responses to mustard oil and garlic. Deficiencies in pain responses induced by topical application of mustard oil are observed in both strains of TRPA1 knock out mice, and Kwan *et. al.* further demonstrate mice lacking TRPA1 are much less aversive to mustard oil in drinking water [166, 173]. However Bautista *et. al.* report TRPA1 (-/-) mice have complete insensitivity to both allyl isothiocyanate or allicin, the active components of mustard oil and garlic respectively, while Kwan *et. al.* report residual effects of mustard oil in DRG neurons of TRPA1 (-/-) mice [166, 173]. Interestingly these currents are not observed in capsaicin sensitive neurons, indicating the effects of mustard oil persist in the absence of TRPV1 expression in neurons. This suggests mustard oil may not be as selective for TRPA1 as first presumed, as the majority of TRPA1

expressing cells also express TRPV1 [173]. However differences in the design of the TRPA1 null mutants must also be taken into consideration. While both target the pore forming domain and flanking transmembrane channels, the incorporation of an endoplasmic reticulum retention signal in the line generated by Kwan *et. al.* ensures disrupted TRPA1 proteins are not transported to the cell surface [173]. Expression of truncated transcripts are observed in the line generated by Baustista *et. al.* and are presumably transported to the cell surface [166]. It is difficult to reconcile the absolute selectivity for TRPA1 by mustard oil observed by Bautista *et. al.* as it and other pungent chemicals react with C-terminal cysteines and not the pore region [171]. These regions are intact in both knock out lines, but it is only the line generated by Kwan *et. al.* that prohibits transport to the cell membrane. Therefore activity observed in the line generated by Kwan *et. al.* should also be observed in that generated by Bautista *et. al.* It is more likely that mustard oil is a non-selective TRPA1 agonist and discrepancies are due to differences between adult DRG and pup trigeminal neurons used in these studies.

TRPA1 as a Mechanosensor

It is clear from the above studies that TRPA1 mediates nociceptive properties, is polymodal and gated via a variety of different mechanisms. Localisation to DRG and nociception auger well for a mechanosensory ability of TRPA1, but do not directly imply it. It was the structural properties of TRPA1, with multiple ankyrin repeats, that first generated interest in its ability to sense mechanical stimuli. In one of the first descriptions of putative mechanosensory properties of TRPA1, Corey *et. al.* undertook extensive analysis of the expression of the entire mammalian TRP family in the mouse inner ear, and of the 33 family members tested, only TRPA1 and TRPML3 positively labelled cells in this area

[174]. The sense of hearing involves movement of hair bristles in the inner ear, a form of mechanosensation. TRPML3 had previously been identified as a gene involved in spontaneous deafness in mice, and postulated to be involved in sensory transduction [225]. Further studies demonstrated localisation to lysosomes within cells where it is likely to be involved in transport of organelles [225-227]. As it is not localised to the plasma membrane it is an unlikely candidate for transduction of mechanosensory stimuli. However the detection of TRPA1 was without precedent, particularly as it was localised to known mechanosensory structures within the inner ear [174]. In studies supporting the involvement of TRPA1 in hearing, antisense knockdown of TRPA1a (a TRPA1 orthologue) in zebrafish and siRNA inhibition of TRPA1 in mice reduced transduction currents in hair cells [174]. Despite these findings, no deficits in hearing or balance are demonstrated in either lines of TRPA1 (-/-) mice [166, 173], indicating TRPA1 is not as important in this sense as the RNA inhibiting experiments first demonstrated.

A more indirect means was used to provide further evidence that TRPA1 is directly gated by mechanical stress. TRPA1 transfected cells were assessed for responsiveness to either trinitrophenol or chlorpromazine, two membrane perturbing compounds demonstrated to influence mechanical gating by mechanisms independent of each other [228]. Both compounds activated TRPA1 gating, trinitrophenol in a robust manner and chlorpromazine in a voltage dependent manner, with an increased open probability only at negative potentials, indicating TRPA1 is directly modulated by mechanical forces [228].

Unlike the ASICs and TRPV4 channels, interest in TRPA1 as a mechanosensor did not originate from studies in *C. elegans*. However more recent studies in this invertebrate model of mechanosensation have demonstrated significant deficits do occur in specific

mechanosensory responses when TRPA1 is disrupted [175]. These deficits are recovered when intact *trpa1* is replaced in these animals indicating the response is specific for TRPA1 [175]. Interestingly the deficits are reported to be less than that previously observed for TRPV4, and it is postulated TRPA1 may not be directly gated by mechanical stimuli but in fact may be modulated by second messenger systems such as the PLC pathway previously described [175]. Another more distant invertebrate orthologue, *Drosophila painless*, reacts to isothiocyanate in a manner similar to that of mammalian TRPA1, and mediates the response to noxious mechanical stimuli, but not light touch [229, 230].

The mechanosensory effects of TRPA1 disruption were also examined in both lines of knock out mice, with mixed results [166, 173]. Kwan *et. al.* report significant deficits in response to acute noxious stimuli in cutaneous afferents, in that activation thresholds are higher and paw withdrawal responses elicited are decreased in mice lacking TRPA1 compared to their wild type litter mates [173]. However Bautista *et. al.* report no observable differences between TRPA1 (+/+) and (-/-) mice when they investigated cutaneous afferent mechanosensitivity [166]. It is important to note there are marked differences between protocols. Kwan *et. al.* examined the response to punctuate noxious stimuli, while Bautista *et. al.* examined the low threshold response. While there is disagreement between these studies, it may be TRPA1 mediates mechanosensation only to noxious stimuli, and is not involved in mediation of non-noxious stimuli.

Aims

While it is clear TRPA1 is nociceptive there is considerable controversy about its involvement in mechanotransduction. Its abundance in DRG is contentious and as yet it has not been identified in colonic DRG. We therefore aimed to determine the expression levels of TRPA1 in colonic DRG and gastric nodose neurons and compare this with whole DRG or nodose populations. Further, its involvement in mechanotransduction is also contentious with current indirect indications implying a role in noxious mechanosensation only. We aimed to determine the contribution TRPA1 imparts toward colonic mechanosensation in afferents with low, medium and high thresholds to mechanical stress to determine whether TRPA1 is restricted to detection of noxious stimuli in the colon or has a more widespread role.

Methodology

Ethics

All studies were performed in accordance with the guidelines of the Animal Ethics Committees of the Institute for Medical and Veterinary Science, and University of Adelaide.

The methodology used for both retrograde labelling and *in situ* hybridization were essentially as outlined in the previous chapters [201].

Colonic and Gastic Retrograde Labelling

Male or female adult (7-10 week) mice were anaesthetised using inhaled halothane, and, following midline laparotomy either three injections (10uL total) or six injections (20uL total) of cholera toxin subunit B conjugated to fluorescein isothiocyanate (CTB-FITC (Sigma,USA)) were made into the submucosal layer of the descending colon or stomach respectively. The viscera was carefully rinsed with sterile saline after each injection to ensure dye was not incorporated into structures other than the wall of the colon or stomach, and the muscle and skin were then sutured closed. Recovery for all animals was under constant observation in a warm environment. A tracing time of three days was used as this had been previously determined to provide optimal results.

FISH

Probe

A 48mer DIG labelled oligonucleotide probe was designed antisense to 1561 to 1609 mRNA of the TRPA1 gene (refer to Table 1 for sequence)**,** with the complementary sense probe used as a negative control. They were each provided unlabelled (Geneworks) and 3' tailed with DIG using the oligonucleotide tailing kit (Roche) according to manufacturer's instructions. The efficiency of this reaction was determined prior to use as per the previous chapter and only those probes that had incorporated sufficient label were used.

gene	sequence (5' to 3')	antisense to
TRPA1	CCAGACTCACATGGGTGGGTACCTCCGCAGTACGTTTCGTCAGGTCGG	1561-1609

Table 1: Oligonucleotide code for TRPA1 probe.

Dorsal Root Ganglion and Nodose Ganglion Preparation

Animals were deeply anaesthetized and transcardial perfusion was performed firstly with warm sterile heparinized saline, followed by ice cold 4% paraformaldehyde (PFA) / 0.1M phosphate buffer then ice cold 20% sucrose in 4% paraformaldehyde (PFA) / 0.1M phosphate buffer. Following fixation, DRG from bilateral spinal levels T10-L1 and L6-S1 or nodose ganglion were removed and pooled separately in 20% sucrose / 0.1M phosphate buffer until sunk, then snap frozen in embedding medium.

Hybridization

Serial frozen sections (12μm) were cut, post fixed in 4% PFA at 4°C for 10 minutes and air dried for one hour at room temperature in a sterile environment. Sections were then rehydrated, endogenous biotin blocked and acetylated before being equilibrated in 5X saline sodium citrate (SSC) buffer. The slides were prehybridised with hybridization buffer for two hours at 37°C. Sections were then washed in 5XSSC for 10 minutes at room temperature. Individual probes were dissolved in hybridization buffer, applied to sections and hybridised overnight in an airtight moist hybridization chamber at 37°C. Following hybridization sections were washed firstly in 1XSSC then 0.5XSSC for 30 minutes each at 55°C. They were then equilibrated to room temperature in 0.5XSSC.

Detection of DIG-Labelled Hybrids

Detection of the DIG label was performed using CARD amplification (Perkin-Elmer) combined with streptavidin conjugated 546 (Invitrogen, La Jolla, CA). Sections were incubated firstly in blocking solution (Perkin-Elmer) for 30 min then anti-DIG horse radish peroxidase conjugated Fab fragments (Roche) at a dilution of 1:100 in blocking solution for a further 30 min. The sections were then incubated for 20 minutes in biotin labelled tyramide (Perkin Elmer) diluted 1:50 in the provided amplification buffer, before being incubated with Alexa Fluor 546 conjugated streptavidin at 1:200 in blocking solution for 50 minutes. Slides were then coverslipped with Prolong antifade (Invitrogen) and screened under an epifluorescent microscope (Olympus BX51) using filters appropriate for FITC and SA546 labelling.

Quantification + Statistics

Digital images were captured (Cool Snap Fx, Photometrics, USA) and processed using V++ software v 4.0 (Digital Optics, New Zealand). Only neurons with intact nucleus were included in this study. UTHSCSA Image tool v3.0 (The University of Texas Health Science Centre, San Antonio, TX, USA) was used to quantify labelled neurons and measure their diameters. The abundance of labelled neurons was expressed as percentage of neurons labelled in whole DRG section. This was counted from at least 6 DRG sections per mouse and averaged across four to six mice. The amount of neurons labelled non-specifically, as detected on the serial sense slide and confirmed using a filter outside the emission spectra of FITC or SA546, was subtracted from the amount of staining recorded on positively labelled tissue. The cross sectional diameter was measured from two different angles (shortest and longest distances) and averaged for measurements of diameter in a representative 96 neurons per tissue (n=6). Exposure times and brightness/contrast levels are constant between TRPV4 probe and its negative control. Unpaired t-tests were used to determine differences between populations ($P<0.05$).

Colonic Electrophysiological Recordings

Electrophysiological recordings from the pelvic nerve were performed essentially as outlined in chapter 5 for TRPV4.

Generation of TRPV4 Knock Out Mice

Mice with disrupted TRPA1 gene were generated at Harvard University, Massachusetts, USA as previously described and kindly donated by D. Corey and K. Kwan [173]. Briefly the gene for TRPA1 was disrupted by BamHI mediated excision of the pore loop domain and adjacent transmembrane domains which were replaced with an endoplasmic retention signal and stop codon. Products of disrupted genes therefore do not have pore forming domains and are retained in the endoplasmic reticulum. Heterozygote pairs (+/-) were mated to generate animals for the current experiments. Homozygous TRPA1 (+/+) or (-/-) mice were randomly selected after genotyping. Mice lacking TRPA1 and their wild type littermates were indistinguishable by body weight, general behaviour or gross anatomical features of the gut or elsewhere.

Pelvic Nerve Dissection

Male and female mice (TRPA1 (+/+) or (-/-)) 20-30 gm were killed via CO_2 inhalation and cervical dislocation. The colon (5-6cm) and mesentery were removed into ice cold Krebs' with the major pelvic ganglion and pelvic nerve attached. Extraneous tissue was removed from pelvic nerve and the distal colon was then opened longitudinally along the anti-mesenteric border and pinned flat, mucosal side up, in a specialized organ bath (Danz

Instrument Service, Adelaide, South Australia). The pelvic nerve was gently extended from the tissue onto a mirror in the adjacent paraffin oil filled recording chamber. The colonic compartment was superfused with a modified Krebs' solution (in mM: 117.9 NaCl, 4.7 KCl, 25 $NaHCO_3$, 1.3 NaH_2PO_4, 1.2 $MgSO4(H_2O)_7$, 2.5 $CaCl_2$, 11.1 d-glucose, 1 µM nifedipine, 3 µM indomethacin), bubbled with carbogen (95% O_2 / 5% CO_2) at a temperature of 34°C. Under a dissecting microscope the pelvic nerve was finely teased into 6-10 bundles. Each bundle was placed individually onto a platinum recording electrode. A platinum reference electrode rested on the mirror in a small pool of Krebs' solution adjacent to the recording electrode.

Characterisation of Pelvic Afferent Properties

As described previously, receptive fields were identified by systematically stroking the mucosal surface with a force sufficient enough to stimulate all afferent types [79-81]. As in the previous chapter, afferents were then distinguished by specific responses to the following stimuli. Serosal afferents responded only to focal compression of the serosa, muscular afferents also responded to circular stretch, mucosal afferents responded to light (10 mg von Frey hair) stroking of the mucosa but not circular stretch, and muscular mucosal afferents responded to both circular stretch and mucosal stroking. Once classified into either of these afferent classes, receptive fields were then assessed according to afferent type. Serosal afferents were assessed by focal compression of the receptive field via a perpendicular probing stimulus with calibrated von Frey hairs (70, 160, 600, 1000 and 2000mg; each force applied 5 times for a period of 3 seconds with a 10 second interval). Muscular afferents were assessed by circular stretch (1-5 gm in 1 gm increments; each weight applied for a period of 1 minute with a 1 minute interval between each application),

applied via a claw and cantilever system to ensure circular and not longitudinal stretch is applied to the system. Mucosal stroking was assessed by stroking the mucosal with calibrated von Frey hairs (10, 200, 500 and 1000mg force); each force applied 10 times.

Drug Addition to Receptive Fields

Chemosensitive properties of pelvic nerve afferents to the TRPA1 agonist trans-Cinnamaldehyde (TCA) (Sigma) were determined after mechanical thresholds and stimulus response functions had been established. A small metal ring was placed over the receptive field of interest, residual Krebs' aspirated, and drug applied to the mucosal surface for 2 minutes. The drug was then aspirated and mechanical sensitivity of receptive field re-determined. Previous descriptions of this route of administration ensure activation of all layers of the colonic wall [79].

Data Recording and Analysis

Electrical signals generated by nerve fibres placed on the platinum recording electrode were fed into a differential amplifier, filtered, sampled at a rate of 20kHz using a 1401 interface (Cambridge Electronic Design, Cambridge, UK) and stored onto PC. The amplified signal was also used for online audio monitoring. Action potentials were analysed off-line using the Spike 2 wavemark function and discriminated as single units on the basis of distinguishable waveform, amplitude and duration. A maximum of two active units on each recorded strand was allowed to avoid potential errors in discrimination. Data are expressed as mean +/- SEM. n = the number of individual afferents. Data were analysed using the Prism 4 software (Graphpad Software, San Diego, CA, USA), and when appropriate, were

analysed using either one or two way analysis of variance (ANOVA). Differences were considered significant at a level of $P < 0.05$.

Results

Expression studies

TRPA1 Expression in whole DRG and nodose ganglia

Using fluorescence *in situ* hybridization (FISH) we investigated the proportion of neurons within thoracolumbar (T10-L1) and lumbosacral (L6-S1) DRG, and nodose ganglia expressing TRPA1 mRNA. Specifically, 42 ± 2% of thoracolumbar DRG neurons, 40 ± 2% of lumbosacral DRG neurons and 36 ± 2% of nodose ganglia neurons expressed transcripts for TRPA1 (N=6 for thoracolumbar and lumbosacral DRG, N=4 for nodose ganglia (Figure 1)). The average diameter of TRPA1 expressing neurons in thoracolumbar DRG was 18.0 ± 0.5 µm, in lumbosacral DRG it was 18.5 ± 0.5 µm and in nodose ganglia it was 15.3 ± 0.5 µm (n=96 cells for thoracolumbar and lumbosacral DRG, n=64 for nodose ganglia). The restricted variability of cellular diameter indicated labelling of a single population of neurons, with diameter from 10 µm to 30 µm, consistent with small-medium diameter cell bodies (Figure 2) [201]. No labelling was evident in non-neuronal cells.

TRPA1 Expression in Colonic DRG

Subserosal CTB-FITC injections in the distal colon resulted in labelling of 4 ± 0.3% (N=6) neurons in thoracolumbar (T10-L1) DRG and 6 ± 0.4% (N=6) of neurons in lumbosacral (L6-S1) DRG, confirming colonic afferents represent a small subpopulation of DRG neurons [69, 71, 79, 201]. In thoracolumbar DRG, the average diameter of retrogradely labelled neurons was 18.9 ± 0.4 µm. In lumbosacral DRG, the average diameter of

retrogradely labelled neurons was 17.9 ± 0.5 µm (Figure 2). The diameter of the majority of retrogradely labelled neurons again ranged from 10 to 25 µm (Figure 2) in both DRG populations, consistent with small-medium cell bodies observed previously [69, 201].

In order to investigate proportions of colonic afferents expressing TRPA1, we carried out FISH experiments in conjunction with retrograde tracing. TRPA1 was observed in 54 ± 4% and 58 ± 2% (N=6) of retrogradely labelled thoracolumbar or lumbosacral DRG neurons respectively (Figure 3).

TRPA1 Expression in Gastric Nodose Neurons

Subserosal CTB-FITC injections in the stomach resulted in labelling of 4 ± 0.6% (N=4) neurons in nodose ganglion, confirming gastric afferents represent a small subpopulation of nodose neuron [205, 206]. The average diameter of retrogradely labelled neurons was 14 ± 0.4 µm, with the majority of labelled neurons ranging from 10 to 25 µm (Figure 2). This is consistent with small-medium diameter cell bodies observed previously [206].

In order to investigate proportions of gastric afferents expressing TRPA1, we carried out FISH experiments in conjunction with retrograde tracing. TRPA1 was observed in 55 ± 2% (N=4) of retrogradely labelled nodose ganglia (Figure 3).

In both DRG populations and nodose ganglia the amount of labelling of TRPA1 was the same regardless of whether ganglia were retrogradely labelled or not, indicating no alterations in TRPA1 expression were induced by the surgical procedure.

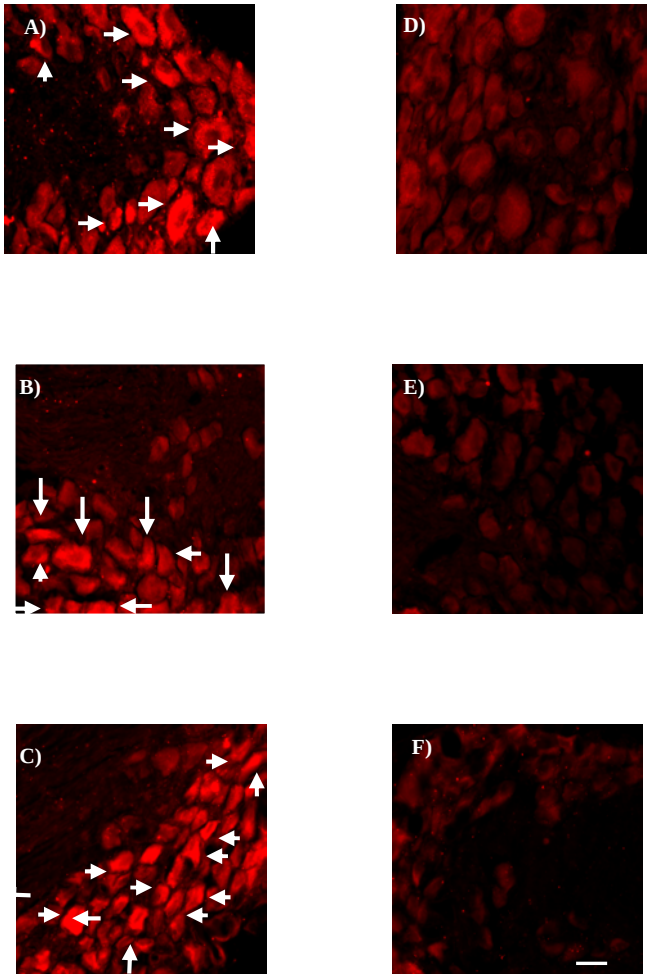

Figure 1: *In situ* hybridisation targeting TRPA1 with streptavidin-546 detection in thoracolumbar (T10-L1) (A), lumbosacral (L6-S1) (B) or nodose (C) ganglia. TRPA1 mRNA expression in **(A)** thoracolumbar, **(B)** lumbosacral, and **(C)** nodose ganglia neurons. Arrows denote examples of positively labelled neurons. **D-F:** The specificity of the mRNA signals were confirmed using negative control studies using the complementary sense probe and serial sections, imaged at identical microscope and software settings. All TRPA1-positive neurons are indicated. Scale bar = 25 μm.

A)

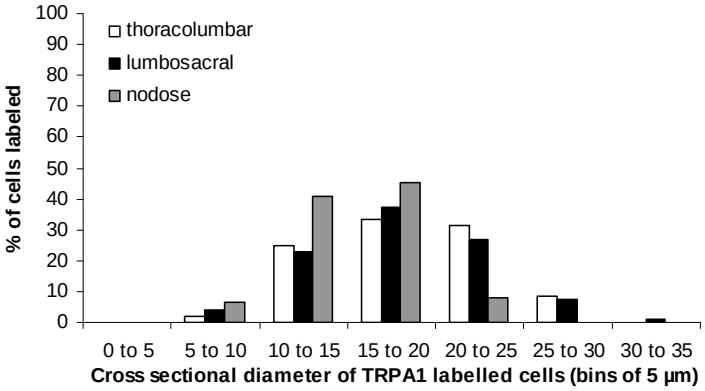

B)

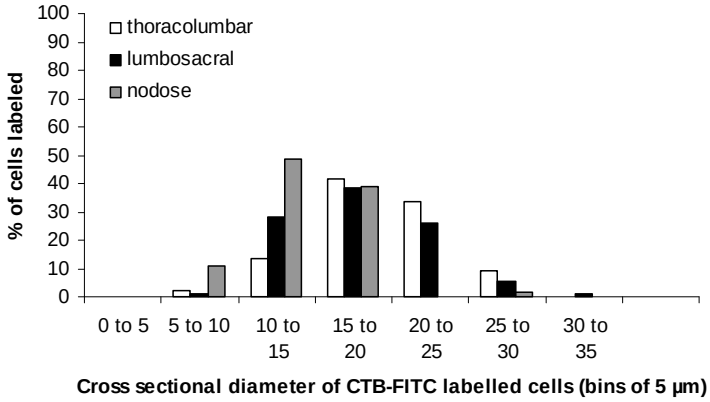

Figure 2: The distribution of the diameters of thoracolumbar or lumbosacral DRG or nodose ganglion neurons labelled by either (A) TRPA1 or (B) CTB-FITC overlap. This graph shows that the neurons expressing TRPA1 have a cross-sectional diameter of 10 – 25 µm, consistent with small-to-medium diameter neurons. Similarly, retrogradely labelled colonic neurons have a similar cross-sectional diameter, consistent with classification as small-to-medium diameter cells

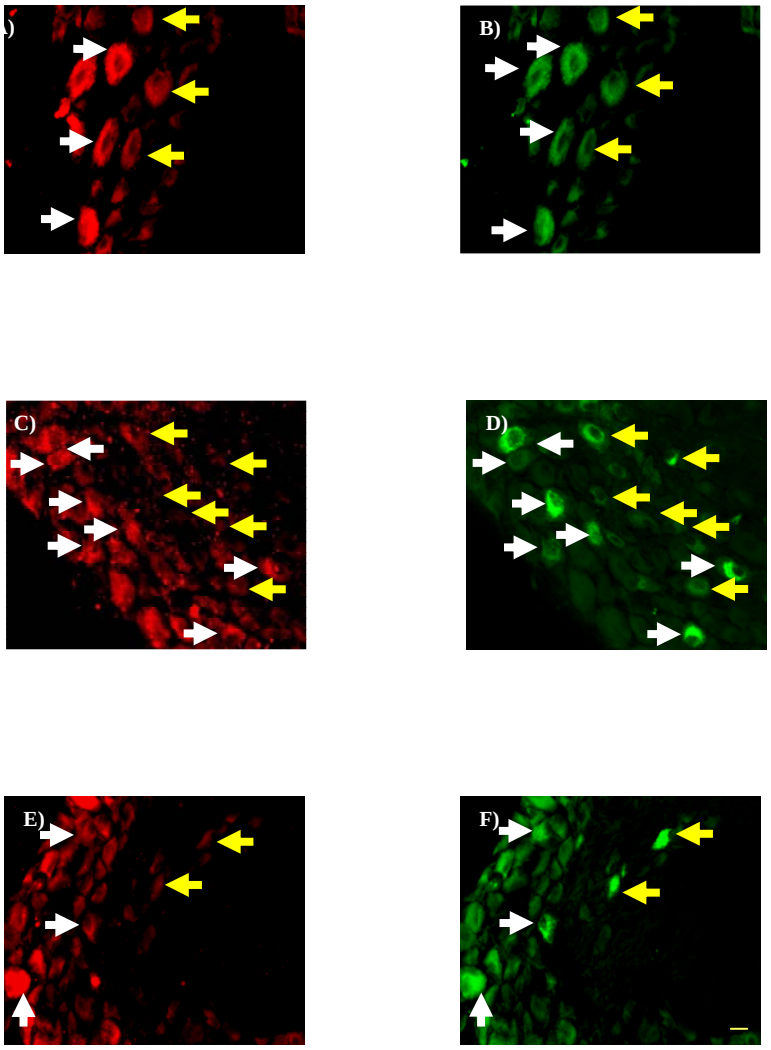

Figure 3: *In situ* hybridisation targeting of TRPA1 in retrogradely labelled colonic or gastric neurons within thoracolumbar and lumbosacral DRG and nodose ganglia. *In situ* hybridisation using probes against TRPA1 labelled with strepavidin-546 (red) in thoracolumbar **(A)**, lumbosacral **(C)** and nodose **(E)** sections, with corresponding retrogradely labelled colonic neurons **(B, D, F)** labelled with CTB-FITC (green). White arrows indicate neurons retrogradely traced from the colon or stomach with CTB-FITC that were also TRPA1-positive. Yellow arrows indicate colonic or gastric neurons, labelled with CTB-FITC, that were TRPA1-negative. Scale bar = 25 μm.

Comparison of colonic, gastric and whole ganglia expression

Significantly ($P < 0.0001$) greater numbers of neurons expressing TRPA1 were observed in colonic thoracolumbar and lumbosacral DRG and gastric nodose ganglia populations compared with unlabelled cells. TRPA1 is 30% more prevalent in colonic thoracolumbar DRG neurons than the general thoracolumbar population, 49% more prevalent in the colonic lumbosacral DRG neurons than the general lumbosacral population and 57% more prevalent in gastric nodose neurons than in the general nodose population (Figure 4). Significant differences in TRPA1 expression were not observed between colonic and gastric populations (Figure 4).

Overall, the results of the *in situ* hybridization experiments indicate a significantly enhanced expression of TRPA1 within colonic neurons and gastric populations, but not between gastric and colonic neurons.

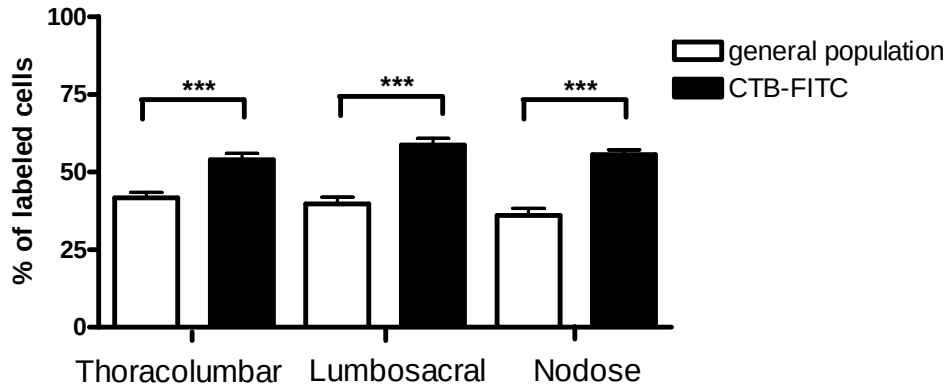

Figure 4: *In situ* hybridisation comparison of the proportions of neurons expressing TRPA1 in the general DRG or nodose population vs colonic (DRG) or gastric (nodose) neurons. Transcript expression of TRPA1 is significantly more abundant in CTB-FITC labelled colonic thoracolumbar and lumbosacral DRG neurons and gastric nodose neurons when compared to expression in the general populations as quantified by *in situ* hybridisation. Data are means ± SEM. (*** P<0.0001)

Colonic Electrophysiological Recordings

Four classes of colonic mechanosensitive afferent were able to be distinguished from pelvic afferent recordings as described previously [78-80]. Characterisations of these classes were based on thresholds to mechanical stimuli as described in chapter 5 for TRPV4 [78-80]. Each of the afferent classes (serosal, mucosal, muscular and muscular mucosal) were observed in TRPA1 (+/+) and (-/-) mice. Each responded to specific mechanical stimuli in a graded manner as described in the previous chapter. Of these four classes, serosal afferents account for 25% of the total afferents observed, mucosal for 37%, muscular for 17% and muscular / mucosal for 21% (Figure 5). No differences were observed between afferent proportions in TRPA1 (+/+) and (-/-) mice.

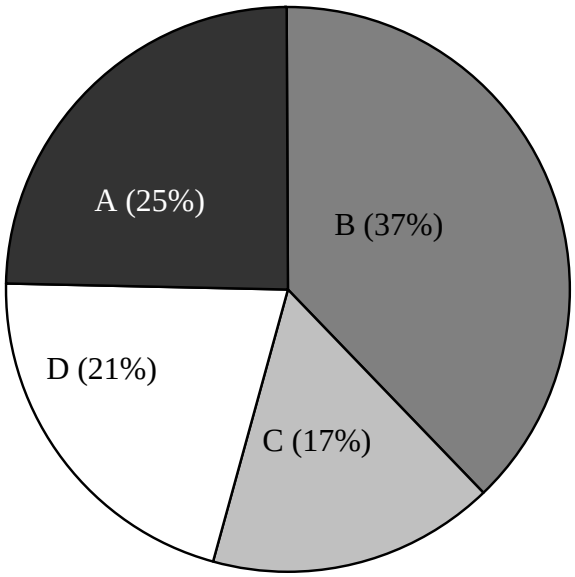

Figure 5: The distribution of afferent classes recorded from the pelvic nerve. The serosal afferent class (A) accounted for 25% of the total afferents observed, mucosal afferents (B) accounted for 37%, muscular afferents (C) accounted for 17%, and muscular mucosal afferents (D) accounted for 21%.

Effect of *trpa1* Deletion on Pelvic Afferents

Significant deficits in mechanosensitivity were observed in TRPA1 (-/-) mice when compared to their intact (+/+) littermates. Specifically, these deficits were observed in the serosal and mucosal afferent classes and in the mucosal component of the muscular mucosal afferent class. The deficits were observed in all analysis paradigms (i.e. mean instantaneous frequency, mean frequency, rate and spikes per second), indicating the reductions observed are not restricted to the initial dynamic phase of the stimuli, but affect mechanotransduction throughout the stimulus period (results not shown). In the serosal afferent class, responses to blunt probing with von Frey hairs were significantly reduced within the stimulus range 600-2000gm, with a maximal reduction of 50% in response to 2000mg (Figure 6). Further, there was a rightward shift in activation threshold, more evident at lower von Frey hair stimulus (Figure 7). This indicates in serosal afferents a greater stimulus is needed for activation and the response generated is lower. In the mucosal afferent class, responses to mucosal stroking with von Frey hairs were significantly reduced within the stimulus range 500 to 1000 mg, with a maximal reduction of 45% observed in response to 1000mg (Figure 8). No significant difference in activation threshold was observed, but this is difficult to measure in mucosal afferents as it is physically impossible to pierce the Krebs meniscus with von Frey hair strength lower than 10 mg. Nonetheless the responses generated by mechanical stimuli are reduced in mice lacking TRPA1. In the mucosal component of the muscular mucosal afferent class, significant reductions in response to mucosal stroking were observed again within the stimulus range 500-1000mg von Frey hair, with a maximal reduction of 52% observed in response to 1000mg (Figure 9). Neither the muscular component of the muscular mucosal

afferent class nor muscular afferents were affected (Figure 10,11). Both male and female mice were used in these experiments and no differences were observed between sexes.

Pharmacological Modulation of TRPA1

TCA Responses in Serosal and Mucosal Afferents

Trans-cinnamaldehyde (TCA) is an agonist of TRPA1 channels [170, 172]. Increases in mechanotransduction were observed in serosal and mucosal afferent classes in response to a single dose of 100 μM when applied for 2 minutes. In serosal afferents, an increase of 39% was observed ($P<0.05$) which was lost in TRPA1 (-/-) mice (Figure 12). In the mucosal afferent class a significant ($P<0.05$) increase of a maximal 42% was observed which was also lost in TRPA1 (-/-) animals (Figure 13). The loss of effect of TCA in both serosal and mucosal afferents in knock out mice in these afferents suggests TCA is selective for TRPA1. Results are expressed as spikes per second (serosal) or spikes per stroke (mucosal), and similar results were produced by other analysis variations (mean instantaneous frequency, mean frequency, rate).

TCA Responses in Muscular and Muscular Mucosal Afferents

In contrast to expected results, TCA significantly inhibited mechanosensation in muscular afferents and muscular mucosal afferents (Figures 14, 15, 16). This is unexpected as deletion of TRPA1 induced significant decreases in the mucosal component of the muscular mucosal afferent class and therefore application of an agonist should induce increases in mechanosensation. Similarly, no changes were observed in muscular afferents

or the muscular component of the muscular mucosal afferent class following the disruption of TRPA1, and application of an agonist should therefore have no effect on mechanosensation. In light of decreases in mechanosensation observed in these afferent classes, and the selectivity for TRPA1 by TCA observed in the serosal and mucosal afferent classes, it was decided dose response relationships (1-1000 μm) would provide further understanding of the effects this agonist is having in these afferent classes.

In muscular afferents, significant ($P<0.01$) decreases in mechanosensation were observed at the highest concentration applied (1000 μm). The deficits observed were nearly absolute, with 91% inhibition observed in response to 3 gm stretch, and 82 % observed in response to 5 gm stretch. While decreases in mechanosensation were observed with lower doses of TCA, they were not of the same magnitude, suggesting desensitisation of the receptor rather than direct inhibition. However when the response to 100 μm TCA was examined in TRPA1 (-/-) animals, decreases in mechanosensation were again observed (Figure 16). While these are not significant ($P<0.08$ at 3gm and 5gm) they are similar to results observed in TRPA1 (+/+) mice. Further, a limited amount of studies (n=2) demonstrated very large deficits occur at the highest dose of TCA (1000 μm) in TRPA1 (-/-) mice, again similar to that observed in TRPA1 (+/+) mice. This indicates the results observed in TRPA1 intact animals are not due to desensitisation of the TRPA1 channel.

Similar responses were observed in the muscular component of the muscular mucosal afferent class, with decreases in mechanosensation observed in both TRPA1 (+/+) and (-/-) mice (FIGURE 15). While the decreases observed are not significant, they are again very large (83% at maximum) and occur independently of TRPA1 presence as observed in the muscular afferents described above.

Interestingly, significant ($P<0.05$) reductions in mechanosensation were also demonstrated in the mucosal component of the muscular mucosal afferent class following the addition of TCA (Figure 14). The decreases observed (53% maximal) were not in the order observed in muscular afferents, but were again observed in a similar manner in TRPA1 (-/-) mice (34% maximal).

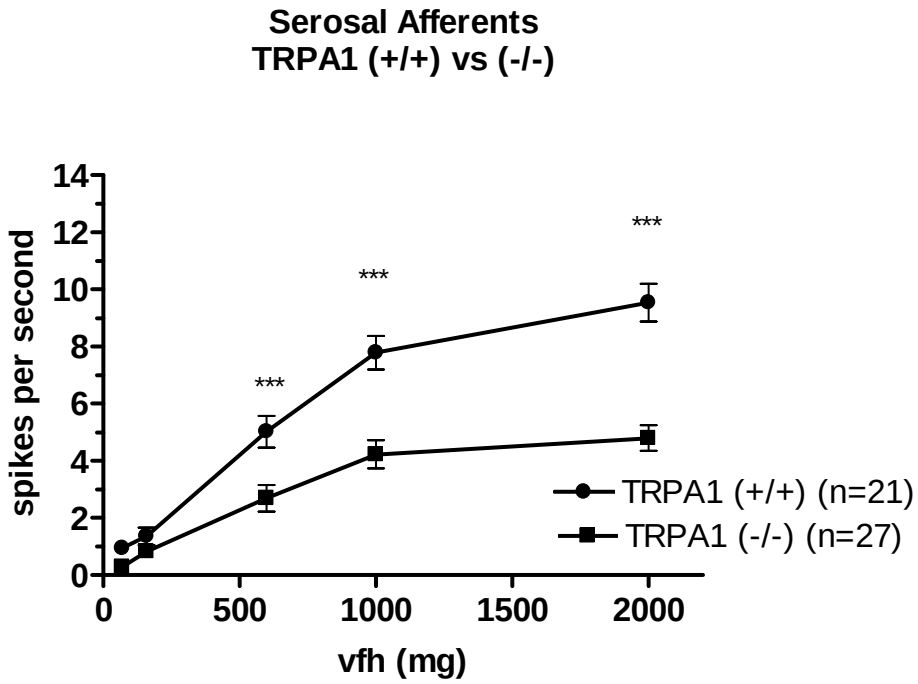

Figure 6: Effect of TRPA1 disruption on pelvic serosal afferent mechanosensitivity. Disruption of TRPA1 resulted in significant decreases in mechanosensitivity (expressed as spikes per second). Data analysed via two way ANOVA with Bonferoni post-hoc test (***P<0.001)

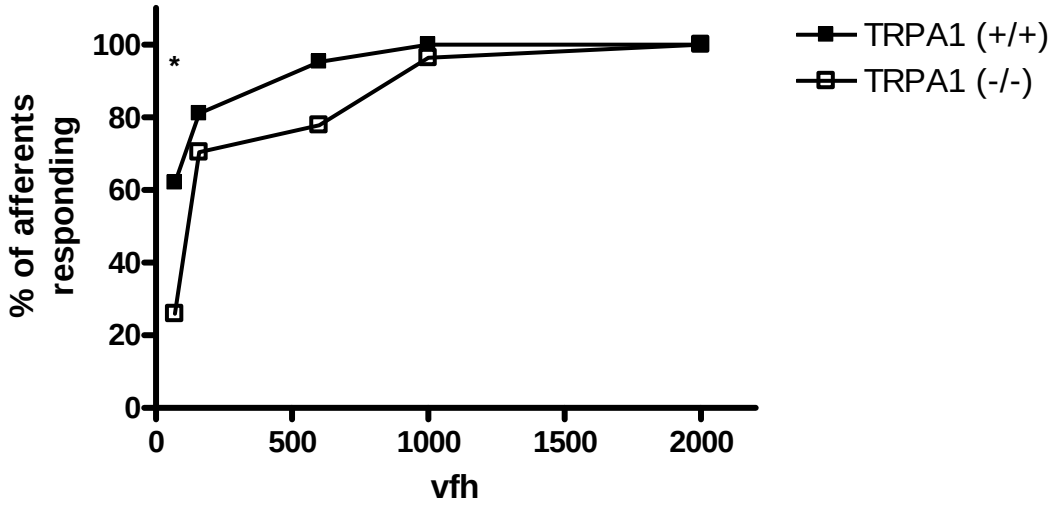

Figure 7: A significant increase in serosal afferent threshold is observed in TRPA1 (-/-) mice. This increase is more pronounced at lower von Frey hair stimuli. Data analysed via Fisher's exact test at each point. (*P<0.05)

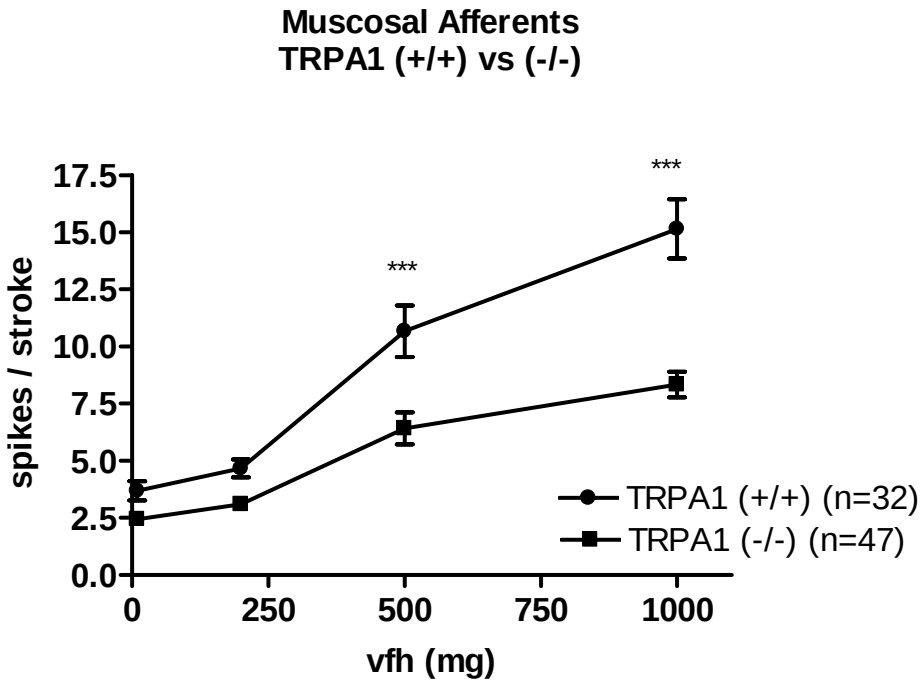

Figure 8: Effect of TRPA1 disruption on pelvic mucosal afferent mechanosensitivity. Disruption of TRPA1 resulted in significant decreases in mechanosensitivity (expressed as spike per stroke). Data analysed via two way ANOVA with Bonferoni post-hoc test (***P<0.001)

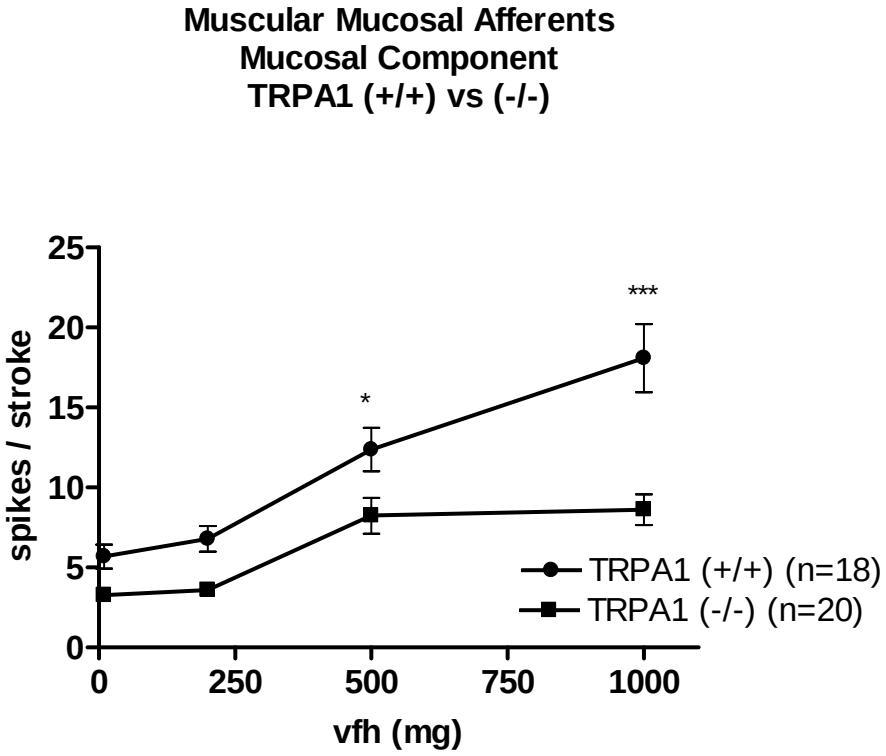

Figure 9: Effect of TRPA1 disruption on the mucosal component of the pelvic muscular mucosal afferent mechanosensitivity. Disruption of TRPA1 resulted in significant decreases in mechanosensitivity (expressed as spikes per second). Data analysed via two way ANOVA with Bonferoni post-hoc test (***P<0.001, **P<0.01, *P<0.05)

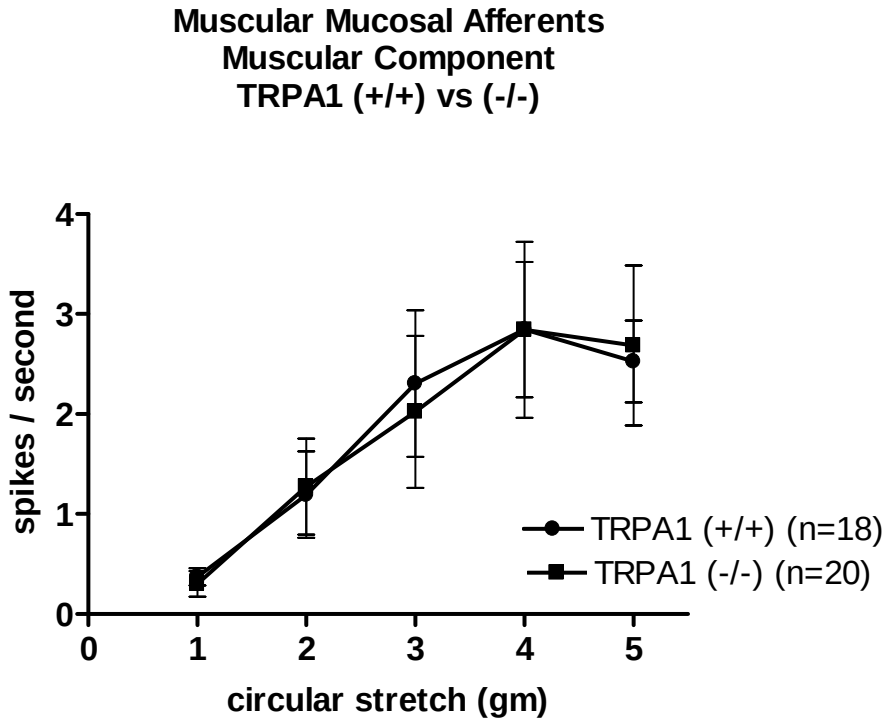

Figure 10: Effect of TRPA1 disruption on the muscular component of the pelvic muscular mucosal afferent mechanosensitivity. Disruption of TRPA1 resulted in no change in mechanosensitivity (expressed as spikes per second). Data analysed via two way ANOVA with Bonferoni post-hoc test

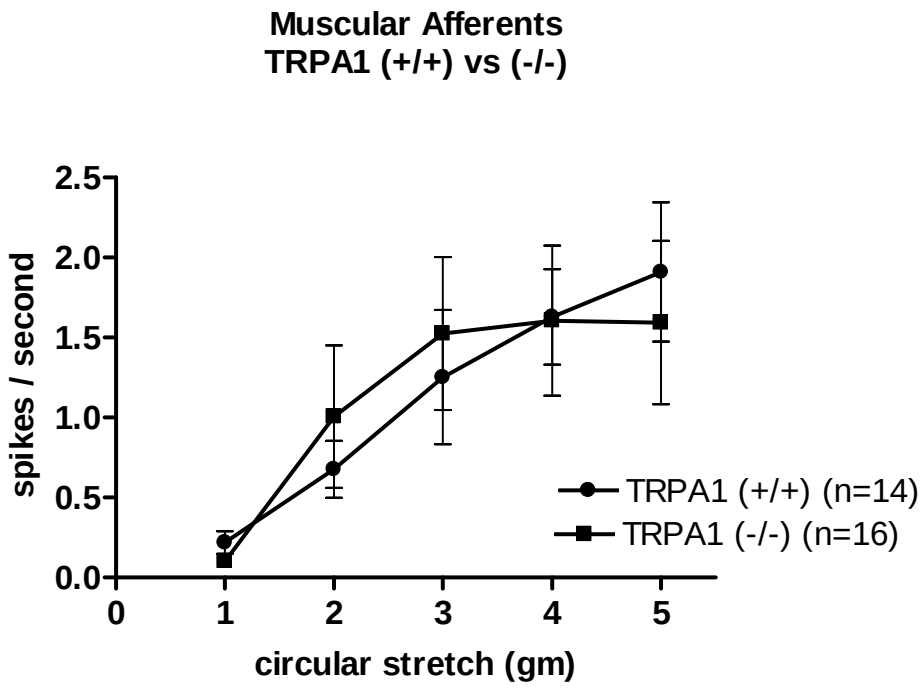

Figure 11: Effect of TRPA1 disruption on pelvic muscular afferent mechanosensitivity. Disruption of TRPA1 resulted in no change in mechanosensitivity (expressed as spikes per second). Data analysed via two way ANOVA with Bonferoni post-hoc test

Effect of TCA on Pelvic Serosal Afferents in TRPA1 (+/+) and (-/-) mice

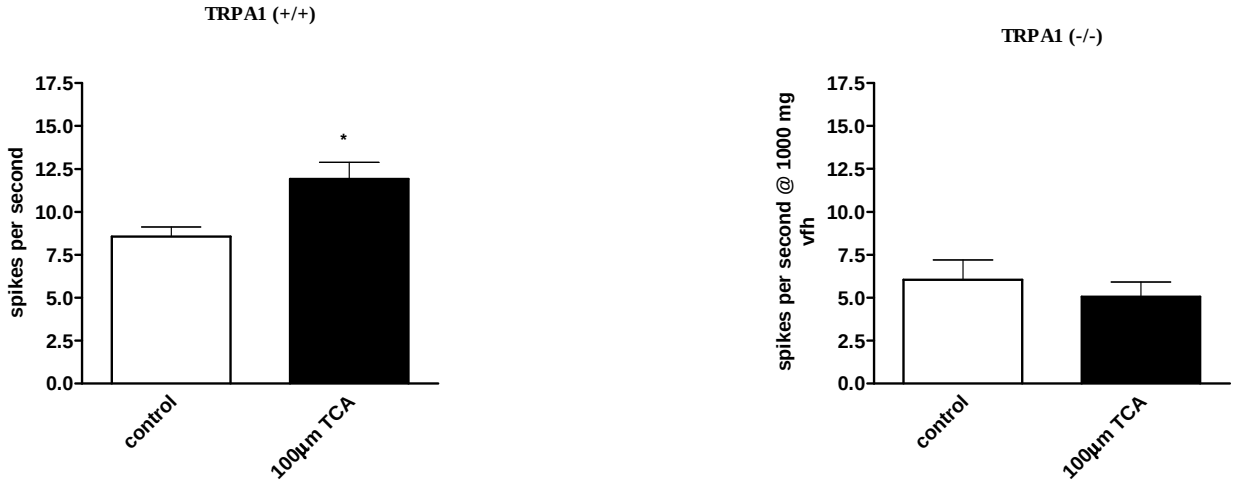

Figure 12: Mechanosensory effect of the TRPA1 agonist TCA on serosal afferents in TRPA1 (+/+) and (-/-) mice. Effect on mechanosensation expressed as change in spikes per second at 1000 mg von Frey hair to 100 µM TCA as compared to control. Addition of TCA resulted in a significant increase in mechanosensation in TRPA1 (+/+) mice (n=6) which was not observed in TRPA1 (-/-) mice (n=7). Data analysed via students t-test (*P<0.05)

Effect of TCA on Pelvic Mucosal Afferents in TRPA1 (+/+) and (-/-) mice

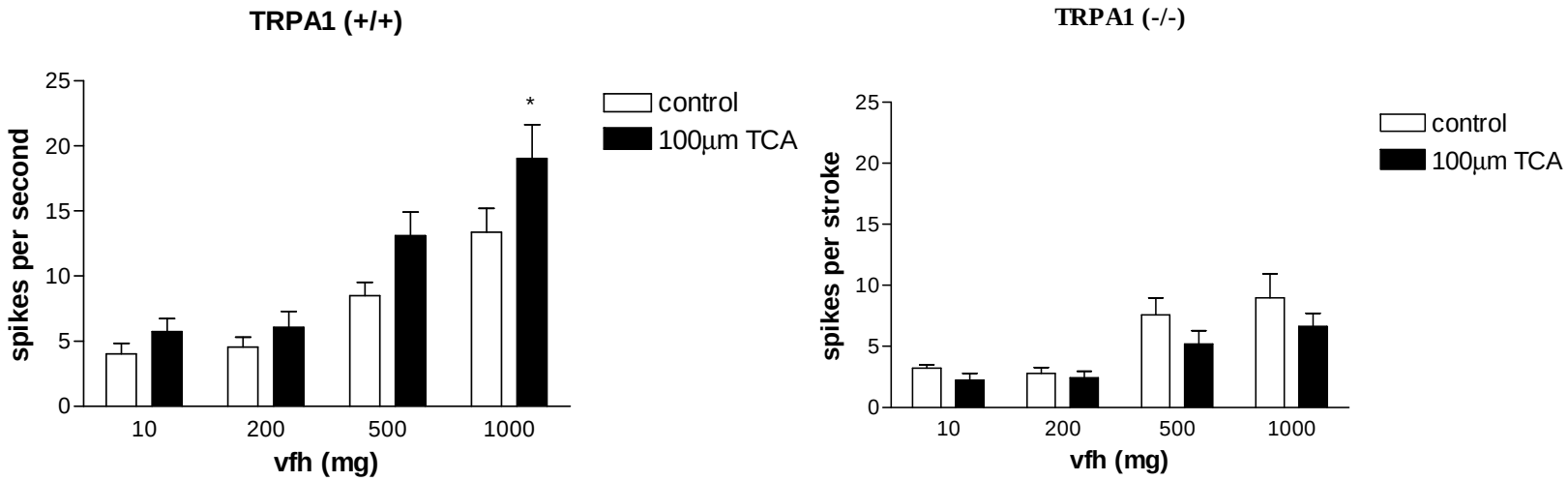

Figure 13: Mechanosensory effect of the TRPA1 agonist TCA on mucosal afferents in TRPA1 (+/+) and (-/-) mice. Effect on mechanosensation expressed as change in spikes per second at 10-1000 mg von Frey hair to 100 µM TCA as compared to control. Addition of TCA resulted in a significant increase in mechanosensation in TRPA1 (+/+) mice (n=11) which was not observed in TRPA1 (-/-) mice (n=8). Data analysed two-way ANOVA with Bonferonni post-hoc test (*P<0.05)

Effect of TCA on Mucosal Component of Muscular Mucosal Afferents in TRPA1 (+/+) and (-/-) mice

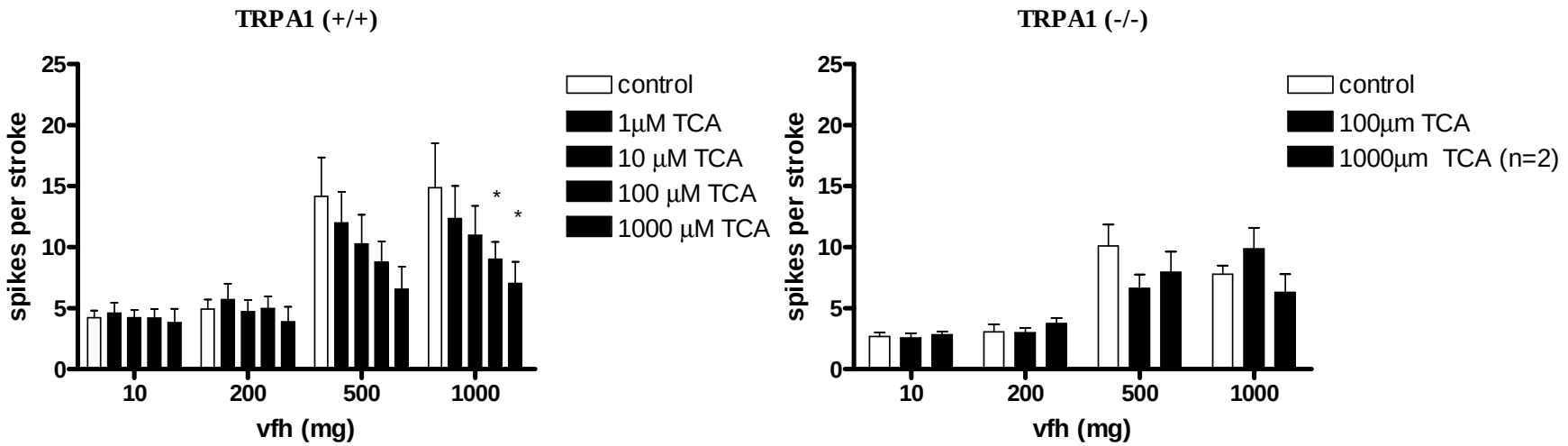

Figure 14: Mechanosensory effect of the TRPA1 agonist TCA on mucosal component of muscular mucosal afferents in TRPA1 (+/+) and (-/-) mice. Effect on mechanosensation expressed as change in spikes per second response at 10-1000 mg von Frey hair to 1-1000 μM TCA as compared to control. Addition of TCA to muscular mucosal afferents resulted in a significant ($P<0.05$) decrease in mechanosensation in the mucosal afferent class in TRPA1 (+/+) mice (n=6). This decrease was also observed in TRPA1 (-/-) mice

Effect of TCA on Muscular Component of Muscular Mucosal Afferents in TRPA1 (+/+) and (-/-) mice

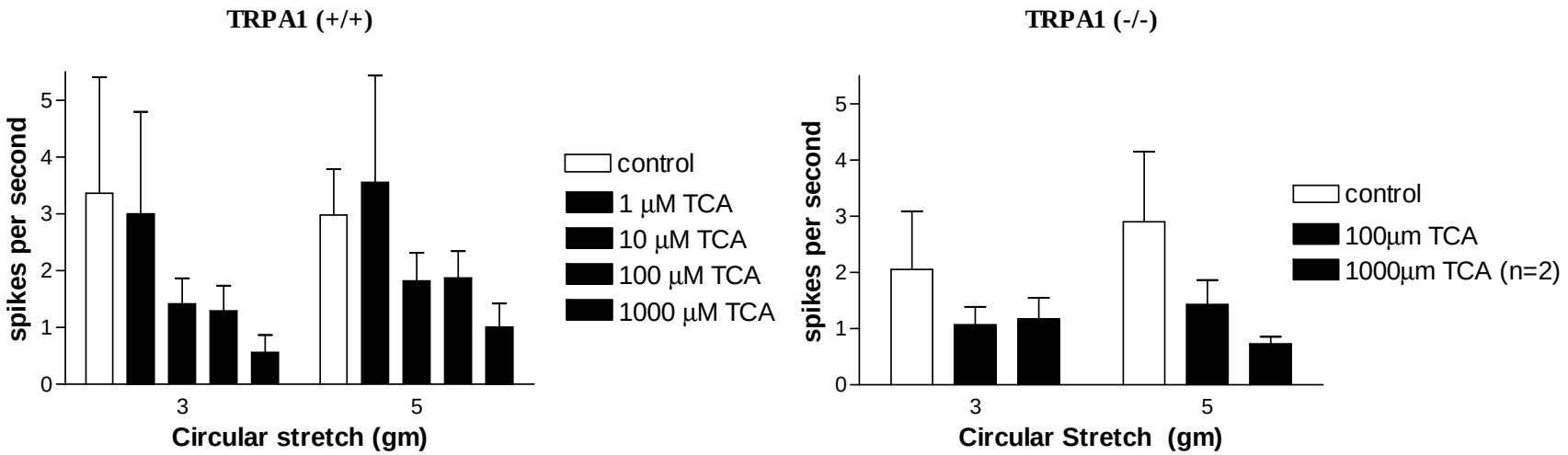

Figure 15: Mechanosensory effect of the TRPA1 agonist TCA on muscular component of muscular mucosal afferents in TRPA1 (+/+) and (-/-) mice. Effect on mechanosensation expressed as change in spikes per second response to 3 or 5 gm circular stretch to increasing concentrations of TCA (1-1000 μM). Decreases in mechanosensation were observed in response to TCA in TRPA1 (+/+) mice (n=6). Decreases were also observed in TRPA1 (-/-) mice (n=10 (control, 100 μM), n=2 (1000 μM)). Data analysed via two way ANOVA with Bonferonni post-hoc test.

Effect of TCA on Pelvic Muscular Afferents in TRPA1 (+/+) and (-/-) mice

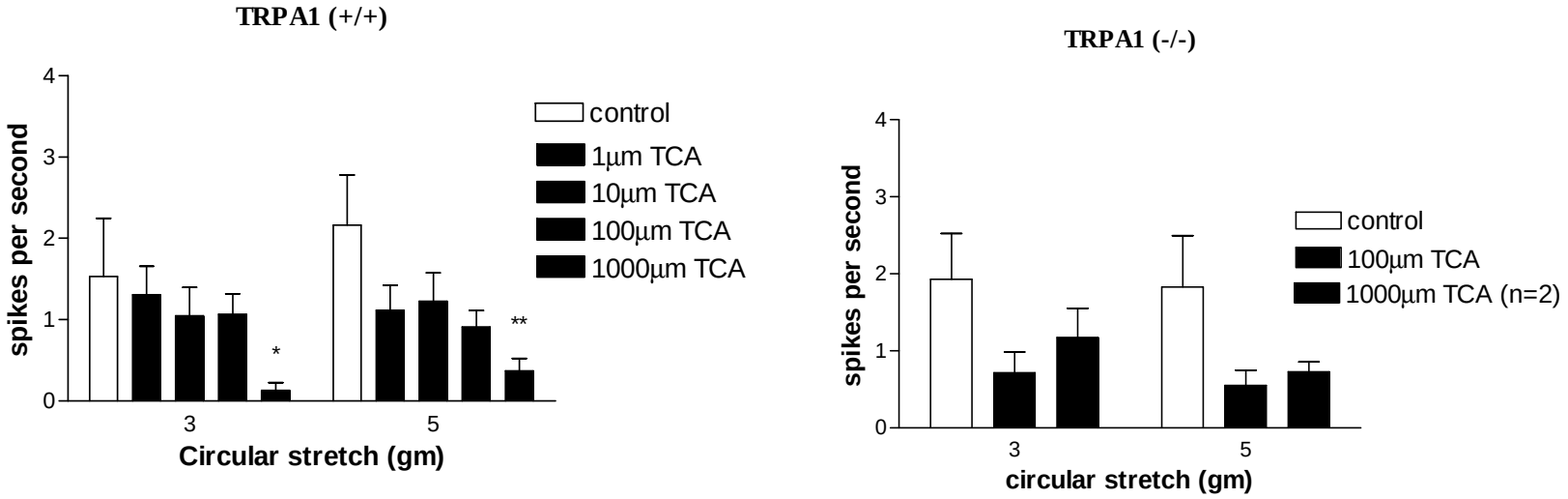

Figure 16: Mechanosensory effect of the TRPA1 agonist TCA on muscular afferents in TRPA1 (+/+) and (-/-) mice. Effect on mechanosensation expressed as change in spikes per second response to 3 or 5 gm circular stretch to increasing concentrations of TCA (1-1000 μM). Significant decreases in mechanosensation were observed in response to 1000 μM TCA in TRPA1 (+/+) mice (n=8). Decreases were also observed in TRPA1 (-/-) mice (n=12 (control and 100 μM) n=2 (1000 μM). Data analysed via two way ANOVA with Bonferonni post-hoc test (**P<0.01, *P<0.05)

Discussion

TRPA1 Expression in the Gastrointestinal Tract

Colonic expression

Transcripts corresponding to TRPA1 were positively identified by PCR in DRG (Figure 17 adapted from Brierley et. al. Neuron in press). The proportion of DRG neurons expressing TRPA1 is currently contentious, and ranges from 5% to 56% of the global DRG population [162-165]. The results of the present study confirm reports at the larger end of this spectrum, with approximately 40% of DRG neurons found to express TRPA1 in either the thoracolumbar or lumbosacral DRG populations. This is the first study to identify TRPA1 expression in DRG neurons specifically innervating the colon. FISH studies indicate TRPA1 was expressed in a significantly greater proportion of colonic neurons compared to the general population, with increases of 30% and 50% observed in thoracolumbar and lumbosacral DRG regions respectively.

Gastric Expression

TRPA1 transcripts have previously been identified in nodose ganglia, but as yet no indication has been provided as to the proportion of nodose neurons expressing TRPA1 [164]. We identified expression of TRPA1 in 36% of nodose neurons, a proportion similar to that observed in DRG populations. A significantly greater proportion of gastric nodose neurons expressed TRPA1 compared to the general population.

Conclusions From Analysis of Expression

This is the first study to demonstrate TRPA1 expression in either colonic DRG or gastric nodose neurons. Previous studies have demonstrated TRPA1 expression in a variety of tissues including DRG, nodose ganglia and colon, but proportions are contentious [159-161, 164, 165, 174]. Our studies confirm TRPA1 is expressed in approximately 50% of the general DRG population. In contrast to ASIC3 and TRPV4, expression of TRPA1 is relatively high in the general population [201, 231]. A greater proportion of colonic and gastric nodose neurons express TRPA1 compared to their respective general populations, but the difference is relatively minor to that observed for other channels [201, 231]. The high proportion of neurons expressing TRPA1 in both colonic DRG and gastric nodose populations suggests it plays an important role in gastrointestinal function. However as TRPA1 is also expressed in a high proportion in the general DRG and nodose populations, and as the colonic and gastric neurons comprise only a small fraction of these populations, this importance is unlikely to be restricted to the gastrointestinal tract.

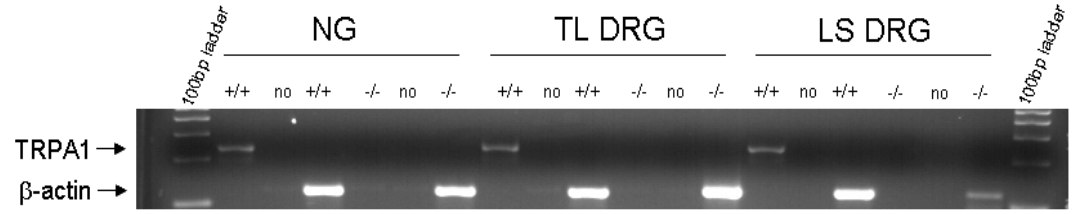

Figure 17: PCR gel of TRPA1 in nodose ganglia (NG), thoracolumbar dorsal root ganglia (TL) and lumbosacral dorsal root ganglia. TRPA1 is present in intact animals (+/+), and not present in TRPV4 knock out animals (-/-) in each of these ganglia. These results are confirmed by the presence of β-actin in (-/-) animals and the absence of product in water controls (no). (adapted from Brierley et. al. Neuron in press)

Influence of TRPA1 on Colonic Mechanosensation

The above studies indicate expression of TRPA1 is widespread, contrary to previously published reports, and that it may have an important influence in the gastrointestinal tract [164, 165]. A great deal of evidence suggests TRPA1 is nociceptive, but the evidence of a specifically mechanosensory role is currently contentious, with a potential role as a detector of noxious mechanical stress a cautious possibility [165, 166, 173, 224].

Effect of TRPA1 Deletion on Colonic Innervation

Mice engineered to lack the TRPA1 gene (*trpa1* (-/-)) and their wild type litter mates (*trpa1* (+/+)) were used in these studies because antagonists specific for TRPA1 are currently not available to study its role. Further, TCA, an agonist purported to be selective for TRPA1 was used to determine whether mechanosensitive responses mediated by TRPA1 are possible to manipulate pharmacologically [170, 172].

TRPA1 (-/-) mice and their (+/+) wild type litter mates were observed to be healthy with no obvious defects. PCR analysis of these mice demonstrates TRPA1 is lacking from the (-/-) mice (Figure 17 adapted from Brierley et. al. Neuron in press). A full complement of afferent classes were observed in both TRPA1 (+/+) and (-/-) mice and no differences were observed between afferent proportions. Conduction velocities were also observed to be similar between TRPA1 (+/+) and (-/-) mice, indicating disruption of TRPA1 does not alter the biophysical properties of colonic afferents (Figure 18 adapted from Brierley et. al. Neuron in press). Hence it is reasonable to infer any alterations in colonic

mechanosensitivity are due entirely to the removal of TRPA1 and not to extraneous effects associated with genetic disruption.

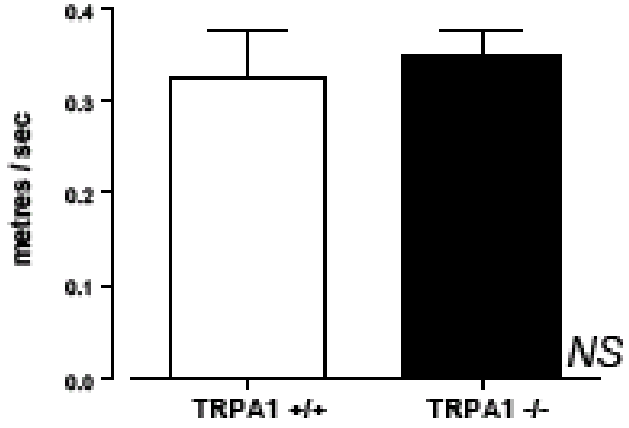

Figure 18: Conduction velocities are similar in TRPA1 (+/+) and (-/-) mice. This indicates no alterations in biophysical properties of colonic afferents occurs from deletion of TRPA1. (adapted from Brierley et. al. Neuron in press)

Pelvic Afferent Mechanosensitivity

Significant reductions in mechanosensation were observed in TRPA1 (-/-) mice in serosal and mucosal afferents. No alterations in mechanosensitivity were observed in muscular afferents. Interestingly the mucosal component of muscular mucosal afferents demonstrated significantly reduced mechanosensation, while the muscular component was unchanged. These results indicate expression of TRPA1 is dependent on the layer of colon innervated rather than afferent type, in that the mucosal component of the muscular mucosal afferents is similar to that of the mucosal afferents, and the muscular component of the muscular mucosal afferent is similar to the muscular afferent. The reductions observed in the serosal class are in the order of those observed previously in mice lacking the TRPV4 gene. Interestingly, the deficits in the mucosal afferent classes are without precedent. Disruption of ASIC3 or TRPV1 have previously been examined using similar means, and while neither channel influenced mechanosensation in mucosal afferents, both affected the function of muscular afferents [78]. These results are therefore unexpected given the demonstrated association of TRPA1 with TRPV1 [159, 165-167, 222]. As TRPA1 is commonly co-expressed with TRPV1 in DRG neurons it would be expected disruption of TRPV1 would result in mechanosensory deficits of at least the extent observed when TRPA1 is disrupted [159, 165, 167]. Either TRPA1 is not always expressed with TRPV1 in colonic DRG neurons, which is unlikely given the extremely high percentages of colocalisation observed in whole DRG populations, or coupling with TRPV1 is not necessary to mediate a mechanosensory signal in mucosal afferents. Previous studies indicate TRPA1 is directly gated by mechanical stimuli, and this may represent yet another gating paradigm for this polymodal receptor [228].

Pharmacological manipulation with TCA further validated these results, with significant increases in mechanosensation observed in the serosal and mucosal afferent classes. These effects were lost in TRPA1 knock out mice, implying selectivity of TCA for TRPA1. However quite unexpected results were obtained in the muscular and muscular mucosal afferent classes, with TCA inducing a potent dose-dependent decrease in mechanosensation in wild type TRPA1 (+/+) mice. This was unexpected as no alterations were induced by TRPA1 disruption in muscular afferents or in the muscular component of muscular mucosal afferents, and potent mechanosensory decreases were observed in the mucosal component of the muscular mucosal afferent class. TCA would therefore not be expected to have an effect on either of the muscular afferent types, and to increase, rather than decrease, mechanosensitivity in the mucosal afferent types. Interestingly, similar results were also observed in TRPA1 (-/-) mice, indicating receptor desensitisation is not the cause. Given the mode of action of TCA is via covalent modification rather than direct pore interaction, it is probable TCA and other related electrophilic agents are not specific for TRPA1. Non-selectivity of pungent chemicals for TRPA1 is somewhat controversial given another electrophilic agent, allyl isothiocyanate, has demonstrated residual effects in one line of TRPA1 (-/-) mice but not another [166, 173]. The TRPA1 activation domain for these electrophilic agents is intact in both lines of knock out mice as only the pore forming domain is disrupted, but in one line truncated TRPA1 is sequestered to the endoplasmic reticulum while in the other truncated transcripts may be transported to the cell membrane [166, 173]. However even in these lines the selectivity is debatable as the residual effects are observed in the absence of cell membrane associated TRPA1, while no effect of TCA is observed in mice with truncated TRPA1 at the cell membrane, which is the opposite of expected results [166, 173].

The non-selectiveness of TCA may be the result of the common electrophilic nature, but may also be due to other as yet unknown actions of these compounds. These include effects on other TRP channels, particularly as high concentrations of AITC inhibit TRPM8 channels [232] . It is clear these actions must have a much greater impact on muscular afferents and the muscular component of muscular mucosal afferents than serosal or mucosal afferents.

The common decrease in mechanosensation following addition of TCA by both components of the muscular mucosal afferent class is contrary to those obtained from the baseline TRPA1 knock out experiments, where responses differed according to stimulus applied. These issues are difficult to resolve as morphological clarification of muscular mucosal afferents is yet to be performed. These afferents may be branched, with separate endings in mucosal and muscular layers of the colon, or may be located between the mucosa and muscular layers in the submucosal plexus. Indications from TRPA1 (+/+) vs (-/-) mice baseline mechanosensation experiments suggest a branched morphology, with receptor expression dependant on the layer of colon innervated, as responses of mucosal and muscular components of the muscular mucosal afferent class resembled those of mucosal or muscular afferents respectively. However this may not be the case as responses induced by TCA incubation, where the mucosal component of the muscular mucosal afferents are decreased similarly to the muscular component of the muscular mucosal afferent rather than increased as is the case with mucosal afferents. These experiments suggest either a branched morphology with afferent expression correlated with afferent class rather than layer of colon innervated, or are suggestive of a single ending in the submucosal plexus that differentially respond to stroking and circular stretch. These issues

are difficult to clarify without the morphology of muscular mucosal afferents and knowledge of the off target actions of TCA.

Lumbar Splanchnic Colonic and Vagal Gastric Afferents

Simultaneous experiments investigating lumbar splanchnic innervation of the colon and vagal innervation of the upper gut provided further evidence of TRPA1 as a mediator of mechanosensation. Significant reductions in mechanosensory responses were observed in both serosal and mesenteric afferents recorded from the lumbar splanchnic nerve (Figure 19 adapted from Brierley et. al. Neuron in press), indicating TRPA1 is involved in detection of mechanical stimuli mediated by high threshold afferent classes. Deletion of TRPA1 induced modest but significant reductions in gastroesophageal vagal mucosal afferent mechanosensitivity, while tension sensitive afferents were not altered (Figure 20 adapted from Brierley et. al. Neuron in press). The results in the upper gut correlate with those recorded from the colon, where pelvic mucosal afferent mechanosensitivity was negatively affected by the deletion of TRPA1, while pelvic muscular afferent mechanosensitivity was unaffected. However the decreased mechanosensitivity observed in gastroesophageal afferents is much more modest than that observed in the colon, indicating that while TRPA1 expression may be similar between gastric nodose and colonic DRG populations differences in functionality exist.

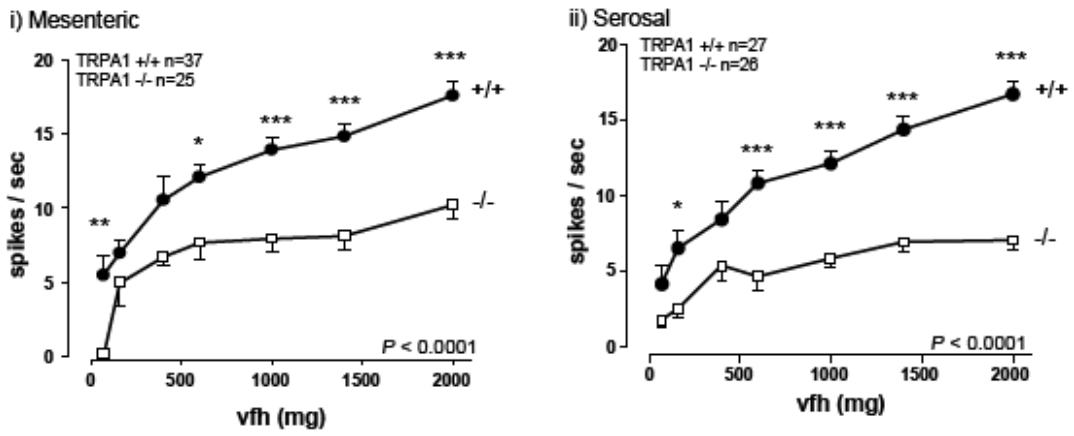

Figure 19: Effect of TRPA1 disruption on lumbar splanchnic i) mesenteric and ii) serosal afferent mechanosensitivity. Disruption of TRPA1 resulted in decreases in mechanosensitivity in both mesenteric and serosal afferent types. Data analysed via two way ANOVA with Bonferoni post-hoc test (***P<0.001, **P<0.01). (adapted from Brierley et. al. Neuron in press)

NOTE:
This figure is included on page 235 of the print copy of the thesis held in the University of Adelaide Library.

Figure 20: Effect of TRPA1 disruption on gastrosophageal vagal i) mucosal and ii) tension afferent mechanosensitivity. Disruption of TRPA1 resulted in modest but significant decreases in mucosal afferent mechanosensitivity in mucosal afferents while muscular afferent mechanosensitivity was unchanged. Data analysed via two way ANOVA with Bonferoni post-hoc test (**P<0.01). (adapted from Brierley et. al. Neuron in press)

Futher Evidence of the involvement of TRPA1 in colonic mechanosensation

Experiments run simultaneously with the above studies provide further evidence of the importance of TRPA1 in colonic mechanosensation. Firstly TRPA1 immunoreactivity was observed in peripheral endings in the mucosa, serosa and mesentery of the colon that were positive for CGRP (Figure 21 adapted from Brierley et. al. Neuron in press). This indicates TRPA1 is indeed present in the colon in areas observed to be disrupted in electrophysiological recordings from TRPA1 knock out mice.

Colorectal balloon distension experiments demonstrated a significantly reduced response to noxious pressure in mice lacking TRPA1 (Figure 22 adapted from Brierley et. al. Neuron in press). This indicates these mice have a reduced ability to detect noxious visceral mechanical stimuli, and correlates well with the electrophysiological experiments performed above.

Figure 21: Colocalisation of CRGP and TRPA1 in peripheral fibres in the mouse colon. TRPA1 colocalised with CGRP in colonic mucosa (A) and on mesenteric blood vessels (B) in TRPA1 (+/+) mice. (adapted from Brierley et. al. Neuron in press)

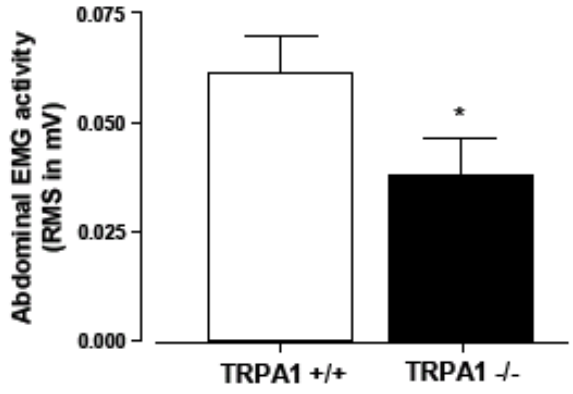

Figure 22: EMG responses to colorectal balloon distension in conscious TRPA1 (+/+) and (-/-) mice. Significantly reduced responses (approx 50%) to colorectal distension were observed in TRPA1 (-/-) mice.

Final Conclusions

We have characterised the role of TRPA1 in detection of mechanical stimuli in the gastrointestinal tract. Our expression studies demonstrate TRPA1 is expressed in a high proportion of colonic DRG and gastric nodose neurons, indicating it may have an important functional relevance in the gastrointestinal tract. However as the proportions are similarly high in the general population this role may not be specific to the gastrointestinal tract. Large deficits in mechanosensation were observed in TRPA1 (-/-) mice for specific colonic afferent subtypes (serosal, mesenteric, mucosal and the mucosal component of muscular mucosal afferents) mediated by either the pelvic or splanchnic nerves, while more modest deficits were observed in vagal gastric mucosal afferents. Notably responses elicited by colonic or gastric muscular afferents and the muscular component of colonic muscular mucosal afferents were unaffected. This is the first report of TRPA1 influencing low threshold afferents and is contrary to previously published results found in mammalian cutaneous and auditory low threshold afferents [166, 173].

TRPA1 is clearly a polymodal receptor with several gating mechanisms. Unclear is whether these mechanisms are similar for serosal and mucosal afferents within the colon, whether this coupling is similar between tissues and whether TRPA1 acts as a primary sensor or acts as a downstream integrator of diffusible messages. Dissecting the various gating paradigms of this channel promises to be an interesting area of future research.

CHAPTER 7

FINAL DISCUSSION

Intestinal hypersensitivity to mechanical stimuli is a hallmark of IBS [7]. The sensations of pain and abdominal cramping mediated by colonic afferents are the most debilitating aspects of this illness [34, 35]. The results from this thesis identify ASIC3, TRPV4 and TRPA1 are potential targets for treatment of colonic mechanical hypersensitivity.

Of the ion channels investigated, expression of ASIC3 and TRPV4 were observed to be much greater in DRG neurons innervating the colon than in the general DRG neuronal population in both thoracolumbar and lumbosacral DRG populations (Figure 1 and 2 respectively). Previous studies have identified ASIC3 as a mediator of painful and non-painful stimuli, in that deletion of ASIC3 induced mechanosensory deficits in high threshold serosal and mesenteric afferent classes, and mid threshold muscular afferents in the colon [78, 125]. We observed TRPV4 to mediate mechanosensation specifically in those colonic afferents involved in detection of noxious events. TRPA1 was also expressed in a high proportion in colonic DRG neurons and also mediated transduction of noxious mechanical stimuli but also mediated the detection of non-noxious stimuli detected by colonic afferents with low thresholds to mechanical stimuli. This is the first study to demonstrate TRPA1 mediates the detection of non-noxious mechanical stimuli. Invertebrate studies have inferred participation in detection of non-noxious mechanical stimuli, particularly that in low threshold afferents involved in hearing, however these studies do not translate to vertebrates as hearing and low threshold cutaneous responses are intact in TRPA1 (-/-) mice [166, 173-175]. It is also the first description of a mechanically sensitive afferent residing in the mucosal layers of the colon. However the expression of TRPA1 is not restricted to colonic cells as high proportions of neurons in the whole DRG population also express TRPA1.

The differential expression between the general DRG population and the colonic DRG population for each of these ion channels investigated in this thesis cautions against inferring abundance of ion channels in specific organs from expression in whole DRG. ASIC3 and TRPV4 provide appropriate examples where expression of either of these channels is low in whole DRG, indicating they are poor targets for colonic physiology, but in fact both are expressed in a high proportion of colonic cells where they do make substantial contributions toward detection of mechanical stimuli. Accurate representations of expression therefore can only be deduced from analysis of subpopulations of DRG cells representing the organ of interest.

The nature of transduction of mechanical stimuli mediated by these channels is unclear with current evidence suggesting both direct and indirect mechanisms. While the pathway involved with direct activation is relatively uncomplicated, it must be noted these experiments are generally performed in isolated cell based systems and may not relate well to normal physiology. On the other hand indirect mechanosensation involves either second messenger systems or functional coupling with accessory proteins. TRPA1 provides a good example of this complexity, with in vitro experiments demonstrating the ability to directly sense mechanical stimuli and intact animal studies demonstrating the majority of TRPA1 colocalises with and is likely to couple with TRPV1 in DRG [159, 163, 165, 166, 173, 228]. Yet co-localisation with TRPV1 is unlikely in the mucosal layers of the colon, as disruption of TRPA1 has a substantial effect on colonic mechanosensation mediated by mucosal afferents, while disruption of TRPV1 has previously shown not to [78]. This indicates separate transduction pathways exist for TRPA1, as there may also be for ASIC3 and TRPV4. Given the polymodality of these receptors, each with numerous distinct gating paradigms, they may each act as integrators of sensory information rather than primary

A) **FISH analysis of Thoracolumbar DRG**

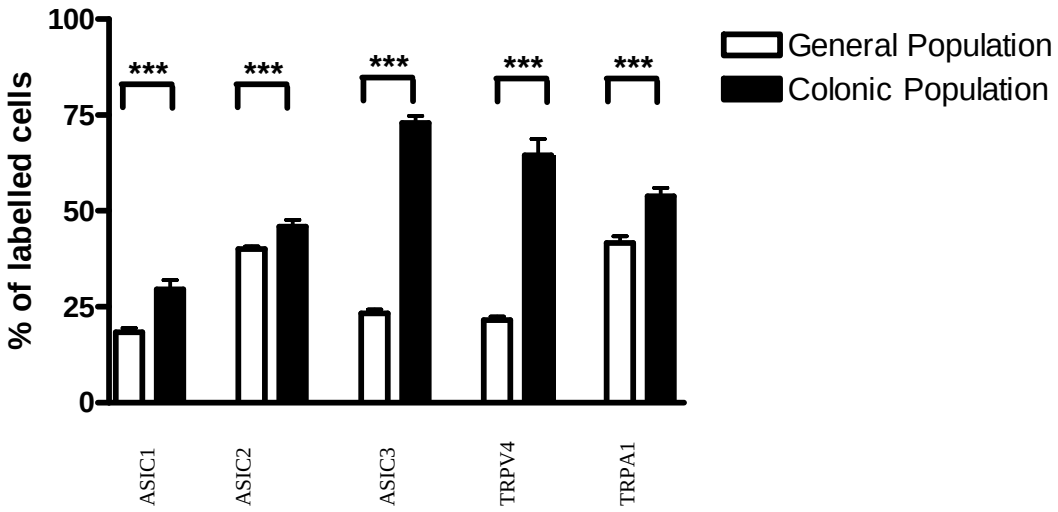

B) **FISH analysis of Lumbosacral DRG**

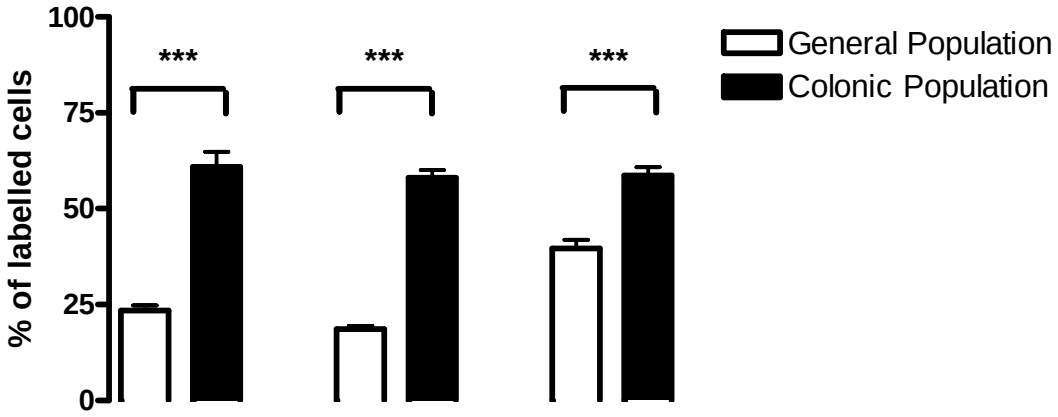

Figure 1 and 2: Significantly more colonic cells express ASIC1, 2 and 3, TRPV4 and TRPV1 in colonic DRG neurons than the general thoracolumbar region (Figure A) and the general lumbosacral region (Figure B). (***P<0.0001).

sensors. Understanding the nature of transduction of mechanical stimuli remains an exciting area of research likely to provide potential targets for modulation of mechanosensation in the future.

Many underlying questions remain regarding IBS. It is currently unclear whether the pain experienced by sufferers of this illness is due to lowering of the activation threshold of specifically the pain sensing serosal and mesenteric afferents, or whether there is a re-wiring event and the afferent barrage from the mucosal and muscular afferents generates painful sensations, or whether both scenarios are applicable. The demonstration of differential expression of receptors throughout the layers of the colon provides more selective targets for treatment should the illness be specifically due to alterations in one layer of the colon.

Final Conclusion

ASIC3, TRPV4 and TRPA1 each represent potential targets for the pharmacotherapy of IBS as each affects specific aspects of colonic mechanosensation. ASIC3 and TRPV4 are both preferentially expressed in colonic DRG neurons, unlike TRPA1, and functionally both are restricted to colonic afferents, unlike TRPA1 which also effects gastro-oesophageal afferent mechanosensation. In the gastrointestinal tract TRPV4 specifically mediates colonic mechano-nociception in healthy mammals making it an attractive target for treatment of sensations of pain experienced by sufferers of IBS. However the pathogenesis of IBS is currently unclear, particularly in regard to the origin of the painful sensations experienced by sufferers. Further delineation of these pathways will provide more specific targets for the future treatment of IBS.

CHAPTER 8

REFERENCES

1. Ringel, Y., A.D. Sperber, and D.A. Drossman, *Irritable bowel syndrome.* Annu Rev Med, 2001. **52**: p. 319-38.
2. Camilleri, M., *Management of the irritable bowel syndrome.* Gastroenterology, 2001. **120**(3): p. 652-68.
3. Camilleri, M., *Dyspepsia, irritable bowel syndrome, and constipation: review and what's new.* Rev Gastroenterol Disord, 2001. **1**(1): p. 2-17.
4. Schwetz, I., S. Bradesi, and E.A. Mayer, *The pathophysiology of irritable bowel syndrome.* Minerva Med, 2004. **95**(5): p. 419-26.
5. Dent, J., *Definitions of reflux disease and its separation from dyspepsia.* Gut, 2002. **50 Suppl 4**: p. iv17-20; discussion iv21-2.
6. Locke, G.R., 3rd, et al., *Overlap of gastrointestinal symptom complexes in a US community.* Neurogastroenterol Motil, 2005. **17**(1): p. 29-34.
7. Ritchie, J., *Pain from distension of the pelvic colon by inflating a balloon in the irritable colon syndrome.* Gut, 1973. **14**(2): p. 125-32.
8. Bouin, M., et al., *Intolerance to visceral distension in functional dyspepsia or irritable bowel syndrome: an organ specific defect or a pan intestinal dysregulation?* Neurogastroenterol Motil, 2004. **16**(3): p. 311-4.
9. Mertz, H., et al., *Altered rectal perception is a biological marker of patients with irritable bowel syndrome.* Gastroenterology, 1995. **109**(1): p. 40-52.
10. Azpiroz, F., et al., *Mechanisms of hypersensitivity in IBS and functional disorders.* Neurogastroenterol Motil, 2007. **19**(1 Suppl): p. 62-88.
11. Naliboff, B.D., et al., *Evidence for two distinct perceptual alterations in irritable bowel syndrome.* Gut, 1997. **41**(4): p. 505-12.
12. Sun, W.M., et al., *Sensory and motor responses to rectal distention vary according to rate and pattern of balloon inflation.* Gastroenterology, 1990. **99**(4): p. 1008-15.
13. Whitehead, W.E., et al., *Tolerance for rectosigmoid distention in irritable bowel syndrome.* Gastroenterology, 1990. **98**(5 Pt 1): p. 1187-92.
14. Delvaux, M., *Role of visceral sensitivity in the pathophysiology of irritable bowel syndrome.* Gut, 2002. **51 Suppl 1**: p. i67-71.
15. Bernstein, C.N., et al., *Rectal afferent function in patients with inflammatory and functional intestinal disorders.* Pain, 1996. **66**(2-3): p. 151-61.
16. Lembo, T., et al., *Symptoms and visceral perception in patients with pain-predominant irritable bowel syndrome.* Am J Gastroenterol, 1999. **94**(5): p. 1320-6.
17. Drossman, D.A., W.E. Whitehead, and M. Camilleri, *Irritable bowel syndrome: a technical review for practice guideline development.* Gastroenterology, 1997. **112**(6): p. 2120-37.
18. Thompson, W.G., et al., *Functional bowel disorders and functional abdominal pain.* Gut, 1999. **45 Suppl 2**: p. II43-7.
19. Drossman, D.A., *The functional gastrointestinal disorders and the Rome II process.* Gut, 1999. **45 Suppl 2**: p. II1-5.
20. Drossman, D.A., et al., *AGA technical review on irritable bowel syndrome.* Gastroenterology, 2002. **123**(6): p. 2108-31.
21. Drossman, D.A. and D.L. Dumitrascu, *Rome III: New standard for functional gastrointestinal disorders.* J Gastrointestin Liver Dis, 2006. **15**(3): p. 237-41.
22. Talley, N.J., et al., *Epidemiology of colonic symptoms and the irritable bowel syndrome.* Gastroenterology, 1991. **101**(4): p. 927-34.
23. Mach, T., *The brain-gut axis in irritable bowel syndrome--clinical aspects.* Med Sci Monit, 2004. **10**(6): p. RA125-31.

24. Gralnek, I.M., *Health care utilization and economic issues in irritable bowel syndrome.* Eur J Surg Suppl, 1998(583): p. 73-6.
25. Maxion-Bergemann, S., et al., *Costs of irritable bowel syndrome in the UK and US.* Pharmacoeconomics, 2006. **24**(1): p. 21-37.
26. Talley, N.J., *Irritable bowel syndrome.* Intern Med J, 2006. **36**(11): p. 724-8.
27. Lembo, T., et al., *Evidence for the hypersensitivity of lumbar splanchnic afferents in irritable bowel syndrome.* Gastroenterology, 1994. **107**(6): p. 1686-96.
28. Verne, G.N., et al., *Central representation of visceral and cutaneous hypersensitivity in the irritable bowel syndrome.* Pain, 2003. **103**(1-2): p. 99-110.
29. Spiller, R.C., *Irritable bowel syndrome.* Br Med Bull, 2004. **72**: p. 15-29.
30. Stanghellini, V., et al., *New developments in the treatment of functional dyspepsia.* Drugs, 2003. **63**(9): p. 869-92.
31. Fass, R. and R. Dickman, *Non-cardiac chest pain: an update.* Neurogastroenterol Motil, 2006. **18**(6): p. 408-17.
32. Richter, J.E., *Investigation and management of non-cardiac chest pain.* Baillieres Clin Gastroenterol, 1991. **5**(2): p. 281-306.
33. Mertz, H., et al., *Symptoms and visceral perception in severe functional and organic dyspepsia.* Gut, 1998. **42**(6): p. 814-22.
34. Gralnek, I.M., et al., *The impact of irritable bowel syndrome on health-related quality of life.* Gastroenterology, 2000. **119**(3): p. 654-60.
35. Drossman, D.A., et al., *Psychosocial aspects of the functional gastrointestinal disorders.* Gut, 1999. **45 Suppl 2**: p. II25-30.
36. Bueno, L., *Gastrointestinal pharmacology: irritable bowel syndrome.* Curr Opin Pharmacol, 2005. **5**(6): p. 583-8.
37. Bueno, L., et al., *Serotonergic and non-serotonergic targets in the pharmacotherapy of visceral hypersensitivity.* Neurogastroenterol Motil, 2007. **19**(1 Suppl): p. 89-119.
38. Gebhart, G.F., *Visceral pain-peripheral sensitisation.* Gut, 2000. **47 Suppl 4**: p. iv54-5; discussion iv58.
39. Liu, C.Y., et al., *The herbal preparation STW 5 (Iberogast) desensitizes intestinal afferents in the rat small intestine.* Neurogastroenterol Motil, 2004. **16**(6): p. 759-64.
40. Simmen, U., et al., *Binding of STW 5 (Iberogast) and its components to intestinal 5-HT, muscarinic M3, and opioid receptors.* Phytomedicine, 2006. **13 Suppl 5**: p. 51-5.
41. Adam, B., et al., *A combination of peppermint oil and caraway oil attenuates the post-inflammatory visceral hyperalgesia in a rat model.* Scand J Gastroenterol, 2006. **41**(2): p. 155-60.
42. McCleskey, E.W. and M.S. Gold, *Ion channels of nociception.* Annu Rev Physiol, 1999. **61**: p. 835-56.
43. Perl, E.R., *Ideas about pain, a historical view.* Nat Rev Neurosci, 2007. **8**(1): p. 71-80.
44. Scholz, J. and C.J. Woolf, *Can we conquer pain?* Nat Neurosci, 2002. **5 Suppl**: p. 1062-7.
45. Costa, M., S.J. Brookes, and G.W. Hennig, *Anatomy and physiology of the enteric nervous system.* Gut, 2000. **47 Suppl 4**: p. iv15-9; discussion iv26.
46. Furness, J.B., W.A. Kunze, and N. Clerc, *Nutrient tasting and signaling mechanisms in the gut. II. The intestine as a sensory organ: neural, endocrine, and immune responses.* Am J Physiol, 1999. **277**(5 Pt 1): p. G922-8.

47. Blackshaw, L.A., et al., *Sensory transmission in the gastrointestinal tract.* Neurogastroenterol Motil, 2007. **19**(1 Suppl): p. 1-19.
48. Grundy, D., *Neuroanatomy of visceral nociception: vagal and splanchnic afferent.* Gut, 2002. **51 Suppl 1**: p. i2-5.
49. Sengupta, J.N., *An overview of esophageal sensory receptors.* Am J Med, 2000. **108 Suppl 4a**: p. 87S-89S.
50. Berthoud, H.R., et al., *Neuroanatomy of extrinsic afferents supplying the gastrointestinal tract.* Neurogastroenterol Motil, 2004. **16 Suppl 1**: p. 28-33.
51. Blackshaw, L.A. and G.F. Gebhart, *The pharmacology of gastrointestinal nociceptive pathways.* Curr Opin Pharmacol, 2002. **2**(6): p. 642-9.
52. Grundy, D., *Signalling the state of the digestive tract.* Auton Neurosci, 2006. **125**(1-2): p. 76-80.
53. Rodrigo, J., et al., *Vegetative innervation of the esophagus. II. Intraganglionic laminar endings.* Acta Anat (Basel), 1975. **92**(1): p. 79-100.
54. Wang, F.B. and T.L. Powley, *Topographic inventories of vagal afferents in gastrointestinal muscle.* J Comp Neurol, 2000. **421**(3): p. 302-24.
55. Neuhuber, W.L., et al., *Vagal efferent and afferent innervation of the rat esophagus as demonstrated by anterograde DiI and DiA tracing: focus on myenteric ganglia.* J Auton Nerv Syst, 1998. **70**(1-2): p. 92-102.
56. Berthoud, H.R., et al., *Distribution and structure of vagal afferent intraganglionic laminar endings (IGLEs) in the rat gastrointestinal tract.* Anat Embryol (Berl), 1997. **195**(2): p. 183-91.
57. Zagorodnyuk, V.P. and S.J. Brookes, *Transduction sites of vagal mechanoreceptors in the guinea pig esophagus.* J Neurosci, 2000. **20**(16): p. 6249-55.
58. Zagorodnyuk, V.P., B.N. Chen, and S.J. Brookes, *Intraganglionic laminar endings are mechano-transduction sites of vagal tension receptors in the guinea-pig stomach.* J Physiol, 2001. **534**(Pt 1): p. 255-68.
59. Zagorodnyuk, V.P., et al., *Mechanotransduction by intraganglionic laminar endings of vagal tension receptors in the guinea-pig oesophagus.* J Physiol, 2003. **553**(Pt 2): p. 575-87.
60. Berthoud, H.R. and T.L. Powley, *Vagal afferent innervation of the rat fundic stomach: morphological characterization of the gastric tension receptor.* J Comp Neurol, 1992. **319**(2): p. 261-76.
61. Powley, T.L. and R.J. Phillips, *Musings on the wanderer: what's new in our understanding of vago-vagal reflexes? I. Morphology and topography of vagal afferents innervating the GI tract.* Am J Physiol Gastrointest Liver Physiol, 2002. **283**(6): p. G1217-25.
62. Wank, M. and W.L. Neuhuber, *Local differences in vagal afferent innervation of the rat esophagus are reflected by neurochemical differences at the level of the sensory ganglia and by different brainstem projections.* J Comp Neurol, 2001. **435**(1): p. 41-59.
63. Dutsch, M., et al., *Vagal and spinal afferent innervation of the rat esophagus: a combined retrograde tracing and immunocytochemical study with special emphasis on calcium-binding proteins.* J Comp Neurol, 1998. **398**(2): p. 289-307.
64. Neuhuber, W.L., *Sensory vagal innervation of the rat esophagus and cardia: a light and electron microscopic anterograde tracing study.* J Auton Nerv Syst, 1987. **20**(3): p. 243-55.
65. Page, A.J. and L.A. Blackshaw, *An in vitro study of the properties of vagal afferent fibres innervating the ferret oesophagus and stomach.* J Physiol, 1998. **512 (Pt 3)**: p. 907-16.

66. Page, A.J., C.M. Martin, and L.A. Blackshaw, *Vagal mechanoreceptors and chemoreceptors in mouse stomach and esophagus.* J Neurophysiol, 2002. **87**(4): p. 2095-103.
67. Sengupta, J.N. and G.F. Gebhart, *Characterization of mechanosensitive pelvic nerve afferent fibers innervating the colon of the rat.* J Neurophysiol, 1994. **71**(6): p. 2046-60.
68. Kirkup, A.J., A.M. Brunsden, and D. Grundy, *Receptors and transmission in the brain-gut axis: potential for novel therapies. I. Receptors on visceral afferents.* Am J Physiol Gastrointest Liver Physiol, 2001. **280**(5): p. G787-94.
69. Robinson, D.R., et al., *Characterization of the primary spinal afferent innervation of the mouse colon using retrograde labelling.* Neurogastroenterol Motil, 2004. **16**(1): p. 113-24.
70. Nadelhaft, I. and A.M. Booth, *The location and morphology of preganglionic neurons and the distribution of visceral afferents from the rat pelvic nerve: a horseradish peroxidase study.* J Comp Neurol, 1984. **226**(2): p. 238-45.
71. Christianson, J.A., R.J. Traub, and B.M. Davis, *Differences in spinal distribution and neurochemical phenotype of colonic afferents in mouse and rat.* J Comp Neurol, 2006. **494**(2): p. 246-59.
72. Ness, T.J. and G.F. Gebhart, *Characterization of neurons responsive to noxious colorectal distension in the T13-L2 spinal cord of the rat.* J Neurophysiol, 1988. **60**(4): p. 1419-38.
73. Neuhuber, W.L., P.A. Sandoz, and T. Fryscak, *The central projections of primary afferent neurons of greater splanchnic and intercostal nerves in the rat. A horseradish peroxidase study.* Anat Embryol (Berl), 1986. **174**(1): p. 123-44.
74. Berthoud, H.R., P.A. Lynn, and L.A. Blackshaw, *Vagal and spinal mechanosensors in the rat stomach and colon have multiple receptive fields.* Am J Physiol Regul Integr Comp Physiol, 2001. **280**(5): p. R1371-81.
75. Hicks, G.A., et al., *Excitation of rat colonic afferent fibres by 5-HT(3) receptors.* J Physiol, 2002. **544**(Pt 3): p. 861-9.
76. Janig, W. and M. Koltzenburg, *Receptive properties of sacral primary afferent neurons supplying the colon.* J Neurophysiol, 1991. **65**(5): p. 1067-77.
77. Su, X. and G.F. Gebhart, *Mechanosensitive pelvic nerve afferent fibers innervating the colon of the rat are polymodal in character.* J Neurophysiol, 1998. **80**(5): p. 2632-44.
78. Jones, R.C., 3rd, L. Xu, and G.F. Gebhart, *The mechanosensitivity of mouse colon afferent fibers and their sensitization by inflammatory mediators require transient receptor potential vanilloid 1 and acid-sensing ion channel 3.* J Neurosci, 2005. **25**(47): p. 10981-9.
79. Brierley, S.M., et al., *Differential chemosensory function and receptor expression of splanchnic and pelvic colonic afferents in mice.* J Physiol, 2005. **567**(Pt 1): p. 267-81.
80. Brierley, S.M., et al., *Splanchnic and pelvic mechanosensory afferents signal different qualities of colonic stimuli in mice.* Gastroenterology, 2004. **127**(1): p. 166-78.
81. Brierley, S.M., et al., *Activation of splanchnic and pelvic colonic afferents by bradykinin in mice.* Neurogastroenterol Motil, 2005. **17**(6): p. 854-62.
82. Lynn, P.A., et al., *Rectal intraganglionic laminar endings are transduction sites of extrinsic mechanoreceptors in the guinea pig rectum.* Gastroenterology, 2003. **125**(3): p. 786-94.

83. Doerffler-Melly, J. and W.L. Neuhuber, *Rectospinal neurons: evidence for a direct projection from the enteric to the central nervous system in the rat.* Neurosci Lett, 1988. **92**(2): p. 121-5.
84. Neuhuber, W.L., et al., *Rectospinal neurons: cell bodies, pathways, immunocytochemistry and ultrastructure.* Neuroscience, 1993. **56**(2): p. 367-78.
85. Suckow, S.K. and R.M. Caudle, *Identification and immunohistochemical characterization of colospinal afferent neurons in the rat.* Neuroscience, 2008.
86. Al-Chaer, E.D. and R.J. Traub, *Biological basis of visceral pain: recent developments.* Pain, 2002. **96**(3): p. 221-5.
87. Hamill, O.P. and B. Martinac, *Molecular basis of mechanotransduction in living cells.* Physiol Rev, 2001. **81**(2): p. 685-740.
88. Gillespie, P.G. and R.G. Walker, *Molecular basis of mechanosensory transduction.* Nature, 2001. **413**(6852): p. 194-202.
89. Christensen, A.P. and D.P. Corey, *TRP channels in mechanosensation: direct or indirect activation?* Nat Rev Neurosci, 2007. **8**(7): p. 510-21.
90. Lumpkin, E.A. and M.J. Caterina, *Mechanisms of sensory transduction in the skin.* Nature, 2007. **445**(7130): p. 858-65.
91. Martinac, B., *Mechanosensitive ion channels: molecules of mechanotransduction.* J Cell Sci, 2004. **117**(Pt 12): p. 2449-60.
92. Blount, P., *Molecular mechanisms of mechanosensation: big lessons from small cells.* Neuron, 2003. **37**(5): p. 731-4.
93. Hill, J.K. and P.G. Gillespie, *Seeing touch: moving closer to the worm mechanotransduction complex.* Curr Biol, 2003. **13**(24): p. R967-9.
94. Syntichaki, P. and N. Tavernarakis, *Genetic models of mechanotransduction: the nematode Caenorhabditis elegans.* Physiol Rev, 2004. **84**(4): p. 1097-153.
95. Chelur, D.S., et al., *The mechanosensory protein MEC-6 is a subunit of the C. elegans touch-cell degenerin channel.* Nature, 2002. **420**(6916): p. 669-73.
96. Honore, E., *The neuronal background K2P channels: focus on TREK1.* Nat Rev Neurosci, 2007. **8**(4): p. 251-61.
97. Julius, D. and A.I. Basbaum, *Molecular mechanisms of nociception.* Nature, 2001. **413**(6852): p. 203-10.
98. Akopian, A.N., et al., *The tetrodotoxin-resistant sodium channel SNS has a specialized function in pain pathways.* Nat Neurosci, 1999. **2**(6): p. 541-8.
99. Nassar, M.A., et al., *Neuropathic pain develops normally in mice lacking both Nav1.7 and Nav1.8.* Mol Pain, 2005. **1**: p. 24.
100. Wood, J.N., et al., *Voltage-gated sodium channels and pain pathways.* J Neurobiol, 2004. **61**(1): p. 55-71.
101. Driscoll, M. and M. Chalfie, *The mec-4 gene is a member of a family of Caenorhabditis elegans genes that can mutate to induce neuronal degeneration.* Nature, 1991. **349**(6310): p. 588-93.
102. Goodman, M.B., et al., *MEC-2 regulates C. elegans DEG/ENaC channels needed for mechanosensation.* Nature, 2002. **415**(6875): p. 1039-42.
103. Goodman, M.B. and E.M. Schwarz, *Transducing touch in Caenorhabditis elegans.* Annu Rev Physiol, 2003. **65**: p. 429-52.
104. Huang, M. and M. Chalfie, *Gene interactions affecting mechanosensory transduction in Caenorhabditis elegans.* Nature, 1994. **367**(6462): p. 467-70.
105. Jospin, M. and B. Allard, *An amiloride-sensitive H+-gated Na+ channel in Caenorhabditis elegans body wall muscle cells.* J Physiol, 2004. **559**(Pt 3): p. 715-20.

106. Liu, J., B. Schrank, and R.H. Waterston, *Interaction between a putative mechanosensory membrane channel and a collagen.* Science, 1996. **273**(5273): p. 361-4.
107. Suzuki, H., et al., *In vivo imaging of C. elegans mechanosensory neurons demonstrates a specific role for the MEC-4 channel in the process of gentle touch sensation.* Neuron, 2003. **39**(6): p. 1005-17.
108. Tavernarakis, N., et al., *unc-8, a DEG/ENaC family member, encodes a subunit of a candidate mechanically gated channel that modulates C. elegans locomotion.* Neuron, 1997. **18**(1): p. 107-19.
109. Zhang, Y., et al., *Identification of genes expressed in C. elegans touch receptor neurons.* Nature, 2002. **418**(6895): p. 331-5.
110. Kellenberger, S. and L. Schild, *Epithelial sodium channel/degenerin family of ion channels: a variety of functions for a shared structure.* Physiol Rev, 2002. **82**(3): p. 735-67.
111. Welsh, M.J., M.P. Price, and J. Xie, *Biochemical basis of touch perception: mechanosensory function of degenerin/epithelial Na+ channels.* J Biol Chem, 2002. **277**(4): p. 2369-72.
112. Waldmann, R. and M. Lazdunski, *H(+)-gated cation channels: neuronal acid sensors in the NaC/DEG family of ion channels.* Curr Opin Neurobiol, 1998. **8**(3): p. 418-24.
113. Waldmann, R., et al., *A proton-gated cation channel involved in acid-sensing.* Nature, 1997. **386**(6621): p. 173-7.
114. Price, M.P., et al., *The mammalian sodium channel BNC1 is required for normal touch sensation.* Nature, 2000. **407**(6807): p. 1007-11.
115. Alvarez de la Rosa, D., et al., *Distribution, subcellular localization and ontogeny of ASIC1 in the mammalian central nervous system.* J Physiol, 2003. **546**(Pt 1): p. 77-87.
116. Alvarez de la Rosa, D., et al., *Functional implications of the localization and activity of acid-sensitive channels in rat peripheral nervous system.* Proc Natl Acad Sci U S A, 2002. **99**(4): p. 2326-31.
117. Chen, C.C., et al., *A role for ASIC3 in the modulation of high-intensity pain stimuli.* Proc Natl Acad Sci U S A, 2002. **99**(13): p. 8992-7.
118. Garcia-Anoveros, J., et al., *Transport and localization of the DEG/ENaC ion channel BNaC1alpha to peripheral mechanosensory terminals of dorsal root ganglia neurons.* J Neurosci, 2001. **21**(8): p. 2678-86.
119. Duggan, A., J. Garcia-Anoveros, and D.P. Corey, *The PDZ domain protein PICK1 and the sodium channel BNaC1 interact and localize at mechanosensory terminals of dorsal root ganglion neurons and dendrites of central neurons.* J Biol Chem, 2002. **277**(7): p. 5203-8.
120. Lingueglia, E., et al., *A modulatory subunit of acid sensing ion channels in brain and dorsal root ganglion cells.* J Biol Chem, 1997. **272**(47): p. 29778-83.
121. Price, M.P., et al., *The DRASIC cation channel contributes to the detection of cutaneous touch and acid stimuli in mice.* Neuron, 2001. **32**(6): p. 1071-83.
122. Ugawa, S., et al., *In situ hybridization evidence for the coexistence of ASIC and TRPV1 within rat single sensory neurons.* Brain Res Mol Brain Res, 2005. **136**(1-2): p. 125-33.
123. Voilley, N., et al., *Nonsteroid anti-inflammatory drugs inhibit both the activity and the inflammation-induced expression of acid-sensing ion channels in nociceptors.* J Neurosci, 2001. **21**(20): p. 8026-33.

124. Page, A.J., et al., *The ion channel ASIC1 contributes to visceral but not cutaneous mechanoreceptor function.* Gastroenterology, 2004. **127**(6): p. 1739-47.
125. Page, A.J., et al., *Different contributions of ASIC channels 1a, 2, and 3 in gastrointestinal mechanosensory function.* Gut, 2005. **54**(10): p. 1408-15.
126. Chen, C.C., et al., *A sensory neuron-specific, proton-gated ion channel.* Proc Natl Acad Sci U S A, 1998. **95**(17): p. 10240-5.
127. Benson, C.J., et al., *Heteromultimers of DEG/ENaC subunits form H+-gated channels in mouse sensory neurons.* Proc Natl Acad Sci U S A, 2002. **99**(4): p. 2338-43.
128. Hesselager, M., D.B. Timmermann, and P.K. Ahring, *pH Dependency and desensitization kinetics of heterologously expressed combinations of acid-sensing ion channel subunits.* J Biol Chem, 2004. **279**(12): p. 11006-15.
129. Xie, J., et al., *DRASIC contributes to pH-gated currents in large dorsal root ganglion sensory neurons by forming heteromultimeric channels.* J Neurophysiol, 2002. **87**(6): p. 2835-43.
130. Mannsfeldt, A.G., et al., *Stomatin, a MEC-2 like protein, is expressed by mammalian sensory neurons.* Mol Cell Neurosci, 1999. **13**(6): p. 391-404.
131. Price, M.P., P.M. Snyder, and M.J. Welsh, *Cloning and expression of a novel human brain Na+ channel.* J Biol Chem, 1996. **271**(14): p. 7879-82.
132. Wetzel, C., et al., *A stomatin-domain protein essential for touch sensation in the mouse.* Nature, 2007. **445**(7124): p. 206-9.
133. Martinez-Salgado, C., et al., *Stomatin and sensory neuron mechanotransduction.* J Neurophysiol, 2007. **98**(6): p. 3802-8.
134. Drummond, H.A., F.M. Abboud, and M.J. Welsh, *Localization of beta and gamma subunits of ENaC in sensory nerve endings in the rat foot pad.* Brain Res, 2000. **884**(1--2): p. 1-12.
135. Drummond, H.A., et al., *A molecular component of the arterial baroreceptor mechanotransducer.* Neuron, 1998. **21**(6): p. 1435-41.
136. Minke, B., *Drosophila mutant with a transducer defect.* Biophys Struct Mech, 1977. **3**(1): p. 59-64.
137. Hardie, R.C. and B. Minke, *The trp gene is essential for a light-activated Ca2+ channel in Drosophila photoreceptors.* Neuron, 1992. **8**(4): p. 643-51.
138. Schaefer, M., *Homo- and heteromeric assembly of TRP channel subunits.* Pflugers Arch, 2005. **451**(1): p. 35-42.
139. Hellwig, N., et al., *Homo- and heteromeric assembly of TRPV channel subunits.* J Cell Sci, 2005. **118**(Pt 5): p. 917-28.
140. Caterina, M.J., et al., *The capsaicin receptor: a heat-activated ion channel in the pain pathway.* Nature, 1997. **389**(6653): p. 816-24.
141. Caterina, M.J., et al., *Impaired nociception and pain sensation in mice lacking the capsaicin receptor.* Science, 2000. **288**(5464): p. 306-13.
142. Liedtke, W., et al., *Vanilloid receptor-related osmotically activated channel (VR-OAC), a candidate vertebrate osmoreceptor.* Cell, 2000. **103**(3): p. 525-35.
143. Colbert, H.A., T.L. Smith, and C.I. Bargmann, *OSM-9, a novel protein with structural similarity to channels, is required for olfaction, mechanosensation, and olfactory adaptation in Caenorhabditis elegans.* J Neurosci, 1997. **17**(21): p. 8259-69.
144. Suzuki, M., et al., *Localization of mechanosensitive channel TRPV4 in mouse skin.* Neurosci Lett, 2003. **353**(3): p. 189-92.

145. Zhang, L., et al., *Thermosensitive transient receptor potential channels in vagal afferent neurons of the mouse.* Am J Physiol Gastrointest Liver Physiol, 2004. **286**(6): p. G983-91.
146. Gao, X., L. Wu, and R.G. O'Neil, *Temperature-modulated diversity of TRPV4 channel gating: activation by physical stresses and phorbol ester derivatives through protein kinase C-dependent and -independent pathways.* J Biol Chem, 2003. **278**(29): p. 27129-37.
147. Guler, A.D., et al., *Heat-evoked activation of the ion channel, TRPV4.* J Neurosci, 2002. **22**(15): p. 6408-14.
148. Smith, P.L., et al., *Bisandrographolide from Andrographis paniculata activates TRPV4 channels.* J Biol Chem, 2006. **281**(40): p. 29897-904.
149. Suzuki, M., et al., *Impaired pressure sensation in mice lacking TRPV4.* J Biol Chem, 2003. **278**(25): p. 22664-8.
150. Watanabe, H., et al., *Activation of TRPV4 channels (hVRL-2/mTRP12) by phorbol derivatives.* J Biol Chem, 2002. **277**(16): p. 13569-77.
151. Watanabe, H., et al., *Anandamide and arachidonic acid use epoxyeicosatrienoic acids to activate TRPV4 channels.* Nature, 2003. **424**(6947): p. 434-8.
152. Caterina, M.J., et al., *A capsaicin-receptor homologue with a high threshold for noxious heat.* Nature, 1999. **398**(6726): p. 436-41.
153. Lee, H., et al., *Altered thermal selection behavior in mice lacking transient receptor potential vanilloid 4.* J Neurosci, 2005. **25**(5): p. 1304-10.
154. Liedtke, W. and J.M. Friedman, *Abnormal osmotic regulation in trpv4-/- mice.* Proc Natl Acad Sci U S A, 2003. **100**(23): p. 13698-703.
155. Liedtke, W., et al., *Mammalian TRPV4 (VR-OAC) directs behavioral responses to osmotic and mechanical stimuli in Caenorhabditis elegans.* Proc Natl Acad Sci U S A, 2003. **100 Suppl 2**: p. 14531-6.
156. Tabuchi, K., et al., *Hearing impairment in TRPV4 knockout mice.* Neurosci Lett, 2005. **382**(3): p. 304-8.
157. Clapham, D.E., *TRP channels as cellular sensors.* Nature, 2003. **426**(6966): p. 517-24.
158. Andrade, E.L., et al., *Contractile mechanisms coupled to TRPA1 receptor activation in rat urinary bladder.* Biochem Pharmacol, 2006. **72**(1): p. 104-14.
159. Frederick, J., et al., *Increased TRPA1, TRPM8, and TRPV2 expression in dorsal root ganglia by nerve injury.* Biochem Biophys Res Commun, 2007.
160. Kunert-Keil, C., et al., *Tissue-specific expression of TRP channel genes in the mouse and its variation in three different mouse strains.* BMC Genomics, 2006. **7**: p. 159.
161. Park, J.J., et al., *Induction of total insensitivity to capsaicin and hypersensitivity to garlic extract in human by decreased expression of TRPV1.* Neurosci Lett, 2007. **411**(2): p. 87-91.
162. Katsura, H., et al., *Antisense knock down of TRPA1, but not TRPM8, alleviates cold hyperalgesia after spinal nerve ligation in rats.* Exp Neurol, 2006. **200**(1): p. 112-23.
163. Kobayashi, K., et al., *Distinct expression of TRPM8, TRPA1, and TRPV1 mRNAs in rat primary afferent neurons with adelta/c-fibers and colocalization with trk receptors.* J Comp Neurol, 2005. **493**(4): p. 596-606.
164. Nagata, K., et al., *Nociceptor and hair cell transducer properties of TRPA1, a channel for pain and hearing.* J Neurosci, 2005. **25**(16): p. 4052-61.
165. Story, G.M., et al., *ANKTM1, a TRP-like channel expressed in nociceptive neurons, is activated by cold temperatures.* Cell, 2003. **112**(6): p. 819-29.

166. Bautista, D.M., et al., *TRPA1 mediates the inflammatory actions of environmental irritants and proalgesic agents.* Cell, 2006. **124**(6): p. 1269-82.
167. Bautista, D.M., et al., *Pungent products from garlic activate the sensory ion channel TRPA1.* Proc Natl Acad Sci U S A, 2005. **102**(34): p. 12248-52.
168. Jordt, S.E., et al., *Mustard oils and cannabinoids excite sensory nerve fibres through the TRP channel ANKTM1.* Nature, 2004. **427**(6971): p. 260-5.
169. Nagata, K., *TRP channels as target sites for insecticides: physiology, pharmacology and toxicology.* Invert Neurosci, 2007. **7**(1): p. 31-7.
170. Bandell, M., et al., *Noxious cold ion channel TRPA1 is activated by pungent compounds and bradykinin.* Neuron, 2004. **41**(6): p. 849-57.
171. Hinman, A., et al., *TRP channel activation by reversible covalent modification.* Proc Natl Acad Sci U S A, 2006. **103**(51): p. 19564-8.
172. Macpherson, L.J., et al., *Noxious compounds activate TRPA1 ion channels through covalent modification of cysteines.* Nature, 2007. **445**(7127): p. 541-5.
173. Kwan, K.Y., et al., *TRPA1 contributes to cold, mechanical, and chemical nociception but is not essential for hair-cell transduction.* Neuron, 2006. **50**(2): p. 277-89.
174. Corey, D.P., et al., *TRPA1 is a candidate for the mechanosensitive transduction channel of vertebrate hair cells.* Nature, 2004. **432**(7018): p. 723-30.
175. Kindt, K.S., et al., *Caenorhabditis elegans TRPA-1 functions in mechanosensation.* Nat Neurosci, 2007. **10**(5): p. 568-77.
176. Caterina, M.J., *Chemical biology: sticky spices.* Nature, 2007. **445**(7127): p. 491-2.
177. Pardue, M.L. and J.G. Gall, *Molecular hybridization of radioactive DNA to the DNA of cytological preparations.* Proc Natl Acad Sci U S A, 1969. **64**(2): p. 600-4.
178. John, H.A., M.L. Birnstiel, and K.W. Jones, *RNA-DNA hybrids at the cytological level.* Nature, 1969. **223**(206): p. 582-7.
179. Hougaard, D.M., H. Hansen, and L.I. Larsson, *Non-radioactive in situ hybridization for mRNA with emphasis on the use of oligodeoxynucleotide probes.* Histochem Cell Biol, 1997. **108**(4-5): p. 335-44.
180. Yang, H., et al., *An optimized method for in situ hybridization with signal amplification that allows the detection of rare mRNAs.* J Histochem Cytochem, 1999. **47**(4): p. 431-46.
181. Schmidt, B.F., et al., *Signal amplification in the detection of single-copy DNA and RNA by enzyme-catalyzed deposition (CARD) of the novel fluorescent reporter substrate Cy3.29-tyramide.* J Histochem Cytochem, 1997. **45**(3): p. 365-73.
182. Wanner, I., et al., *Subcellular localization of specific mRNAs and their protein products in Purkinje cells by combined fluorescence in situ hybridization and immunocytochemistry.* Histochem Cell Biol, 1997. **108**(4-5): p. 345-57.
183. Bobrow, M.N., et al., *Catalyzed reporter deposition, a novel method of signal amplification. Application to immunoassays.* J Immunol Methods, 1989. **125**(1-2): p. 279-85.
184. Bobrow, M.N., et al., *The use of catalyzed reporter deposition as a means of signal amplification in a variety of formats.* J Immunol Methods, 1992. **150**(1-2): p. 145-9.
185. Bobrow, M.N., K.J. Shaughnessy, and G.J. Litt, *Catalyzed reporter deposition, a novel method of signal amplification. II. Application to membrane immunoassays.* J Immunol Methods, 1991. **137**(1): p. 103-12.
186. Akopian, A.N., L. Sivilotti, and J.N. Wood, *A tetrodotoxin-resistant voltage-gated sodium channel expressed by sensory neurons.* Nature, 1996. **379**(6562): p. 257-62.
187. Schaeren-Wiemers, N. and A. Gerfin-Moser, *A single protocol to detect transcripts of various types and expression levels in neural tissue and cultured cells: in situ*

hybridization using digoxigenin-labelled cRNA probes. Histochemistry, 1993. **100**(6): p. 431-40.
188. Lichtman, J.W. and J.A. Conchello, *Fluorescence microscopy.* Nat Methods, 2005. **2**(12): p. 910-9.
189. Garcia-Anoveros, J., et al., *BNaC1 and BNaC2 constitute a new family of human neuronal sodium channels related to degenerins and epithelial sodium channels.* Proc Natl Acad Sci U S A, 1997. **94**(4): p. 1459-64.
190. Waldmann, R., et al., *The mammalian degenerin MDEG, an amiloride-sensitive cation channel activated by mutations causing neurodegeneration in Caenorhabditis elegans.* J Biol Chem, 1996. **271**(18): p. 10433-6.
191. Babinski, K., K.T. Le, and P. Seguela, *Molecular cloning and regional distribution of a human proton receptor subunit with biphasic functional properties.* J Neurochem, 1999. **72**(1): p. 51-7.
192. de Weille, J.R., et al., *Identification, functional expression and chromosomal localisation of a sustained human proton-gated cation channel.* FEBS Lett, 1998. **433**(3): p. 257-60.
193. Akopian, A.N., et al., *A new member of the acid-sensing ion channel family.* Neuroreport, 2000. **11**(10): p. 2217-22.
194. Grunder, S., et al., *Acid-sensing ion channel (ASIC) 4 gene: physical mapping, genomic organisation, and evaluation as a candidate for paroxysmal dystonia.* Eur J Hum Genet, 2001. **9**(9): p. 672-6.
195. Grunder, S., et al., *A new member of acid-sensing ion channels from pituitary gland.* Neuroreport, 2000. **11**(8): p. 1607-11.
196. Drew, L.J., et al., *Acid-sensing ion channels ASIC2 and ASIC3 do not contribute to mechanically activated currents in mammalian sensory neurones.* J Physiol, 2004. **556**(Pt 3): p. 691-710.
197. Wemmie, J.A., et al., *The acid-activated ion channel ASIC contributes to synaptic plasticity, learning, and memory.* Neuron, 2002. **34**(3): p. 463-77.
198. Livak, K.J. and T.D. Schmittgen, *Analysis of relative gene expression data using real-time quantitative PCR and the 2(-Delta Delta C(T)) Method.* Methods, 2001. **25**(4): p. 402-8.
199. Waldmann, R., et al., *Molecular cloning of a non-inactivating proton-gated Na+ channel specific for sensory neurons.* J Biol Chem, 1997. **272**(34): p. 20975-8.
200. Grant AD, B.N., *protease activated receptor 2 sensitises the transient receptor potential vallinoid 4 ion channel to cause mechanical hyperalgesia.* 2006.
201. Hughes, P.A., et al., *Localization and comparative analysis of acid-sensing ion channel (ASIC1, 2, and 3) mRNA expression in mouse colonic sensory neurons within thoracolumbar dorsal root ganglia.* J Comp Neurol, 2007. **500**(5): p. 863-75.
202. Alessandri-Haber, N., et al., *A transient receptor potential vanilloid 4-dependent mechanism of hyperalgesia is engaged by concerted action of inflammatory mediators.* J Neurosci, 2006. **26**(14): p. 3864-74.
203. Vriens, J., et al., *Cell swelling, heat, and chemical agonists use distinct pathways for the activation of the cation channel TRPV4.* Proc Natl Acad Sci U S A, 2004. **101**(1): p. 396-401.
204. Koltzenburg, M., C.L. Stucky, and G.R. Lewin, *Receptive properties of mouse sensory neurons innervating hairy skin.* J Neurophysiol, 1997. **78**(4): p. 1841-50.
205. Bielefeldt, K., et al., *Phenotypic characterization of gastric sensory neurons in mice.* Am J Physiol Gastrointest Liver Physiol, 2006. **291**(5): p. G987-97.
206. Zhong, F., et al., *Dichotomizing Axons in Spinal and Vagal Afferents of the Mouse Stomach.* Dig Dis Sci, 2007.

207. Garcia-Martinez, C., et al., *Identification of an aspartic residue in the P-loop of the vanilloid receptor that modulates pore properties.* J Biol Chem, 2000. **275**(42): p. 32552-8.
208. Nilius, B., et al., *Pharmacological modulation of monovalent cation currents through the epithelial Ca2+ channel ECaC1.* Br J Pharmacol, 2001. **134**(3): p. 453-62.
209. Szallasi, A., et al., *The vanilloid receptor TRPV1: 10 years from channel cloning to antagonist proof-of-concept.* Nat Rev Drug Discov, 2007. **6**(5): p. 357-72.
210. Ness, T.J. and G.F. Gebhart, *Visceral pain: a review of experimental studies.* Pain, 1990. **41**(2): p. 167-234.
211. Doring, B., et al., *Ablation of connexin43 in smooth muscle cells of the mouse intestine: functional insights into physiology and morphology.* Cell Tissue Res, 2007. **327**(2): p. 333-42.
212. Jaquemar, D., T. Schenker, and B. Trueb, *An ankyrin-like protein with transmembrane domains is specifically lost after oncogenic transformation of human fibroblasts.* J Biol Chem, 1999. **274**(11): p. 7325-33.
213. Walker, R.G., A.T. Willingham, and C.S. Zuker, *A Drosophila mechanosensory transduction channel.* Science, 2000. **287**(5461): p. 2229-34.
214. Sidi, S., R.W. Friedrich, and T. Nicolson, *NompC TRP channel required for vertebrate sensory hair cell mechanotransduction.* Science, 2003. **301**(5629): p. 96-9.
215. Sotomayor, M., D.P. Corey, and K. Schulten, *In search of the hair-cell gating spring elastic properties of ankyrin and cadherin repeats.* Structure, 2005. **13**(4): p. 669-82.
216. Fujita, F., et al., *Methyl p-hydroxybenzoate causes pain sensation through activation of TRPA1 channels.* Br J Pharmacol, 2007. **151**(1): p. 153-60.
217. Xu, H., N.T. Blair, and D.E. Clapham, *Camphor activates and strongly desensitizes the transient receptor potential vanilloid subtype 1 channel in a vanilloid-independent mechanism.* J Neurosci, 2005. **25**(39): p. 8924-37.
218. Cebi, M. and U. Koert, *Reactivity Recognition by TRPA1 Channels.* Chembiochem, 2007. **8**(9): p. 979-980.
219. Peterlin, Z., A. Chesler, and S. Firestein, *A painful trp can be a bonding experience.* Neuron, 2007. **53**(5): p. 635-8.
220. Wang, S., et al., *Phospholipase C and protein kinase A mediate bradykinin sensitization of TRPA1: a molecular mechanism of inflammatory pain.* Brain, 2008. **131**(Pt 5): p. 1241-51.
221. Couture, R., et al., *Kinin receptors in pain and inflammation.* Eur J Pharmacol, 2001. **429**(1-3): p. 161-76.
222. Doerner, J.F., et al., *Transient receptor potential channel A1 is directly gated by calcium ions.* J Biol Chem, 2007. **282**(18): p. 13180-9.
223. Zurborg, S., et al., *Direct activation of the ion channel TRPA1 by Ca2+.* Nat Neurosci, 2007. **10**(3): p. 277-9.
224. Story, G.M. and R.W.t. Gereau, *Numbing the senses: role of TRPA1 in mechanical and cold sensation.* Neuron, 2006. **50**(2): p. 177-80.
225. Di Palma, F., et al., *Mutations in Mcoln3 associated with deafness and pigmentation defects in varitint-waddler (Va) mice.* Proc Natl Acad Sci U S A, 2002. **99**(23): p. 14994-9.b
226. Corey, D.P., *What is the hair cell transduction channel?* J Physiol, 2006. **576**(Pt 1): p. 23-8.

227. Atiba-Davies, M. and K. Noben-Trauth, *TRPML3 and hearing loss in the varitint-waddler mouse.* Biochim Biophys Acta, 2007.
228. Hill, K. and M. Schaefer, *TRPA1 is differentially modulated by the amphipathic molecules trinitrophenol and chlorpromazine.* J Biol Chem, 2007. **282**(10): p. 7145-53.
229. Tracey, W.D., Jr., et al., *painless, a Drosophila gene essential for nociception.* Cell, 2003. **113**(2): p. 261-73.
230. Al-Anzi, B., W.D. Tracey, Jr., and S. Benzer, *Response of Drosophila to wasabi is mediated by painless, the fly homolog of mammalian TRPA1/ANKTM1*. Curr Biol, 2006. **16**(10): p. 1034-40.
231. Brierley, S.M., et al., *Selective Role for TRPV4 Ion Channels in Visceral Sensory Pathways.* Gastroenterology, 2008.
232. Niforatos, W., et al., *Activation of TRPA1 channels by the fatty acid amide hydrolase inhibitor 3'-carbamoylbiphenyl-3-yl cyclohexylcarbamate (URB597).* Mol Pharmacol, 2007. **71**(5): p. 1209-16.

APPENDIX 1

PUBLICATIONS ARISING FROM THIS THESIS

THE JOURNAL OF COMPARATIVE NEUROLOGY 500:863–875 (2007)

Localization and Comparative Analysis of Acid-Sensing Ion Channel (ASIC1, 2, and 3) mRNA Expression in Mouse Colonic Sensory Neurons within Thoracolumbar Dorsal Root Ganglia

PATRICK A. HUGHES,[1,2] STUART M. BRIERLEY,[1,2] RICHARD L. YOUNG,[1,3] AND L. ASHLEY BLACKSHAW[1–3]*

[1]Nerve-Gut Research Laboratory, Department of Gastroenterology, Hepatology and General Medicine, Royal Adelaide Hospital, Adelaide, South Australia, 5000, Australia
[2]Discipline of Physiology, School of Molecular and Biomedical Sciences, University of Adelaide, Adelaide, South Australia, 5005, Australia
[3]Discipline of Medicine, University of Adelaide, Adelaide, South Australia, 5005, Australia

ABSTRACT

Reducing colonic mechanosensitivity is an important potential strategy for reducing visceral pain. Mice lacking acid-sensing ion channels (ASIC) 1, 2, and 3 show altered colonic mechanosensory function, implicating ASICs in the mechanotransduction process. Deletion of ASICs affects mechanotransduction in visceral and cutaneous afferents differently, suggesting differential expression. We determined relative expression of ASIC1, 2, and 3 in mouse thoracolumbar dorsal root ganglia (DRG) by quantitative reverse-transcriptase polymerase chain reaction (RT-PCR) analysis (QPCR) and specifically in retrogradely traced colonic neurons isolated via laser capture microdissection. Localization of ASIC expression in DRG was determined with fluorescence in situ hybridization (FISH) and retrograde tracing. QPCR of whole thoracolumbar DRG revealed and abundance of ASIC2 > ASIC1 > ASIC3. Similarly, FISH of all neurons in thoracolumbar DRG demonstrated that ASIC2 was expressed in the most (40 ± 1%) neurons, followed by ASIC3 (24 ± 1%), then ASIC1 (18 ± 1%). Retrograde tracing from the distal colon labeled 4 ± 1% of neurons in T10-L1 DRG. In contrast to whole DRG, FISH of colonic neurons showed ASIC3 expression in 73 ± 2%, ASIC2 in 47 ± 0.5%, and ASIC1 in 30 ± 2%. QPCR of laser captured colonic neurons revealed that ASIC3 was the most abundant ASIC transcript, followed by ASIC1, then ASIC2. We conclude that ASIC1, 2, and 3 are expressed preferentially in colonic neurons within thoracolumbar DRG. In particular ASIC3, the least abundant in the general population, is the most abundant ASIC transcript in colonic neurons. The prevalence of ASIC3 in neurons innervating the colon supports electrophysiological data showing that it makes a major contribution to colonic mechanotransduction and therefore may be a target for the treatment of visceral pain. J. Comp. Neurol. 500:863–875, 2007.

Indexing terms: visceral afferents; fluorescent in situ hybridization; laser capture microdissection; quantitative RT-PCR; retrograde labeling; visceral pain

Grant support: National Health and Medical Research Council of Australia (NHMRC) Senior Research Fellowship (to L.A.B.); Grant sponsor: NHMRC Australia; Grant number: 298942 (to L.A.B.); Grant sponsor: GlaxoSmithKline Young Investigator Award in the Biology of Functional Bowel Disorders (to S.M.B.); Grant sponsor: Dawes Scholarship/University of Adelaide Faculty of Science Postgraduate Award (to P.A.H.).

The first two authors contributed equally to this work.

*Correspondence to: L. Ashley Blackshaw, Nerve Gut Research Laboratory, Level 1 Hanson Institute, Frome Road, Adelaide, SA 5000, Australia.

E-mail: ablacksh@mail.rah.sa.gov.au

Received 18 June 2006; Revised 21 August 2006; Accepted 28 August 2006

DOI 10.1002/cne.21204

Published online in Wiley InterScience (www.interscience.wiley.com).

Hughes, P.A., Brierley, S.M., Young, R.L. & Blackshaw, L.A. (2007). Localization and comparative analysis of acid-sensing ion channel (ASIC1, 2, and 3) mRNA expression in mouse colonic sensory neurons within thoracolumbar dorsal root ganglia. *Journal of Comparative Neurology, v. 500 (5), pp. 863-875*

GASTROENTEROLOGY 2008;134:2059–2069

Selective Role for TRPV4 Ion Channels in Visceral Sensory Pathways

STUART M. BRIERLEY,[*,§] AMANDA J. PAGE,[*,‡,§] PATRICK A. HUGHES,[*,§] BIRGIT ADAM,[§] TOBIAS LIEBREGTS,[§] NICOLE J. COOPER,[§] GERALD HOLTMANN,[‡,§] WOLFGANG LIEDTKE,[‖] and L. ASHLEY BLACKSHAW[*,‡,§]

[*]Discipline of Physiology, School of Molecular and Biomedical Sciences, The University of Adelaide, Adelaide, Australia; [‡]Discipline of Medicine, The University of Adelaide, Adelaide, Australia; [§]Nerve-Gut Research Laboratory, Department of Gastroenterology and Hepatology, Hanson Institute, Royal Adelaide Hospital, Adelaide, Australia; [‖]Center for Translational Neuroscience, Duke University, Durham, North Carolina

Background & Aims: **Although there are many candidates as molecular mechanotransducers, so far there has been no evidence for molecular specialization of visceral afferents. Here, we show that colonic afferents express a specific molecular transducer that underlies their specialized mechanosensory function: the transient receptor potential channel, vanilloid 4 (TRPV4).** ***Methods:*** **We found TRPV4 mRNA is highly enriched in colonic sensory neurons compared with other visceral and somatic sensory neurons. TRPV4 protein was found in colonic nerve fibers from patients with inflammatory bowel disease, and it colocalized in a subset of fibers with the sensory neuropeptide CGRP in mice. We characterized the responses of 8 subtypes of vagal, splanchnic, and pelvic mechanoreceptors.** ***Results:*** **Mechanosensory responses of colonic serosal and mesenteric afferents were enhanced by a TRPV4 agonist and dramatically reduced by targeted deletion of TRPV4 or by a TRP antagonist. Other subtypes of vagal and pelvic afferents, by contrast, were unaffected by these interventions. The behavioral responses to noxious colonic distention were also substantially reduced in mice lacking TRPV4.** ***Conclusions:*** **These data indicate that TRPV4 contributes to mechanically evoked visceral pain, with relevance to human disease. In view of its distribution in favor of specific populations of visceral afferents, we propose that TRPV4 may present a selective novel target for the reduction of visceral pain, which is an important opportunity in the absence of current treatments.**

Abbreviations used in this paper: 5,6-EET, 5,6-epoxyeicosatrienoic acid; ANOVA, analysis of variance; CGRP, calcitonin gene-related peptide; CRD, colorectal distention; CTB-FITC, cholera toxin subunit B conjugated to fluorescein isothiocyanate; DRG, dorsal root ganglia; EMG, electromyographic; QRT-PCR, quantitative reverse transcription–polymerase chain reaction; RR, ruthenium red; TRP, transient receptor potential; TRPV4, transient receptor potential channel, vanilloid 4.

0016-5085/08/$34.00
doi:10.1053/j.gastro.2008.01.074

Brierley, S.M., Page, A.J., Hughes, P.A., Adam, B., Liebregts, T., Cooper, N.J., Holtmann, G., Liedtke, W. & Blackshaw, L.A. (2008). Selective Role for TRPV4 ion channels in visceral sensory pathways.
Gastroenterology, v. 134 (7), pp. 2059-2069

TRPA1 mediates mechanotransduction in sensory neurons and is modulated by algesic stimuli

Stuart M. Brierley [1,2], Patrick A. Hughes [1,2]*, Amanda J. Page [1,2,3]*, Kelvin Y. Kwan [4], Christopher M. Martin [1] Tracey A. O'Donnell [1], Nicole J. Cooper [1], Andrea M. Harrington[1], Birgit Adam [1], Tobias Liebregts [1], Gerald Holtmann [1,3], David P. Corey [4], Grigori Y. Rychkov [2] & L. Ashley Blackshaw [1,2,3].*

[1]Nerve-Gut Research Laboratory, Department of Gastroenterology & Hepatology, Hanson Institute, Royal Adelaide Hospital, Adelaide, South Australia, AUSTRALIA 5000.

[2]Discipline of Physiology, School of Molecular and Biomedical Sciences, [3] Discipline of Medicine, The University of Adelaide, Adelaide, South Australia, AUSTRALIA 5000.

[4]Department of Neurobiology and Howard Hughes Medical Institute, Harvard Medical School, Boston, Massachusetts, USA, 02115.

** These authors contributed equally to this work*

Correspondence: L. Ashley Blackshaw, Nerve-Gut Research Laboratory, Department of Gastroenterology & Hepatology, Hanson Institute, Royal Adelaide Hospital, Adelaide, South Australia, AUSTRALIA 5000.
Phone: +61 8 8222 5644
Fax: +61 8 8222 5934
Email: ashley.blackshaw@adelaide.edu.au

Acknowledgements:

We thank the following for financial support: National Health and Medical Research Council of Australia for project grant support (L.A.B, S.M.B), Senior Research Fellowships (L.A.B and G.Y.R) and an Australian Biomedical Fellowship (S.M.B), GlaxoSmithKline Young Investigator Award (S.M.B), University of Adelaide Postgraduate Scholarship (P.A.H).

Summary

Transient receptor potential (TRP) channels transduce diverse stimuli in sensory neurons. TRPA1 mediates cold- and chemical-induced pain, and interacts with G-protein-coupled receptors, but its role in mechanosensation remains enigmatic. Chronic pain states often involve the viscera, from which sensory information is conducted via 5 afferent subtypes along 3 pathways. Visceral mechanosensory function was dramatically reduced in TRPA1-/- mice, but only in particular afferent subtypes. These subtypes showed increased TRPA1 function after inflammation. Bradykinin and capsaicin directly excited sensory endings, which was unchanged in TRPA1-/- mice. Bradykinin responses were followed by increased mechanosensitivity, whereas capsaicin reduced mechanosensitivity. These changes were lost in TRPA1-/-, indicating that TRPA1 is not required for direct activation by algesic compounds, but it provides a mechanism for alteration of mechanosensation. In contrast, no interaction between protease receptor activation and TRPA1 was evident. This study reveals multiple, discrete roles for TRPA1 in mechanosensation and nociception.

Running title: TRPA1: a mechanotransducer in mammalian sensory neurons

Brierley, S.M., Hughes, P.A., Page, A.J., Kwan, K.Y., Martin, C.M., O'Donnell, T.A., Cooper, N.J., Harrington, A.M., Adam, B., Liebregts, T., Holtmann, G., Corey, D.P., Rychkov, G. & Blackshaw, A. (2008) TRPA1 mediates mechanotransduction in sensory neurons and is modulated by algesic stimuli.
Neuron (in press)